

THE FLORIDA STATE UNIVERSITY

COLLEGE OF ARTS AND SCIENCES

SEMILEPTONIC DECAY OF HEAVY BARYONS IN
A CONSTITUENT QUARK MODEL

By

MUSLEMA PERVIN

A dissertation submitted to the
Department of Physics
in partial fulfillment of the
requirements for the degree of
Doctor of Philosophy

Degree Awarded:
Summer Semester, 2005

The members of the Committee approve the dissertation of Muslema Pervin defended on June 24, 2005.

Simon Capstick
Professor Co-Directing dissertation

Winston Roberts
Professor Co-Directing dissertation

Christopher Hunter
Outside Committee Member

Jorge Piekarewicz
Committee Member

Paul Eugenio
Committee Member

Laura Reina
Committee Member

The Office of Graduate Studies has verified and approved the above named committee members.

To my mother.

ACKNOWLEDGEMENTS

I would like to thank Professor Simon Capstick for providing me the opportunity to be a graduate student at FSU, and for his guidance and help in my research. This has been especially important in the last six months leading to the dissertation defense. I am also indebted to him for his kind help and understanding during some difficult times at FSU.

I offer my full gratitude to Professor Winston Roberts for his guidance, cooperation and patience throughout this research project. Without his support it would have been very difficult for me to carry this project to completion, and attain my most significant accomplishment to date.

Many thanks to Professor Jorge Piekarewicz, Professor Laura Reina and Professor Paul Eugenio for their invaluable discussions and insightful suggestions about the project. Special thanks to Professor Christopher Hunter for his kind cooperation as an outside committee member. I would also like to thank Professor Kirby Kemper (former department chair) and Professor David Van Winkle (current chair) for their help and support.

At this auspicious moment I would also like to acknowledge the moral support of my parents (Md. Maniruzzaman and Mrs. Hashmat Ara Begum) and my sisters (Mimi, Rimi, and Luma) and express my heartfelt gratitude to them. Special thanks go to my mother, who has always inspired me to strive for accomplishments.

I would also like to thank the adviser for my MS research, Professor Lalit M. Nath (of Dhaka University): he was the person who first inspired me to dream of being a researcher.

Many thanks to Boudi (Jhumur), Professor Yazdani, Sraboni, Hafiz bhai and Rifat for being with me in my good and bad times in last five years of my graduate study. I also thank those who helped me after my accident (at FSU) and surgery. Too numerous to list, I am nevertheless grateful to them all.

This research was supported by the U.S. Department of Energy under contracts DE-FG02-92ER40750 (M.P. and S.C.) and DE-FG05-94ER40832 (W.R.).

TABLE OF CONTENTS

List of Tables	vii
List of Figures	ix
Abstract	x
1. Introduction	1
1.1 Standard Model	2
1.2 Quark model and QCD	8
1.3 Semileptonic Decay	12
1.4 Heavy Quark Effective Theory	15
1.5 HQET and Semileptonic Decays	16
1.6 Existing Models of Semileptonic Decay	18
1.7 Motivation	20
2. Matrix Elements, Decay rates and HQET	22
2.1 Matrix Elements	22
2.2 Decay Rates	23
2.3 Heavy Quark Effective Theory	25
3. The Model	35
3.1 Wave Function Components	35
3.2 Expansion Bases	39
3.3 Hamiltonian	40
3.4 Obtaining the Form Factors	41
4. Comparison of HQET and Quark Model Results	46
4.1 Λ_Q decay	46
4.2 Ω_Q decay	49
5. Numerical Results	56
5.1 Model Parameters, Mass Spectra and Wave Functions	56
5.2 Form Factors and Decay Rates: Λ_Q	62
5.3 Form Factors and Decay Rates: Ω_Q	81
5.4 Conclusions and Outlook	91

A.	Wave Functions and Semileptonic Operators	95
A.1	Λ_Q Baryon	95
A.2	Ω_Q Baryon	97
A.3	Semileptonic Operators	99
B.	Integrals in the SturmianBasis	101
C.	Quark Model Form Factors	105
C.1	Form factors for Λ_Q decay	105
C.2	Form factors for Ω_Q decay	114
C.3	HQET Quark Model Form Factors	135
D.	Hadronic Tensor	148
E.	Constructing Higher Spin Representations and Quark Matrix Elements	156
	REFERENCES	158
	BIOGRAPHICAL SKETCH	163

LIST OF TABLES

5.1	Hamiltonian parameters obtained from the four different fits.	56
5.2	Wave function size parameters, α_ρ and α_λ , for states of different J^P and with spin-flavor antisymmetric light diquark, in different models.	57
5.3	Wave function size parameters, α_ρ and α_λ , for states of different J^P and with spin-flavor symmetric light diquark.	58
5.4	Baryon masses in GeV in different quark models-1.	59
5.5	Baryon masses in GeV in different quark models-2.	60
5.6	Mixing coefficients (η_i) of the two lowest lying $1/2^+$ states in different flavor sectors.	61
5.7	Mixing coefficients (η_i) of the two lowest lying $1/2^+, 3/2^+$ states of Ξ and Ω_c	62
5.8	Form factor components \mathcal{F}_i and \mathcal{G}_i evaluated at the non-recoil point for $\Lambda_Q \rightarrow \Lambda_q$	63
5.9	The form factors for $\Lambda_c \rightarrow \Lambda^{(*)}$ transitions, calculated at the non-recoil point, in the four models we used.	64
5.10	The ratio ξ_2/ξ_1 for $\Lambda_c \rightarrow \Lambda(1/2^+)$	65
5.11	Integrated decay rates for $\Lambda_c \rightarrow \Lambda^{(*)}$ in units of $10^{11}s^{-1}$, for different Λ states in the four models.	67
5.12	Form factors of $\Lambda_b \rightarrow \Lambda_c^{(*)}$, calculated at the non-recoil point, in the four models.	70
5.13	Slope of the Isgur-Wise function, evaluated at the non-recoil point, for the elastic decay of the Λ_b	73
5.14	Rates for $\Lambda_b \rightarrow \Lambda_c^{(*)}$ decays in units of $10^{10}s^{-1}$	76
5.15	Decay rates of $\Lambda_b \rightarrow N^{(*)+}\ell\bar{\nu}_\ell$ in units of $10^{12}s^{-1} \times V_{ub} ^2$	80
5.16	The form factors for $\Omega_b \rightarrow \Omega_c^{(*)}$ transitions, calculated at the non-recoil point.	83
5.17	Integrated decay rates for $\Omega_b \rightarrow \Omega_c^{(*)}$ in units of $10^{10}s^{-1}$	86

5.18	The form factors for $\Omega_c \rightarrow \Xi^{(*)}$ transitions, calculated at the non-recoil point.	87
5.19	Integrated decay rates for $\Omega_c \rightarrow \Xi^{(*)}$ in units of $10^{10}s^{-1}$, for different Ξ states.	90
5.20	Integrated decay rates for $\Omega_c \rightarrow \Omega^{(*)}$ in units of $10^{11}s^{-1}$	90
A.1	Quark matrix elements of $\langle q(p_Q, s_Q) \mathcal{O}_i Q(p_q, s_q) \rangle$	99
A.2	Quark matrix elements of $\langle q(p_Q, s_Q) \mathcal{O}_i Q(p_q, s_q) \rangle$ in terms of spherical harmonics.	100

LIST OF FIGURES

1.1	Baryon semileptonic decay: $B_Q \rightarrow B_q \ell \nu_\ell$	14
5.1	Form factors for $\Lambda_c \rightarrow \Lambda(1/2^+)$ obtained using harmonic oscillator wave functions and Sturmian wave functions	65
5.2	The differential decay rates for different $\Lambda_c \rightarrow \Lambda^{(*)}$ transitions, in the different models	66
5.3	Form factors for $\Lambda_b \rightarrow \Lambda_c(1/2^+)$ obtained using harmonic oscillator wave functions and Sturmian wave functions	71
5.4	The elastic form factors for the decay of the Λ_b as functions of w in the harmonic oscillator and Sturmian model.	72
5.5	The differential decay rates for different $\Lambda_b \rightarrow \Lambda_c^{(*)}$ transitions, in the various models that we use	75
5.6	Form factors $\xi_1^{(V)}$, $\xi_1^{(A)}$ and ξ_2 for the transitions $\Lambda_c \rightarrow n$ and $\Lambda_b \rightarrow p$	78
5.7	Differential decay rates for $\Lambda_b \rightarrow N^{(*)+}$ in the HONR and HOSR models.	79
5.8	Differential decay rate for $\Lambda_c \rightarrow n$ in the HONR and HOSR models.	81
5.9	Form factors for $\Omega_b \rightarrow \Omega_c(1/2^+)$ obtained using harmonic oscillator wave functions and Sturmian wave functions	84
5.10	The differential decay rates for different $\Omega_b \rightarrow \Omega_c^{(*)}$ transitions, in the various models that we use	85
5.11	Form factors for $\Omega_c \rightarrow \Xi(1/2^+)$ obtained using harmonic oscillator wave functions and Sturmian wave functions	88
5.12	The differential decay rates for different $\Omega_c \rightarrow \Xi^{(*)}$ transitions, in the various models that we use	89

ABSTRACT

The semileptonic decays of heavy baryons, Λ_Q and Ω_Q are treated in the framework of a constituent quark model. Both nonrelativistic and semirelativistic Hamiltonians are used to obtain the baryon wave functions from a fit to the spectra, and the wave functions are expanded in both the harmonic oscillator and Sturmian bases. The latter basis leads to form factors in which the kinematic dependence on the square of the momentum transfer (q^2) is in the form of multipoles, and the resulting form factors fall faster as a function of q^2 in the available kinematic ranges. As a result, decay rates obtained in the two models using the Sturmian basis are significantly smaller than those obtained using the harmonic oscillator basis. In the case of the Λ_c , decay rates calculated using the Sturmian basis are closer to the experimentally reported rates. However, we find a semileptonic branching fraction for the Λ_c to decay to excited Λ^* states of 11% to 19%, in contradiction with what is assumed in available experimental analyses. Our prediction for the Λ_b semileptonic decays is that decays to the ground state Λ_c provide a little less than 70% of the total semileptonic decay rate. For the decays $\Lambda_b \rightarrow \Lambda_c$, the analytic form factors we obtain satisfy the relations expected from heavy-quark effective theory at the non-recoil point, at leading and next-to-leading orders in the heavy-quark expansion. In addition, some features of the heavy-quark limit are shown to naturally persist as the mass of the heavy quark in the daughter baryon is decreased.

For the case of Ω_Q decays there are no experimentally determined rates. However, we find that our analytical and numerical results for the form factors and rates of Ω_Q decays compare well with HQET predictions. Our results indicate a significant inelastic branching fraction for $\Omega_b \rightarrow \Omega_c^{(*)}$ decays, which is about 37% in all of our models. For $\Omega_c \rightarrow \Xi^{(*)}$ decays the elastic fraction dominates (about 82%) but it does not saturate the decay.

CHAPTER 1

Introduction

Curiosity about nature sets humans apart from other creatures. Questions about the origin of the universe, and the forces behind the formation and binding of tiny atoms to giant stars have driven the curiosity of philosophers and scientists, and have led them to strive for knowledge throughout the history of mankind. Among these questions, the nature of the four fundamental forces (gravity, electromagnetic, weak and strong) has always been the central focus of physicists.

Gravity, the weakest of all forces, is a fundamental force which acts between any pair of material objects, and is the source of attraction between the Earth and any massive object on the Earth. It is also the force responsible for the orbital motion of planets and stars. While gravity works in one extreme, in the macroscopic world of very massive objects, it is the strong force (10^{40} times stronger than gravity) which dominates in the other extreme, the nuclear and sub-nuclear world. The strong interaction binds protons and neutrons into a nucleus. It is also responsible for binding quarks into protons and neutrons, and for providing most of the mass of these objects. The positively charged nucleus and negatively charged electrons are then combined to form a neutral atom. The force involved between these moving charged particles is known as the electromagnetic force, $1/137$ times weaker than the strong force. The last is the weak force, which was not known until radioactivity was discovered.

In the early twentieth century it was observed that the nuclei of certain chemical elements were not stable, but decayed into other nuclei. It was soon discovered that a neutron inside this kind of unstable nucleus decayed to a proton, and an electron was emitted at the same time. This process is known as beta decay, and its description lead to the concept of weak interactions. At present a vast number of different decays and interactions are described by

the weak interaction, which has been the focus of the attention of leading physicists from the moment of its discovery. Some revolutionary new concepts, such as violation of some apparently well established symmetries like parity (P), charge conjugation (C) and later on CP, are involved in the description of the weak interactions.

Although the fundamental forces are reasonably well understood, with the exception of the strong interaction, there still remain at least two fundamental challenges for 21st century particle and nuclear physicists. The first is the unification of all four forces and their description in terms of a single coupling constant at some higher energy scale. So far the Standard Model couples the strong and electroweak forces. However, it does not unify the forces up to a single coupling constant. Extensive research has been carried out to include gravity in the unification of forces, and string theory is one of the most popular approaches in that direction. The second challenge is to understand the strong interaction well in the ‘soft’ region, where momenta are smaller or distances between interacting particles are large.

Neutrons and protons are not fundamental particles but are made of quarks, which are elementary particles having fractional charge. The existence of quarks has been established indirectly in deep inelastic scattering [1]. However, isolated quarks have never been seen, despite much experimental effort. Quarks always bind together for example, to form a meson (a quark with an antiquark) or a baryon (three quarks), known collectively as hadrons. The presently accepted theory of the strong interactions is described in terms of a ‘running’ coupling constant which is small at short distances and becomes large (order of unity) at large distances. This makes any perturbative approach to the calculation of the consequences of QCD (Quantum Chromodynamics) at large distance impossible. Therefore much of the phenomenology of the strong interaction and how the quarks are bound remains poorly understood.

1.1 Standard Model

The Standard Model (SM) of particle physics describes the fundamental particles of nature and the interactions between them. The Lagrangian of the Standard Model has the underlying symmetry $SU(3)_c \times SU(2)_w \times U(1)_y$. This means that the Lagrangian is constructed in such a way that it is invariant under this symmetry group. The Abelian $U(1)_y$ group is associated with the quantum number y , known as weak hypercharge, which is related to the electric charge Q by $Q = t_3 + y/2$ where t_3 is the third component of the

weak isospin quantum number. The $SU(2)_w$ group is associated with weak isospin, and in $SU(3)_c$ the c stands for the color quantum number. The $SU(2)_w \times U(1)_y$ symmetry describes the unified weak and electromagnetic forces, and is widely known as the Glashow-Salam-Weinberg [2] model of the electroweak interaction. The strong (color) interaction $SU(3)_c$ was incorporated later into the Standard Model to complete the description of the three interactions. It should be noted here that three independent coupling constants are required by the structure of the direct product group $SU(3)_c \times SU(2)_w \times U(1)_y$.

In this section we will focus on the electroweak interaction. The electroweak gauge group $SU(2)_w \times U(1)_y$ requires four gauge bosons: 3 \mathbf{b}_μ for $SU(2)$ and a_μ for $U(1)$. The constituent particles are spin-1/2 fermions (six quarks and six leptons). There is also a scalar particle known as the Higgs. The Lagrangian density of this model can be written as the sum of terms

$$\mathcal{L} = \mathcal{L}_g + \mathcal{L}_{f-g} + \mathcal{L}_s + \mathcal{L}_{f-s},$$

where \mathcal{L}_g represents the Lagrangian for the gauge fields, \mathcal{L}_{f-g} describes the fermion fields and their couplings to the gauge fields, \mathcal{L}_s is the contribution from scalar fields, and \mathcal{L}_{f-s} describes the coupling between fermion and scalar fields. For brevity we will focus on those parts of the Lagrangian that are most relevant for this project.

1.1.1 \mathcal{L}_{f-g} and the weak current

The Lagrangian density that describes the interaction between the fermions and the gauge fields may be written as

$$\begin{aligned} \mathcal{L}_{f-g} = & \sum_{j=1}^3 \left[\bar{R}_{hj} i\gamma^\mu \left(\partial_\mu + i\frac{g'}{2} a_\mu y \right) R_{hj} + \bar{R}'_{hj} i\gamma^\mu \left(\partial_\mu + i\frac{g'}{2} a_\mu y \right) R'_{hj} \right. \\ & + \bar{L}_{hj} i\gamma^\mu \left(\partial_\mu + i\frac{g'}{2} a_\mu y + i\frac{g}{2} \boldsymbol{\tau} \cdot \mathbf{b}_\mu \right) L_{hj} + \bar{R}'_{\ell j} i\gamma^\mu \left(\partial_\mu + i\frac{g'}{2} a_\mu y \right) R'_{\ell j} \\ & \left. + \bar{L}_{\ell j} i\gamma^\mu \left(\partial_\mu + i\frac{g'}{2} a_\mu y + i\frac{g}{2} \boldsymbol{\tau} \cdot \mathbf{b}_\mu \right) L_{\ell j} \right], \end{aligned} \quad (1.1)$$

where the index j represents the generation of the fermion family, and h and ℓ correspond to the hadronic and leptonic part of the Lagrangian. Neutrinos only appear in a left-handed doublet since there is no right-handed neutrino. The members of the lepton families are

(ν_e, e) , (ν_μ, μ) and (ν_τ, τ) . Quarks are grouped into weak isospin doublet as (u, d) , (c, s) and (t, b) . The right and left-handed fermions are defined as

$$\begin{aligned} R_j &= u_{jR} = \frac{1}{2}(1 + \gamma_5)u_j, R'_j = d_{jR} = \frac{1}{2}(1 + \gamma_5)d_j, \\ L_j &= \begin{pmatrix} u_j \\ d_j \end{pmatrix}_L = \frac{1}{2}(1 - \gamma_5) \begin{pmatrix} u_j \\ d_j \end{pmatrix}, \end{aligned}$$

where u_j and d_j represent the gauge (weak) eigenstates of the corresponding Dirac spinors for up and down type fermions (quarks and leptons).

To preserve the gauge invariance of the symmetry group there is no mass term for either the fermion fields or the gauge bosons. However, $SU(2)_w \times U(1)_y$ is not a symmetry that occurs in nature. Within the SM, it is spontaneously broken by the Higgs mechanism [3]. The remaining symmetry is $U(1)_{QED}$ and consequently electrical charge is conserved. After spontaneous symmetry breaking (SSB), the four gauge bosons are coupled to give three massive vector bosons (W_μ^+ , W_μ^- and Z_μ^0) and a massless vector boson, the photon (A_μ), for the $U(1)_{QED}$ symmetry. The scalar field also acquires a mass, and becomes the Higgs particle. The other very important aspect of SSB is that it makes the fermion fields massive. Without going into the details of the procedure, we mention here that under SSB the original scalar field in the \mathcal{L}_{f-s} of the Lagrangian density is shifted. As a consequence the gauge eigenstates of fermion fields transform into mass eigenstates with a finite mass for all the quarks and down type leptons. The neutrino remains massless because it has no right-handed component.

After SSB, the hadronic charged current of \mathcal{L}_{f-g} has the form

$$\mathcal{L}_{f-g}^{charged} = -\frac{g}{\sqrt{2}} [V_{ij}\bar{u}'_i\gamma^\mu(1 - \gamma_5)d'_jW_\mu^+ + \text{H.C.}], \quad (1.2)$$

where H.C. denotes the Hermitian conjugate and V is the Cabibbo-Kobayashi-Maskawa (CKM) [4] matrix. This matrix appears in the hadronic current due to the transformation of quark fields from the gauge eigenstates (unprimed) to the mass eigenstates (primed). The values of the CKM matrix elements are of prime interest, and we discuss their current values and the ways in which they are extracted in the next section.

The coupling constant g is related to the Fermi coupling constant, G_F , (which describes the four-point coupling of the weak interaction) by

$$g^2 = \frac{8}{\sqrt{2}}G_F m_W^2,$$

where m_W is the W -boson mass. The leptonic charged current has a form that is very similar to that of the hadronic current but without the CKM matrix elements. However, recent experimental discoveries of neutrino oscillation indicate that neutrinos might have tiny masses. If that is the case, the leptonic sector of the SM will have to be modified and a similar mixing matrix will be present in the model. Extensive research is being carried out to incorporate neutrino masses into the SM, and to determine whether the neutrinos are Dirac or Majorana spinors. In the present work we will ignore the tiny mass of neutrinos and use the well-established form of the leptonic current without the mixing matrix elements for neutrinos.

1.1.2 The CKM matrix

The CKM matrix is a quark mixing matrix and for the case of three families of quarks, it is a 3×3 unitary matrix. To see the matrix explicitly we write the hadronic current in matrix form as

$$J_c^\mu = (\bar{u}' \quad \bar{c}' \quad \bar{t}')_L \gamma_\mu \begin{pmatrix} V_{ud} & V_{us} & V_{ub} \\ V_{cd} & V_{cs} & V_{cb} \\ V_{td} & V_{ts} & V_{tb} \end{pmatrix} \begin{pmatrix} d' \\ s' \\ b' \end{pmatrix}_L,$$

The diagonal matrix elements are the largest, and correspond to mixing within the same family. Mixing becomes smaller as we move away from the diagonal elements, and the mixings between the first and third families, such as V_{ub} , are the smallest.

There are several parametrizations available for this matrix, including the original CKM parametrization. The matrix is described by four independent parameters, namely three mixing angles and a complex phase, as required for a 3×3 unitary matrix. A non-vanishing value for the complex phase implies CP violation within the SM.

It is very important to determine the values of the CKM matrix elements with high precision. Uncertainties in these parameters reduce the predictive power of the SM and our ability to test it. Semileptonic decays have been the main means of measuring these matrix elements. Both theoretical and experimental expertise are essential for precise extraction of the matrix elements. Their current absolute magnitudes and uncertainties as described in the *Review of Particle Properties* [5] are

$$V_{CKM} = \begin{pmatrix} 0.974 \sim 0.975 & 0.221 \sim 0.227 & 0.003 \sim 0.0045 \\ 0.221 \sim 0.227 & 0.973 \sim 0.974 & 0.039 \sim 0.044 \\ 0.005 \sim 0.014 & 0.039 \sim 0.43 & 0.999 \sim 0.9992 \end{pmatrix} \quad (1.3)$$

Not all the values of the matrix elements presented are extracted by direct experiments, as unitarity of the CKM matrix has been used to obtain the tightest bounds on some of the elements. Our present knowledge of the matrix elements comes from the following sources[5]:

1. $|V_{ud}|$: The analysis of nuclear beta decay has been used to extract a value for $|V_{ud}|$, and the current world average is

$$|V_{ud}| = 0.9738 \pm 0.0005.$$

The theoretical uncertainties in extracting a value for $|V_{ud}|$ from neutron beta decay are significantly smaller than for decays of mirror nuclei, but the value depends on both the value of g_A/g_V and the neutron lifetime.

2. $|V_{us}|$: The original analysis of K_{e3} decays yields

$$|V_{us}| = 0.2196 \pm 0.0023.$$

The notation K_{e3} refers to the decay of a kaon semileptonically to a pion, an electron, and a neutrino, with a total of three particles in the final state.

The values of $|V_{us}|$ extracted from two K_{e3} ($K_L^0 \rightarrow \pi^\pm e^\mp \nu_e$, $K^+ \rightarrow \pi^0 e^+ \nu_e$) decays can be brought into agreement at the 1% level of accuracy. A new measurement of the K^+ semileptonic branching ratio indicates a higher value for this quantity. The PDG [5] average of the new results with the older one is

$$|V_{us}| = 0.220 \pm 0.0026.$$

3. $|V_{cd}|$: The value of $|V_{cd}|$ can be extracted from neutrino and antineutrino production of charmed quarks off valence ‘d’ quarks. The dimuon production cross sections of the CDHS group [6] yield $\overline{B}_c |V_{cd}|^2 = (0.41 \pm 0.07) \times 10^{-2}$, where \overline{B}_c is the semileptonic branching fraction of the charmed hadron produced. A more recent value from the CCFR collaboration at FNAL [7] is $\overline{B}_c |V_{cd}|^2 = (0.534 \pm 0.046) \times 10^{-2}$. Averaging these two results and supplementing this data with measurements of the semileptonic branching fraction of the charmed meson to give $\overline{B}_c = 0.0923 \pm 0.0073$ yields

$$|V_{cd}| = 0.224 \pm 0.012.$$

4. $|V_{cs}|$: Neutrino production of charm and semileptonic D decays were used to obtain values for $|V_{cs}|$. Recently these values have been superseded by direct measurements [8] of $|V_{cs}|$ in charmed W decays that give $|V_{cs}| = 0.97 \pm 0.09(\text{stat}) \pm 0.07(\text{syst})$. The constraint of unitarity gives a much tighter bound.
5. $|V_{cb}|$: HQET [9, 10] provides a nearly model-independent description of the B meson decaying semileptonically to charmed mesons. Measurements of the exclusive decay $B \rightarrow \bar{D}^* \ell^+ \nu_\ell$ have been used to extract a value of $|V_{cb}|$. Analysis of inclusive semileptonic bottom hadron decays is also used to extract a value of this matrix element. A more detailed discussion can be found in the *Review of Particle Physics* [11]. The average of exclusive and inclusive results gives

$$|V_{cb}| = 0.041 \pm 0.015.$$

6. $|V_{ub}|$: In the semileptonic decays of B mesons the decays $b \rightarrow u \ell^+ \bar{\nu}_\ell$ can be observed by measuring the lepton energy spectrum above the endpoint of the bottom to charm decay spectrum. The interpretation of this inclusive $b \rightarrow u \ell^+ \bar{\nu}_\ell$ decay in terms of $|V_{ub}|$ depends fairly strongly on the theoretical model used to generate the lepton energy spectrum. At LEP, the separation between u -like and c -like decays is based on up to twenty different event parameters, and it requires a detailed understanding of the decay $b \rightarrow c \ell^+ \bar{\nu}_\ell$. Exclusive semileptonic decays, such as, $B \rightarrow \pi \ell^+ \bar{\nu}_\ell$ can also be used to extract a value for $|V_{ub}|$, but there is an associated model dependence in the values of the hadronic matrix elements of the weak current [12].

The average of the inclusive and exclusive result of $|V_{ub}|$, in which the uncertainties are dominated by theoretical uncertainties, is

$$|V_{ub}| = (3.67 \pm 0.47) \times 10^{-3}.$$

7. $|V_{tb}|$: The discovery of the top quark by the CDF and D0 collaborations utilized in part the semileptonic decays of t to b . The CDF experiment has published a limit on the fraction $t \rightarrow b \ell^+ \nu_\ell$, of [13]

$$\frac{|V_{tb}|^2}{|V_{td}|^2 + |V_{ts}|^2 + |V_{tb}|^2} = 0.94_{-0.24}^{+0.31}.$$

The above discussion clarifies the pivotal role of semileptonic decay processes in the extraction of the CKM matrix elements. We also note that in some matrix elements the current uncertainties are still large, so there remains the necessity of improvement in both the experimental and theoretical sectors. In later sections, we will discuss the complementary role that baryon semileptonic decays can play in the extraction of CKM matrix elements.

1.2 Quark model and QCD

1.2.1 The Origins of the Quark Model

From a historical perspective, quarks were proposed as the fundamental constituents of hadrons and were discovered before QCD, the gauge theory that describes the interaction between quarks and the way they are bound inside a hadron. The large number of newly discovered particles in the 1950's gave rise to the necessity of a classification scheme. One of the most successful proposals was the 'Eight-fold Way' proposed by Gell-Mann and Ne'eman [14] which was based on the flavor group $SU(3)_f$. This classification scheme grouped the hadrons into representation of this symmetry group. Mesons were described in the singlet and octet representations and baryons fit into an octet and decuplet. The most notable achievement of this symmetry scheme was the successful prediction of the Ω^- baryon to complete the baryon decuplet.

The success of this model soon led Zweig [15] and Gell-Mann [16] to propose a quark model for the underlying structure of hadrons. In 1964 they both independently proposed that hadrons are made up of constituents, Zweig named them 'aces' while Gell-Mann called them 'quarks'. These constituents, quarks, are spin- $\frac{1}{2}$ objects with fractional charge. Quarks in this model are in the fundamental representation of $SU(3)_f$, denoted by $\mathbf{3}$, and come in three flavors, up (u), down (d) and strange (s). The meson and baryon groupings are now seen as being built up by direct products of $\mathbf{3}$ and its conjugate $\bar{\mathbf{3}}$ (representing the antiquarks),

$$\begin{aligned}\mathbf{3} \times \bar{\mathbf{3}} &= \mathbf{1} \oplus \mathbf{8}, \\ \mathbf{3} \times \mathbf{3} \times \mathbf{3} &= \mathbf{1} \oplus \mathbf{8} \oplus \mathbf{8} \oplus \mathbf{10}.\end{aligned}$$

This quark model was also extended to an $SU(6)$ symmetry assuming that the strong interactions are not only flavor independent but also independent of quark spin. Then quarks are grouped in a $\mathbf{6}$ of $SU(6)$ and baryons appear in $SU(6)$ supermultiplets made up of $\mathbf{6} \times \mathbf{6} \times \mathbf{6}$.

However, despite all of its successes, this naive constituent quark model does not provide an explanation of why quarks only appeared in states like $q\bar{q}$ and qqq but not, for example, in the qq state.

1.2.2 Color and QCD

The concept of color was first introduced to explain the required symmetry property of certain baryons, particularly the $\Delta^{++}(1232)$. In the naive quark model, the ground state Δ^{++} consists of three u quarks with a spin and parity of $J^P = 3/2^+$. When combined with an orbital angular momentum zero, exchange symmetric, spatial wave function, the result is a state completely symmetric under the exchange of any pair of quarks. This violates the spin-statistic theorem, or generalized Pauli principle, since quarks are fermions. As a solution to this problem Greenberg [17], Nambu and Han [18] proposed that quarks had an additional internal degree of freedom, which was later called color. A quark can have one of three different colors, usually denoted red, green and blue, and it transforms as the fundamental representation $\mathbf{3}$ of the group $SU(3)$ of color. The spin-statistics problem was resolved by assuming an anti-symmetric color wave function for the baryon. This color symmetry group could also be used to explain the lack of quark states other than $q\bar{q}$ and qqq , by postulating that only color singlet (antisymmetric) states of quarks are present in nature. The color concept was also successful in explaining other phenomena known at the time. For example the factor of nine discrepancy between theory and experiment in the electromagnetic decay of the pion, $\pi^0 \rightarrow \gamma\gamma$, was resolved by taking into account the three colors of quarks [19].

The success of the color hypothesis was the beginning of the idea that there was a color-dependent force between the quarks which bind them together to form a hadron. A Lagrangian which is locally invariant under the non-Abelian symmetry group $SU(3)_c$ was proposed to describe the strong interaction. The strong interaction could then be put in the same framework as the electroweak interaction by extending the GSW model of the symmetry group $SU(2)_w \times U(1)_y$ to include the $SU(3)_c$ group as another direct product. As mentioned before, the extended Standard Model is described by a Lagrangian invariant

under the gauge symmetry group $SU(3)_c \times SU(2)_w \times U(1)_y$.

The theory of the color-dependent strong force between quarks is known as Quantum Chromodynamics (QCD), in analogy with Quantum Electrodynamics (which describes the charge dependent electromagnetic force). The forces between the colored quarks are mediated by eight massless vector bosons known as gluons, one for each generator of the $SU(3)_c$ gauge group. The QCD Lagrangian density for quark of mass m is of the form

$$\mathcal{L}_{QCD} = \bar{\psi}(i\gamma^\mu D_\mu - m)\psi - \frac{1}{4}(F_{\mu\nu}^i)^2, \quad (1.4)$$

where

$$\begin{aligned} D_\mu &= \partial_\mu - ig_s A_\mu^i \frac{\lambda_i}{2}, \\ F_{\mu\nu}^i &= \partial_\mu A_\nu^i - \partial_\nu A_\mu^i + g_s f^{ijk} A_\mu^j A_\nu^k. \end{aligned}$$

The λ_i are the three dimensional Gell-Mann representation of the generators and f^{ijk} are the structure constants of $SU(3)_c$. The A_μ^i are the gauge fields for gluons, and g_s is the strong coupling constant. We note here that when \mathcal{L}_{QCD} is embedded in the SM there is no mass term in the Lagrangian, and quark masses are generated by SSB within the SM.

In the renormalized theory of QED the coupling ($\alpha = e^2/4\pi$) is replaced by an running coupling constant $\alpha(Q^2)$, which gives the Q^2 dependence of the renormalized vertex function. The contributions to this vertex function come from all possible vacuum polarization graphs which describe the charged lepton loop corrections to the photon propagator. The effective coupling constant of QED is of the form

$$\alpha(Q^2) = \frac{\alpha(\mu^2)}{1 - \frac{\alpha(\mu^2)}{3\pi} \ln(\frac{Q^2}{\mu^2})}. \quad (1.5)$$

where μ^2 is the renormalization point. The important point to note about this coupling constant is that it increases with Q^2 .

In QCD the analogous calculation is complicated by gluon self couplings. However, the leading logarithm contribution to the effective quark-gluon vertex can be summed to all orders in g_s . The renormalization group analysis for QCD leads to

$$\alpha_s(Q^2) = \frac{\alpha_s(\mu^2)}{1 + \frac{\alpha_s(\mu^2)}{2\pi} (11 - 2/3N_f) \ln(\frac{Q^2}{\mu^2})},$$

for the running coupling constant for QCD. After some manipulations this can be written in terms of a parameter with the dimension of energy, called Λ_{QCD}

$$\alpha_s(Q^2) = \frac{12\pi}{(33 - 2N_f) \ln(\frac{Q^2}{\Lambda_{QCD}^2})}, \quad (1.6)$$

where, N_f is the number of quark flavors with masses below $\sqrt{Q^2}$. If Λ_{QCD} is known, then QCD is entirely defined by Eqs. (1.4) and (1.6). The value for Λ_{QCD} obtained by measuring α_s and Q^2 is between 100 and 400 MeV.

For $N_f < 16$ we see from Eq. (1.6) that at large Q^2 or at short distances the effective quark gluon coupling goes to zero. This property of QCD is known as ‘asymptotic freedom’ and was first proposed in 1973 by Gross, Wilczek [20] and Politzer [21]. As recognition for this revolutionary work they received the Nobel Prize in 2004. At short distances or at high Q^2 quarks behave like free particles. However as $Q^2 \rightarrow 0$, for Q^2 of the order of Λ_{QCD}^2 , the effective coupling constant, α_s is no longer small and a perturbative picture breaks down. We also note that quarks are bound within hadrons, as the coupling increases with distance. The failure of perturbative approach at the hadronic scale and the limited success of non-perturbative techniques has made it difficult for us to arrive at an understanding of the confinement of quarks from first principles. It is one of the outstanding problems of modern theoretical physics that this non-perturbative property of QCD has not yet been established.

1.2.3 The Constituent Quark Model and the Baryon Spectrum

In 1964 Dalitz and Greenberg [22] and their collaborators used a Breit-Fermi type potential model to calculate the masses of non-strange negative parity baryons. A different approach where the strengths of the potential terms were described by the non-relativistic reduction of one-gluon exchange amplitude, was taken by de Rujula, Georgi and Glashow [23] and the MIT group. Isgur and Karl [24, 25] put the two approaches to baryon spectroscopy together. In their model for the low-lying negative-parity baryons they solved a three body problem in a harmonic long-range confining potential, with a one-gluon exchange potential at short range. Both the contact and tensor parts of the spin dependent forces were included, but in contrast to the model by Dalitz and Greenberg, the spin-orbit potential was left out in the Isgur-Karl model.

This model was quite successful in predicting the low-lying negative-parity baryon masses. It verified that the short distance behavior of quarks in baryons is dominated by one-gluon-exchange effects, and established that the confining potential between a pair of quarks is

independent of quark masses. However, it did not explain the reasons for the importance of the contact force, nor did it explain the reason for the negligible spin-orbit force. A partial explanation to the second concern was given by Isgur and Karl [24, 25], along with other authors [26] by noting that the source of spin-orbit coupling was not only the one-gluon exchange but it could also arise from the Thomas precession of the quark spins in a confining potential. They showed that these two contributions came with opposite signs and result in an almost complete cancellation of the spin-orbit terms.

Isgur and Karl [27] then extended their analysis to the low-lying positive-parity baryons. In their analysis they introduced non-harmonic potential terms to correspond to the expected Coulomb plus linear nature of confinement. This model showed an impressive agreement for the masses of a large number of ground and excited baryon states. Their work has been extended to include the spectroscopy of other baryons such as the strange and charmed baryons, missing resonances etc., in many subsequent papers [28]. However, there are several shortcomings in the Isgur-Karl model, such as different parameter sets were used for negative and positive-parity excited states, a large value for the coupling α_s was required to fit the contact interaction, etc. The Isgur-Karl model was improved by Capstick and Isgur [29]. A few successes of the Capstick and Isgur model are that it used a single set of parameters for all baryon states, the model was expanded in a large harmonic oscillator basis, and it had a smaller value for α_s .

In our project we use a model which is very similar to the model to the Capstick and Isgur, but with a few simplifications, to obtain the baryon spectrum. We discuss our model in Section 3.3.

1.3 Semileptonic Decay

Semileptonic decays have been of interest to the physics community ever since neutron beta decay was first observed. This particular type of weak decay process played a crucial role in the development of our understanding of particle physics. The massless and neutral neutrinos were first predicted by Pauli [30] to describe the end point energy-momentum spectrum of the electron in the beta decay. Neutrinos were discovered later [31] and have continued to receive a lot of attention from particle-, nuclear- and astro-physicists.

Semileptonic decay is a flavor changing weak decay process which involves the CKM matrix elements. These matrix elements have not been determined with the precision

necessary for a detailed testing of the SM. Very precise knowledge of these matrix elements is important as they play a crucial role in the search for answers to some fundamental questions, such as the nature of CP violation and the unitarity of the CKM matrix. Semileptonic decays of hadrons have been, and will continue to be, the main source of information on the CKM matrix elements. The precision with which the CKM matrix elements are extracted from these semileptonic decays is strongly dependent on how well the form factors that describe the matrix elements of the hadronic currents are known. The vast literature on these form factors is a testament to the importance of these parameters.

In addition to their importance for the extraction of CKM matrix elements, semileptonic decays can provide information that will increase our understanding of the structure of hadrons in the non-perturbative region. Furthermore, knowledge of the semileptonic decay of hadrons has impacts on other decay modes of the same hadron. As an example, knowledge of the branching fraction for the semileptonic decay $\Lambda_c \rightarrow \Lambda^* e \nu_e$ is necessary to normalize all other decay modes of Λ_c [32].

In semileptonic decays a hadron decays weakly into another hadron with the emission of a lepton and a neutrino, and a detailed understanding of these processes necessitates an understanding of the interesting interplay between the weak and the strong interactions. A Feynman diagram representing the semileptonic decay of a baryon B_Q made up of quarks $q_1 q_2 Q$ into a baryon B_q with quarks $q_1 q_2 q$ is shown in Figure 1.1.

The transition matrix element for this decay is

$$T = \frac{G_F}{\sqrt{2}} V_{qQ} J_\mu L^\mu,$$

where $J_\mu = \bar{q} \gamma_\mu (1 - \gamma_5) Q$ is the flavor changing hadronic current and $L^\mu = \bar{\ell} \gamma^\mu (1 - \gamma_5) \nu_\ell$ is the leptonic current. We know that isolated quarks have never been found, so it is necessary to take the matrix element of the hadronic current between the initial and final baryons, B_Q and B_q respectively. Thus, we are interested in

$$H_\mu = \langle B_q | \bar{q} \gamma_\mu (1 - \gamma_5) Q | B_Q \rangle \equiv \langle B_q | V_\mu - A_\mu | B_Q \rangle,$$

where $V_\mu \equiv \bar{q} \gamma_\mu Q$ and $A_\mu \equiv \bar{q} \gamma_\mu \gamma_5 Q$, are the vector and the axial vector weak current respectively. The leptonic current of the semileptonic decay can be calculated from first principles of Quantum mechanics but the hadronic matrix element, H_μ , is not. Several

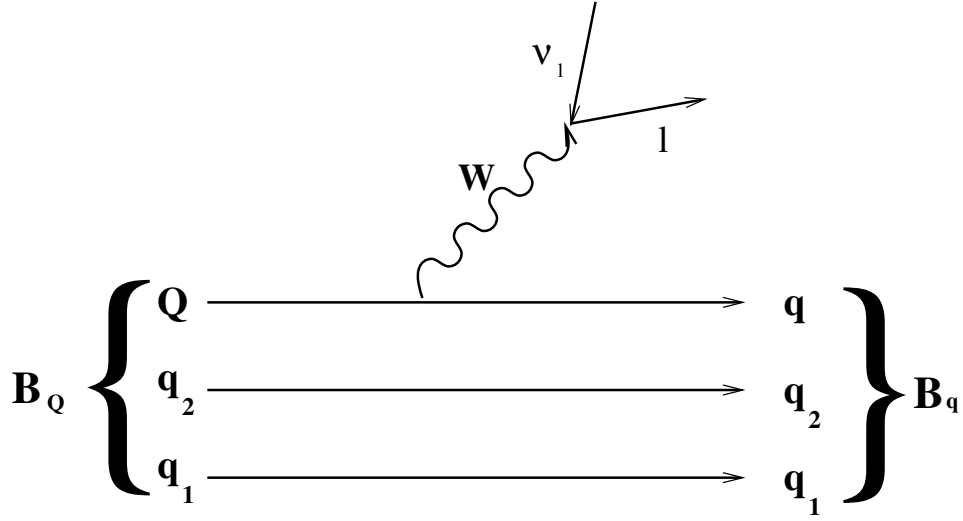


Figure 1.1: Baryon semileptonic decay: $B_Q \rightarrow B_q \ell \nu_\ell$.

models and approximation schemes have been used to describe the hadronic matrix element in semileptonic decay, but so far no first principles calculation has been carried out.

The hadronic matrix element of a semileptonic decay process cannot be calculated from first principles because of the non-perturbative nature of QCD. However, the matrix element of the vector current, V_μ , must be a vector, and can only be expressed in terms of the initial and final hadron momenta and γ_μ for baryon decay. It is usually expressed in terms of unknown Lorentz invariant form factors. For example, the matrix element of V_μ for transitions between ground state ($J^P = 1/2^+$) baryons is written as

$$\langle B_q(p', s') | V_\mu | A_Q(p, s) \rangle = \bar{u}(p', s') \left(F_1(q^2) \gamma_\mu + F_2(q^2) \frac{p_\mu}{m_A} + F_3(q^2) \frac{p'_\mu}{m_B} \right) u(p, s),$$

where the F_i are known as the vector form factors for baryons, $p(p')$ and $s(s')$ are the momentum and spin of the initial (final) baryon, and $q^2 = (p - p')^2$ is the momentum transfer squared between the initial and final baryon. The matrix element of the axial-vector current, A_μ , can be expressed in terms of axial-vector form factors in a similar manner.

The discussion of semileptonic decay of baryons will be extended in later sections of this chapter. In the next section we will give a brief overview of heavy quark effective theory (HQET) which has important implications for semileptonic decays of heavy hadrons.

1.4 Heavy Quark Effective Theory

The strong interactions of hadrons containing a heavy quark are easier to understand than those of hadrons containing only light quarks. This is because the presence of the heavy quark in a hadron leads to two additional symmetries. These two symmetries are the heavy quark flavor symmetry, and the heavy-quark spin symmetry. It is important to emphasize that these are not symmetries of the Lagrangian of QCD, but rather symmetries of an effective theory which is a good approximation to QCD in a certain kinematic region. These heavy quark symmetries were first pointed out by Isgur and Wise [9].

The heavy quark symmetries have a close analog in the familiar properties of atoms. To a good approximation the electronic wave functions of atoms are independent of the mass of the nucleus, meaning that different isotopes of the same nuclei have the same chemical properties. In addition the hyperfine levels in atoms are nearly degenerate, indicating that these levels are largely independent of the spin of the atomic nucleus. In hadronic systems containing a heavy quark, similar things happen.

When the mass of a quark Q , m_Q , is much larger than the QCD scale, $m_Q \gg \Lambda_{QCD}$, the quark Q can be thought of as a heavy quark. This heavy quark is surrounded by a complicated, strongly interacting cloud of light quarks, antiquarks and gluons, sometimes termed the ‘brown muck’. As $m_Q \rightarrow \infty$, the heavy quark and the hadron that contains it have the same velocity: in the hadron’s rest frame the heavy quark is also at rest. In this limit two new symmetries beyond those usually associated with QCD arise. These are the flavor symmetry and the spin symmetry of the heavy quark mentioned earlier.

In a heavy hadron the spin of the heavy quark and that of the light quark system decouple, so that the light quark system is blind to the spin orientation of the heavy quark. The spectrum of the hadron is determined largely by the light degrees of freedom, and is largely independent of the heavy quark spin. This phenomenon constitutes the spin symmetry of the heavy quark. One consequence of this is the existence of nearly-degenerate multiplets of states. For example, in a baryon comprised of a light diquark and a heavy quark, if the light diquark has spin one, then the spin symmetry implies that there are two degenerate states, one with $J = 1/2$ and the other with $J = 3/2$. The analogous observation in an atomic system is that the hydrogen spectrum is largely independent of the spin of the proton.

The other important symmetry of the heavy quark is the flavor symmetry. The spectra

of heavy hadrons are independent of the flavor of the heavy quark contained in the hadron. This means that the spectrum of, say Λ_b baryons containing a bottom quark will be similar to that of Λ_c baryons that contain a charm quark. For a particular excited state, we expect $M_{\Lambda_b^*} - M_{\Lambda_b} = M_{\Lambda_c^*} - M_{\Lambda_c}$ in the limit of infinitely heavy b and c quarks. Here Λ_c and Λ_b are the ground state baryons, Λ_c^* denotes an excited charmed baryon, and Λ_b^* denotes its b -flavored analog. This flavor symmetry would allow us to predict the spectrum of excited b -hadrons, if the corresponding spectrum of excited charmed hadrons is known.

1.5 HQET and Semileptonic Decays

The heavy quark symmetries discussed in the last section have important consequences for the description of strong interactions, including the hadronic currents that contribute to semileptonic decays. Even though these extra symmetries do not allow us to explicitly deduce the detailed structure of hadronic systems, they provide important relations among and constraints on the properties of heavy hadrons. The description of these symmetries has been formalized into the heavy quark effective theory (HQET). This effective theory provides a framework within which calculations of matrix elements for different phenomena can be carried out in a systematic expansion in $1/m_Q$.

Weak decays of hadrons involving one or more heavy quarks ($m_Q \gg \Lambda_{QCD}$) have an additional symmetry in the effective Lagrangian which was first pointed out by Isgur and Wise [9]. There, they used the additional heavy quark symmetry to obtain normalized, model-independent predictions for all the form factors for the decays of heavy hadrons to daughter hadrons that are also heavy. This led to many subsequent calculations by many authors.

For the hadronic matrix elements of the electroweak currents between two heavy mesons, the application of HQET provides a number of features that simplify the extraction of CKM matrix elements from such decays. First, the number of form factors is reduced, so that the six form factors that describe the decays of heavy pseudoscalar mesons to heavy pseudoscalar and vector mesons are replaced by a single form factor, at leading order in HQET. This form factor has become known as the Isgur-Wise function. Second, the absolute normalization of this form factor at the so-called non-recoil point is known. Third, corrections to this normalization do not arise at order $1/m_Q$ in the heavy quark expansion, but at order $1/m_Q^2$. This is known as Luke's Theorem [10], and is an analog of the Ademollo-Gatto theorem [33].

This means that some predictions made at leading order are more robust than might be expected. Finally, the corrections that do arise can be estimated systematically in the heavy quark expansion. As a result, HQET has become the tool of choice in the extraction of $|V_{cb}|$ [11].

For the semileptonic decays of a heavy meson to a light meson, the predictions of HQET are not quite as powerful: there is no reduction in the number of form factors needed to describe the decay, nor are the normalizations of any of the form factors known. However, the heavy quark symmetry, along with SU(2) or SU(3) flavor symmetry for the light mesons, can be used to relate the form factors for $D \rightarrow \pi$ and $D \rightarrow \rho$ decays, for instance, to those for $B \rightarrow \pi$ and $B \rightarrow \rho$ decays, respectively. Thus, even though it is not as predictive in the decays of heavy to light mesons, there is still a great deal of reliance on HQET for extracting V_{ub} from meson decays.

For the semileptonic decays of a heavy baryon to another heavy baryon, HQET makes predictions that are completely analogous to those made for heavy-to-heavy meson decays: (i) the six form factors that describe the decays to the ground-state heavy baryons are replaced by fewer form factors, also called Isgur-Wise functions; (ii) the normalization of at least one of the Isgur-Wise function is known at the non-recoil point; (iii) corrections to this normalization first appear at order $1/m_Q^2$; (iv) corrections can be systematically estimated in a $1/m_Q$ expansion. Note that in the case of baryons, the number of Isgur-Wise functions needed at leading order depends on the flavor-spin structure of the parent and daughter baryons.

In the case of a heavy baryon decaying to a light baryon, HQET makes predictions that are not as powerful as in the heavy-to-heavy case, but which are significantly more powerful than for the heavy-to-light transitions of mesons. Among the baryons, the leading-order prediction is that the number of independent form factors decreases from six to two in the case of Λ_Q decays, or four in the case of Ω_Q decays. In addition, as with mesons, the heavy quark symmetry can be used to relate the form factors for the decay $\Lambda_c^+ \rightarrow n$ to those for $\Lambda_b \rightarrow p$, for instance. This, in principle, could facilitate the extraction of V_{ub} from semileptonic decays of the Λ_b , and since the number of unknown form factors is reduced from six to two, the theoretical uncertainty in the extraction from these decays should be significantly smaller than extractions from meson decays.

While HQET has been tremendously successful and useful in treating semileptonic decays

of heavy hadrons, it is not without its limitations. It is a limit of QCD that applies only to hadrons containing heavy quarks. For the decays of such hadrons, it only predicts the relationships among form factors, not their kinematic dependence; ansätze, models of one kind or another, or lattice simulations, are still needed for this. In addition, the predictions of HQET are valid only as long as the energy of the daughter hadron is not comparable to the mass of the heavy quark. For heavy to heavy decays, this means that the predictions are valid for all of the available phase space, but for heavy to light decays, such as $B \rightarrow \pi$, a large portion of the available phase space is beyond the region of reliable applicability of HQET. These limitations mean that the predictions of HQET must be complemented/supplemented by information arising from other approaches to hadron structure.

1.6 Existing Models of Semileptonic Decay

The semileptonic decays of heavy mesons have been studied extensively in the last two decades. Wirbel, Stech and Bauer [34, 35] assumed monopole type form factors for the decays of heavy mesons. In Ref. [36, 37], a non-relativistic quark model (NRQM) was used to treat the semileptonic decays of B and D mesons, and relatively simple forms for the form factors were presented. The first of those articles, along with the work of Shifman and Voloshin [38], ultimately lead to the development of the heavy quark effective theory (HQET). In addition, Ivanov and Santorelli [39] used a relativistic quark model to find the form factors. These are just a very few of the very large number of articles that treat semileptonic decays of mesons in some kind of model.

While some work has been done in modeling the form factors for the semileptonic decays of heavy baryons, to the best of our knowledge little has been done in treating the decays to excited baryons. Predictions for the number of independent form factors for decays to excited states have been made in the framework of HQET [40], and Leibovich and Stewart [41] have examined the form factors for decays to the $1/2^-$ and $3/2^-$ ll_q states, using large N_c arguments. In the semileptonic decays of B mesons to those with charm, it is known that B^0 decays to the ground state pseudoscalar and vector mesons provide only about 75% of the total semileptonic decay rate, while for the B^\pm , the corresponding fraction is about 85%. Any assumption that decay of a heavy baryon to the ground state will saturate the semileptonic decay rate is therefore subject to potentially large corrections.

In some of the work done in this area, the predictions of HQET, along with various ansätze

for the form factors, have been used to estimate some decay rates. Leibovich and Stewart [41] follow such a procedure to estimate the rates for decays of the Λ_b to the $J^P = 1/2^-$ and $3/2^-$ Λ_c states. Polarization effects in semileptonic Λ_b and Λ_c decays have been studied by Körner and Krämer [42], using the predictions of HQET to estimate the dominant form factors for both $b \rightarrow c$ and $c \rightarrow s$ transitions. They have also calculated the asymmetry parameters that characterize the angular dependence of the decay distributions.

A number of authors have constructed explicit quark models of the form factors for the decays of Λ_Q baryons to ground state baryons. The decays of Λ_b and Ω_b have been treated by Singleton using a spectator quark model [43]. He also discusses the polarization of the W boson and the daughter baryon in these processes. Albertus *et al.* [44] use a NRQM to evaluate the form factors for $\Lambda_b \rightarrow \Lambda_c$, explicitly applying heavy quark symmetry to their trial wave functions. To date, there appear to be only two lattice studies of the semileptonic decays of heavy baryons. A first study of Λ_b and Ξ_b semileptonic decays was made by Bowler *et al.* [45], while Gottlieb and Tamhankar [46] have examined the decay of the Λ_b . Pérez-Marcial and collaborators [47] have studied the semileptonic decays of a number of charmed baryons, both in a non-relativistic quark model and in the MIT bag model. There have been light-front calculations [48], as well as ones using sum rules [49], Bethe-Salpeter formalisms [50], bag models [51], and quark model calculations [52]. Large N_c arguments have also been applied to these form factors [53], as well as perturbative QCD arguments [54]. For the decays of a heavy baryon to a light one, work has been done using QCD sum rules [55], and there's one quark model calculation [56] apart from the work of Scora [57], to the best of our knowledge. For the decays of Ω_Q baryons, the literature is very scant [58].

1.6.1 Experimental Status of Heavy Baryon Semileptonic Decays

The experimental status of heavy baryon semileptonic decays is somewhat rudimentary. The semileptonic decay rate for $\Lambda_c \rightarrow \Lambda$ has been measured by the CLEO and Argus collaborations [59, 60], while the Delphi collaboration has only recently published an analysis of the exclusive semileptonic decay of the Λ_b [61]. Prior to this, only the inclusive semileptonic branching fraction $\Lambda_b \rightarrow \Lambda_c \ell \nu X$ had been reported in the PDG [5]. In their analysis of the $\Lambda_c \rightarrow \Lambda$ semileptonic decay, the CLEO collaboration have assumed that the ground state Λ saturates the semileptonic decays of the Λ_c , and cite the absence of any final states of the form $\Lambda \ell \nu$ with additional decay products from the Λ_c to support their assumption [60]. No

experiments have yet reported results for the decay $\Lambda_c \rightarrow n$, while Ω_c semileptonic decays have been reported as ‘seen’.

The major difficulty in the baryon sector is that there is no source of heavy baryons as there is for mesons. Electron-positron colliders have produced billions of B mesons, utilizing the fact that the $\Upsilon(4s)$ is just above the $B\bar{B}$ threshold. In principle, a similar abundance can be duplicated among D mesons, by using the $\Psi(3s)$. With baryons, production at such machines will be continuum production, as there are no (known) resonances to enhance the rate of production. Hadron colliders can provide larger yields, but they provide large yields of everything, and the heavy baryons will then have to be separated from everything else that is produced. However, the recent CLEO measurement suggests that some optimism regarding the future measurement of these decays might be warranted. In addition, there might be prospects for such studies at Jefferson Laboratory upgraded to 12 GeV or higher, or at E907 at FNAL. The advantage in these cases is that the target will be a baryon, unlike the continuum production of e^+e^- machines.

1.7 Motivation

In this dissertation we study the semileptonic decay of two types of heavy baryons, namely Λ_Q and Ω_Q . Our first motivation is the importance of the CKM matrix elements V_{ub} and V_{cb} , and the fact that baryon semileptonic decays can provide complementary extractions of these quantities, despite the difficulties mentioned above. In particular, a model such as ours, coupled with constraints provided by HQET, may lead to a more precise extraction of V_{ub} than provided by meson decays.

Our second motivation is to examine the predictions for these decays of a quark model developed very much in the spirit of the work by Capstick and Isgur [29], which builds on the work of Isgur and Karl [24, 25]. Such a model has been applied, with some success, to the strong [62] and electromagnetic [63, 64] couplings of baryons, and the semileptonic decays of baryons is a useful complementary extension of such a model. Indeed, a similar model, applied to the semileptonic decays of mesons [36], gave rise to HQET. We note that the thesis of Scora [57] treats a number of baryon semileptonic decays in a framework very similar to that used in the treatment of mesons in [36]. We use a similar framework, but we extend the model to examine the decays to excited baryons, whereas Scora [57] examined only decays to ground state baryons. We also use a more sophisticated treatment of baryon

structure.

The dissertation is organized as follows: in Chapter II we discuss the hadronic matrix elements and decay rates, and provide a brief outline of HQET predictions for the relationships between semileptonic form factors as they relate to the decays that we discuss. In Chapter III we describe the model we use to obtain the form factors, including some description of the Hamiltonian. We also discuss briefly the procedure to obtain the form factors analytically within the quark models we use for various decay modes. The comparison of our analytic results with HQET predictions are discussed in Chapter IV. Our numerical results, including the parameters of the quark model, the values of some of the form factors at the non-recoil point, predictions for the semileptonic decay rates and estimates of branching fractions, as well as comparisons with experimental results where available, are given in Chapter V. Chapter VI presents our conclusions and outlook. A number of details of the calculation, including the explicit expressions for the form factors, are shown in a number of Appendices.

CHAPTER 2

Matrix Elements, Decay rates and HQET

2.1 Matrix Elements

The transition matrix element for semileptonic decay of any baryon B_Q , ($B_Q \rightarrow B_q \ell \nu_\ell$) where B_Q can be either a Λ_Q or Ω_Q and B_q can be a Λ_q , a nucleon, an Ω_q , or a Ξ , is

$$T = \frac{G_F}{\sqrt{2}} V_{Qq} \bar{u}_\ell \gamma^\mu (1 - \gamma_5) u_{\nu_\ell} \langle B_q(p', s') | J_\mu | B_Q(p, s) \rangle, \quad (2.1)$$

where $G_F/\sqrt{2} = g^2/(8M_W^2)$ is the Fermi coupling constant, M_W is the intermediate vector boson mass, V_{Qq} is the CKM matrix element, and $\bar{u}_\ell \gamma^\mu (1 - \gamma_5) u_{\nu_\ell}$ is the lepton current. Since quarks are confined, the matrix element of the hadron current is described in terms of a number of form factors. We will build a model of the baryons we wish to study, and obtain approximations to the form factors that describe the hadronic matrix elements.

For transitions between ground state ($J^P = 1/2^+$) baryons, the hadronic matrix elements of the vector and axial currents are

$$\langle B_q(p', s') | V_\mu | B_Q(p, s) \rangle = \bar{u}(p', s') \left(F_1(q^2) \gamma_\mu + F_2(q^2) \frac{p_\mu}{m_{B_Q}} + F_3(q^2) \frac{p'_\mu}{m_{B_q}} \right) u(p, s), \quad (2.2)$$

$$\langle B_q(p', s') | A_\mu | B_Q(p, s) \rangle = \bar{u}(p', s') \left(G_1(q^2) \gamma_\mu + G_2(q^2) \frac{p_\mu}{m_{B_Q}} + G_3(q^2) \frac{p'_\mu}{m_{B_q}} \right) \gamma_5 u(p, s), \quad (2.3)$$

where the F_i and G_i are form factors which depend on the square of the momentum transfer $q = p - p'$ between the initial and the final baryons. Similarly, the matrix elements for decays to a daughter baryon with $J^P = 3/2^-$ are

$$\begin{aligned} \langle B_q^{3/2}(p', s') | V_\mu | B_Q(p, s) \rangle &= \bar{u}^\alpha(p', s') \left[\frac{p_\alpha}{m_{B_Q}} \left(F_1 \gamma_\mu + F_2 \frac{p_\mu}{m_{B_Q}} + F_3 \frac{p'_\mu}{m_{B_q^{3/2}}} \right) + F_4 g_{\alpha\mu} \right] u(p, s), \\ \langle B_q^{3/2}(p', s') | A_\mu | B_Q(p, s) \rangle &= \bar{u}^\alpha(p', s') \left[\frac{p_\alpha}{m_{B_Q}} \left(G_1 \gamma_\mu + G_2 \frac{p_\mu}{m_{B_Q}} + G_3 \frac{p'_\mu}{m_{B_q^{3/2}}} \right) + G_4 g_{\alpha\mu} \right] \gamma_5 u(p, s). \end{aligned} \quad (2.4)$$

The spinor $\bar{u}^\alpha(p', s')$ satisfies the conditions

$$p'_\alpha \bar{u}^\alpha(p', s') = 0, \quad \bar{u}^\alpha(p', s') \gamma_\alpha = 0, \quad \bar{u}^\alpha(p', s') \not{p}' = m_{B_q^{3/2}} \bar{u}^\alpha(p', s'). \quad (2.5)$$

The corresponding matrix elements for decay to a baryon with $J^P = 5/2^+$ are

$$\begin{aligned} \langle B_q^{5/2}(p', s') | V_\mu | B_Q(p, s) \rangle &= \bar{u}^{\alpha\beta}(p', s') \frac{p_\alpha}{m_{B_Q}} \left[\frac{p_\beta}{m_{B_Q}} \left(F_1 \gamma_\mu + F_2 \frac{p_\mu}{m_{B_Q}} \right. \right. \\ &\quad \left. \left. + F_3 \frac{p'_\mu}{m_{B_q^{5/2}}} \right) + F_4 g_{\beta\mu} \right] u(p, s), \\ \langle B_q^{5/2}(p', s') | A_\mu | B_Q(p, s) \rangle &= \bar{u}^{\alpha\beta}(p', s') \frac{p_\alpha}{m_{B_Q}} \left[\frac{p_\beta}{m_{B_Q}} \left(G_1 \gamma_\mu + G_2 \frac{p_\mu}{m_{B_Q}} \right. \right. \\ &\quad \left. \left. + G_3 \frac{p'_\mu}{m_{B_q^{5/2}}} \right) + G_4 g_{\beta\mu} \right] \gamma_5 u(p, s), \end{aligned}$$

where the spinor $\bar{u}^{\alpha\beta}(p', s')$ is symmetric in the indices α and β , and satisfies

$$\begin{aligned} p'_\alpha \bar{u}^{\alpha\beta}(p', s') &= p'_\beta \bar{u}^{\alpha\beta}(p', s') = 0, \\ \bar{u}^{\alpha\beta}(p', s') \gamma_\alpha &= \bar{u}^{\alpha\beta}(p', s') \gamma_\beta = 0, \\ \bar{u}^{\alpha\beta}(p', s') \not{p}' &= m_{B_q^{5/2}} \bar{u}^{\alpha\beta}(p', s'), \\ \bar{u}^{\alpha\beta}(p', s') g_{\alpha\beta} &= 0. \end{aligned} \quad (2.6)$$

Here we have only presented the form factor equations involving spinors having natural parity. The equations for unnatural parity spinors can be constructed in a similar manner by switching γ_5 from the equations defining the G_i to the equations defining the F_i .

2.2 Decay Rates

The decay rate that arises from any of these matrix elements is

$$d\Gamma = \frac{1}{2m_{B_Q}} \frac{G_F^2}{2} |V_{Qq}|^2 \left(\prod_f \frac{d^3 p_f}{(2\pi)^3 2E_f} \right) L^{\mu\nu} H_{\mu\nu} (2\pi)^4 \delta^{(4)}(p_A - \sum p_f), \quad (2.7)$$

where A refers to the initial hadron. The leptonic tensor $L^{\mu\nu}$ is

$$L^{\mu\nu} = \sum_{\text{spin}} L^{\dagger\nu} L^\mu = 8[p_\ell^\mu p_{\nu_\ell}^\nu + p_{\nu_\ell}^\mu p_\ell^\nu - g^{\mu\nu} p_\ell \cdot p_{\nu_\ell} + i\epsilon^{\mu\nu\alpha\beta} p_{\ell\alpha} p_{\nu_\ell\beta}]. \quad (2.8)$$

The hadronic tensor $H_{\mu\nu}$ is

$$H_{\mu\nu} = \sum_{\text{spin}} \langle B_Q | J_\nu^\dagger | B_q \rangle \langle B_q | J_\mu | B_Q \rangle, \quad (2.9)$$

where B_Q and B_q refer to the initial and final baryons, respectively. The tensor $H_{\mu\nu}$ must have the Lorentz structure

$$\begin{aligned} H_{\mu\nu} \equiv & -\alpha g_{\mu\nu} + \beta_{++}(p+p')_\mu(p+p')_\nu + \beta_{+-}(p+p')_\mu(p-p')_\nu \\ & + \beta_{-+}(p-p')_\mu(p+p')_\nu + \beta_{--}(p-p')_\mu(p-p')_\nu \\ & + i\gamma\epsilon_{\mu\nu\rho\sigma}(p+p')^\rho(p-p')^\sigma, \end{aligned}$$

where the coefficients α , β_{++} , etc., are expressed in terms of the form factors that describe the hadronic matrix element $H_{\mu\nu}$. The complete expression for the differential decay rate is

$$\frac{d^2\Gamma}{dx dy} = \frac{|V_{Qq}|^2 G_F^2 m_{B_Q}^5}{64\pi^3} [\alpha C_\alpha + \beta_{++} C_{\beta_{++}} + \beta_{-+} C_{\beta_{-+}} + \beta_{+-} C_{\beta_{+-}} + \beta_{--} C_{\beta_{--}} + \gamma C_\gamma], \quad (2.10)$$

where

$$\begin{aligned} C_\alpha &= \frac{2}{m_{B_Q}^2} \left(y - \frac{m_\ell^2}{m_{B_Q}^2} \right), \\ C_{\beta_{++}} &= 8 \left[x(2x_m + y) - 2x^2 - y/2 \right] - \frac{m_\ell^2}{m_{B_Q}^2} \left(\frac{m_\ell^2}{m_{B_Q}^2} - \frac{4m_{B_q}^2}{m_{B_Q}^2} - 8x + 3y \right), \\ C_{\beta_{-+}} &= C_{\beta_{+-}} = \frac{m_\ell^2}{m_{B_Q}^2} \left[4(x - x_m) - y - \frac{m_\ell^2}{m_{B_Q}^2} \right], \\ C_{\beta_{--}} &= \frac{m_\ell^2}{m_{B_Q}^2} \left(y - \frac{m_\ell^2}{m_{B_Q}^2} \right), \\ C_\gamma &= \mp 2y \left[2x_m - 4x + y + \frac{m_\ell^2}{m_{B_Q}^2} (2x_m + y) \right]. \end{aligned} \quad (2.11)$$

In these expressions, $x = E_\ell/m_{B_Q}$, where E_ℓ is the lepton energy, $x_m = (m_{B_Q}^2 - m_{B_q}^2)/(2m_{B_Q}^2)$, and $y = q^2/m_{B_Q}^2 = (p-p')^2/m_{B_Q}^2$. The \mp sign in C_γ is determined by the charge of the lepton, with the upper (negative) sign corresponding to decays to $\ell\nu_\ell$. The lepton energy has the range

$$\frac{-K}{2\sqrt{y}} \left(y - \frac{m_\ell^2}{m_{B_Q}^2} \right)^{1/2} + \frac{(2x_m + y)}{4y} \left(y + \frac{m_\ell^2}{m_{B_Q}^2} \right) \leq x \leq \frac{K}{2\sqrt{y}} \left(y - \frac{m_\ell^2}{m_{B_Q}^2} \right)^{1/2} + \frac{(2x_m + y)}{4y} \left(y + \frac{m_\ell^2}{m_{B_Q}^2} \right)$$

with $K = \frac{1}{2}[(2x_m - y)^2 - 4m_{B_q}^2/m_{B_Q}^2]^{1/2}$, and y has the kinematic range $m_\ell^2/m_{B_Q}^2 \leq y \leq (m_{B_Q} - m_{B_q})^2/m_{B_Q}^2$. If the lepton mass is neglected, the terms in β_{+-} , β_{-+} and β_{--} vanish, and the differential decay rate becomes

$$\frac{d^2\Gamma}{dx dy} = \frac{|V_{Qq}|^2 G_F^2 m_{B_Q}^5}{32\pi^3} \left[\frac{\alpha y}{m_{B_Q}^2} + 2\beta_{++} [2x(2x_m + y) - 4x^2 - y] \mp \gamma y (2x_m - 4x + y) \right], \quad (2.12)$$

where the lepton energy is now constrained by $-K/2 + (2x_m + y)/4 \leq x \leq K/2 + (2x_m + y)/4$, and the lower limit on y is zero. In this case the differential rate depends only on α , β_{++} and γ . The explicit expressions for α , β_{++} and γ in terms of form factors for different final baryon spins are given in Appendix D.

2.3 Heavy Quark Effective Theory

2.3.1 Introduction

The heavy quark effective theory [65, 66] has been a very useful tool in the study of electroweak decays of heavy hadrons. This effective theory has been applied to a number of processes, both inclusive and exclusive, to higher and higher order in the $1/m_Q$ expansion, where m_Q is the mass of the heavy quark. In most applications, the aim has been to constrain the hadronic uncertainties in the extraction of CKM matrix elements such as V_{ub} and V_{cb} . In this section, we take a different tack; we examine the predictions of HQET for decays of a heavy Λ or Ω into a number of the allowed excited daughter baryons, whether this daughter baryon is heavy or light, with the aim of comparing these predictions with the form factors that we obtain in our model. We will discuss the predictions for Λ and Ω baryons in separate subsections because the structures of the light quark system spin-flavor wave function are very different in the ground states of these two baryons. In the Λ_Q ground state the light quark system is flavor antisymmetric and the spatial wave function is symmetric so that the spin wave function must also be antisymmetric. This corresponds to spin zero. The Ω_Q ground state has a symmetric flavor wave function for the light diquark, and so has a symmetric spin one wave function.

2.3.2 Structure of States and Parity Considerations

In a heavy excited baryon, the light quark system has some total angular momentum j , so that the total angular momentum of the baryon can be $J = j \pm 1/2$. These two states are degenerate because of the heavy quark spin symmetry. It is useful to show explicitly the representation we use for these two degenerate baryons. In the notation of Falk [67], we write $u_{j+1/2}^{\mu_1 \dots \mu_j}(v') = u^{\mu_1 \dots \mu_j}(v') - u_{j-1/2}^{\mu_1 \dots \mu_j}(v')$, with

$$u^{\mu_1 \dots \mu_j}(v') = A^{\mu_1 \dots \mu_j}(v') u_Q(v'). \quad (2.13)$$

Here, $u_Q(v)$ is the spinor of the heavy quark, with v being the four-velocity and $A^{\mu_1 \dots \mu_j}(v')$ is a tensor that describes the spin- j light quark system. This tensor is symmetric in all of its Lorentz indices, meaning that the $u^{\mu_1 \dots \mu_j}(v')$ is also symmetric in all its Lorentz indices. Both $u_{j\pm 1/2}^{\mu_1 \dots \mu_j}(v')$ satisfy the conditions

$$\begin{aligned} \psi' u^{\mu_1 \dots \mu_j}(v') &= u^{\mu_1 \dots \mu_j}(v'), \\ v'_{\mu_i} u^{\mu_1 \dots \mu_i \dots \mu_j} &= 0, \quad g_{\mu_k \mu_l} u^{\mu_1 \dots \mu_j}(v) = 0, \end{aligned} \quad (2.14)$$

where μ_k and μ_l indicate any pair of the indices $\mu_1 \dots \mu_j$. The state with $J = j + 1/2$ also satisfies

$$\gamma_{\mu_i} u_{j+1/2}^{\mu_1 \dots \mu_i \dots \mu_j} = 0. \quad (2.15)$$

Further details of the structure and properties of these tensors are given in Falk's article [67].

At this point, it is useful to discuss the parity of the states, which is determined by the parity of the light component. A spin- j light quark component with parity $(-1)^j$ is said to have 'natural' parity, unnatural parity otherwise. The natural-parity light quark systems therefore have $j^P = (2n)^+$ or $j^P = (2n+1)^-$, with n a positive integer or zero. The natural-parity light quark systems are represented by tensors, while those with unnatural parity are represented by pseudo-tensors. Since the parity of the baryon is that of the light quark system, we may refer to the baryons as being tensors or pseudo-tensors, with the understanding that this really refers to the light-quark component of the baryon. It is thus convenient to divide the decays we discuss into two classes, those in which the daughter baryons are tensors, and those in which they are pseudo-tensors.

2.3.3 Heavy to Heavy Λ Decay

As outlined above we may divide daughter baryons into two groups, those we call tensors, and those that are pseudo-tensors. The ground state Λ_Q is a tensor and we begin by discussing the tensor decays. In general, we are interested in the matrix element

$$\mathcal{A} = \langle \Lambda_c^*(v', j) | \bar{c} \Gamma b | \Lambda_b(v) \rangle, \quad (2.16)$$

where c and b are the heavy quark fields, and Γ is an arbitrary combination of Dirac matrices. With the use of HQET, we may write this as

$$\langle \Lambda_c^*(v', j) | \bar{c} \Gamma b | \Lambda_b(v) \rangle = \bar{u}^{\mu_1 \dots \mu_j}(v') \Gamma u(v) M_{\mu_1 \dots \mu_j}, \quad (2.17)$$

to leading order. In writing this form, we are omitting multiplicative QCD corrections of order unity that arise from matching of the effective theory to full QCD at different mass scales. Here, $M_{\mu_1 \dots \mu_j}$ is the most general tensor that we can construct, given the kinematic variables at our disposal. Clearly, $M_{\mu_1 \dots \mu_j}$ may not contain any factors of v'_{μ_i} or $g_{\mu_i \mu_j}$, and therefore takes the form

$$M_{\mu_1 \dots \mu_j} = \eta^{(j)}(v \cdot v') v_{\mu_1} \dots v_{\mu_j}. \quad (2.18)$$

Thus, a single form factor, $\eta^{(j)}(v \cdot v')$ is needed to this order, regardless of the spin of the final baryon. In addition, spin symmetry allows us to relate the form factors for $\Gamma = \gamma_\mu$ to those for $\Gamma = \gamma_\mu \gamma_5$.

The case of $J^P = 1/2^+$, $j = 0$ requires a special comment. Some of these states may be thought of as radial excitations of the ground state Λ_c^+ . Because of the heavy quark symmetry, and the orthogonality of these states with respect to the ground state, we must have

$$\langle \Lambda_c^*(v', j^P = 0^+)_{(n)} | \bar{c} \Gamma b | \Lambda_b(v) \rangle = (v \cdot v' - 1) \eta_{(n)}^{(0)}(v \cdot v') \bar{u}(v') \Gamma u(v), \quad (2.19)$$

where the subscripts (n) denote the n th radial excitation. That is, these amplitudes must vanish as $v' \rightarrow v$. This result has been pointed out by Isgur, Wise and Youssefmir [68]. Note, too, that all of the other amplitudes ($j \neq 0$) vanish trivially at the non-recoil point.

Applying these results to the specific case of the ground state with $j^P = 0^+$, for the $J^P = 1/2^+$ state, we find

$$F_1 = G_1 = \eta^{(0)}(w), \quad F_2 = F_3 = G_2 = G_3 = 0. \quad (2.20)$$

Here, $\eta^{(0)}(w)$ is an Isgur-Wise function, and $w = v \cdot v'$. At the non-recoil point, $v = v'$, $\eta^{(0)}(w = 1) = 1$.

For the case of $j^P = 1^-$, we find, for $J^P = 1/2^-$,

$$F_1 = \frac{w-1}{\sqrt{3}}\eta^{(1)}(w), \quad F_2 = G_2 = -\frac{2}{\sqrt{3}}\eta^{(1)}(w), \quad G_3 = F_3 = 0, \quad G_1 = \frac{w+1}{\sqrt{3}}\eta^{(1)}(w). \quad (2.21)$$

For $3/2^-$,

$$F_2 = F_3 = G_2 = G_3 = F_4 = G_4 = 0, \quad F_1 = G_1 = -\eta^{(1)}(w). \quad (2.22)$$

In these two sets of equations $\eta^{(1)}$ is a universal function of the Isgur-Wise type.

For $j^P = 2^+$, we find for $J^P = 3/2^+$,

$$\begin{aligned} F_3 = G_3 = F_4 = G_4 = 0, \quad F_1 &= \frac{2(w-1)}{\sqrt{10}}\eta^{(2)}(w), \\ F_2 = G_2 = -\frac{4}{\sqrt{10}}\eta^{(2)}(w), \quad G_1 &= \frac{2(w+1)}{\sqrt{10}}\eta^{(2)}(w), \end{aligned} \quad (2.23)$$

and for $5/2^+$

$$F_2 = F_3 = F_4 = G_4 = G_2 = G_3 = 0, \quad F_1 = G_1 = -\eta^{(2)}(w). \quad (2.24)$$

As with the previous example, the function $\eta^{(2)}$ is an Isgur-Wise form factor common to both decays. The normalizations of $\eta^{(1)}$ and $\eta^{(2)}$ in the expressions above are not known.

For the elastic decays, as well as for decays to the $1/2^-$, $3/2^-$ doublet, the matrix elements have been evaluated at order $1/m_c$ and $1/m_b$ in the heavy quark expansion [41]. When we present our results for the form factors, we will compare our expressions with the predictions of HQET.

For the pseudo-tensor decays, we write exactly the same form, but $M_{\mu_1 \dots \mu_j}$ must now be a pseudo-tensor object, and must therefore be constructed by using the ε tensor. Inspection shows that no such pseudo-tensor can be constructed, given that we have only two kinematic variables at our disposal, namely v and v' , and that the spinor-tensor used to describe the daughter baryon is symmetric in its indices. Thus, decay amplitudes for transitions to pseudo-tensor daughter baryons vanish at leading order in HQET.

2.3.4 Heavy to Light Λ Decay

For the heavy to light transitions, we may no longer describe the daughter baryons in terms of the spin structure of the light quark system that helps to make up the baryon. Instead,

we are forced to use the total angular momentum of the baryon concerned, as well as its parity. As before, we may represent one of these baryons, denoted Λ^* , by a generalized Rarita-Schwinger field $u^{\mu_1 \dots \mu_n}(p')$, where the auxiliary conditions now are

$$\begin{aligned} \not{p}' u^{\mu_1 \dots \mu_n}(p') &= m_{\Lambda^*} u^{\mu_1 \dots \mu_n}(p'), \quad \gamma_{\mu_1} u^{\mu_1 \dots \mu_n}(p') = 0, \\ p'_{\mu_1} u^{\mu_1 \dots \mu_n}(p') &= 0, \quad u_{\mu}^{\mu_1 \dots \mu_n}(p') = 0, \end{aligned} \quad (2.25)$$

and a baryon with angular momentum and parity J^P is represented by a spinor-tensor with $n = J - 1/2$ indices. As was the case with the heavy to heavy transitions, we need to divide the possible transitions into two classes, which we call tensor and pseudo-tensor, with the obvious meaning.

As before, we begin with the transitions to tensor states. Here, we say a state of total angular momentum J is a tensor if its parity is $(-1)^{(J-1/2)}$, and is a pseudo-tensor otherwise. The matrix element of interest is

$$\langle \Lambda^*(p')_{JP} | \bar{s} \Gamma c | \Lambda_c^+(v) \rangle = \bar{u}^{\mu_1 \dots \mu_n}(p') M_{\mu_1 \dots \mu_n} \Gamma u(v), \quad (2.26)$$

where $M_{\mu_1 \dots \mu_n}$ is the most general tensor that one can construct. As with the heavy to heavy transitions, we may not use any factors of γ_{μ_i} , p'_{μ_i} or $g_{\mu_i \mu_j}$ in constructing $M_{\mu_1 \dots \mu_n}$, which must therefore have the form

$$M_{\mu_1 \dots \mu_n} = v_{\mu_1} \dots v_{\mu_n} \mathcal{A}_n. \quad (2.27)$$

Here, \mathcal{A}_n is the most general Lorentz scalar that we can build. On inspection, we find that

$$\mathcal{A}_n = \xi_1^{(n)} + \not{p}' \xi_2^{(n)}, \quad (2.28)$$

so that each of these transitions is described by two form factors, at leading order in HQET.

For the transitions into pseudotensor daughter baryons, we write exactly the same form as in Eq. (2.26), but now $M_{\mu_1 \dots \mu_n}$ must be a pseudo-tensor. This may involve the use of the ε tensor, but since $u^{\mu_1 \dots \mu_n}(p')$ is symmetric in its indices, at most one of these indices may be contracted with the indices of the ε tensor. With some patience, and the use of a few well chosen identities, one can show that any pseudo-tensor term constructed with the ε tensor may always be reduced to an ordinary tensor multiplying a γ_5 matrix. We will therefore leave out much of the tedium, and simply write for these transitions

$$M_{\mu_1 \dots \mu_n} = v_{\mu_1} \dots v_{\mu_n} \left(\zeta_1^{(n)} + \not{p}' \zeta_2^{(n)} \right) \gamma_5, \quad (2.29)$$

where the ξ_i and ζ_i are functions of the kinematic variable $v \cdot p'$. Thus, any of the heavy to light transitions is described by a pair of form factors, to this order in HQET. Note that for both sets of heavy to light transitions, we may use the spin symmetry of HQET to relate the two form factors necessary for $\Gamma = \gamma_\mu$ to those for $\Gamma = \gamma_\mu \gamma_5$.

For $1/2^+$, we find

$$F_3 = G_3 = 0, \quad F_2 = G_2 = 2\xi_2^{(0)}, \quad F_1 = \xi_1^{(0)} - \xi_2^{(0)}, \quad G_1 = \xi_1^{(0)} + \xi_2^{(0)}, \quad (2.30)$$

while for $1/2^-$, the form factors are

$$F_3 = G_3 = 0, \quad F_2 = G_2 = -2\zeta_2^{(0)}, \quad F_1 = -(\zeta_1^{(0)} + \zeta_2^{(0)}), \quad G_1 = -(\zeta_1^{(0)} - \zeta_2^{(0)}). \quad (2.31)$$

For $3/2^-$,

$$F_3 = G_3 = F_4 = G_4 = 0, \quad F_2 = G_2 = 2\xi_2^{(1)}, \quad F_1 = \xi_1^{(1)} - \xi_2^{(1)}, \quad G_1 = \xi_1^{(1)} + \xi_2^{(1)}. \quad (2.32)$$

For $3/2^+$,

$$F_3 = G_3 = F_4 = G_4 = 0, \quad F_2 = G_2 = -2\zeta_2^{(1)}, \quad F_1 = -(\zeta_1^{(1)} + \zeta_2^{(1)}), \quad G_1 = -(\zeta_1^{(1)} - \zeta_2^{(1)}). \quad (2.33)$$

For $5/2^+$,

$$F_3 = G_3 = F_4 = G_4 = 0, \quad F_2 = G_2 = 2\xi_2^{(2)}, \quad F_1 = \xi_1^{(2)} - \xi_2^{(2)}, \quad G_1 = \xi_1^{(2)} + \xi_2^{(2)}. \quad (2.34)$$

Note that, in principle, the form factors for the decays to $1/2^-$ have no relationship with those for decays to $3/2^-$, in the heavy quark limit. In addition, the normalizations of none of the heavy to light form factors are known.

2.3.5 Heavy to Heavy Ω Decay

First, we note that the Falk representation of the ground state Ω_Q is

$$\Omega_\nu(v) = \frac{1}{\sqrt{3}} (\gamma_\nu + v_\nu) \gamma_5 u(v), \quad (2.35)$$

where $u(v)$ is a Dirac spinor. This state is a pseudotensor, and we begin with a discussion of decays to other pseudotensor states. As with Λ_Q decays, we are interested in the matrix element

$$\mathcal{A} = \langle \Omega_c^{(*)}(v', j) | \bar{c} \Gamma b | \Omega_b(v) \rangle, \quad (2.36)$$

where c and b are the heavy quark fields, and Γ is an arbitrary combination of Dirac matrices. With the use of HQET, we may write this matrix element as

$$\langle \Omega_c^{(*)}(v', j) | \bar{c} \Gamma b | \Omega_b(v) \rangle = \bar{u}^{\mu_1 \dots \mu_j}(v') \Gamma \Omega^\nu M_{\mu_1 \dots \mu_j \nu}, \quad (2.37)$$

to leading order. Here, $M_{\mu_1 \dots \mu_j \nu}$ is the most general tensor that we can construct. $M_{\mu_1 \dots \mu_j \nu}$ may not contain any factors of v'_{μ_i} or $g_{\mu_i \mu_j}$, and therefore takes the form

$$M_{\mu_1 \dots \mu_j \nu} = \left(\eta_1^{(j)} g_{\mu_1 \nu} + \eta_2^{(j)} v_{\mu_1} v'_\nu \right) v_{\mu_2} \dots v_{\mu_j}. \quad (2.38)$$

Thus, two independent form factors, $\eta_{1,2}^{(j)}(v \cdot v')$ are needed to this order, regardless of the spin of the final baryon.

Applying these pseudotensor results to the specific case of $j^P = 0^-$, we find, for $J^P = 1/2^-$

$$F_1 = \frac{w-1}{\sqrt{3}} \eta_2^{(0)}(w), \quad F_2 = G_2 = 0, \quad F_3 = -G_3 = \frac{2}{\sqrt{3}} \eta_2^{(0)}(w), \quad G_1 = \frac{w+1}{\sqrt{3}} \eta_2^{(0)}(w). \quad (2.39)$$

In this case, the daughter baryon is a singlet, and has no Lorentz indices. This means that the term in $g_{\mu\nu}$ is not present, and only the term in η_2 contributes to the matrix element.

When $j^P = 1^+$, we find, for $J^P = 1/2^+$,

$$\begin{aligned} F_1 &= G_1 = \frac{1}{3} \left[w \eta_1^{(1)} + (w^2 - 1) \eta_2^{(1)} \right], & F_2 &= F_3 = \frac{2}{3} \left[-\eta_1^{(1)} + (1 - w) \eta_2^{(1)} \right], \\ G_2 &= -G_3 = -\frac{2}{3} \left[\eta_1^{(1)} + (1 + w) \eta_2^{(1)} \right], \end{aligned} \quad (2.40)$$

and for $J^P = 3/2^+$

$$\begin{aligned} F_1 &= -\frac{1}{\sqrt{3}} \left[\eta_1^{(1)} + (w - 1) \eta_2^{(1)} \right], & F_2 &= 0, & F_3 &= -\frac{2}{\sqrt{3}} \eta_2^{(1)}, & F_4 &= -\frac{2}{\sqrt{3}} \eta_1^{(1)}, \\ G_1 &= -\frac{1}{\sqrt{3}} \left[\eta_1^{(1)} + (w + 1) \eta_2^{(1)} \right], & G_2 &= 0, & G_3 &= \frac{2}{\sqrt{3}} \eta_2^{(1)}, & G_4 &= \frac{2}{\sqrt{3}} \eta_1^{(1)}. \end{aligned} \quad (2.41)$$

In these two sets of equations $\eta_{1,2}^{(1)}$ are two universal functions of the Isgur-Wise type. We note that there exist several multiplets that have the same quantum numbers as this ground state multiplet. The same is true in the case of Λ_Q baryons, and these excited Λ_Q s were identified as radial excitations of the ground state. In the case of the Ω_Q , such baryons are indeed excitations of the ground state, but they are not necessarily radial excitations. Some of these excitations are orbital excitations. However, independent of whether the daughter baryon

belongs to the ground state ($1/2^+$, $3/2^+$) or one of the excited multiplets, the expressions above for the form factors are valid. The explicit forms of the $\eta_i^{(1)}$ will depend on the details of the structure of the daughter baryon. For the ground state we know that at the non-recoil point, $\eta_1^{(1)}(v.v' = 1) = -1$, while the normalization of $\eta_2^{(1)}$ is not known. The negative sign on the normalization of $\eta_1^{(1)}$ arises because we have chosen a positive sign on the $g_{\mu_1\nu}$ term in Eq. (2.38).

For $j^P = 2^-$, we find for $J^P = 3/2^-$,

$$\begin{aligned}
F_1 &= \frac{1}{\sqrt{30}} \left[(2w-1)\eta_1^{(2)} + 2(w^2-1)\eta_2^{(2)} \right], & F_2 &= -2\sqrt{\frac{2}{15}} \left[\eta_1^{(2)} + (w-1)\eta_2^{(2)} \right], \\
F_3 &= -\sqrt{\frac{2}{15}} \left[\eta_1^{(2)} + 2(w-1)\eta_2^{(2)} \right], & F_4 &= -\sqrt{\frac{2}{15}}(w-1)\eta_1^{(2)}, \\
G_1 &= \frac{1}{\sqrt{30}} \left[(2w+1)\eta_1^{(2)} + 2(w^2-1)\eta_2^{(2)} \right], & G_2 &= -2\sqrt{\frac{2}{15}} \left[\eta_1^{(2)} + (w+1)\eta_2^{(2)} \right], \\
G_3 &= \sqrt{\frac{2}{15}} \left[\eta_1^{(2)} + 2(w+1)\eta_2^{(2)} \right], & G_4 &= \sqrt{\frac{2}{15}}(w+1)\eta_1^{(2)},
\end{aligned} \tag{2.42}$$

and for $J^P = 5/2^-$

$$\begin{aligned}
F_1 &= -\frac{1}{\sqrt{3}} \left[\eta_1^{(2)} + (w-1)\eta_2^{(2)} \right], & F_2 &= 0, & F_3 &= -\frac{2}{\sqrt{3}}\eta_2^{(2)}, & F_4 &= -\frac{2}{\sqrt{3}}\eta_1^{(2)}, \\
G_1 &= -\frac{1}{\sqrt{3}} \left[\eta_1^{(2)} + (w+1)\eta_2^{(2)} \right], & G_2 &= 0, & G_3 &= \frac{2}{\sqrt{3}}\eta_2^{(2)}, & G_4 &= \frac{2}{\sqrt{3}}\eta_1^{(2)}.
\end{aligned} \tag{2.43}$$

As with the previous example, the functions $\eta_{1,2}^{(2)}$ are Isgur-Wise form factors common to both decays.

For $j^P = 3^+$, we find for $J^P = 5/2^+$,

$$\begin{aligned}
F_1 &= \frac{1}{3\sqrt{7}} \left[(3w-2)\eta_1^{(3)} + 3(w^2-1)\eta_2^{(3)} \right], & F_2 &= -2\sqrt{\frac{1}{7}} \left[\eta_1^{(3)} + (w-1)\eta_2^{(3)} \right], \\
F_3 &= -\frac{2}{3\sqrt{7}} \left[\eta_1^{(3)} + 3(w-1)\eta_2^{(3)} \right], & F_4 &= -\frac{4}{3\sqrt{7}}(w-1)\eta_1^{(3)}, \\
G_1 &= \frac{1}{3\sqrt{7}} \left[(3w+2)\eta_1^{(3)} + 3(w^2-1)\eta_2^{(3)} \right], & G_2 &= -2\sqrt{\frac{1}{7}} \left[\eta_1^{(3)} + (w+1)\eta_2^{(3)} \right], \\
G_3 &= \frac{2}{3\sqrt{7}} \left[\eta_1^{(3)} + 3(w+1)\eta_2^{(3)} \right], & G_4 &= \frac{4}{3\sqrt{7}}(w+1)\eta_1^{(3)},
\end{aligned} \tag{2.44}$$

and for $J^P = 7/2^+$

$$\begin{aligned}
F_1 &= -\frac{1}{\sqrt{3}} \left[\eta_1^{(3)} + (w-1)\eta_2^{(3)} \right], \quad F_2 = 0, \quad F_3 = -\frac{2}{\sqrt{3}}\eta_2^{(3)}, \quad F_4 = -\frac{2}{\sqrt{3}}\eta_1^{(3)}, \\
G_1 &= -\frac{1}{\sqrt{3}} \left[\eta_1^{(3)} + (w+1)\eta_2^{(3)} \right], \quad G_2 = 0, \quad G_3 = \frac{2}{\sqrt{3}}\eta_2^{(3)}, \quad G_4 = \frac{2}{\sqrt{3}}\eta_1^{(3)},
\end{aligned} \tag{2.45}$$

The functions $\eta_{1,2}^{(3)}$ are Isgur-Wise form factors common to both decays. The normalization of $\eta_2^{(1,2)}$ and $\eta_3^{(1,2)}$ are not known.

For the tensor decays, the matrix element again takes the form shown in Eq. (2.37), but $M_{\mu_1 \dots \mu_j \nu}$ must now be a pseudotensor. The only form that we can write is

$$M_{\mu_1 \dots \mu_j \nu} = \tau^{(j)}(w) v_{\mu_2} \dots v_{\mu_j} \varepsilon_{\nu \mu_1 \rho \lambda} v^\rho v'^\lambda. \tag{2.46}$$

When applied to the $1/2^+$ singlet daughter baryon, there is no way to create this pseudotensor, so such amplitudes vanish at leading order. For the other spin states, after some manipulation, we can express the form factors in terms of a set of Isgur-Wise functions $\tau^{(j)}(w)$.

For $j^P = 1^-$, we find for the $1/2^-$ state

$$F_1 = G_1 = 0, \quad F_2 = F_3 = -G_2 = G_3 = -\frac{2}{3}\tau^{(1)}, \tag{2.47}$$

while for $3/2^-$ state, the form factors are

$$F_2 = G_2 = 0, \quad G_3 = -F_3 = 2F_1 = -2G_1 = -\frac{2}{\sqrt{3}}\tau^{(1)}, \quad F_4 = -\frac{2}{\sqrt{3}}(w-1)\tau^{(1)}, \quad G_4 = \frac{2}{\sqrt{3}}(w+1)\tau^{(1)}. \tag{2.48}$$

For $j^P = 2^+$, starting with $3/2^+$, the form factors are

$$\begin{aligned}
F_1 &= \frac{1}{\sqrt{30}}(1-w)\tau^{(2)}, \quad F_2 = -2\sqrt{\frac{2}{15}}\tau^{(2)}, \quad F_3 = \sqrt{\frac{2}{15}}(w-2)\tau^{(2)}, \quad F_4 = \sqrt{\frac{2}{15}}(1-w^2)\tau^{(2)}, \\
G_1 &= \frac{1}{\sqrt{30}}(1+w)\tau^{(2)}, \quad G_2 = 2\sqrt{\frac{2}{15}}\tau^{(2)}, \quad G_3 = -\sqrt{\frac{2}{15}}(w+2)\tau^{(2)}, \quad G_4 = -\sqrt{\frac{2}{15}}(1-w^2)\tau^{(2)}.
\end{aligned} \tag{2.49}$$

For the $5/2^+$ state, the form factors are

$$F_2 = G_2 = 0, \quad G_3 = -F_3 = 2F_1 = -2G_1 = -\frac{2}{\sqrt{3}}\tau^{(2)}, \quad F_4 = -\frac{2}{\sqrt{3}}(w-1)\tau^{(2)}, \quad G_4 = \frac{2}{\sqrt{3}}(w+1)\tau^{(2)}. \tag{2.50}$$

The normalizations of none of the $\tau^{(i)}$ are known.

We do not present the predictions for the heavy to light Ω_Q decays as the HQET predictions are not as useful as they are in the case of heavy to light Λ_Q decays. For instance, the decays of the ground state Ω_Q to Ω are described in terms of four form factors in HQET, instead of six in general. While this small simplification is no doubt useful we do not pursue it here.

CHAPTER 3

The Model

3.1 Wave Function Components

Our calculation of the form factors describing the semileptonic decays of heavy baryons follows the spirit of the work by ISGW [36]. In our model, a baryon state has the form

$$|A_Q(\mathbf{p}, s)\rangle = 3^{3/4} \int d^3 p_\rho d^3 p_\lambda C^A \Psi_{A_Q}^S |q_1(\mathbf{p}_1, s_1) q_2(\mathbf{p}_2, s_2) q_3(\mathbf{p}_3, s_3)\rangle,$$

where $\mathbf{p}_\rho = \frac{1}{\sqrt{2}}(\mathbf{p}_1 - \mathbf{p}_2)$, $\mathbf{p}_\lambda = \frac{1}{\sqrt{6}}(\mathbf{p}_1 + \mathbf{p}_2 - 2\mathbf{p}_3)$ are the Jacobi momenta, C^A is the totally antisymmetric color wave function, and $\Psi_{A_Q}^S = \phi_{A_Q} \psi_{A_Q} \chi_{A_Q}$ is a symmetric combination of flavor, momentum and spin wave functions.

For Λ_Q the flavor wave function we use is

$$\phi_{\Lambda_Q} = \frac{1}{\sqrt{2}}(ud - du)Q, \quad (3.1)$$

which is antisymmetric in quarks 1 and 2. The momentum-spin portion of the wave function must therefore be antisymmetric in quarks 1 and 2. For states like the neutron and proton, we use the ‘*uds*’ basis used in Refs. [24, 29]. In that basis, the wave function of the proton is simply *uud*, while that for the neutron is *ddu*. This flavor wave function provides some simplification in dealing with matrix elements of the Hamiltonian. However, the treatment of current matrix elements, such as those that describe semileptonic decays, will require some extra care, as will be explained later.

The flavor wave function of Ω_Q is

$$\phi_{\Omega_Q} = ssQ,$$

which is symmetric in quarks 1 and 2. The momentum-spin part of the wave function must therefore be symmetric in quarks 1 and 2 to keep the overall symmetry.

The total spin of the three spin-1/2 quarks can be either 3/2 or 1/2. The spin wave functions for the maximally stretched state in each case are

$$\begin{aligned}\chi_{3/2}^S(+3/2) &= |\uparrow\uparrow\uparrow\rangle, \\ \chi_{1/2}^\rho(+1/2) &= \frac{1}{\sqrt{2}}(|\uparrow\downarrow\uparrow\rangle - |\downarrow\uparrow\uparrow\rangle), \\ \chi_{1/2}^\lambda(+1/2) &= -\frac{1}{\sqrt{6}}(|\uparrow\downarrow\uparrow\rangle + |\downarrow\uparrow\uparrow\rangle - 2|\uparrow\uparrow\downarrow\rangle),\end{aligned}$$

where S labels the state as totally symmetric, while λ/ρ denotes the mixed symmetric states that are symmetric/anti-symmetric under the exchange of quarks 1 and 2. The momentum wave function for total $L = \ell_\rho + \ell_\lambda$ is constructed from a Clebsch-Gordan sum of the wave functions of the two Jacobi coordinates \mathbf{p}_ρ and \mathbf{p}_λ , and takes the form

$$\psi_{LMn_\rho\ell_\rho n_\lambda\ell_\lambda}(\mathbf{p}_\rho, \mathbf{p}_\lambda) = \sum_m \langle LM|\ell_\rho m, \ell_\lambda M - m\rangle \psi_{n_\rho\ell_\rho m}(\mathbf{p}_\rho) \psi_{n_\lambda\ell_\lambda M-m}(\mathbf{p}_\lambda).$$

The momentum and spin wave functions are then coupled to give symmetric wave functions corresponding to total spin J and parity $(-1)^{(\ell_\rho+\ell_\lambda)}$,

$$\Psi_{JM} = \sum_{M_L} \langle JM|LM_L, SM - M_L\rangle \psi_{LM_L n_\rho\ell_\rho n_\lambda\ell_\lambda} \chi_S(M - M_L).$$

The full wave function for a state A is built from a linear superposition of such components as

$$\Psi_{A, J^P M} = \phi_A \sum_i \eta_i^A \Psi_{JM}^i. \quad (3.2)$$

Here ϕ_A is the flavor wave function of the state A , and the η_i^A are coefficients that are determined by diagonalizing a Hamiltonian in the basis of the Ψ_{JM} . For this calculation, we limit the expansion in the last equation to components that satisfy $N \leq 2$, where $N = 2(n_\rho + n_\lambda) + \ell_\rho + \ell_\lambda$. Consistent with this is the fact that the states we discuss all correspond to $N \leq 2$.

3.1.1 Λ_Q Wave Functions

With the limitation mentioned above, the wave function for a Λ_Q with $J^P = 1/2^+$ takes the form

$$\begin{aligned}
\Psi_{\Lambda_Q, 1/2^+ M} &= \phi_{\Lambda_Q} \left(\left[\eta_1^{\Lambda_Q} \psi_{000000}(\mathbf{p}_\rho, \mathbf{p}_\lambda) + \eta_2^{\Lambda_Q} \psi_{001000}(\mathbf{p}_\rho, \mathbf{p}_\lambda) + \eta_3^{\Lambda_Q} \psi_{000010}(\mathbf{p}_\rho, \mathbf{p}_\lambda) \right] \chi_{1/2}^\rho(M) \right. \\
&+ \eta_4^{\Lambda_Q} \psi_{000101}(\mathbf{p}_\rho, \mathbf{p}_\lambda) \chi_{1/2}^\lambda(M) + \eta_5^{\Lambda_Q} \left[\psi_{1M_L 0101}(\mathbf{p}_\rho, \mathbf{p}_\lambda) \chi_{3/2}^S(M - M_L) \right]_{1/2, M} \\
&+ \eta_6^{\Lambda_Q} \left[\psi_{1M_L 0101}(\mathbf{p}_\rho, \mathbf{p}_\lambda) \chi_{1/2}^\lambda(M - M_L) \right]_{1/2, M} \\
&\left. + \eta_7^{\Lambda_Q} \left[\psi_{2M_L 0101}(\mathbf{p}_\rho, \mathbf{p}_\lambda) \chi_{3/2}^S(M - M_L) \right]_{1/2, M} \right), \tag{3.3}
\end{aligned}$$

where $[\psi_{LM_L n_\rho \ell_\rho n_\lambda \ell_\lambda}(\mathbf{p}_\rho, \mathbf{p}_\lambda) \chi_S(M - M_L)]_{J, M}$ is a shorthand notation that denotes the Clebsch-Gordan sum $\sum_{M_L} \langle JM | LM_L, SM - M_L \rangle \psi_{LM_L n_\rho \ell_\rho n_\lambda \ell_\lambda}(\mathbf{p}_\rho, \mathbf{p}_\lambda) \chi_S(M - M_L)$. When we diagonalize the Hamiltonian, this expansion will provide the wave functions for seven states with $J^P = 1/2^+$, the lowest of which will be taken to be the ground state of the system.

A simplified version of the model would truncate this expansion after the first component, giving

$$\Psi_{\Lambda_Q, 1/2^+ M} = \phi_\Lambda \psi_{000000}(\mathbf{p}_\rho, \mathbf{p}_\lambda) \chi_{1/2}^\rho(M),$$

while the first radial excitation of interest in this model would be

$$\Psi_{\Lambda_Q, 1/2_1^+ M} = \phi_\Lambda \psi_{000010}(\mathbf{p}_\rho, \mathbf{p}_\lambda) \chi_{1/2}^\rho(M).$$

There exists a second radial excitation which, in the truncated basis would be

$$\Psi_{\Lambda_Q, 1/2_2^+ M} = \phi_\Lambda \psi_{001000}(\mathbf{p}_\rho, \mathbf{p}_\lambda) \chi_{1/2}^\rho(M).$$

The latter state has its radial excitation in the ρ coordinate, which means that it has a very small overlap with the ground state in the spectator model that we use. For some states, this truncation provides a very good approximation to the wave function, but there are important configuration mixing effects for a number of states. In the spectator assumption that we use, not all of these states have an overlap with the initial ground-state Λ_Q . The possible Λ_q states which can be connected to the ground state are the states with $J^P = 1/2^+, 1/2_1^+, 1/2^-, 3/2^-, 3/2^+, 5/2^+$, where $1/2^+$ and $1/2_1^+$ denote the ground state and the first (radially) excited state. Wave functions are shown in [Appendix A](#)

It is useful for us to list the single-component representations of these states. The states with $J^P = 1/2^+$ have already been given. For the remaining states, we have

$$\begin{aligned}
\Psi_{\Lambda_Q, 1/2^- M} &= \phi_\Lambda \left[\psi_{1M_L 0001}(\mathbf{p}_\rho, \mathbf{p}_\lambda) \chi_{1/2}^\rho(M - M_L) \right]_{1/2, M}, \\
\Psi_{\Lambda_Q, 3/2^- M} &= \phi_\Lambda \left[\psi_{1M_L 0001}(\mathbf{p}_\rho, \mathbf{p}_\lambda) \chi_{1/2}^\rho(M - M_L) \right]_{3/2, M}, \\
\Psi_{\Lambda_Q, 3/2^+ M} &= \phi_\Lambda \left[\psi_{2M_L 0002}(\mathbf{p}_\rho, \mathbf{p}_\lambda) \chi_{1/2}^\rho(M - M_L) \right]_{3/2, M}, \\
\Psi_{\Lambda_Q, 5/2^+ M} &= \phi_\Lambda \left[\psi_{2M_L 0002}(\mathbf{p}_\rho, \mathbf{p}_\lambda) \chi_{1/2}^\rho(M - M_L) \right]_{5/2, M}.
\end{aligned} \tag{3.4}$$

From these representations, the multiplet structure expected in the heavy quark limit is easily identified, with the $1/2^-$ and $3/2^-$ states forming a multiplet, and the $3/2^+$ and $5/2^+$ states forming another. Both of the $1/2^+$ states we consider are singlets.

3.1.2 Ω_Q Wave Functions

The wave functions for Ω_Q with $J^P = 1/2^+$ has the form

$$\begin{aligned}
\Psi_{1/2^+ M}^{\Omega_Q} &= \phi_{\Omega_Q} \left(\left[\eta_1^{\Omega_Q} \psi_{000000}(\mathbf{p}_\rho, \mathbf{p}_\lambda) + \eta_2^{\Omega_Q} \psi_{001000}(\mathbf{p}_\rho, \mathbf{p}_\lambda) + \eta_3^{\Omega_Q} \psi_{000010}(\mathbf{p}_\rho, \mathbf{p}_\lambda) \right] \chi_{1/2}^\lambda(M) \right. \\
&+ \eta_4^{\Omega_Q} \psi_{000101}(\mathbf{p}_\rho, \mathbf{p}_\lambda) \chi_{1/2}^\rho(M) + \eta_5^{\Omega_Q} \left[\psi_{1M_L 0101}(\mathbf{p}_\rho, \mathbf{p}_\lambda) \chi_{1/2}^\rho(M - M_L) \right]_{1/2, M} \\
&+ \eta_6^{\Omega_Q} \left[\psi_{2M_L 0200}(\mathbf{p}_\rho, \mathbf{p}_\lambda) \chi_{3/2}^S(M - M_L) \right]_{1/2, M} \\
&\left. + \eta_7^{\Omega_Q} \left[\psi_{2M_L 0002}(\mathbf{p}_\rho, \mathbf{p}_\lambda) \chi_{3/2}^S(M - M_L) \right]_{1/2, M} \right).
\end{aligned} \tag{3.5}$$

The complete expressions for Ω_Q wave functions of different spins and parities are also shown in Appendix A. In the rest of this section we present a list of the truncated wave functions for Ω_Q with different J^P , analogous to what was done for Λ_Q in the previous section. We note that the number of possible states which can have an overlap with the ground state Ω_Q is significantly larger than for the Λ_Q case: there are three states with $J^P = 1/2^+$, two with $J^P = 1/2^-$, two with $J^P = 3/2^-$, four with $J^P = 3/2^+$, one with $J^P = 5/2^-$, two with $J^P = 5/2^+$, and one with $J^P = 7/2^+$, all of which occur in the $N \leq 2$ band. The

single-component representations of these states are

$$\begin{aligned}
\Psi_{\Omega_Q,1/2^+M} &= \phi_\Omega \psi_{000000}(\mathbf{p}_\rho, \mathbf{p}_\lambda) \chi_{1/2}^\lambda(M), \\
\Psi_{\Omega_Q,1/2_1^+M} &= \phi_\Omega \psi_{000010}(\mathbf{p}_\rho, \mathbf{p}_\lambda) \chi_{1/2}^\lambda(M), \\
\Psi_{\Omega_Q,1/2_2^+M} &= \phi_\Omega [\psi_{2M_L0002}(\mathbf{p}_\rho, \mathbf{p}_\lambda) \chi_{3/2}^S(M - M_L)]_{1/2,M}, \\
\Psi_{\Omega_Q,1/2^-M} &= \phi_\Omega [\psi_{1M_L0001}(\mathbf{p}_\rho, \mathbf{p}_\lambda) \chi_{1/2}^\lambda(M - M_L)]_{1/2,M}, \\
\Psi_{\Omega_Q,1/2_1^-M} &= \phi_\Omega [\psi_{1M_L0001}(\mathbf{p}_\rho, \mathbf{p}_\lambda) \chi_{3/2}^S(M - M_L)]_{1/2,M}, \\
\Psi_{\Omega_Q,3/2^-M} &= \phi_\Omega [\psi_{1M_L0001}(\mathbf{p}_\rho, \mathbf{p}_\lambda) \chi_{1/2}^\lambda(M - M_L)]_{3/2,M}, \\
\Psi_{\Omega_Q,3/2_1^-M} &= \phi_\Omega [\psi_{1M_L0001}(\mathbf{p}_\rho, \mathbf{p}_\lambda) \chi_{3/2}^S(M - M_L)]_{3/2,M}, \\
\Psi_{\Omega_Q,5/2^-M} &= \phi_\Omega [\psi_{1M_L0001}(\mathbf{p}_\rho, \mathbf{p}_\lambda) \chi_{3/2}^S(M - M_L)]_{5/2,M}, \\
\Psi_{\Omega_Q,3/2^+M} &= \phi_\Omega \psi_{000000}(\mathbf{p}_\rho, \mathbf{p}_\lambda) \chi_{3/2}^S(M), \\
\Psi_{\Omega_Q,3/2_1^+M} &= \phi_\Omega \psi_{000010}(\mathbf{p}_\rho, \mathbf{p}_\lambda) \chi_{3/2}^S(M), \\
\Psi_{\Omega_Q,3/2_2^+M} &= \phi_\Omega [\psi_{2M_L0002}(\mathbf{p}_\rho, \mathbf{p}_\lambda) \chi_{3/2}^S(M - M_L)]_{3/2,M}, \\
\Psi_{\Omega_Q,3/2_3^+M} &= \phi_\Omega [\psi_{2M_L0002}(\mathbf{p}_\rho, \mathbf{p}_\lambda) \chi_{1/2}^\lambda(M - M_L)]_{3/2,M}, \\
\Psi_{\Omega_Q,5/2^+M} &= \phi_\Omega [\psi_{2M_L0002}(\mathbf{p}_\rho, \mathbf{p}_\lambda) \chi_{1/2}^\lambda(M - M_L)]_{5/2,M}, \\
\Psi_{\Omega_Q,5/2_1^+M} &= \phi_\Omega [\psi_{2M_L0002}(\mathbf{p}_\rho, \mathbf{p}_\lambda) \chi_{3/2}^S(M - M_L)]_{5/2,M}, \\
\Psi_{\Omega_Q,7/2^+M} &= \phi_\Omega [\psi_{2M_L0002}(\mathbf{p}_\rho, \mathbf{p}_\lambda) \chi_{3/2}^S(M - M_L)]_{7/2,M}. \tag{3.6}
\end{aligned}$$

3.2 Expansion Bases

A common choice for constructing baryon wave function is the harmonic oscillator basis. One advantage of using this basis is that it facilitates calculation of the required matrix elements. However, it leads to form factors that fall off too rapidly at large values of momentum transfer. We therefore also use the so-called Sturmian basis [69]. In this basis, form factors have multipole dependence on q^2 , which is what is expected experimentally. The full wave functions in momentum space are

$$\psi_{nLm}^{\text{h.o.}}(\mathbf{p}) = \left[\frac{2n!}{(n + L + \frac{1}{2})!} \right]^{\frac{1}{2}} (i)^L (-1)^n \frac{1}{\alpha^{L+\frac{3}{2}}} e^{-\frac{p^2}{2\alpha^2}} L_n^{L+\frac{1}{2}}(p^2/\alpha^2) \mathcal{Y}_{Lm}(\mathbf{p}) \tag{3.7}$$

in the harmonic oscillator basis, and

$$\psi_{nLm}^{\text{St}}(\mathbf{p}) = \frac{2 [n!(n+2L+2)!]^{\frac{1}{2}}}{(n+L+\frac{1}{2})!} (i)^L \frac{1}{\beta^{L+\frac{3}{2}}} \frac{1}{\left(\frac{p^2}{\beta^2} + 1\right)^{L+2}} P_n^{(L+\frac{3}{2}, L+\frac{1}{2})} \left(\frac{p^2 - \beta^2}{p^2 + \beta^2}\right) \mathcal{Y}_{Lm}(\mathbf{p}) \quad (3.8)$$

in the Sturmian basis. The $L_n^\nu(x)$ are generalized Laguerre polynomials and the $P_n^{(\mu, \nu)}(y)$ are Jacobi polynomials, with $p = |\mathbf{p}|$. The corresponding wave functions in coordinate space are

$$\psi_{nLm}^{\text{h.o.}}(\mathbf{r}) = \left[\frac{2n!}{(n+L+\frac{1}{2})!} \right]^{\frac{1}{2}} \alpha^{L+\frac{3}{2}} e^{-\frac{\alpha^2 r^2}{2}} L_n^{L+\frac{1}{2}}(\alpha^2 r^2) \mathcal{Y}_{Lm}(\mathbf{r})$$

in the harmonic oscillator basis, and

$$\psi_{nLm}^{\text{St}}(\mathbf{r}) = \left[\frac{n!}{(n+2L+2)!} \right]^{\frac{1}{2}} (2\beta)^{L+\frac{3}{2}} e^{-\beta r} L_n^{2L+2}(2\beta r) \mathcal{Y}_{Lm}(\mathbf{r}) \quad (3.9)$$

in the Sturmian basis.

3.3 Hamiltonian

We use a non-relativistic quark model similar to that of Isgur and Karl [24, 25], with some of the modifications suggested by Capstick and Isgur [29, 71]. The Isgur-Karl model evolved from the pioneering work of others; an extensive list of references to the origins of the model can be found in Ref. [29].

The phenomenological Hamiltonian we use takes the form

$$H = \sum_{i=1}^3 K_i + \sum_{i<j=1}^3 (V_{\text{conf}}^{ij} + H_{\text{hyp}}^{ij}), \quad (3.10)$$

where $\sum_{i=1}^3 K_i$ is a sum of the kinetic energies of each quarks. For this, we use two forms, the usual non-relativistic form given by

$$K_i = \left(m_i + \frac{p_i^2}{2m_i} \right), \quad (3.11)$$

and a semirelativistic form given by

$$K_i = \sqrt{p_i^2 + m_i^2}. \quad (3.12)$$

The spin independent confining potential is a simplified version of that used by Capstick and Isgur [29], with

$$V_{\text{conf}}^{ij} = C_{qqq} + \frac{br_{ij}}{2} - \frac{2\alpha_{\text{Coul}}}{3r_{ij}}, \quad (3.13)$$

with $r_{ij} = |\mathbf{r}_i - \mathbf{r}_j|$. Here H_{hyp}^{ij} is the hyperfine interaction, assumed to have the form

$$H_{\text{hyp}}^{ij} = \frac{2\alpha_{\text{hyp}}}{3m_i m_j} \left\{ \frac{8\pi}{3} \mathbf{S}_i \cdot \mathbf{S}_j \delta^3(\mathbf{r}_{ij}) + \frac{1}{r_{ij}^3} \left[\frac{3(\mathbf{S}_i \cdot \mathbf{r}_{ij})(\mathbf{S}_j \cdot \mathbf{r}_{ij})}{r_{ij}^2} - \mathbf{S}_i \cdot \mathbf{S}_j \right] \right\} \quad (3.14)$$

The first term is a contact term, while the second is a tensor term. The spin-orbit interaction is neglected. We note here that α_{Coul} , α_{hyp} , b , C_{qqq} , and m_i are not fundamental, but are phenomenological parameters obtained from a fit to the spectrum of baryon states.

3.4 Obtaining the Form Factors

3.4.1 $B_Q \rightarrow B_q$

Here, we illustrate the procedure we follow to obtain the form factors, using the decay of the B_Q to the ground state B_q as an example. We note here that B_Q represents either Λ_Q or Ω_Q and B_q refers to any of the Λ_q , Ω_q or Ξ in their ground state. We begin with the vector current matrix element from Eq. (2.2), with the assumption that the parent B_Q is at rest and the daughter B_q has three momentum \mathbf{p} . The left-hand side of Eq. (2.2) is evaluated using the quark model, after the operator $V_\mu = \bar{q}\gamma_\mu Q$ has been reduced to its Pauli (non-relativistic) form. Specific values for the index μ are chosen, as well as specific values of s and s' . By making three sets of such choices, three equations for the F_i in terms of the quark-model matrix elements of three operators are obtained. This system of equations is then solved to obtain the expressions for the form factors. In the specific case at hand, choosing $s = s' = +1/2$ and $\mu = 0$, for instance, leads to

$$\begin{aligned} \langle B_q(\mathbf{p}, +) | \bar{q}\gamma_0 Q | B_Q(0, +) \rangle &= \int d^3 p'_\rho d^3 p'_\lambda d^3 p_\rho d^3 p_\lambda C^{A*} C^A \Psi_{B_q}^{*S}(+) \\ &\times \langle q'_1 q'_2 q | q^\dagger \gamma_0 Q | q_1 q_2 Q \rangle \Psi_{B_Q}^S(+). \end{aligned} \quad (3.15)$$

where

$$\langle q'_1 q'_2 q | q^\dagger \gamma_0 Q | q_1 q_2 Q \rangle = \langle q'_1 q'_2 | q_1 q_2 \rangle \langle q | q^\dagger \gamma_0 Q | Q \rangle.$$

In the specific case of $\Lambda_Q \rightarrow \Lambda_q$,

$$\langle B_q(\mathbf{p}, +) | \bar{q} \gamma_0 Q | B_Q(0, +) \rangle = F_1 + F_2 + F_3.$$

The matrix element $\langle q'_1 q'_2 | q_1 q_2 \rangle$ gives δ -functions in spin, momentum and flavor in the spectator approximation. Using the δ -functions in momentum and flavor, the integral is simplified to

$$\langle B_q(\mathbf{p}, +) | \mathcal{O}_0 | B_Q(\mathbf{0}, +) \rangle = \int d^3 p_\rho d^3 p_\lambda \psi_{B_q}^*(\mathbf{p}'_\rho, \mathbf{p}'_\lambda) \mathcal{A}_{B_Q B_q}^{++}(\mathcal{O}_0) \psi_{B_Q}(\mathbf{p}_\rho, \mathbf{p}_\lambda), \quad (3.16)$$

with $\mathbf{p}'_\rho = \mathbf{p}_\rho$, $\mathbf{p}'_\lambda = \mathbf{p}_\lambda - 2\sqrt{3/2} m_\sigma \mathbf{p} / m_{B_q}$, where m_σ is the mass of the light quark and $\mathcal{O}_0 = q^\dagger \gamma_0 Q$. It is useful for us to define

$$\mathcal{A}_{B_Q B_q}^{s's}(\mathcal{O}_\mu) = \chi_{B_q}^*(s') \delta_{s'_1 s_1} \delta_{s'_2 s_2} \langle q(\mathbf{p}'_3, s'_3) | \mathcal{O}_\mu | Q(\mathbf{p}_3, s_3) \rangle \chi_{B_Q}(s). \quad (3.17)$$

where $\mathbf{p}'_3 = \mathbf{p} - \sqrt{\frac{2}{3}} \mathbf{p}_\lambda$ and $\mathbf{p}_3 = -\sqrt{\frac{2}{3}} \mathbf{p}_\lambda$.

The spin structures of the Λ_q states that we consider are different from those of the Ω_q and Ξ states. It is therefore also useful to write the spin matrix elements explicitly for these two types of baryons. For $B = \Lambda$ we find that

$$\begin{aligned} \mathcal{A}_{\Lambda_Q \Lambda_q}^{++}(\mathcal{O}_\mu) &= \langle q(\mathbf{p}'_3, \uparrow) | \mathcal{O}_\mu | Q(\mathbf{p}_3, \uparrow) \rangle \\ \mathcal{A}_{\Lambda_Q \Lambda_q}^{+-}(\mathcal{O}_\mu) &= \langle q(\mathbf{p}'_3, \uparrow) | \mathcal{O}_\mu | Q(\mathbf{p}_3, \downarrow) \rangle, \end{aligned} \quad (3.18)$$

and for $B = \Omega$ or Ξ we have

$$\begin{aligned} \mathcal{A}_{\Omega_Q \Omega_q}^{++}(\mathcal{O}_\mu) &= \frac{1}{3} \langle q(\mathbf{p}'_3, \uparrow) | \mathcal{O}_\mu | Q(\mathbf{p}_3, \uparrow) \rangle + \frac{2}{3} \langle q(\mathbf{p}'_3, \downarrow) | \mathcal{O}_\mu | Q(\mathbf{p}_3, \downarrow) \rangle \\ \mathcal{A}_{\Omega_Q \Omega_q}^{+-}(\mathcal{O}_\mu) &= -\frac{1}{3} \langle q(\mathbf{p}'_3, \uparrow) | \mathcal{O}_\mu | Q(\mathbf{p}_3, \downarrow) \rangle, \end{aligned} \quad (3.19)$$

where both parent and daughter baryons are in the ground state in both sets of expressions.

Here we only show the structure of $\mathcal{A}_{B_Q B_q}^{++}(\mathcal{O}_\mu)$ for decays to a $J^P = 1/2^+$ baryon. The matrix elements $\langle q(\mathbf{p}'_3, s'_3) | \mathcal{O}_\mu | Q(\mathbf{p}_3, s_3) \rangle$ for various components of \mathcal{O}_μ with different possible combinations of spin projections are shown in Appendix A

After the spin matrix elements are evaluated, there remain the momentum integrals to be performed. These are done using both bases for the momentum wave function shown

earlier. The analytic results for the form factors for Λ_Q decaying into various Λ_q final states, as well as for the $\Omega_Q \rightarrow \Omega_q$ decays are given in Appendix C. For decays to excited states, the calculation of the form factors is a little more involved, but the basic idea is as outlined here.

3.4.2 $\Lambda_Q \rightarrow N$

For decays in which the daughter baryon is a nucleon, the procedure is much the same as outlined in the previous subsection, with one modification. To illustrate, let us take the specific example of $\Lambda_b \rightarrow p$. The flavor wave functions of these two states have been chosen to be

$$\phi_{\Lambda_b} = \frac{1}{\sqrt{2}}(ud - du)b, \quad \phi_p = uud. \quad (3.20)$$

For the transition to occur, the third quark in the parent baryon, the b quark, undergoes the transition $b \rightarrow u$, leaving a final state that is $\frac{1}{\sqrt{2}}(ud - du)u$. This has no overlap with the flavor wave function that we use for the proton. We must now permute the third quark with the first and second quarks, giving

$$\{13\} \frac{1}{\sqrt{2}}(ud - du)u = \frac{1}{\sqrt{2}}(udu - udu), \quad \{23\} \frac{1}{\sqrt{2}}(ud - du)u = \frac{1}{\sqrt{2}}(uud - duu), \quad (3.21)$$

both of which now have some overlap with the proton flavor wave function we use. This requires that the sum of matrix elements

$$\langle N(\mathbf{p}, +) | \{13\} O_i | \Lambda_Q(\mathbf{0}, +) \rangle + \langle N(\mathbf{p}, +) | \{23\} O_i | \Lambda_Q(\mathbf{0}, +) \rangle$$

be evaluated, where we apply the permutation to the wave function of the daughter nucleon. The permutation operators also transform the spin and momentum wave function of the nucleon. The transformed spin wave functions are

$$\{13\} \chi^\lambda(s) = -\frac{\sqrt{3}}{2} \chi^\rho(s) - \frac{1}{2} \chi^\lambda(s), \quad \{23\} \chi^\lambda(s) = \frac{\sqrt{3}}{2} \chi^\rho(s) - \frac{1}{2} \chi^\lambda(s). \quad (3.22)$$

After carrying out the transformation on the nucleon wave function, and using the fact that the ground state momentum space wave function is totally symmetric, we find

$$\langle p(\mathbf{p}, s) | O_i | \Lambda_Q(\mathbf{0}, s') \rangle = (-\sqrt{3/4}) \int d^3 p_\rho d^3 p_\lambda \psi_p^*(\mathbf{p}'_\rho, \mathbf{p}'_\lambda) A^{ss'}(O_i) \psi_{\Lambda_Q}(\mathbf{p}_\rho, \mathbf{p}_\lambda), \quad (3.23)$$

where $A^{ss'}(O_i)$ is the Pauli reduction of the operator O_i . The integrations required for the Λ_b to proton form factors are the same as those in Eq. (3.16) in the previous subsection, and

so the form factors are the same up to a multiplicative factor. For excited states, however, the procedure is slightly more involved, and is easily illustrated by examining the decays to the radially excited nucleon.

Assuming single components, the wave function of the radially excited state is

$$\Psi_{N,1/2_1^+ M} = \phi_N \psi_{000010}(\mathbf{p}_\rho, \mathbf{p}_\lambda) \chi_{1/2}^\lambda(M). \quad (3.24)$$

The $\{13\}$ transformation, acting on the spin-space part of this wave function, produces

$$\begin{aligned} \{13\} \Psi_{000010}(\mathbf{p}_\rho, \mathbf{p}_\lambda) \chi_{1/2}^\lambda(M) &= \Psi_{000010}(\mathbf{p}'_\rho, \mathbf{p}'_\lambda) \left[-\frac{\sqrt{3}}{2} \chi_{1/2}^\rho(M) - \frac{1}{2} \chi_{1/2}^\lambda(M) \right] \\ &= -\frac{1}{8} \left[\sqrt{27} \psi_{001000}(\mathbf{p}_\rho, \mathbf{p}_\lambda) \chi_{1/2}^\rho(M) + 3 \psi_{001000}(\mathbf{p}_\rho, \mathbf{p}_\lambda) \chi_{1/2}^\lambda(M) \right. \\ &\quad + \sqrt{3} \psi_{000010}(\mathbf{p}_\rho, \mathbf{p}_\lambda) \chi_{1/2}^\rho(M) + \psi_{000010}(\mathbf{p}_\rho, \mathbf{p}_\lambda) \chi_{1/2}^\lambda(M) \\ &\quad \left. + \sqrt{18} \psi_{000101}(\mathbf{p}'_\rho, \mathbf{p}_\lambda) \chi_{1/2}^\rho(M) + \sqrt{6} \psi_{000101}(\mathbf{p}_\rho, \mathbf{p}_\lambda) \chi_{1/2}^\lambda(M) \right], \end{aligned} \quad (3.25)$$

with a similar expression for the $\{23\}$ transformation. Here $\mathbf{p}_{\rho'} = \frac{1}{\sqrt{2}}(\mathbf{p}_3 - \mathbf{p}_2)$, $\mathbf{p}_{\lambda'} = \frac{1}{\sqrt{6}}(\mathbf{p}_3 + \mathbf{p}_2 - 2\mathbf{p}_1)$ are the Jacobi coordinates in the transformed basis. Of these components, only the first, third and fifth have spin wave functions that overlap with the decaying Λ_Q , while only the first and third have non-zero spatial overlaps. The integrals that arise from the first component are simply a numerical factor ($\sqrt{27}/8$) times those that arise in the $\Lambda_Q \rightarrow \Lambda_q$ matrix elements, for the radially excited Λ_q . The integrals that arise from the third term are also a numerical factor ($\sqrt{3}/8$) times the $\Lambda_Q \rightarrow \Lambda_q$ ground-state integrals, multiplied by a factor that arises from the spectator overlap. In this case, this overlap is expected to be small, since the spectators are in a radially excited state in the daughter baryon, but in their ground state in the parent.

3.4.3 $\Omega_c \rightarrow \Omega^{(*)}$

The calculation of form factors for $\Omega_c \rightarrow \Omega^{(*)}$ decays is very similar to that described in Section 3.4, but for a question of symmetry. The flavor wave functions of Ω_c and Ω are $\phi_{\Omega_c} = ssc$ and $\phi_\Omega = sss$. In a semileptonic decay process the charm quark of Ω_c decays into a s quark, which can be any of the three s quarks of the Ω . Thus, in analogy with the nucleon final states, we need to evaluate

$$\frac{1}{\sqrt{3}} \left(\langle \Omega(\mathbf{p}, +) | \mathcal{O}_\mu | \Omega_Q(\mathbf{0}, +) \rangle + \langle \Omega(\mathbf{p}, +) | \{13\} \mathcal{O}_\mu | \Omega_Q(\mathbf{0}, +) \rangle + \langle \Omega(\mathbf{p}, +) | \{23\} \mathcal{O}_\mu | \Omega_Q(\mathbf{0}, +) \rangle \right).$$

The factor $\frac{1}{\sqrt{3}}$ comes from the normalization. The wave functions for the Ω states are fully symmetric under interchange of any of the quarks, so each of the permuted matrix elements reproduces the unpermuted one. The result is that we must calculate

$$\sqrt{3}\langle\Omega(\mathbf{p}, +)|\mathcal{O}_\mu|\Omega_Q(\mathbf{0}, +)\rangle,$$

to obtain the form factors for $\Omega_c \rightarrow \Omega$.

3.4.4 The Sturmian Basis

The procedures described in the sections above are relatively straightforward to implement in the harmonic oscillator basis, largely due to the fact that the Moshinsky rotations have been treated by a number of authors, and are also fairly simple to calculate. In particular, the fact that the ‘permuted’ wave function can be written in terms of a finite set of transformed wave function components is another feature that makes the harmonic oscillator basis attractive for calculations like these. In the Sturmian basis, however, the permutation of particles requires an infinite sum of transformed wave functions. This sum could be truncated at some point in a calculation such as this. However, at this point we do not examine decays to daughter nucleons or Ω ’s in the Sturmian basis.

CHAPTER 4

Comparison of HQET and Quark Model Results

The analytic expressions that we obtain for the form factors are shown in Appendix C, for both the Sturmian and harmonic oscillator bases. The results shown there are valid when the wave function for a particular state is written as a single component, in either expansion basis.

As mentioned earlier, one of the advantages of the Sturmian basis is that it leads to form factors that behave like multipoles in the kinematic variable, and this is seen in the forms that we display. At this point, it is instructive to compare, as far as possible, these analytic forms with the predictions of HQET. While HQET does not give the explicit forms of the form factors, a number of relationships among the form factors are expected, and any model should reproduce these relationships. In what follows, we restrict our comparison to the predictions that are valid at the non-recoil point, as we have ignored any kinematic dependence beyond the Gaussian or multipole factors shown in Appendix C. In addition, we focus on the predictions for heavy to heavy transitions.

4.1 Λ_Q decay

4.1.1 Natural Parity Daughter Baryons

We begin by discussing the form factors for decays to daughter baryons of natural parity. In this work, this means daughter baryons with $J^P = 1/2^+$ (both ground state and first excited state), $J^P = 1/2^-$ and $3/2^-$ (which constitute a degenerate doublet when the daughter baryons are also treated as heavy) and $J^P = 3/2^+$ and $5/2^+$ (also a doublet). In our discussion of these results, we implicitly assume that the wave functions for the states are dominated by a single component of the wave function expansions that we use. These single-component wave functions have been described in Section 3.1.

For elastic decays, predictions have been made at least to order $1/m_q^2$ and $1/m_Q^2$. However, we will restrict our discussion to the predictions valid to order $1/m_q$ and $1/m_Q$. To this order, using the results of Falk and Neubert [72], the relationships among form factors are

$$\begin{aligned} F_2 &= G_2 = \frac{m_Q}{m_q} F_3 = -\frac{m_Q}{m_q} G_3, \\ F_1 &= G_1 - F_2 \left(1 + \frac{m_q}{m_Q} \right). \end{aligned} \quad (4.1)$$

Our expressions for the form factors satisfy these relationships, in both bases, to the appropriate order. In fact, the analytic forms obtained exactly match the structure predicted by HQET [72].

For the $(1/2^-, 3/2^-)$ doublet, there are 14 form factors in general, which Leibovitch and Stewart [41] write in terms of a number of universal functions and constants, valid at order $1/m_q$ and $1/m_Q$. Using their expressions, and writing form factors for the $1/2^-$ state as primed quantities, the relationships expected are

$$\begin{aligned} F'_1 &= \frac{1}{2\sqrt{3}m_q} (3m_Q - m_q) F_4, \\ F'_3 &= 3G'_3 + \frac{2}{\sqrt{3}} (G_3 - 2F_4), \\ F_3 &= -G_3, \quad G_2 = F_2, \quad F_1 - G_2 = G_3 - F_2, \\ G_4 &= -3F_4 + 2\sqrt{3}G'_3, \quad F'_2 - G'_2 = -\frac{2}{\sqrt{3}}G_3, \\ F'_2 + G'_2 + 2G'_1 &= \sqrt{3}F_4 \left(1 + \frac{m_Q}{m_q} \right) - 2G'_3 - \frac{2}{\sqrt{3}}G_3, \end{aligned} \quad (4.2)$$

where terms that vanish at the non-recoil point have been ignored. Our results for these states also satisfy all eight of the relationships shown above, in both bases. Thus, there is a very good correspondence between the predictions of HQET and those of the quark model that we use, and this correspondence is independent of the wave function basis chosen.

For the $(3/2^+, 5/2^+)$ doublet, the available predictions are at leading order, shown in Eqs. (2.23) and (2.24). These are also satisfied by our analytic expressions for the form factors, in both bases.

For the excited state with $J^P = 1/2_1^+$, the predictions of HQET are that the form factors should vanish at the non-recoil point, by reason of the orthogonality of the wave functions. In the treatments in the literature, this is achieved by assuming that the form factors have an explicit factor that vanishes as $w \rightarrow 1$. In the expressions that we have obtained for the

leading order form factors, this orthogonality arises explicitly from the size parameters of the wave functions.

It is instructive to examine the expression for F_1 for this decay, in the limit when the Hamiltonian is that of a harmonic oscillator. The expression for F_1 is

$$F_1 = I_H \frac{1}{2\alpha_{\lambda\lambda'}^2} \left[(\alpha_\lambda^2 - \alpha_{\lambda'}^2) - \frac{m_\sigma}{3\alpha_{\lambda\lambda'}^2} \left(\frac{\alpha_\lambda^2}{m_Q} (7\alpha_{\lambda'}^2 - 3\alpha_\lambda^2) - \frac{\alpha_{\lambda'}^2}{m_q} (7\alpha_\lambda^2 - 3\alpha_{\lambda'}^2) \right) \right], \quad (4.3)$$

where

$$I_H = \sqrt{\frac{3}{2}} \left(\frac{\alpha_\lambda^{3/2} \alpha_{\lambda'}^{3/2}}{\alpha_{\lambda\lambda'}^3} \right) \exp \left(-\frac{3m_\sigma^2 p^2}{2m_{\Lambda_q}^2 \alpha_{\lambda\lambda'}^2} \right). \quad (4.4)$$

In the above expressions, $\alpha_\lambda(\alpha_{\lambda'})$ is the size parameter of the initial (final) wave function associated with the Jacobi coordinate λ , and $\alpha_{\lambda\lambda'}^2 = (\alpha_\lambda^2 + \alpha_{\lambda'}^2)/2$. If the Hamiltonian is taken to be a harmonic oscillator of the form

$$V = \frac{K}{2} (|\mathbf{r}_1 - \mathbf{r}_2|^2 + |\mathbf{r}_1 - \mathbf{r}_3|^2 + |\mathbf{r}_2 - \mathbf{r}_3|^2) = 3K (\rho^2 + \lambda^2) \quad (4.5)$$

where \mathbf{r}_i is the position of the i -th quark and $\boldsymbol{\rho} = (\mathbf{r}_1 - \mathbf{r}_2)/\sqrt{2}$ and $\boldsymbol{\lambda} = (\mathbf{r}_1 + \mathbf{r}_2 - 2\mathbf{r}_3)/\sqrt{6}$ are the Jacobi coordinates, then

$$\alpha_\lambda = \left(\frac{3Km_\sigma m_Q}{m_Q + 2m_\sigma} \right)^{1/4}, \quad \alpha_{\lambda'} = \left(\frac{3Km_\sigma m_q}{m_q + 2m_\sigma} \right)^{1/4}. \quad (4.6)$$

With these forms, the term in F_1 proportional to m_σ (mass of the light quark) vanishes identically, while the term in $(\alpha_\lambda^2 - \alpha_{\lambda'}^2)$ becomes proportional to $1/m_q - 1/m_Q$, and so vanishes in the heavy quark limit. The terms in p^2 , which we do not include here, will be those that contribute, despite the orthogonality of the wave functions, as expected. Note that even though the p^2 terms will appear with explicit factors of $1/m_q^2$, p will range from small values (of order Λ_{QCD}), to a maximum of $(m_{\Lambda_Q}^2 - m_{\Lambda_q}^2)/(2m_{\Lambda_Q})$. Such terms are therefore not necessarily negligible. However, in the non-relativistic model that we use for the form factors, we have neglected such terms.

4.1.2 Unnatural Parity Daughter Baryons

For the decays to baryons with unnatural parity, HQET predicts that the form factors should vanish at leading order. In the present model, we first have to identify such states, which we

do in the heavy quark limit, using the single-component wave functions. The wave functions of interest are

$$\begin{aligned}
\Psi_{\Lambda_Q, 1/2^+ M} &= \phi_\Lambda [\psi_{000101}(\mathbf{p}_\rho, \mathbf{p}_\lambda) \chi_{1/2}^\lambda(M - M_L)]_{1/2, M}, \\
\Psi_{\Lambda_Q, 3/2^+ M} &= \phi_\Lambda [\psi_{000101}(\mathbf{p}_\rho, \mathbf{p}_\lambda) \chi_{3/2}^S(M - M_L)]_{3/2, M}, \\
\Psi_{\Lambda_Q, 3/2^- M} &= \phi_\Lambda [\psi_{1M_L 0100}(\mathbf{p}_\rho, \mathbf{p}_\lambda) \chi_{3/2}^S(M - M_L)]_{3/2, M}, \\
\Psi_{\Lambda_Q, 5/2^- M} &= \phi_\Lambda [\psi_{1M_L 0100}(\mathbf{p}_\rho, \mathbf{p}_\lambda) \chi_{3/2}^S(M - M_L)]_{5/2, M}.
\end{aligned} \tag{4.7}$$

In the spectator assumption that we use, none of these states have any overlap with the ground state parent Λ_Q . In fact, there is a ‘two-fold’ orthogonality at play. The spin wave function of the two spectator quarks is orthogonal to the corresponding wave function in the parent baryon. The spatial wave functions of these two quarks are also orthogonal in parent and daughter. Thus, decays to these states will only occur through configuration mixing in the wave function, induced by various terms in the Hamiltonian.

In the model that we use, configuration mixing in the spin wave functions arises from hyperfine terms involving the heavy quark, which means that such mixing will be small. Thus we expect that decays to such states should be significantly suppressed. Interestingly, the suppression of the decays to these unnatural parity doublets persists as the mass of the heavy quark in the daughter baryon is decreased, as such configuration mixing remains small. In this case, even though the definition of unnatural parity is different for light states, there are still a number of decays (in $\Lambda_c \rightarrow \Lambda$, for instance) that are predicted to be significantly suppressed. We will comment on this later, when we examine the numerical results of our model.

4.2 Ω_Q decay

The quark model states we use are constructed in the coupling scheme

$$|J^P, L, S \rangle = |[(\ell_\rho \ell_\lambda)_L (s_{12} s_3)]_J \rangle, \tag{4.8}$$

where the notation $(ab)_c$ means angular momenta a and b are added vectorially to give angular momentum c . The parity P is $(-1)^{\ell_\rho + \ell_\lambda}$, the total spin of the two light quarks in the baryon is s_{12} , and s_3 is the spin of the third quark, taken to be the heavy quark when the baryon contains a heavy quark.

The HQET states are assumed to have the coupling scheme

$$|J^P, j \rangle = \left| \left\{ [(\ell_\rho \ell_\lambda)_L s_{12}]_j s_3 \right\}_J \right\rangle, \quad (4.9)$$

where j is the total spin of the light component of the baryon, so that $J = j \pm 1/2$. The states of one coupling scheme are linear combinations of the states of the second. In particular, we find

$$\begin{aligned} & \left| \left\{ [(\ell_\rho \ell_\lambda)_L s_{12}]_j s_3 \right\}_J \right\rangle = (-1)^{1/2+s_{12}+L+J} \sqrt{2j+1} \\ & \times \sum_S \sqrt{2S+1} \left\{ \begin{array}{ccc} 1/2 & s_{12} & S \\ L & J & j \end{array} \right\} \left| [(\ell_\rho \ell_\lambda)_L (s_{12} s_3)_S]_J \right\rangle, \end{aligned} \quad (4.10)$$

where $\left\{ \begin{array}{ccc} 1/2 & s_{12} & S \\ L & J & j \end{array} \right\}$ is a 6-J symbol.

For the states that we consider, the explicit expressions for the HQET states in terms of the quark model ones are

$$\begin{aligned} |1/2^-, j=1\rangle &= \sqrt{\frac{2}{3}} |1/2^-, L=1, S=1/2\rangle + \frac{1}{\sqrt{3}} |1/2^-, L=1, S=3/2\rangle, \\ |1/2^-, j=0\rangle &= -\frac{1}{\sqrt{3}} |1/2^-, L=1, S=1/2\rangle + \sqrt{\frac{2}{3}} |1/2^-, L=1, S=3/2\rangle, \\ |3/2^-, j=2\rangle &= \sqrt{\frac{5}{6}} |3/2^-, L=1, S=1/2\rangle + \frac{1}{\sqrt{6}} |3/2^-, L=1, S=3/2\rangle, \\ |3/2^-, j=1\rangle &= -\frac{1}{\sqrt{6}} |3/2^-, L=1, S=1/2\rangle + \sqrt{\frac{5}{6}} |3/2^-, L=1, S=3/2\rangle, \\ |3/2^+, j=2\rangle &= \frac{1}{\sqrt{2}} (|3/2^+, L=2, S=1/2\rangle + |3/2^+, L=2, S=3/2\rangle), \\ |3/2^+, j=1\rangle &= \frac{1}{\sqrt{2}} (-|3/2^+, L=2, S=1/2\rangle + |3/2^+, L=2, S=3/2\rangle), \\ |5/2^+, j=3\rangle &= \frac{\sqrt{7}}{3} |5/2^+, L=2, S=1/2\rangle + \frac{\sqrt{2}}{3} |5/2^+, L=2, S=3/2\rangle, \\ |5/2^+, j=2\rangle &= -\frac{\sqrt{2}}{3} |5/2^+, L=2, S=1/2\rangle + \frac{\sqrt{7}}{3} |5/2^+, L=2, S=3/2\rangle. \end{aligned} \quad (4.11)$$

For all of the quark model states shown on the r.h.s of these equations, $S = 1/2$ corresponds to spin wave function of the χ^λ type. The form factors that describe transitions to these states are shown in Appendix C.3.

Other states not shown above are single component states in both representations, and

these are

$$\begin{aligned}
|1/2^+, j = 1\rangle &= |1/2^+, L = 0, S = 1/2\rangle, \\
|3/2^+, j = 1\rangle &= |3/2^+, L = 0, S = 3/2\rangle, \\
|1/2_1^+, j = 1\rangle &= |1/2_1^+, L = 0, S = 1/2\rangle, \\
|3/2_1^+, j = 1\rangle &= |3/2_1^+, L = 0, S = 3/2\rangle, \\
|1/2_2^+, j = 1\rangle &= |1/2_2^+, L = 2, S = 3/2\rangle, \\
|5/2^-, j = 2\rangle &= |5/2^-, L = 1, S = 3/2\rangle.
\end{aligned} \tag{4.12}$$

The subscripts ‘1’ denotes the first radially-excited copy of the ground state multiplet. The ‘2’ denotes an orbitally-excited state with $J^P = 1/2^+$. This state forms an $j = 1$ multiplet with the second $3/2^+$ state listed in Eq. (4.11).

We now examine the form factors of Appendix C.3, along with some of the form factors in Appendix C, and compare these with the predictions of HQET shown in Section 2.3.5. We begin with a discussion of the decays to pseudotensor final states.

4.2.1 $1/2^-$

The HQET predictions for decays to this state are shown in Eq. (2.39), while the quark model form factors are shown in Section C.3.1. Noting that $w - 1 \approx \mathcal{O}(1/m_q)$, the leading order predictions are that $F_1 = F_2 = G_2 = 0$, and $F_3 = -G_3 = G_1$. The form factors of Section C.3.1 satisfy these relations, and allow us to identify

$$\eta_2^{(0)} = \frac{m_\sigma}{\alpha_\lambda} \left(\frac{\alpha_\lambda \alpha_{\lambda'}}{\alpha_{\lambda\lambda'}^2} \right)^{5/2} \exp \left(-\frac{3m_\sigma^2}{2m_{\Omega_q}^2} \frac{p^2}{\alpha_{\lambda\lambda'}^2} \right),$$

in the harmonic oscillator models, or

$$\eta_2^{(0)} = \frac{m_\sigma}{\beta_\lambda} \sqrt{2} \frac{\left(\frac{\beta_\lambda \beta_{\lambda'}}{\beta_{\lambda\lambda'}^2} \right)^{5/2}}{\left[1 + \frac{3}{2} \frac{m_\sigma^2}{m_{\Omega_q}^2} \frac{p^2}{\beta_{\lambda\lambda'}^2} \right]^3} \tag{4.13}$$

in the Sturmian models.

4.2.2 $(1/2^+, 3/2^+)$

The HQET predictions for decays to this state are shown in Eqs. (2.40) and (2.41). As there are three multiplets with these quantum numbers, we discuss each one separately.

Ground State

The quark model form factors for the ground state doublet are shown in Sections C.2.1 and C.2.8. Comparison of these form factors with the predictions of HQET leads to

$$\eta_2^{(1)} = -\frac{1}{2}\eta_1^{(1)} \quad (4.14)$$

at the non-recoil point, and allows us to identify

$$\eta_1^{(1)} = \left(\frac{\alpha_\lambda \alpha_{\lambda'}}{\alpha_{\lambda\lambda'}^2} \right)^{3/2} \exp \left(-\frac{3m_\sigma^2}{2m_{\Omega_q}^2} \frac{p^2}{\alpha_{\lambda\lambda'}^2} \right), \quad (4.15)$$

in the harmonic oscillator models, or

$$\eta_1^{(1)} = \frac{\left(\frac{\beta_\lambda \beta_{\lambda'}}{\beta_{\lambda\lambda'}^2} \right)^{3/2}}{\left[1 + \frac{3}{2} \frac{m_\sigma^2}{m_{\Omega_q}^2} \frac{p^2}{\beta_{\lambda\lambda'}^2} \right]^3} \quad (4.16)$$

in the Sturmian models. In the heavy quark limit, both forms yield the expected normalization at the non-recoil point, namely $\eta_1^{(1)}(w=1) = 1$. It must be emphasized that the relationship between $\eta_1^{(1)}$ and $\eta_2^{(1)}$ given above is one that arises only in the context of the quark model. In HQET, these two Isgur-Wise functions are *a priori* independent of each other. A more complete expression of the relationship between $\eta_1^{(1)}$ and $\eta_2^{(1)}$ can be obtained by noting that G_2 and G_3 for the $1/2^+$ final state both vanish at leading order in the quark model. This leads to

$$\eta_1^{(1)}(w) = -(1+w)\eta_2^{(1)}(w), \quad (4.17)$$

valid at leading order in the heavy quark expansion.

Radial Excitation

The form factors for decays to the radially excited $(1/2^+, 3/2^+)$ multiplet are shown in Sections C.2.2 and C.2.9. Comparison of these form factors with the predictions of HQET again leads to

$$\eta_2^{(1)} = -\frac{1}{2}\eta_1^{(1)}, \quad (4.18)$$

and allows us to identify

$$\eta_1^{(1)} = \sqrt{\frac{3}{8}} \frac{\alpha_\lambda^2 - \alpha_{\lambda'}^2}{\alpha_\lambda \alpha_{\lambda'}} \left(\frac{\alpha_\lambda \alpha_{\lambda'}}{\alpha_{\lambda\lambda'}^2} \right)^{5/2} \exp \left(-\frac{3m_\sigma^2}{2m_{\Omega_q}^2} \frac{p^2}{\alpha_{\lambda\lambda'}^2} \right), \quad (4.19)$$

in the harmonic oscillator models, or

$$\eta_1^{(1)} = \frac{\sqrt{3} \beta_\lambda^2 - \beta_{\lambda'}^2}{4 \beta_\lambda \beta_{\lambda'}} \frac{\left(\frac{\beta_\lambda \beta_{\lambda'}}{\beta_{\lambda\lambda'}^2}\right)^{3/2}}{\left[1 + \frac{3}{2} \frac{m_\sigma^2}{m_{\Omega_q}^2} \frac{p^2}{\beta_{\lambda\lambda'}^2}\right]^3} \quad (4.20)$$

in the Sturmian models. As with decays to the ground state multiplet, the full relationship between $\eta_1^{(1)}$ and $\eta_2^{(1)}$ can be deduced to be

$$\eta_1^{(1)}(w) = -(1+w)\eta_2^{(1)}(w), \quad (4.21)$$

valid at leading order in the heavy quark expansion.

Orbital Excitation

The orbitally excited $(1/2^+, 3/2^+)$ multiplet has a very different structure from either of the two multiplets discussed previously, and the form factors that are non-vanishing at leading order are different. For the ground state and radially excited multiplets, F_1 , F_2 , F_3 and G_1 are the non-vanishing form factors at leading order for the $1/2^+$ state, for instance, and this pattern is repeated with the radially excited multiplet (ignoring, for the moment, the fact that $\alpha_\lambda^2 - \alpha_{\lambda'}^2 \approx \mathcal{O}(1/m_q)$). For the orbitally excited states, whose form factors are shown in Sections C.2.3 and C.3.3, the pattern is different, with G_2 and G_3 being the non-vanishing form factors for the $1/2^+$ state.

Comparing these quark model form factors with the predictions of HQET allows us to deduce that

$$\begin{aligned} \eta_1^{(1)} &= 0, \\ \eta_2^{(1)} &= -\sqrt{\frac{27}{10}} \frac{m_\sigma^2}{\alpha_\lambda^2} \left(\frac{\alpha_\lambda \alpha_{\lambda'}}{\alpha_{\lambda\lambda'}^2}\right)^{7/2} \exp\left(-\frac{3m_\sigma^2}{2m_{\Omega_q}^2} \frac{p^2}{\alpha_{\lambda\lambda'}^2}\right) \end{aligned} \quad (4.22)$$

in the harmonic oscillator basis, or

$$\begin{aligned} \eta_1^{(1)} &= 0, \\ \eta_2^{(1)} &= -\frac{9}{\sqrt{5}} \frac{m_\sigma^2}{\beta_\lambda^2} \frac{\left(\frac{\beta_\lambda \beta_{\lambda'}}{\beta_{\lambda\lambda'}^2}\right)^{7/2}}{\left[1 + \frac{3}{2} \frac{m_\sigma^2}{m_{\Omega_q}^2} \frac{p^2}{\beta_{\lambda\lambda'}^2}\right]^4} \end{aligned} \quad (4.23)$$

in the Sturmian basis.

4.2.3 $(3/2^-, 5/2^-)$

The HQET predictions for this multiplet are shown in Eqs. (2.42) and (2.43), while the quark model predictions for these states are shown in Sections C.2.12 and C.3.6. Comparison of these two sets of equations yields

$$\eta_1^{(2)}(w) = -(1+w)\eta_2^{(2)}(w) = -\sqrt{3}\frac{m_\sigma}{\alpha_\lambda} \left(\frac{\alpha_\lambda\alpha_{\lambda'}}{\alpha_{\lambda\lambda'}^2}\right)^{5/2} \exp\left(-\frac{3m_\sigma^2}{2m_{\Omega_q}^2}\frac{p^2}{\alpha_{\lambda\lambda'}^2}\right) \quad (4.24)$$

in the harmonic oscillator models, or

$$\eta_1^{(2)}(w) = -(1+w)\eta_2^{(2)}(w) = -\sqrt{6}\frac{m_\sigma}{\beta_\lambda} \frac{\left(\frac{\beta_\lambda\beta_{\lambda'}}{\beta_{\lambda\lambda'}^2}\right)^{5/2}}{\left[1 + \frac{3}{2}\frac{m_\sigma^2}{m_{\Omega_q}^2}\frac{p^2}{\beta_{\lambda\lambda'}^2}\right]^3} \quad (4.25)$$

in the Sturmian models.

4.2.4 $(5/2^+, 7/2^+)$

The HQET predictions for this multiplet are shown in Eqs. (2.44) and (2.45), while the quark model predictions for the $5/2^+$ state are shown in section C.3.8. We have not calculated the form factors for the $7/2^+$ state in our models. Comparison of the HQET predictions with the results of the quark model calculation yields

$$\eta_1^{(3)}(w) = -(1+w)\eta_2^{(3)}(w) = -\frac{3}{\sqrt{2}}\frac{m_\sigma^2}{\alpha_\lambda^2} \left(\frac{\alpha_\lambda\alpha_{\lambda'}}{\alpha_{\lambda\lambda'}^2}\right)^{7/2} \exp\left(-\frac{3m_\sigma^2}{2m_{\Omega_q}^2}\frac{p^2}{\alpha_{\lambda\lambda'}^2}\right) \quad (4.26)$$

in the harmonic oscillator models, or

$$\eta_1^{(3)}(w) = -(1+w)\eta_2^{(3)}(w) = -3\sqrt{3}\frac{m_\sigma^2}{\beta_\lambda^2} \frac{\left(\frac{\beta_\lambda\beta_{\lambda'}}{\beta_{\lambda\lambda'}^2}\right)^{7/2}}{\left[1 + \frac{3}{2}\frac{m_\sigma^2}{m_{\Omega_q}^2}\frac{p^2}{\beta_{\lambda\lambda'}^2}\right]^4} \quad (4.27)$$

in the Sturmian models.

We now turn to a discussion of the decays to daughter baryons having tensor light diquark. We note, first that there exists a $1/2^+$, $j = 0$ singlet state. At leading order, the form factors for decays to such a state vanish in HQET. In the quark model, such a state can be constructed, but the overlap of its wave function with that of the decaying parent baryon is zero to the approximation to which we work, and is strongly suppressed beyond that. Thus we do not have form factors for such a state. For the remaining decays of this type, there is a single Isgur-Wise type form factor.

4.2.5 $(1/2^-, 3/2^-)$

The HQET predictions for this multiplet are shown in Eqs. (2.47) and (2.48), while the quark model predictions are shown in Sections C.3.2 and C.3.5. Comparison of these two sets yields

$$\tau^{(1)} = \sqrt{\frac{3}{2}} \frac{m_\sigma}{\alpha_\lambda} \left(\frac{\alpha_\lambda \alpha_{\lambda'}}{\alpha_{\lambda\lambda'}^2} \right)^{7/2} \exp \left(-\frac{3m_\sigma^2}{2m_{\Omega_q}^2} \frac{p^2}{\alpha_{\lambda\lambda'}^2} \right) \quad (4.28)$$

in the harmonic oscillator models, or

$$\tau^{(1)} = \sqrt{3} \frac{m_\sigma}{\beta_\lambda} \frac{\left(\frac{\beta_\lambda \beta_{\lambda'}}{\beta_{\lambda\lambda'}^2} \right)^{5/2}}{\left[1 + \frac{3}{2} \frac{m_\sigma^2}{m_{\Omega_q}^2} \frac{p^2}{\beta_{\lambda\lambda'}^2} \right]^3} \quad (4.29)$$

in the Sturmian model.

4.2.6 $(3/2^+, 5/2^+)$

The HQET predictions for this multiplet are shown in Eqs. (2.49) and (2.50), while the quark model predictions are shown in Sections C.3.4 and C.3.7. Comparison of these two sets yields

$$\tau^{(2)} = \sqrt{3} \frac{m_\sigma^2}{\alpha_\lambda^2} \left(\frac{\alpha_\lambda \alpha_{\lambda'}}{\alpha_{\lambda\lambda'}^2} \right)^{5/2} \exp \left(-\frac{3m_\sigma^2}{2m_{\Omega_q}^2} \frac{p^2}{\alpha_{\lambda\lambda'}^2} \right) \quad (4.30)$$

in the harmonic oscillator models, or

$$\tau^{(2)} = 3\sqrt{2} \frac{m_\sigma^2}{\beta_\lambda^2} \frac{\left(\frac{\beta_\lambda \beta_{\lambda'}}{\beta_{\lambda\lambda'}^2} \right)^{5/2}}{\left[1 + \frac{3}{2} \frac{m_\sigma^2}{m_{\Omega_q}^2} \frac{p^2}{\beta_{\lambda\lambda'}^2} \right]^3} \quad (4.31)$$

in the Sturmian model.

CHAPTER 5

Numerical Results

5.1 Model Parameters, Mass Spectra and Wave Functions

In Section 3.3, we introduced the two Hamiltonians we diagonalize to obtain the baryon spectrum. They differ only in the form chosen for the kinetic portion, one of which is non-relativistic (NR), while the other is semirelativistic (SR). In addition, we use two different expansion bases to obtain the wave functions: the harmonic oscillator (HO) basis, and the Sturmian (ST) basis. In the following, the four spectra we obtain will be denoted HONR, HOSR, STNR and STSR, in what should be an obvious notation.

Table 5.1: Hamiltonian parameters obtained from the four different fits. In the first column, HO refers to the harmonic oscillator basis, while ST refers to the Sturmian basis. In the same column, NR indicates a non-relativistic Hamiltonian, while SR indicates a semirelativistic one. The form of the Hamiltonian is described in Section 3.3.

model	m_σ (GeV)	m_s (GeV)	m_c (GeV)	m_b (GeV)	b (GeV ²)	α_{Coul}	α_{hyp}	C_{qqq} (GeV)
HONR	0.40	0.65	1.89	5.28	0.14	0.45	0.81	-1.20
HOSR	0.38	0.61	1.83	5.17	0.17	0.09	0.26	-1.45
STNR	0.40	0.64	1.89	5.29	0.13	0.41	0.31	-1.18
STSR	0.34	0.57	1.78	5.22	0.15	0.19	0.11	-1.23

There are eight free parameters to be obtained for each spectrum: four quark masses (m_σ , m_s , m_c and m_b), and 4 parameters of the potential (α_{hyp} , α_{Coul} , b and C_{qqq}). We have investigated the effects of a tensor interaction in the two harmonic oscillator models, and found the effects to be small. In the results we present, the tensor interaction has been

ignored. The eight parameters are determined from a ‘variational diagonalization’ of the Hamiltonian. The variational parameters are the size parameters α_ρ and α_λ of Eq. (3.7), or β_ρ and β_λ of Eq. (3.8). This variational diagonalization is accompanied by a fit to the known spectrum. In this fit, the eight parameters mentioned before are varied. The values we obtain for the Hamiltonian parameters are shown in Table 5.1, while some of the wave function size parameters are shown in Tables 5.2 and 5.3.

Table 5.2: Wave function size parameters, α_ρ and α_λ , for states of different J^P and with spin-flavor antisymmetric light diquark, in different models. All values are in GeV. For the Sturmian basis, the size parameters have been denoted β in the text.

J^P	model	Λ_b	Λ_c	Λ	N
		$(\alpha_\lambda, \alpha_\rho)$	$(\alpha_\lambda, \alpha_\rho)$	$(\alpha_\lambda, \alpha_\rho)$	$(\alpha_\lambda, \alpha_\rho)$
1/2 ⁺	HONR	(0.59, 0.61)	(0.55, 0.58)	(0.49, 0.53)	0.48
1/2 ⁺	HOSR	(0.68, 0.68)	(0.60, 0.61)	(0.52, 0.57)	0.54
1/2 ⁺	STNR	(0.44, 0.66)	(0.41, 0.69)	(0.35, 0.75)	-
1/2 ⁺	STSR	(0.46, 0.64)	(0.43, 0.67)	(0.38, 0.72)	-
1/2 ⁻	HONR	-	(0.47, 0.49)	(0.40, 0.47)	0.37
1/2 ⁻	HOSR	-	(0.55, 0.59)	(0.48, 0.54)	0.46
1/2 ⁻	STNR	-	(0.60, 0.50)	(0.55, 0.54)	-
1/2 ⁻	STSR	-	(0.61, 0.49)	(0.58, 0.51)	-
3/2 ⁺	HONR	-	-	-	0.35
3/2 ⁺	HOSR	-	-	-	0.44
5/2 ⁺	HONR	-	-	-	0.35
5/2 ⁺	HOSR	-	-	-	0.46

We note that the value of b , the slope of the linear potential, tends to be smaller than in most published studies of the baryon spectrum. The same is true for the strength of the hyperfine interaction, α_{hyp} . In the case of the latter, the small strength arises because the hyperfine interaction is treated as a contact interaction, and this can lead to very strong attractive forces between the quarks. One result of this is that, for sufficiently large values of α_{hyp} , the masses of the lightest baryon states can become negative. The small value of this parameter that results from our fits is therefore driven largely by the need for positive baryon masses. One direct consequence is that hyperfine splittings are not well reproduced in all but the HONR model, with the $\Delta - N$ mass splitting being about one third of its experimental value. In general, we allow the values of α_ρ to be different from α_λ . The exceptions occur

Table 5.3: Wave function size parameters, α_ρ and α_λ , for states of different J^P and with spin-flavor symmetric light diquark, in different models. All values are in GeV.

J^P	model	Ω_b	Ω_c	Ξ	Ω
		$(\alpha_\lambda, \alpha_\rho)$	$(\alpha_\lambda, \alpha_\rho)$	$(\alpha_\lambda, \alpha_\rho)$	$(\alpha_\lambda, \alpha_\rho)$
1/2 ⁺	HONR	(0.68, 0.49)	(0.64, 0.49)	(0.50, 0.55)	0.54
1/2 ⁺	HOSR	(0.68, 0.52)	(0.61, 0.51)	(0.52, 0.57)	0.53
1/2 ⁺	STNR	(0.61, 0.43)	(0.62, 0.42)	(0.41, 0.46)	-
1/2 ⁺	STSR	(0.63, 0.50)	(0.64, 0.50)	(0.51, 0.56)	-
1/2 ⁻	HONR	-	(0.54, 0.44)	(0.39, 0.44)	0.44
1/2 ⁻	HOSR	-	(0.56, 0.49)	(0.45, 0.50)	0.49
1/2 ⁻	STNR	-	(0.61, 0.43)	(0.44, 0.60)	-
1/2 ⁻	STSR	-	(0.66, 0.48)	(0.49, 0.65)	-
3/2 ⁺	HONR	-	(0.56, 0.46)	(0.39, 0.44)	0.45
3/2 ⁺	HOSR	-	(0.58, 0.50)	(0.45, 0.50)	0.49
3/2 ⁺	STNR	-	(0.64, 0.40)	(0.37, 0.42)	-
3/2 ⁺	STSR	-	(0.66, 0.48)	(0.46, 0.51)	-
5/2 ⁻	HONR	-	(0.52, 0.44)	(0.38, 0.43)	0.42
5/2 ⁻	HOSR	-	(0.55, 0.49)	(0.45, 0.50)	0.48
5/2 ⁻	STNR	-	(0.61, 0.43)	(0.52, 0.57)	-
5/2 ⁻	STSR	-	(0.66, 0.48)	(0.65, 0.70)	-

in cases when the three quarks are identical, as they are in the nucleon or the Ω . In that case, the variational diagonalization automatically selects $\alpha_\rho = \alpha_\lambda$. In Tables 5.2 and 5.3, we show only some values of the size parameters. Table 5.2 shows the size parameters of Λ_Q baryons and nucleons, while Table 5.3 shows the corresponding parameters of Ω_Q and Ξ baryons. The other size parameters, for the states that are significant for this work, are related to those presented. For instance, for the $1/2_1^+$ states, the size parameters are the same as for the $1/2^+$ states. Furthermore, since we do not include a spin-orbit interaction in our Hamiltonian, the size parameters for the $1/2^-$ and $3/2^-$ states are identical. We do not show the size parameters for the Λ_Q states with $Q = c, s$ and $J^P = 3/2^+$ or $5/2^+$, nor do we show Ξ, Ω_Q states with $Q = c, s$ and $J^P = 5/2^+$ or $7/2^+$ mainly because we find that semileptonic decay rates to these states are very small.

5.1.1 Mass Spectra

Portions of the four mass spectra we obtain are shown in Tables 5.4 and 5.5. In these tables, the first two columns identify the state and its experimental mass, while the next four columns show the masses that result from the models that we use. The small hyperfine interaction that we alluded to in the previous subsection has resulted in ground state nucleons that are too heavy, in all models. In addition, the ground state Δ (not shown in the tables) is too light in all models. Similar patterns emerge when the various Λ_Q and Σ_Q (not shown) states are compared. The size of this interaction also results in ‘radial’ excitations that are too heavy, even heavier than usually result in models like these. We note, too, that the different

Table 5.4: Baryon masses in GeV fitted in different quark models. The first two columns identify the state and its experimental mass, while the next four columns show the masses that result from the models that we use.

State	Experimental Mass	HONR	HOSR	STNR	STSR
$N(1/2^+)$	0.94	1.00	1.08	1.08	1.08
$N(1/2_1^+)$	1.44	1.76	1.60	1.81	1.70
$N(1/2^-)$	1.54	1.45	1.44	1.50	1.47
$N(3/2^-)$	1.52	1.45	1.44	1.50	1.47
$N(3/2^+)$	1.72	1.72	1.69	1.78	1.77
$N(5/2^+)$	1.68	1.72	1.69	1.78	1.77
$\Lambda(1/2^+)$	1.12	1.23	1.23	1.12	1.10
$\Lambda(1/2_1^+)$	1.60	1.73	1.81	1.61	1.55
$\Lambda(1/2^-)$	1.41	1.54	1.62	1.50	1.56
$\Lambda(3/2^-)$	1.52	1.54	1.62	1.50	1.56
$\Lambda(3/2^+)$	1.89	1.81	1.81	1.77	1.87
$\Lambda(5/2^+)$	1.82	1.82	1.81	1.77	1.87
$\Lambda_c(1/2^+)$	2.28	2.35	2.32	2.26	2.22
$\Lambda_c(1/2^-)$	2.59	2.61	2.70	2.61	2.68
$\Lambda_c(3/2^-)$	2.63	2.61	2.70	2.61	2.68
$\Lambda_b(1/2^+)$	5.62	5.62	5.62	5.62	5.62

models give very similar results for many of the states such as the $N(1/2^+)$, $N(1/2^-)$, $\Lambda(1/2^+)$ and $\Lambda_b(1/2^+)$, for instance, but for some states such as $N(1/2_1^+)$ (1440), there are striking differences in the masses obtained. To obtain the results shown in Tables 5.4 and 5.5, we fit the hamiltonian parameters only to those states where the experimental masses

are known. We note that for the Ω and Ξ states, the predicted masses are in satisfactory agreement with the available experimental values.

Table 5.5: Baryon masses in GeV in different quark models. Hamiltonian parameters for each model are fit to the experimental masses where known; the other masses are predictions of each quark models. The first two columns identify the state and its experimental mass, while the next four columns show the masses that result from the models that we use.

State	Experimental Mass	HONR	HOSR	STNR	STSR
$\Xi(1/2^+)$	1.32	1.36	1.43	1.43	1.42
$\Xi(1/2_1^+(\text{rad}))$		2.04	1.93	2.10	2.00
$\Xi(1/2_2^+(\text{orb}))$		2.29	2.08	2.24	2.18
$\Xi(3/2^+)$	1.53	1.51	1.50	1.49	1.47
$\Xi(3/2_1^+(\text{rad}))$		2.12	2.03	2.25	2.16
$\Xi(3/2_2^+(\text{orb}))$		2.15	2.05	2.41	2.35
$\Xi(3/2^-)$	1.82	1.83	1.79	1.89	1.89
$\Xi(5/2^-)$		1.84	1.80	1.83	1.89
$\Omega(3/2^+)$	1.67	1.67	1.67	1.63	1.62
$\Omega(3/2_1^+(\text{rad}))$		2.19	2.14	2.38	2.24
$\Omega(3/2_2^+(\text{orb}))$		2.24	2.21	2.21	2.24
$\Omega(1/2_1^+(\text{rad}))$		2.40	2.09	2.28	2.18
$\Omega(1/2_2^+(\text{orb}))$		2.41	2.22	2.53	2.24
$\Omega(3/2^-)$		1.97	1.95	1.93	1.95
$\Omega(5/2^-)$		1.97	1.95	1.94	1.96
$\Omega_c(1/2^+)$		2.70	2.70	2.74	2.74
$\Omega_c(1/2_1^+(\text{rad}))$	3.22		3.17	3.29	3.24
$\Omega_c(1/2_2^+(\text{orb}))$	3.35		3.24	3.34	3.34
$\Omega_c(3/2^+)$	2.76		2.74	2.76	2.72
$\Omega_c(3/2_1^+(\text{rad}))$	3.23		3.19	3.33	3.26
$\Omega_c(3/2_2^+(\text{orb}))$	3.26		3.23	3.30	3.33
$\Omega_c(1/2^-)$	3.02		3.00	3.08	3.06
$\Omega_c(5/2^-)$	3.02		3.00	3.08	3.06
$\Omega_b(1/2^+)$		6.04	6.01	6.09	6.09

5.1.2 Wave Functions

For many of the states that we treat, the wave functions that result are, to a very good approximation, the single component wave functions shown in Section 3.1. This turns out to be a particularly good approximation for the orbitally excited states such as the $1/2^-$

and $3/2^-$ states, for all but the nucleon states. For the $\Lambda(1/2^-)$ and $\Lambda(3/2^-)$, for instance, the dominant component has a coefficient [the η_i of Eq. (A.2)] of at least 0.985 in all of the models. We treat such states as being single component states, and this will introduce errors of about a few percent (typically less than three percent for the particular states mentioned, usually much less for the states containing a c or b quark).

Table 5.6: Mixing coefficients (η_i) of the two lowest lying $1/2^+$ states in different flavor sectors. The η_i are defined in Appendix A.

Baryon states	HONR			HOSR		
	η_1	η_2	η_3	η_1	η_2	η_3
$N(1/2^+)$	0.979	-0.150	0.034	0.989	-0.110	0.028
$N(1/2_1^+)$	0.022	0.522	0.825	-0.026	0.579	0.800
$\Lambda(1/2^+)$	0.994	0.005	-0.069	0.998	0.003	-0.035
$\Lambda(1/2_1^+)$	0.047	0.149	0.962	0.018	0.650	0.750
$\Lambda_c(1/2^+)$	0.999	0.001	-0.020	0.999	<0.001	-0.012
$\Lambda_c(1/2_1^+)$	0.017	0.100	0.993	0.010	0.361	0.931
$\Lambda_b(1/2^+)$	0.999	<0.000	-0.003	0.999	<0.001	-0.004
Baryon states	STNR			STSR		
	η_1	η_2	η_3	η_1	η_2	η_3
$\Lambda(1/2^+)$	0.900	0.208	0.382	0.875	0.313	0.368
$\Lambda(1/2_1^+)$	-0.177	0.977	-0.115	-0.279	0.950	-0.152
$\Lambda_c(1/2^+)$	0.917	0.137	0.374	0.877	0.289	0.382
$\Lambda_c(1/2_1^+)$	-0.138	0.989	-0.059	-0.257	0.957	-0.132
$\Lambda_b(1/2^+)$	0.915	0.141	0.378	0.876	0.286	0.390

Significant mixing occurs only in the $1/2^+$ sector, for all flavors of baryons, particularly in the Sturmian models. The mixings that result are tabulated in Tables 5.6 and 5.7, for all four models. In these tables, we show the wave function coefficients for the two lowest $1/2^+$ states, in each flavor sector, in each model (in the case of the nucleon, we show only the results from the HO models) for the Λ_Q baryons. In the same way significant mixing occurs in the ground states ($1/2^+, 3/2^+$) of the Ξ and Ω_Q baryons, in the Sturmian models. Harmonic oscillator wave functions for these states have essentially one component. In Table 5.7 we show only the mixing of the $1/2^+$ and $3/2^+$ states of Ξ and Ω_Q in the Sturmian models.

The mixing shown in these tables complicates the extraction of the form factors. However, in all results that we show for the form factors and the decay rates, this mixing of the three

Table 5.7: Mixing coefficients (η_i) of the two lowest lying $1/2^+$, $3/2^+$ states of Ξ and Ω_c . The η_i are defined in Appendix A.

Baryon states	STNR			STSR		
	η_1	η_2	η_3	η_1	η_2	η_3
$\Xi(1/2^+)$	0.947	0.208	0.244	0.964	0.154	0.217
$\Xi(1/2_1^+)$	-0.313	0.771	0.554	-0.263	0.669	0.694
$\Xi(3/2^+)$	0.937	0.240	0.253	0.949	0.203	0.239
$\Xi(3/2_1^+)$	-0.237	-0.097	0.967	-0.152	-0.370	0.916
$\Omega_c(1/2^+)$	0.943	0.315	0.106	0.949	0.273	0.152
$\Omega_c(1/2_1^+)$	-0.181	0.220	0.958	-0.218	0.231	0.948
$\Omega_c(3/2^+)$	0.942	0.331	0.044	0.950	0.297	0.097
$\Omega_c(3/2_1^+)$	-0.124	0.224	0.967	-0.166	0.215	0.962
$\Omega_b(1/2^+)$	0.933	0.291	0.210	0.933	0.253	0.256

quark states is properly accounted for. Note that in the wave functions for Λ and N shown in Table 5.6, there is also some contribution from the term in η_4 . However, this component of the wave function has negligible overlap with the wave function of the parent baryon, and so is neglected here.

5.2 Form Factors and Decay Rates: Λ_Q

In our calculation of the form factors, we have assumed that we can use non-relativistic approximations for the operators. This means that we have ignored terms in the various quark model operators that appear at order $1/m_q^2$, $1/m_Q^2$, and above. Such terms have also been ignored in writing the hadronic matrix elements. However, in extracting the form factors for the semileptonic decays of the Λ_Q , we have kept, and shown, terms that are of order $1/(m_q m_Q)$. To examine the validity of this treatment, we write each form factor as

$$\begin{aligned}
 F_i &= F_i^{(0)} + \frac{1}{m_q} F_i^{(q)} + \frac{1}{m_Q} F_i^{(Q)} + \frac{1}{m_q m_Q} F_i^{(qQ)}, \\
 &\equiv \mathcal{F}_i^{(0)} + \mathcal{F}_i^{(q)} + \mathcal{F}_i^{(Q)} + \mathcal{F}_i^{(qQ)}
 \end{aligned} \tag{5.1}$$

and show the values for $\mathcal{F}_i^{(0)}$, $\mathcal{F}_i^{(q)}$, etc., in Table 5.8. In this table, we show only the results for the HONR and STNR models.

For the elastic decays, the form factors F_1 and G_1 are dominant, while all other form factors are subdominant. For $1/2^-$ final states, F_2 , G_1 and G_2 are dominant, while for $3/2^-$,

F_1 and G_1 are the dominant form factors (not shown in Table 5.8). In each case, we see that the $\mathcal{F}^{(0)}$ or $\mathcal{G}^{(0)}$ term is significantly larger than the ‘higher order’ terms, as expected. The numbers in this table suggest that the convergence in $1/m_q$ is rapid, modulo the model dependence.

Table 5.8: Form factor components \mathcal{F}_i and \mathcal{G}_i as defined in Eq. (5.1), evaluated at the non-recoil point. The components are shown for the HONR (HO) and STNR (St.) models. The columns labeled ‘ Λ_c ’ are for the $\Lambda_c \rightarrow \Lambda^{(*)}$ form factors, while those labeled ‘ Λ_b ’ are for the $\Lambda_b \rightarrow \Lambda_c^{(*)}$ form factors.

form factor	$J^P = 1/2^+$				$J^P = 1/2^-$			
	Λ_c		Λ_b		Λ_c		Λ_b	
	H.O.	St.	H.O.	St.	H.O.	St.	H.O.	St.
$\mathcal{F}_1^{(0)}$	0.98	0.97	0.99	0.99	0	0	0	0
$\mathcal{F}_1^{(q)}$	0.54	0.78	0.20	0.28	0.36	0.32	0.16	0.12
$\mathcal{F}_1^{(Q)}$	0.23	0.15	0.08	0.05	-0.04	-0.04	-0.04	-0.01
$\mathcal{F}_2^{(0)}$	0	0	0	0	-1.24	-1.71	-1.34	-1.60
$\mathcal{F}_2^{(q)}$	-0.54	-0.72	0.20	-0.26	0.36	0.32	0.16	0.12
$\mathcal{F}_2^{(Q)}$	0	0	0	0	-0.34	-0.43	-0.11	-0.14
$\mathcal{F}_3^{(0)}$	0	0	0	0	0	0	0	0
$\mathcal{F}_3^{(q)}$	0	0	0	0	0	0	0	0
$\mathcal{F}_3^{(Q)}$	-0.21	-0.11	-0.07	-0.04	0.34	0.43	0.08	0.14
$\mathcal{G}_1^{(0)}$	0.98	0.97	0.99	0.99	1.24	1.71	1.34	1.60
$\mathcal{G}_1^{(q)}$	0	0	0	0	0	0	0	0
$\mathcal{G}_1^{(Q)}$	0	0	0	0	0.04	0.02	0.02	0.01
$\mathcal{G}_2^{(0)}$	0	0	0	0	-1.24	-1.71	-1.34	-1.60
$\mathcal{G}_2^{(q)}$	-0.54	-0.72	-0.20	-0.26	0.36	0.32	0.16	0.12
$\mathcal{G}_2^{(Q)}$	0	0	0	0	0.08	0.06	0.04	0.03
$\mathcal{G}_3^{(0)}$	0	0	0	0	0	0	0	0
$\mathcal{G}_3^{(q)}$	0	0	0	0	0	0	0	0
$\mathcal{G}_3^{(Q)}$	0.23	0.11	0.08	0.04	0.08	0.07	0.04	0.03

5.2.1 $\Lambda_c \rightarrow \Lambda^{(*)}$ Decay

In Table 5.9 we show the values of the form factors at the non-recoil point, for the decays $\Lambda_c \rightarrow \Lambda$, for both elastic and inelastic channels. In this table, the results from all four

models are presented. The results we obtain for the elastic channel are consistent with the predictions of HQET as estimated by Scora [57].

Table 5.9: The form factors for $\Lambda_c \rightarrow \Lambda^{(*)}$ transitions, calculated at the non-recoil point, in the four models used here.

spin	model	F_1	F_2	F_3	F_4	G_1	G_2	G_3	G_4
1/2 ⁺	HONR	1.75	-0.54	-0.23	-	0.98	-0.54	0.23	-
1/2 ⁺	HOSR	1.76	-0.55	-0.24	-	0.98	-0.55	0.24	-
1/2 ⁺	STNR	1.90	-0.72	-0.11	-	0.97	-0.72	0.11	-
1/2 ⁺	STSR	1.78	-0.66	-0.09	-	0.92	-0.66	0.09	-
1/2 ⁻	HONR	0.32	-1.22	0.34	-	1.20	-0.80	0.08	-
1/2 ⁻	HOSR	0.42	-1.02	0.30	-	1.14	-0.61	0.10	-
1/2 ⁻	STNR	0.28	-1.82	0.43	-	1.73	-1.42	0.07	-
1/2 ⁻	STSR	0.36	-1.30	0.31	-	1.38	-1.04	0.08	-
3/2 ⁻	HONR	-1.83	0.46	0.37	-0.14	-1.00	0.46	-0.37	0.14
3/2 ⁻	HOSR	-1.81	0.52	0.35	-0.18	-0.94	0.52	-0.35	0.16
3/2 ⁻	STNR	-2.61	0.76	0.43	-0.13	-1.42	0.76	-0.47	0.13
3/2 ⁻	STSR	-2.03	0.58	0.34	-0.13	-1.11	0.57	-0.38	0.13

In their treatment of the process $\Lambda_c \rightarrow \Lambda e^+ \nu$, the CLEO Collaboration have used the leading order predictions of HQET to analyze the decay rate in terms of two form factors, ξ_1 and ξ_2 . In terms of the form factors that we have been using, these HQET form factors are

$$\begin{aligned}
 \xi_1 &= F_1 + F_2/2, & \xi_2 &= F_2/2, \\
 \xi_1 &= G_1 - G_2/2, & \xi_2 &= G_2/2
 \end{aligned}
 \tag{5.2}$$

The two sets of equations above arise from inverting Eqs. (2.30) either in terms of the F_i or the G_i . In Table 5.10, we show the values we obtain for the ratio ξ_2/ξ_1 , evaluated at the non-recoil point. We also show the value obtained by the CLEO Collaboration in their analysis. We note that CLEO present a single value for the ratio of form factors, while we have two sets of values, arising from the two equations above. These two expressions give values for this ratio that are different, but not disturbingly so. The vector ratio (involving the F_i) tends to be smaller than the axial-vector ratio (involving the G_i), and both are smaller than the ratio extracted by the CLEO collaboration. The differences among the numbers we

obtain using the two methods can be traced back to the $1/m_Q$ terms in F_1 ; if those terms are ignored, both methods give the same value for the ratio.

Table 5.10: The ratio ξ_2/ξ_1 for $\Lambda_c \rightarrow \Lambda(1/2^+)$. The first row is obtained using the vector relation defined in the text, while the second row is obtained using the axial-vector relation.

ξ_2/ξ_1	HONR	HOSR	STNR	STSR	CLEO
Vector	-0.18	-0.18	-0.23	-0.23	-0.31
Axial Vector	-0.21	-0.22	-0.27	-0.26	-0.31

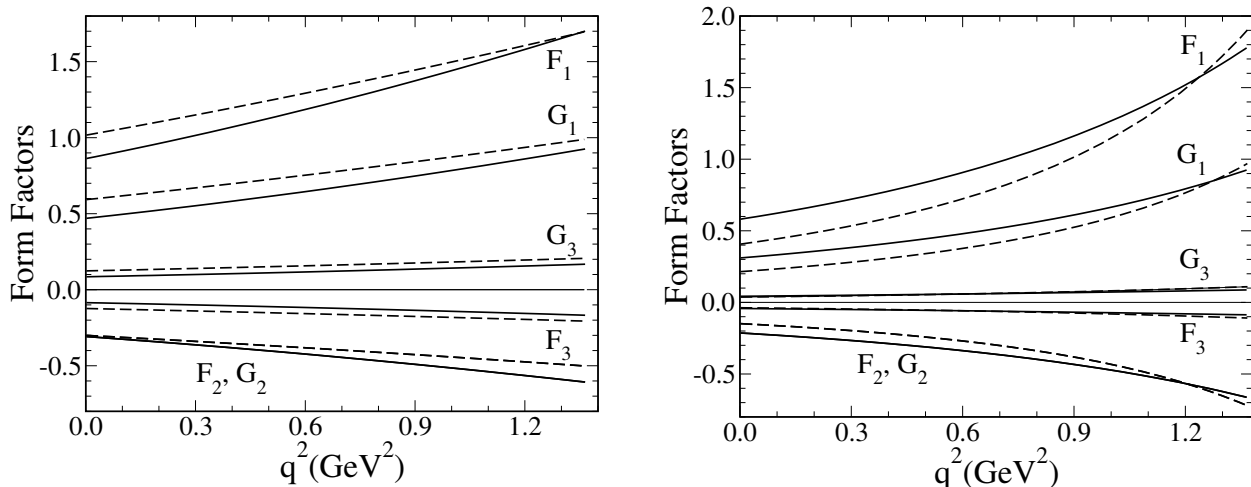


Figure 5.1: Form factors for $\Lambda_c \rightarrow \Lambda(1/2^+)$ obtained using harmonic oscillator wave functions (left panel, HOSR and HONR models) and Sturmian wave functions (right panel, STSR and STNR models). In each panel, the solid curves arise from the semirelativistic version of the model, while the dashed curves arise from the non-relativistic version. Note that F_2 is indistinguishable from G_2 in all cases.

Figure 5.1 shows the q^2 dependence of the form factors for the elastic transition $\Lambda_c \rightarrow \Lambda(1/2^+)$, calculated in the HONR and HOSR models on the left, and in the STSR and STNR models on the right. In each panel, the solid curves arise from the SR version of the model, while the dashed curves are from the NR version. If we compare the form factors shown in Figure 5.1, we see that those calculated using the Sturmian wave functions

have larger slopes near the non-recoil point (maximum q^2) than those calculated using the harmonic oscillator wave functions. The form factors calculated in the different models all have similar values near the non-recoil point (as seen in Table 5.9). The larger slopes in the case of the Sturmian model form factors means that we can expect smaller integrated rates from the STSR and STNR models.

The differential decay rates, $d\Gamma/dq^2$, that we obtain in the four models are shown in Figure 5.2. For these rates, we use $|V_{cs}| = 0.974$. In these figures, we show the differential rates for decays to the elastic channel, as well as for two orbital excitations, the states with $J^P = 1/2^-$ and $3/2^-$. We have also examined the differential decay rates to the $3/2^+$ and $5/2^+$ orbitally excited states, as well as to the $1/2^+$ radially excited state. With the exception of the latter, we find these rates to be significantly smaller than those shown in this figure.

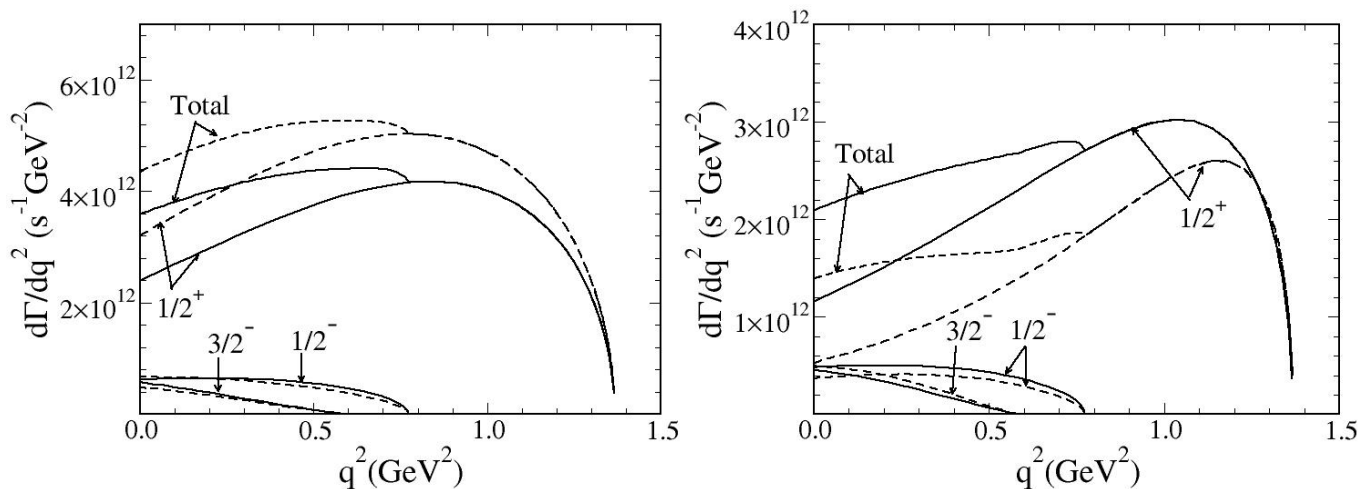


Figure 5.2: The differential decay rates for different $\Lambda_c \rightarrow \Lambda^{(*)}$ transitions, in the different models that we use. The curves on the left arise from the two versions of the harmonic oscillator model, while those on the right are from the Sturmian models. The curves are for exclusive final states with $J^P = 1/2^+$, $1/2^-$ and $3/2^-$. Also shown are the differential decay rates obtained by adding the exclusive modes described (labeled as ‘total’). In each panel, the solid curves arise from the semirelativistic version of the model, while the dashed curves arise from the non-relativistic version.

As expected from the plots for the form factors, the differential decay rates that arise from the Sturmian wave functions for the ground state show a larger variation over the

Table 5.11: Integrated decay rates for $\Lambda_c \rightarrow \Lambda^{(*)}$ in units of $10^{11} s^{-1}$, for different Λ states in the four models we consider. The last row shows the ‘elastic fraction’ obtained in our model, where the decays shown in the table are assumed to saturate the semileptonic decays.

Spin	$\Gamma(\text{HONR})$	$\Gamma(\text{HOSR})$	$\Gamma(\text{STNR})$	$\Gamma(\text{STSR})$	Expt. [60]
$1/2^+$	2.10	2.36	0.79	1.11	1.05 ± 0.35
$1/2^-$	0.19	0.29	0.12	0.15	-
$3/2^-$	0.04	0.06	0.06	0.05	-
$1/2_1^+$	0.02	0.02	<0.01	<0.01	-
total	2.35	2.73	0.97	1.31	-
$\Gamma_\Lambda/\Gamma_{\text{total}}$	0.89	0.86	0.81	0.85	1.0 (assumed)

allowed q^2 range. We also point out that the most noticeable difference between the NR and SR versions of a particular model is seen in the differential rate for the elastic decay.

The integrated decay rate for the different final states in the different models are shown in Table 5.11. As anticipated above, the total semileptonic decay rates that we obtain in the harmonic oscillator models are significantly larger than those obtained in the Sturmian models. This effect is largest in the elastic decays, where the HO models predict decay rates that are more than twice as large as the ST models. We note that the elastic rates predicted by the ST models are much closer to the experimentally reported rate [60] than those predicted by the HO models. From Table 5.11, it is clear that, while the elastic channel dominates the decay rate of the Λ_c , it does not saturate the decay. In each model, we find that the decay rate to the $1/2^-$ state is roughly one tenth of the elastic decay rate, while the decay rate to the $3/2^-$ state is about five percent of the elastic. Decays to these two excited states account for about 15% of the total decays of the Λ_c , assuming that decays to other excited states are negligible. It is also interesting to note that the ratio $\Gamma_\Lambda/\Gamma_{\text{total}}$ is almost independent of the model that we use, even though the absolute rates are very different in the different models.

The assumption that the channels we explore saturate the resonant decays of the Λ_c is certainly consistent with the results we have obtained with the other states that we consider. First we point out that phase space limits how many excited Λ states can be considered, and the higher the excitation, the more limited the phase space available for producing such a state. For some final states for which there might be sufficient phase space to allow

the decay, the spin-space structure of the state allows little overlap with the initial baryon, and configuration mixing that could involve components with larger overlap with the initial baryon is very small. In addition, angular momentum factors (in orbitally excited states) lead to suppression of the decay rate.

We can compare our predictions for decays to the excited Λ states with the assumption made by the CLEO Collaboration [60], that the elastic channel saturates the semileptonic decays of the Λ_c . In our models, we find that between 11% and 19% of the Λ_c semileptonic decays are to excited states. In addition, our branching fraction (of 81% to 89%) to the ground state Λ must represent an upper limit, as we have not included any non-resonant production of multi-particle final states. It appears difficult to understand the lack of evidence for any decays to excited states in Ref. [60]. This article reports no signal for decays of the kind $\Lambda_c \rightarrow \Lambda X e^+ \nu$, and this is taken as evidence of saturation. However, the excited Λ states that we consider do not decay to $\Lambda\pi$, the most obvious decay mode to search for, as this decay is isospin violating. They will predominantly decay to $\Sigma\pi$ final states. In fact, the $1/2^-$ state, the $\Lambda(1405)$, has a 100% branching fraction to $\Sigma\pi$, while the $\Lambda(1520)$, the $3/2^-$ state, has roughly equal dominant branching ratios to $\Sigma\pi$ and NK , with only about ten percent going into $\Lambda\pi\pi$. Thus, our suggestion is that CLEO should investigate final states like $\Sigma\pi\ell\nu$ and $NK\ell\nu$, and not states like $\Lambda\pi\pi\ell\nu$.

The results discussed above are obtained using the assumption that the lightest of the $J^P = 1/2^-$ Λ states, identified with the S_{01} state $\Lambda(1405)$ found in analyses of scattering data, is a three-quark state. There are a number of other descriptions of this state in the literature, such as a dynamically generated bound state [73], and a multi-quark state [74]. If the CLEO Collaboration (or other groups) search for decays of the Λ_c to excited Λ states, especially the $\Lambda(1405)$, and find no such decays, this would be a strong hint that this state is not a simple three quark state, as we have assumed.

Our estimate of the fraction of Λ_c decays to excited states has important consequences for the absolute normalization of the branching fractions to the more than sixty observed final states in Λ_c^+ decay. Most of these branching fractions are measured relative to the decay mode $\Lambda_c^+ \rightarrow pK^-\pi^+$, and the absolute branching fraction of this mode cannot be extracted from data without introducing model dependence. One of the two important techniques for this extraction is based on measurements [75, 76] of the cross section for $\Lambda_c^+ X$ production in e^+e^- annihilation, with the subsequent semileptonic decay $\Lambda_c^+ \rightarrow \Lambda\ell^+\nu_\ell$. The

extraction relies on the assumption that the fraction f of decays $\Lambda_c^+ \rightarrow X_s \ell^+ \nu_\ell$ that have X_s as the ground state Λ is unity (the elastic channel saturates the semileptonic decays), with a significant uncertainty. Our calculated value $f = 0.85$, with an error of 0.04 estimated by evaluating f in four different models, changes the central value of this parameter and may allow a reduction in the assumed error from model dependence in the extracted absolute branching fractions.

5.2.2 $\Lambda_b \rightarrow \Lambda_c^{(*)}$ Decay

In Table 5.12 we show the values of the form factors at the non-recoil point, for the decays $\Lambda_b \rightarrow \Lambda_c^{(*)}$, where this notation means that the Λ_c may be in an excited state. The results from all four models are shown, along with the results from a lattice study [45]. The lattice results are actually given as multiples of $\xi(w)$, evaluated at the non-recoil point, and Ref. [45] reports a number of different values for $\xi(w)$. In the ‘physical’ limit, values $\xi^{(A)}(1) = 1.03_{-0.19}^{+0.18}$ and $\xi^{(V)}(1) = 0.87 \pm 0.22$ are quoted, where the two extractions are from the axial and vector currents, respectively. The results we obtain for the elastic decays are consistent with the predictions of HQET as estimated by Scora [57], as well as with these lattice simulations.

Figure 5.3 shows the q^2 dependence of the form factors for the elastic decay of the Λ_b , calculated in the HONR and HOSR models on the left, and in the STSR and STNR models on the right. In each panel, the solid curves arise from the SR version of the model, while the dashed curves are from the NR version. As we noted in the case of the $\Lambda_c \rightarrow \Lambda(1/2^+)$, the form factors obtained in the Sturmian basis have significantly larger slopes than the corresponding form factors calculated in the harmonic oscillator basis, at the non-recoil point.

In terms of the Isgur-Wise function $\xi(w)$ for the elastic decay of the Λ_b , the form factor F_1 is

$$F_1 = \left[1 + \bar{\Lambda} \left(\frac{1}{2m_c} + \frac{1}{2m_b} \right) \right] \xi(w), \quad (5.3)$$

where $\bar{\Lambda} = m_{\Lambda_b} - m_b = m_{\Lambda_c} - m_c$ at leading order in the heavy quark expansion. From the forms given in Appendix C, and with the identification $\bar{\Lambda} \approx 2m_\sigma$, we can extract

$$\xi(w) \approx \exp \left(-\frac{3m_\sigma^2 p^2}{2m_{\Lambda_c}^2 \alpha^2} \right) \quad (5.4)$$

Table 5.12: Form factors of $\Lambda_b \rightarrow \Lambda_c^{(*)}$, calculated at the non-recoil point, in the four models we use.

J^P	model	F_1	F_2	F_3	F_4	G_1	G_2	G_3	G_4
$1/2^+$	HONR	1.27	-0.20	-0.08	-	0.99	-0.20	0.08	-
$1/2^+$	HOSR	1.24	-0.18	-0.08	-	0.97	-0.18	0.08	-
$1/2^+$	STNR	1.28	-0.26	-0.04	-	0.98	-0.26	0.04	-
$1/2^+$	STSR	1.20	-0.22	-0.03	-	0.92	-0.22	0.03	-
$1/2^+$	Lattice	1.28 ± 0.06	-0.19 ± 0.04	$-0.06^{+0.02}_{-0.01}$	-	0.99	$-0.24^{+0.05}_{-0.04}$	0.09 ± 0.02	-
$1/2^-$	HONR	0.12	-1.20	0.11	-	1.21	-1.05	0.03	-
$1/2^-$	HOSR	0.15	-0.95	0.09	-	1.01	-0.82	0.04	-
$1/2^-$	STNR	0.10	-1.63	0.14	-	1.61	-1.50	0.03	-
$1/2^-$	STSR	0.11	-1.21	0.10	-	1.24	-1.12	0.03	-
$3/2^-$	HONR	-1.33	0.17	0.13	-0.06	-1.03	0.17	-0.13	0.06
$3/2^-$	HOSR	-1.13	0.15	0.12	-0.05	-0.87	0.15	-0.12	0.05
$3/2^-$	STNR	-1.75	0.25	0.15	-0.05	-1.36	0.25	-0.22	0.05
$3/2^-$	STSR	-1.31	0.16	0.11	-0.05	-1.04	0.16	-0.18	0.05

in the harmonic oscillator basis, or

$$\xi(w) \approx \frac{1}{\left[1 + \frac{3m_\sigma^2}{2m_{\Lambda_c}^2} \frac{p^2}{\beta^2}\right]^2} \quad (5.5)$$

in the Sturmian basis (assuming single-component wave functions), and we have assumed that $\alpha_\lambda = \alpha_{\lambda'} \equiv \alpha$, $\beta_\lambda = \beta_{\lambda'} \equiv \beta$ in the heavy quark limit. Writing

$$p^2 = m_{\Lambda_c}^2 (w^2 - 1) \approx 2m_{\Lambda_c}^2 (w - 1), \quad (5.6)$$

the above expressions become

$$\xi(w) \approx \exp\left(-\frac{3m_\sigma^2}{\alpha^2}(w - 1)\right) \quad (5.7)$$

in the harmonic oscillator basis, or

$$\xi(w) \approx \frac{1}{\left[1 + \frac{3m_\sigma^2}{\beta^2}(w - 1)\right]^2} \quad (5.8)$$

in the Sturmian basis.

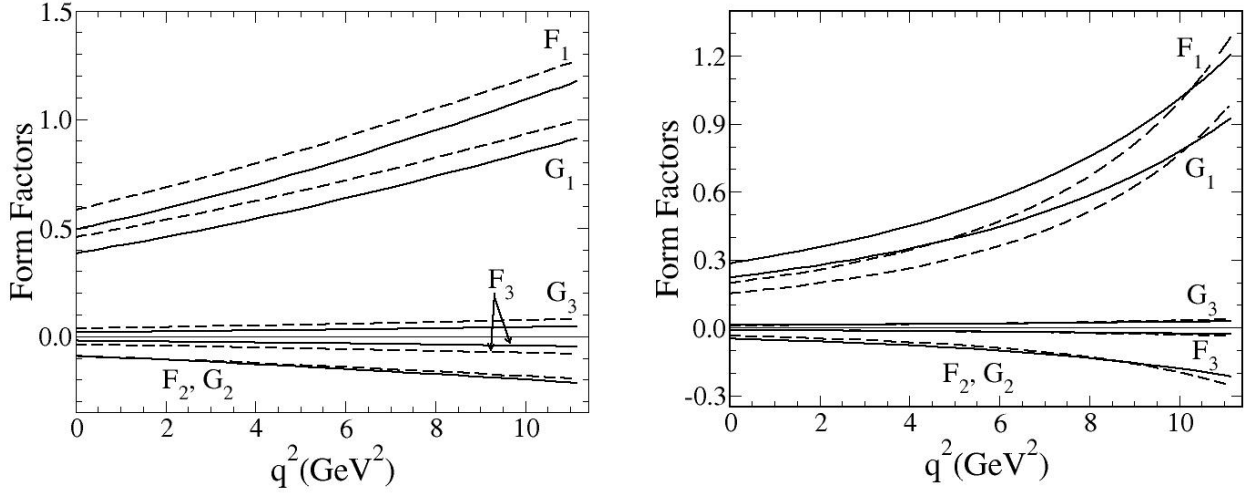


Figure 5.3: Form factors for $\Lambda_b \rightarrow \Lambda_c(1/2^+)$ obtained using harmonic oscillator wave functions (left panel, HOSR and HONR models) and Sturmian wave functions (right panel, STSR and STSR models). In each panel, the solid curves arise from the semirelativistic version of the model, while the dashed curves arise from the non-relativistic version. Note that F_2 is indistinguishable from G_2 in all cases.

The Isgur-Wise function may be expanded as

$$\xi(w) = 1 - \rho^2(w - 1) + \frac{\sigma^2}{2}(w - 1)^2 + \dots, \quad (5.9)$$

where the slope of the form factor at the non-recoil point has been denoted ρ^2 , and the curvature is denoted σ^2 . Rigorous bounds have been placed on the values of both the slope and curvature parameters for meson decays, and some models have difficulty in satisfying those bounds. In particular, in the model of ISGW [36], a factor κ was introduced by hand (see the discussion between Eqs. (B2) and (B3) of Ref. [36]) to modify the q^2 dependence of the form factors. In our model, the equivalent procedure would be to change I_H in Eq. (C.1) from

$$I_H = \left(\frac{\alpha_\lambda^{3/2} \alpha_{\lambda'}^{3/2}}{\alpha_{\lambda\lambda'}^3} \right) \exp \left(- \frac{3m_\sigma^2}{2m_{\Lambda_q}^2} \frac{p^2}{\alpha_{\lambda\lambda'}^2} \right)$$

as calculated to

$$I_H = \left(\frac{\alpha_\lambda^{3/2} \alpha_{\lambda'}^{3/2}}{\alpha_{\lambda\lambda'}^3} \right) \exp \left(- \frac{3m_\sigma^2}{2m_{\Lambda_q}^2} \frac{p^2}{\kappa^2 \alpha_{\lambda\lambda'}^2} \right).$$

The argument used by ISGW was that this factor of κ would take into account ‘relativistic effects’. The effect of this change is shown in Figure 5.4, where the form factors for $\Lambda_b \rightarrow \Lambda_c$ are plotted as functions of $w = v \cdot v'$, for the two harmonic oscillator models (upper graphs). For comparison, the lower graph shows form factors obtained in the Sturmian basis, also as functions of w . The graph on the upper left shows our calculated form factors, while that on the upper right shows form factors including the factor of κ .

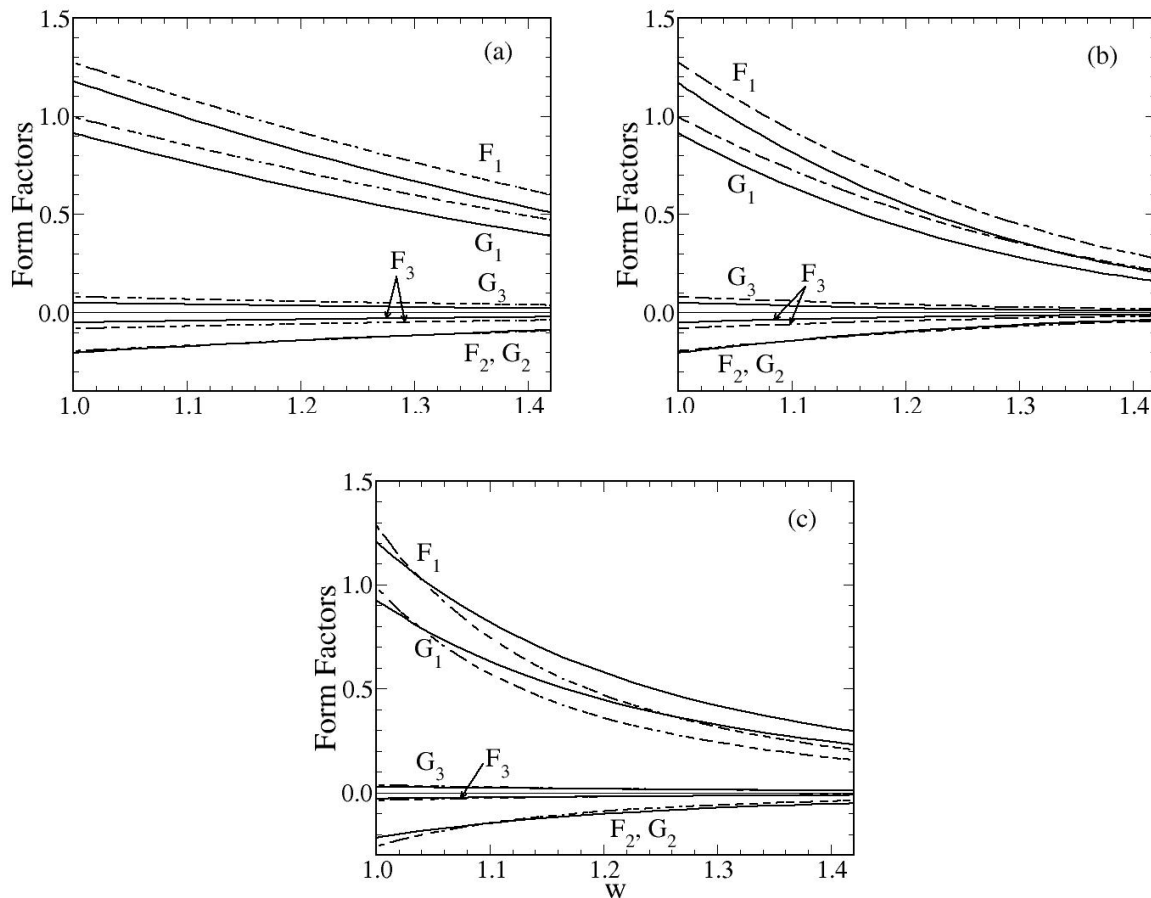


Figure 5.4: The elastic form factors for the decay of the Λ_b as functions of w . The upper two graphs arise from the harmonic oscillator model, while the lower graph is from the Sturmian version of our model. Among the upper graphs, the panel on the left shows the form factors obtained in this work, while those on the right incorporate a ‘relativistic’ factor in the exponential (see text).

Table 5.13 lists the slope of the Isgur-Wise function that we have extracted, at the

non-recoil point, in both the harmonic oscillator and Sturmian models, as well as in the ‘relativistically modified’ harmonic oscillator model (using the factor κ). The slopes of the form factor near the non-recoil point are larger in the Sturmian models than in the harmonic oscillator models. This is easily understood by noting that the value of ρ^2 is

$$\rho^2 = 3 \frac{m_\sigma^2}{\alpha^2} \quad (5.10)$$

in the HO models, and

$$\rho^2 = 6 \frac{m_\sigma^2}{\beta^2} \quad (5.11)$$

in the ST models. The extra factor of two in the latter case arises because the form factors in the ST models have a dipole dependence on w . A corresponding monopole form would give the same slope as the HO models. Since the values of m_σ are similar in the two sets of models, and the values of α are not very different from the values of β , the ST models will give slopes that are roughly twice as large as the HO models. In the same way, it is easily shown that the ST models lead to curvatures that are about six times as large as those obtained in the HO models.

Table 5.13: Slope of the Isgur-Wise function, evaluated at the non-recoil point, for the elastic decay of the Λ_b .

model	HONR	HOSR	HONR κ	HOSR κ	STNR	STSR
$d\xi(w)/dw$	-1.38	-1.33	-2.82	-2.71	-5.71	-3.27

The κ -modified harmonic oscillator model leads to slopes that are similar to those obtained in the Sturmian models, since the value chosen for κ was 0.7 (so that $1/\kappa^2 \approx 2$). Relativistic effects do not need to be invoked to obtain the large slopes obtained in the Sturmian models. The differences in the slopes are simply artifacts of the expansion bases used for the wave functions.

In the follow-up article to Ref. [36], Scora and Isgur [77] rewrite the quark model form factors, explicitly replacing the exponential factor that arises with the harmonic oscillator wave functions. The change they make is

$$\exp \left\{ -\frac{1}{6} r_{\text{wf}}^2 [(m_B - m_D)^2 - q^2] \right\} \longrightarrow \frac{1}{\left\{ 1 + \frac{1}{6N} r^2 [(m_B - m_D)^2 - q^2] \right\}^N}, \quad (5.12)$$

where r_{wf}^2 is the value obtained from the harmonic oscillator wave functions, and

$$r^2 = \frac{3}{4m_Q m_q} + r_{\text{wf}}^2 + r_{\text{QCD}}^2, \quad (5.13)$$

where the last term arises from matching of currents in HQET with full QCD. In Eq. (5.12), the integer $N = 2 + n + n'$, where n and n' are the harmonic oscillator principal quantum numbers for the initial and final wave functions. The final forms that they used are therefore very similar to the forms that we have obtained in the Sturmian models.

The values we have obtained for the slope of the Isgur-Wise function in our Sturmian models are significantly larger than the value obtained recently by Huang *et al.* [78] using a HQET approach based on QCD sum rules: their value for ρ^2 is less than 1.5, similar to the values we obtain in the HO models. In a recent analysis of the Λ_b form factor measured in hadronic Z decays, the DELPHI Collaboration [61] found $\rho^2 = 2.03 \pm 0.46$, where the error shown is statistical. They also reported two sets of systematic errors, each comparable to the statistical error. This result means that for the Sturmian models, we will obtain integrated decay rates that are significantly smaller than the DELPHI rate. In the lattice study by Bowler *et al.* [45], the reported slope is 1.1 ± 1.0 . A more recent lattice study with $\mathcal{O}(a^2, \alpha_s a^2)$ improved lattices [46] does not quote values for the slope. However, a conservative estimate from the graphs they present gives values for ρ^2 that appear to be consistent with the large values we obtain in the ST models.

Also of some interest is the curvature of the Isgur-Wise function, denoted σ^2 . In the HO models with no modifications, the prediction is that $\sigma_{\text{HO}}^2 = (\rho_{\text{HO}}^2)^2$, while the ST models give $\sigma_{\text{ST}}^2 = 3(\rho_{\text{ST}}^2)^2/2$. Bounds on the curvature of the Isgur-Wise function for meson decays have been derived by Le Yaouanc, Oliver and Raynal [79]. To the best of our knowledge, no such bounds have been derived for baryon decays. However, the values of the curvature we obtain using both the HO and ST models easily satisfy the known bounds for meson decays. Note that the large slope *and* large curvature we obtain suggest that the common procedure of parametrizing the Isgur-Wise function only in terms of its slope parameter, can potentially lead to significant errors in the extraction of CKM matrix elements.

The differential decay rates $d\Gamma/dq^2$ that we obtain in the four models are shown in Figure 5.5 (assuming $|V_{cb}| = .041$). In these plots, we show the differential rates for the elastic channel, for the radially excited $1/2_1^+$ state, as well as for decays to two orbital excitations, the states with $J^P = 1/2^-$ and $3/2^-$. We have also examined the decay rates

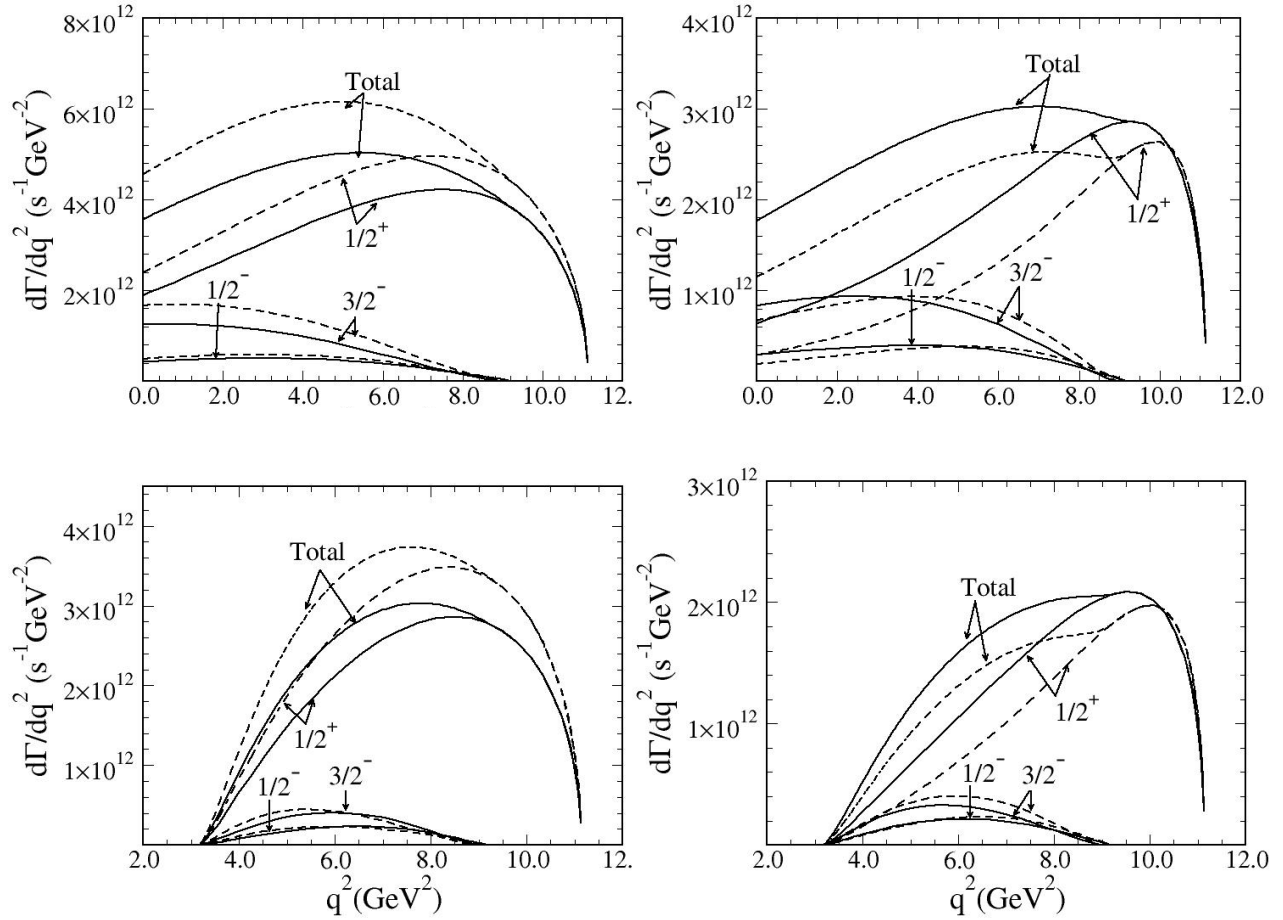


Figure 5.5: The differential decay rates for different $\Lambda_b \rightarrow \Lambda_c^{(*)}$ transitions, in the various models that we use. The curves on the left arise from the two versions of the harmonic oscillator model, while those on the right are from the Sturmian models. The upper panels are for $\Lambda_b \rightarrow \Lambda_c^{(*)} \ell \bar{\nu}_\ell$, where ℓ is e^- or μ^- . The lower panels are for $\Lambda_b \rightarrow \Lambda_c^{(*)} \tau \bar{\nu}_\tau$. The curves are for final states with $J^P = 1/2^+, 1/2^-$ and $3/2^-$.

to the $3/2^+, 5/2^+$ states, and found them to be smaller than those shown in this figure, contributing of the order of one or two percent to the total rate.

The integrated decay rate for the different final states in the different models are shown in Table 5.14. As anticipated above, the total semileptonic decay rates that we obtain in the harmonic oscillator models are significantly larger than those obtained in the Sturmian models. This effect is largest in the elastic decays, where HO models predict decay rates that are more than twice as large as the ST models. Note that, in all models, the decay rate

to the $3/2^-$ state is roughly twice the decay rate to the $1/2^-$ state. In the heavy quark limit, this ratio of decay rates is expected to be two, and results from arguments that are similar to spin-counting arguments.

Table 5.14: Rates for $\Lambda_b \rightarrow \Lambda_c^{(*)}$ decays in units of $10^{10}s^{-1}$. The first five rows of numbers are for decays with a muon or electron in the final state, while the last four rows are for decays with a τ in the final state. The rows labeled ‘total’ are obtained by adding the exclusive decay rates shown in the table, while the row with the branching fractions assumes that the exclusive channels shown saturate the semileptonic decays of the Λ_b . The elastic fraction reported by the DELPHI collaboration (fifth row of numbers, sixth column) is actually $\frac{\Gamma(\Lambda_b \rightarrow \Lambda_c \ell \bar{\nu}_\ell)}{\Gamma(\Lambda_b \rightarrow \Lambda_c \ell \bar{\nu}_\ell) + \Gamma(\Lambda_b \rightarrow \Lambda_c \pi \pi \ell \bar{\nu}_\ell)}$. The errors on both numbers from DELPHI are statistical and systematic, respectively.

J^P	$\Gamma(\text{HONR})$	$\Gamma(\text{HOSR})$	$\Gamma(\text{STNR})$	$\Gamma(\text{STSR})$	Γ_{DELPHI}
$1/2^+$	4.60	5.39	1.47	2.00	$4.07^{+0.90+1.30}_{-0.65-0.98}$
$1/2^-$	0.45	0.52	0.26	0.27	-
$3/2^-$	0.95	0.90	0.63	0.60	-
Total ($\Lambda_c^{(*)} \ell^- \bar{\nu}_\ell$)	5.95	6.81	2.36	2.87	-
$\Gamma_{\Lambda_c} / \Gamma_{\text{total}}$	0.76	0.79	0.62	0.69	$0.47^{+0.10+0.07}_{-0.08-0.06}$
$1/2^+$	1.90	2.09	0.82	1.00	-
$1/2^-$	0.10	0.11	0.08	0.07	-
$3/2^-$	0.15	0.13	0.14	0.12	-
Total ($\Lambda_c^{(*)} \tau^- \bar{\nu}_\tau$)	2.15	2.33	1.04	1.19	-

Table 5.14 also shows that a significant fraction of the semileptonic decay of the Λ_b is inelastic. This is analogous to what has been seen in B semileptonic decays, where the elastic channels account for no more than about 80% of the total semileptonic decay rate. For the Λ_b , our predicted ratios are similar, ranging from 62% to 77% of the total semileptonic decay rate. We have estimated the total semileptonic decay rate by assuming that the three exclusive modes shown in Table 5.14 saturate the semileptonic decays (rates to other states that we have examined are significantly smaller than those shown in the table). Using these numbers, we obtain predictions for the total semileptonic decay rate of the Λ_b , also shown in Table 5.14.

For comparison, the PDG [5] gives a rate of $7.486 \pm 2.105 \times 10^{10}s^{-1}$ for the inclusive semileptonic decay $\Lambda_b \rightarrow \Lambda_c \ell \bar{\nu} + \text{anything}$. This is significantly larger than any of the total semileptonic widths we obtain, but the authors of the PDG emphasize that this value

results from assumptions about the fragmentation of b quarks into baryons, and ‘cannot be thought of as measurements’ [5]. The DELPHI value for the elastic semileptonic decay rate is also shown in Table 5.14. As anticipated, the rates we obtain in the Sturmian models are significantly smaller than the DELPHI rate, while those obtained in the harmonic oscillator models are consistent with the DELPHI measurement.

The above examination of the decays of the Λ_c found that the Sturmian models provided rates that were consistent with the CLEO measurements, while the harmonic oscillator models gave rates that were twice as large. This suggested that the Sturmian models might be more reliable. For the Λ_b decays, we see that the harmonic oscillator models provide rates that are more consistent with the single measurement available to date. For the Sturmian models, the predicted rates are about 2σ away from the reported value, if the systematic and statistical errors are treated in quadrature.

The DELPHI Collaboration also reported on the elastic fraction of the semileptonic decays of the Λ_b . For the ratio $\frac{\Gamma(\Lambda_b \rightarrow \Lambda_c \ell \bar{\nu}_\ell)}{\Gamma(\Lambda_b \rightarrow \Lambda_c \ell \bar{\nu}_\ell) + \Gamma(\Lambda_b \rightarrow \Lambda_c \pi \pi \ell \bar{\nu}_\ell)}$, they find a value of $0.47_{-0.08-0.06}^{+0.10+0.07}$, with no evidence for resonant decays. This ratio is smaller than we predict, in all models. However, our predictions must be thought of as upper limits for the elastic fraction, as we do not include any non-resonant semileptonic decays. We note that our predicted ratios are already somewhat smaller than those reported in the decays of B mesons, while the DELPHI ratio is smaller still, suggesting that there are significant differences between the semileptonic decays of the heavy baryons and those of the heavy mesons. If the DELPHI results for both the elastic rate and the elastic fraction are not modified by future experiments, this aspect of the physics of heavy hadrons will require further scrutiny.

5.2.3 $\Lambda_Q \rightarrow N^{(*)}$ Decay

The decays of the Λ_Q to final states consisting solely of light quarks are interesting as they provide an alternate means of extracting CKM matrix elements like V_{ub} . The expectation from HQET is, modulo $1/m_Q$ effects, that the form factors that describe the $\Lambda_c \rightarrow n$ semileptonic decays will be the same as those describing the $\Lambda_b \rightarrow p$ semileptonic decays. To explore this, we now examine the form factors for these two decays.

In Figure 5.6 we show the form factors $\xi_1^{(V)}$, $\xi_1^{(A)}$ and ξ_2 for the transitions $\Lambda_c \rightarrow n$ and $\Lambda_b \rightarrow p$, obtained in the two harmonic oscillator models. The two forms $\xi_1^{(V,A)}$ are found using the two sets of equations in Eq. (5.2). The value of ξ_2 is independent of which of the

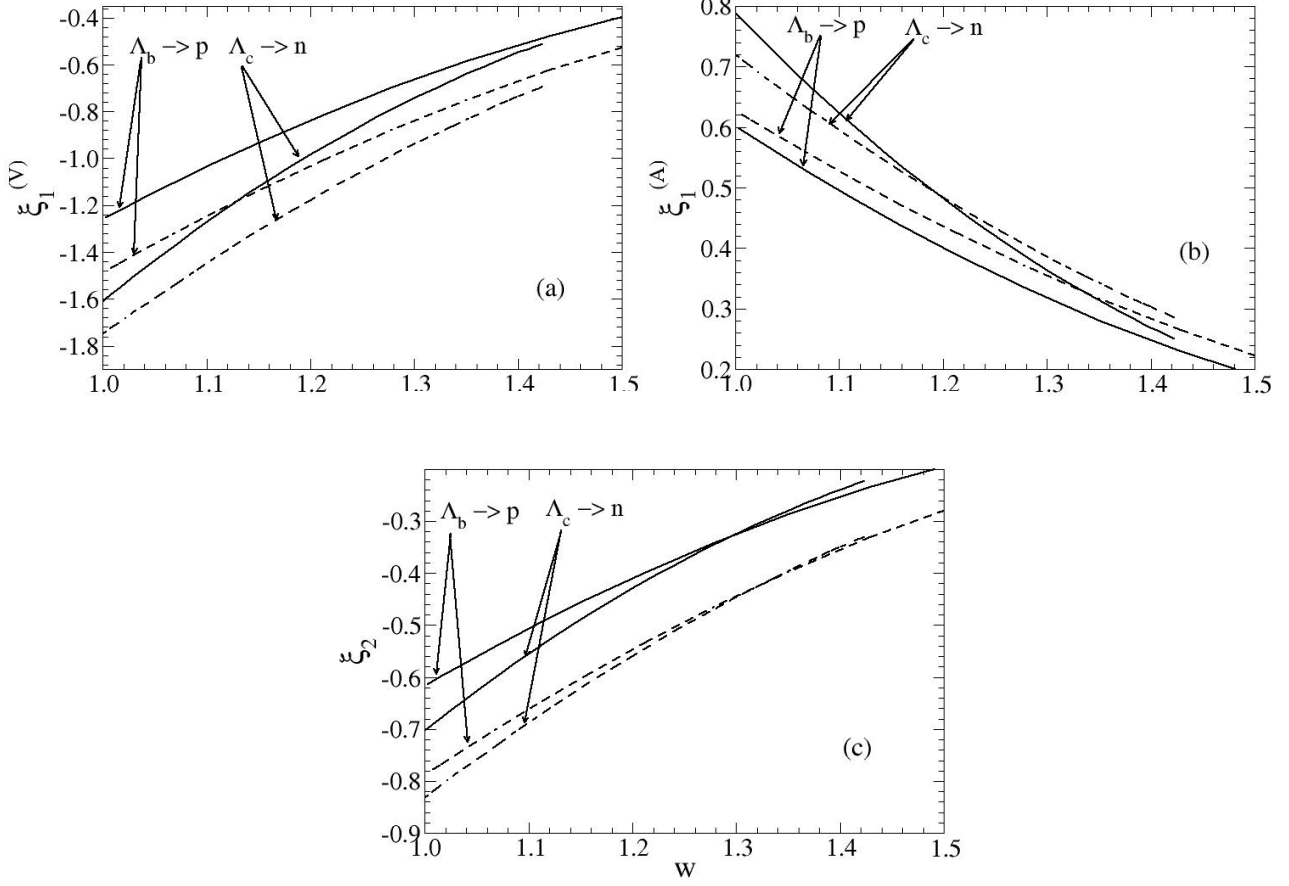


Figure 5.6: Form factors $\xi_1^{(V)}$ (top left), $\xi_1^{(A)}$ (top right) and ξ_2 (bottom) for the transitions $\Lambda_c \rightarrow n$ and $\Lambda_b \rightarrow p$. All curves arise from the harmonic oscillator models, with the solid curves corresponding to HOSR, and the dashed curves to HONR. The two plots for ξ_1 arise from the two ways of evaluating this form factor, shown in eqn. (5.2).

two sets of equations we use, up to the order to which we calculate the form factors. In both the non-relativistic and semirelativistic versions of the model, the two curves for $\xi_1^{(A)}$ (top right plot in Fig. 5.6) are very similar, indicating that the HQET prediction, that this form factor should be the same for both transitions, indeed holds up to small corrections. For the semirelativistic version, the two curves are closer than in the non-relativistic case. The differences seen in the curves for ξ_2 , which are consistent with those in the curves for $\xi_1^{(A)}$, arise mainly from the differences in the size parameters (α_ρ and α_λ) between the Λ_c and Λ_b

states in the models (see Table 5.2). The curves for $\xi_1^{(V)}$ (top left plot in Fig. 5.6) show the biggest differences in going from $\Lambda_b \rightarrow p$ to $\Lambda_c \rightarrow n$, in both models. Here, the differences get some contribution from the $1/m_Q$ term that is present in F_1 .

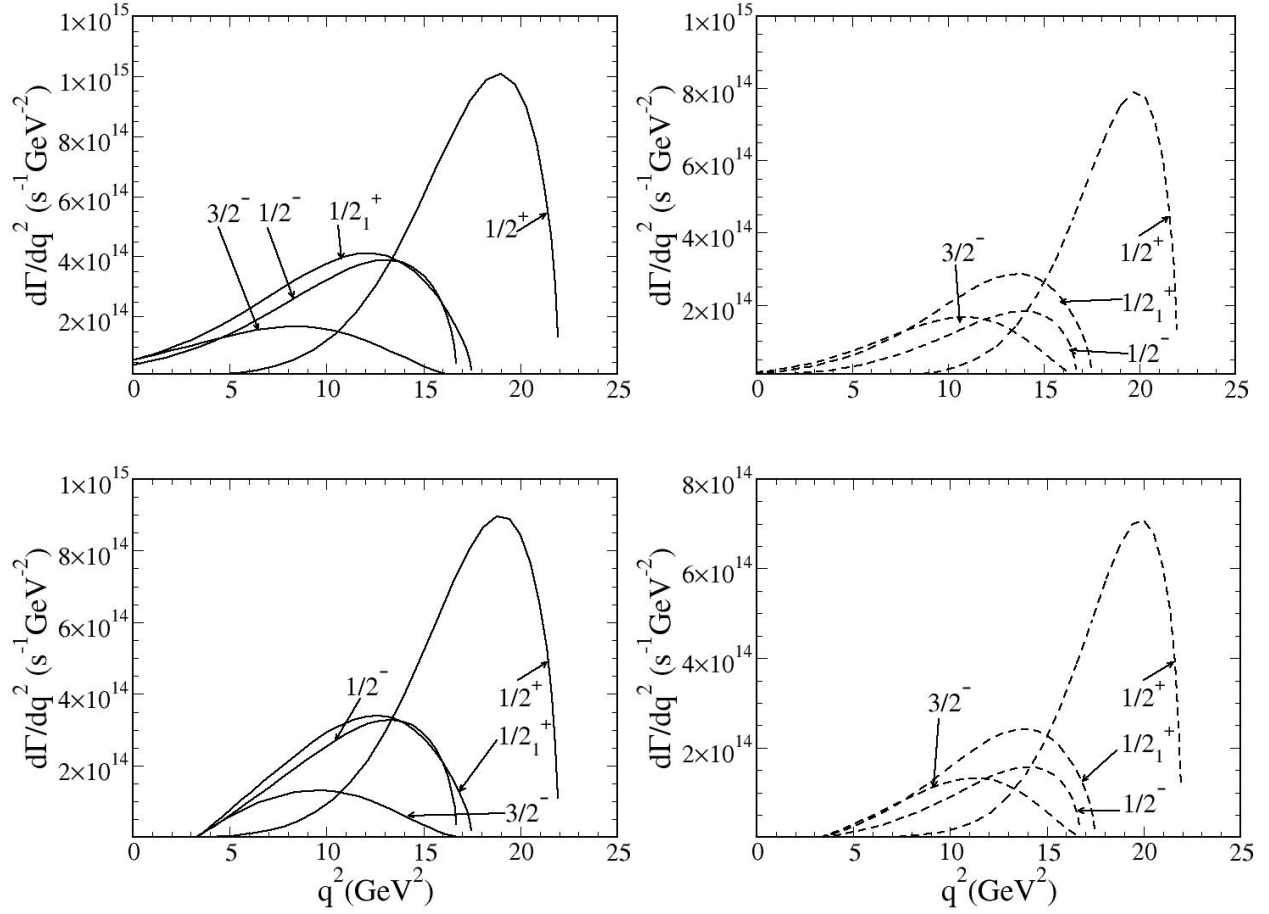


Figure 5.7: Differential decay rates for $\Lambda_b \rightarrow N^{(*)+}$ in the HONR and HOSR models. The upper panels show the rates for $\Lambda_b \rightarrow N^{(*)+} e^- \bar{\nu}_e$, while the lower panels show the rates for $\Lambda_b \rightarrow N^{(*)+} \tau^- \bar{\nu}_\tau$, both in units of $|V_{ub}|^2$. The panels on the left are from the HOSR model, while those on the right are from the HONR model.

In Figure 5.7, we show the differential decay rates for Λ_b decaying semileptonically into the four lowest-lying nucleon states, while Table 5.15 shows the integrated rates into six exclusive states. Also shown in this figure and table are the rates that we obtain when the final lepton is a τ . The ground state nucleon is the largest of the CKM suppressed decays of

Table 5.15: Decay rates of $\Lambda_b \rightarrow N^{(*)+} \ell^- \bar{\nu}_\ell$ in units of $10^{12} s^{-1} \times |V_{ub}|^2$. Also shown are the rates for $\Lambda_c \rightarrow N^{(*)0} \ell^+ \nu_\ell$ in units of $10^{10} s^{-1}$, obtained using $|V_{cd}| = 0.224$.

J^P	$\Lambda_b \rightarrow N^{(*)+} \ell^- \bar{\nu}_\ell$		$\Lambda_b \rightarrow N^{(*)+} \tau^- \bar{\nu}_\tau$	
	$\Gamma(\text{HONR})$	$\Gamma(\text{HOSR})$	$\Gamma(\text{HONR})$	$\Gamma(\text{HOSR})$
$1/2^+$	4.55	7.55	4.01	6.55
$1/2_1^+$	2.92	4.44	2.20	3.05
$1/2^-$	1.42	3.85	1.10	2.73
$3/2^-$	1.52	1.77	1.02	1.04
$3/2^+$	1.06	2.21	0.61	1.14
$5/2^+$	0.78	1.47	0.37	0.52
Total	12.23	21.29	9.31	15.03
	$\Lambda_c \rightarrow N^{(*)0} \ell^+ \nu_\ell$		-	-
$1/2^+$	1.02	1.35	-	-
$1/2^-$	0.02	0.04	-	-

the Λ_b , but it accounts for less than 50% of these decays, in both of the harmonic oscillator models. A large fraction (about 20%) goes into the first excited state, the Roper resonance, usually treated as a radial excitation of the ground-state nucleon, as it is in this model. As with the $\Lambda(1405)$ in the decays of the Λ_c , this result hinges on the assumption that the Roper resonance is a three-quark state, and that it is the first radial excitation of the nucleon. A number of hypotheses for the internal structure of this state have been made, such as pentaquark partner [80], dynamically generated state [81], and hybrid state [82]. In each of these scenarios, the rate at which the Λ_b decays semileptonically into this state is affected by its internal structure. For the three-quark, radially-excited scenario, the prediction is that decays to this state are about 60% of the decays to the ground state nucleon, a rather large fraction. If ample Λ_b 's can be produced, their semileptonic decays may therefore provide information that can be used in understanding the structure of the Roper resonance.

We have examined decays to other excited nucleons, and those shown in Table 5.15 are by far the dominant ones. We have also examined one additional $1/2^+$ nucleon state, two additional nucleon states with $J^P = 3/2^+$, and one additional nucleon state with $J^P = 5/2^+$, none of which are shown in Table 5.15. Of these, the rate to the additional $1/2^+$ state is less than 1% of the ‘total’ rate that we have estimated, while rates to the additional $3/2^+$ and $5/2^+$ states are similarly small or even smaller. These small rates are a direct consequence

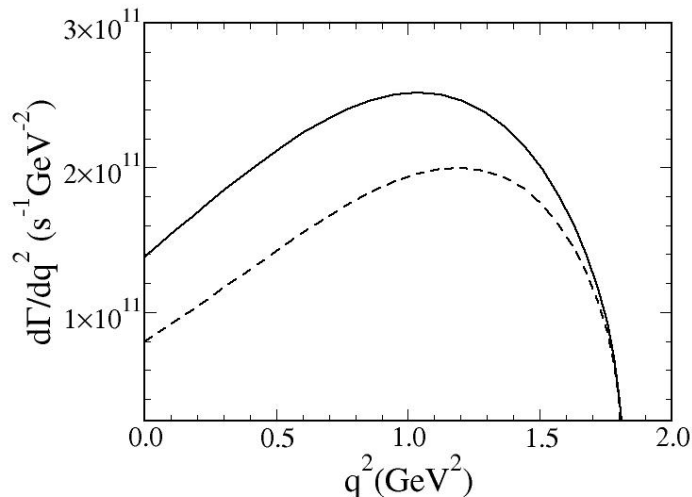


Figure 5.8: Differential decay rate for $\Lambda_c \rightarrow n$ in the HONR and HOSR models.

of the structure of these states, as their overlaps with the decaying Λ_b , in the spectator assumption, are very small. The only other excited nucleons that may occur with ‘significant’ rate in the semileptonic decays of the Λ_b are those with higher spins, such as $7/2^+$ and $5/2^-$. However, for such states, orbital angular momentum centrifugal factors will lead to some suppression of the decay rate.

Figure 5.8 shows the differential decay rate for $\Lambda_c \rightarrow n$, while the integrated decay rates for two exclusive modes $\Lambda_c \rightarrow N^{(*)0}$, obtained using $|V_{cd}| = 0.224$, are shown in Table 5.15. It is clear from this table that decays of the Λ_c to excited states of the nucleon are strongly suppressed, due in part to the reduced phase space.

5.3 Form Factors and Decay Rates: Ω_Q

5.3.1 $\Omega_b \rightarrow \Omega_c^{(*)}$ Decay

The form factors at the non-recoil point for the $\Omega_b \rightarrow \Omega_c^{(*)}$ decays are shown in Table 5.16 in all four models we use in this work. In this table we show only the form factors for the decays to final states with $J^P = 1/2^+$ and $3/2^+$. These constitute the elastic decays. We note that the two harmonic oscillator model (HONR and HOSR) form factor values at the non-recoil points are very close to each other, while the Sturmian model (STNR and STSR)

form factor values are slightly different from each other. The origin of this difference lies in the mixing of the wave functions of the Ω_b and Ω_c states with spin $1/2^+$ and $3/2^+$, as shown in Table 5.7.

It is instructive to compare our form factor values at the non-recoil point with the HQET predictions for the ground state doublet. For the state with $J^P = 1/2^+$, the HQET prediction is $F_1 = G_1 = \eta_1^{(1)}/3$. With the known normalization condition on $\eta_1^{(1)}$, this means that we expect $F_1 = G_1 = -1/3$ at the non-recoil point. We see that our results for G_1 are very close to this, but those for F_1 are not. The deviations from the HQET predictions can easily be traced to the presence of $1/m_q$ and $1/m_Q$ terms in the quark model results for F_1 , while no such terms exist in the model predictions for G_1 . If such terms are ignored in F_1 then the HQET prediction is indeed satisfied in the quark models. Similarly, HQET predicts that F_2 and F_3 should each have the value of $2/3$ at the non-recoil point. The model results agree with this prediction for F_2 but not for F_3 , and the differences can again be traced to the presence of $1/m_q$ terms in the quark model results. The HQET predictions for G_2 and G_3 are less easily interpreted, but comparison of those predictions with the quark model calculations suggests that the Isgur-Wise function $\eta_2^{(1)}$ is normalized to $1/2$ at the non-recoil point. We have already raised this point in Section 2.3.5 where we discuss the HQET predictions.

For the state with $J^P = 3/2^+$, HQET predicts that $F_4 = -G_4 = 2/\sqrt{3}$. This is well satisfied by the model predictions for G_4 , but the model predictions for F_4 include $1/m_q$ contributions. Assuming that $\eta_2^{(1)}$ is indeed normalized to $1/2$ at the non-recoil point, the HQET prediction is then that $G_1 = 0$ and $F_3 = -G_3 = -1/\sqrt{3}$. The quark model results for G_3 are close to the HQET prediction, but those for F_3 deviate from this prediction because of the presence of $1/m_q$ terms in the quark model results.

Figure 5.9 shows the q^2 dependence of the form factors for the elastic transition $\Omega_b \rightarrow \Omega_c(1/2^+)$ calculated in the HONR and HOSR models on the left, and in the STSR and STNR models on the right. In each panel, the solid curves arise from the SR version of the model, while the dashed curves are from the NR version. Once again the difference in the STNR and STSR form factor curves near the non-recoil point arise because of the different mixing of the ground state wave functions of Ω_b and Ω_c . Here we note that the form factors calculated using the Sturmian wave functions have larger slopes near the non-recoil point than those calculated using the harmonic oscillator wave functions. As we have seen in the Λ_Q decay rates, we expect the integrated Ω_b decay rates obtained using Sturmian wave

Table 5.16: The form factors for $\Omega_b \rightarrow \Omega_c^{(*)}$ transitions, calculated at the non-recoil point, in the four models used here.

spin	model	F_1	F_2	F_3	F_4	G_1	G_2	G_3	G_4
$1/2^+$	HONR	-0.48	0.64	0.83	-	-0.33	0.11	-0.04	-
$1/2^+$	HOSR	-0.47	0.65	0.81	-	-0.33	0.10	-0.04	-
$1/2^+$	STNR	-0.57	0.69	1.03	-	-0.38	0.15	-0.04	-
$1/2^+$	STSR	-0.47	0.56	0.86	-	-0.32	0.13	-0.03	-
$3/2^+$	HONR	0.80	0.0	-0.80	1.59	0.0	-0.15	0.64	-1.12
$3/2^+$	HOSR	0.80	0.0	-0.80	1.60	0.0	-0.16	0.64	-1.13
$3/2^+$	STNR	0.97	0.0	-0.97	1.94	0.0	-0.27	0.70	-1.29
$3/2^+$	STSR	0.82	0.0	-0.82	1.65	0.0	-0.22	0.60	-1.11

functions to be smaller than those obtained using harmonic oscillator wave functions.

The differential decay rates, $d\Gamma/dq^2$, that we obtain in the four models for different final states in $\Omega_b \rightarrow \Omega_c^{(*)} \ell \nu_\ell$, with $\ell = e^-, \mu^-$, are shown in Figure 5.10. For these rates, we use $|V_{cb}| = 0.041$. In these figures, we only show the differential rates for the dominant decays to the two elastic channels, with $J^P = 3/2^+$ and $J^P = 1/2^+$, and for two orbital excitations, the states with $J^P = 3/2^-$ and $5/2^-$. We have also examined the differential decay rates to the $1/2^-$, $1/2_1^-$, and $3/2_1^-$ orbitally excited states, as well as to the radially excited state $1/2_1^+$ and $3/2_1^+$ (notations defined in Section 3.1.2). We have found that the branching fraction for the radially excited states (not shown in the Table 5.17) are small, whereas the branching fraction for the decays to the orbitally excited states are not insignificant, as shown in Table 5.17. The bottom panel of Figure 5.10 shows the differential decay rates of Ω_b decaying to different Ω_c final states but with a τ lepton.

In Table 5.17 we show the integrated decay rates for the different final states in the four quark models we use. The first part of this table shows the rate with vanishing lepton mass, whereas the second part shows the rate when the final lepton is a τ . The last two rows of the first part of the table present the total decay rate and the ratio of the elastic decay rate to the total semileptonic rate. As anticipated, the integrated rates obtained in the Sturmian models are smaller than those obtained in the harmonic oscillator models. However, the branching fraction for the elastic decay mode is almost independent of the models we used. In two (HOSR, STSR) of our four models we predict about 61% of Ω_b decays to the ground states

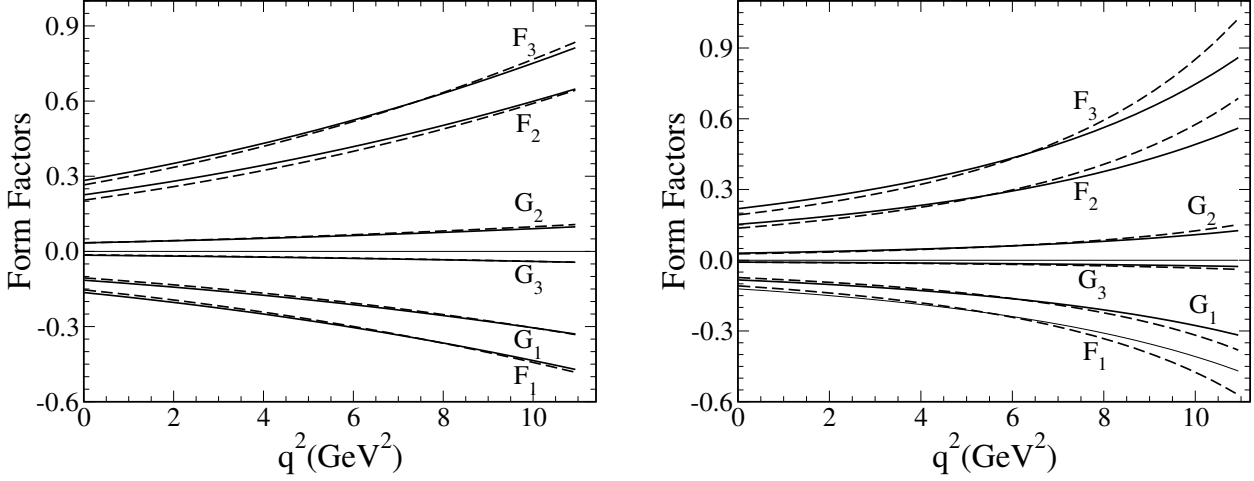


Figure 5.9: Form factors for $\Omega_b \rightarrow \Omega_c(1/2^+)$ obtained using harmonic oscillator wave functions (left panel, HOSR and HONR models) and Sturmian wave functions (right panel, STSR and STSR models). In each panel, the solid curves arise from the semirelativistic version of the model, while the dashed curves arise from the non-relativistic version.

of Ω_c and the HONR and STNR models predict about 62% and 67% for the same branching fraction. This implies that the elastic decay processes dominate the Ω_b semileptonic decay but do not saturate it: there is some significant branching fraction to the orbitally excited decay modes.

We may also compare our decay rates with HQET predictions. As discussed in Section 2.3.5, there are a number of pairs of degenerate states, such as states with $J^P = (1/2^+, 3/2^+)$, $J^P = (1/2^-, 3/2^-)$, $J^P = (3/2_1^-, 5/2^-)$. In the heavy quark limit, the ratio between the rates of the ground state heavy baryon decaying to the states in the first two degenerate pairs is expected to be 1 : 2, and for the third pair it is 2 : 3. In other words, for example, we expect the rate for $\Omega_b(1/2^+) \rightarrow \Omega_c(3/2^+)$ to be twice as large as the rate for $\Omega_b(1/2^+) \rightarrow \Omega_c(1/2^+)$. The expected pattern of the rates coming from the HQET prediction is reflected in all of our quark model calculations, as shown in Table 5.17. Departures from these predictions are due to $1/m_Q$ and $1/m_Q$ corrections, and the fact that, for instance, the $3/2^-$ state shown in the table is not exactly the state in the $(1/2^-, 3/2^-)$ multiplet, but contains some admixture of the $3/2^-$ state from $(3/2_1^-, 5/2^-)$ multiplet.

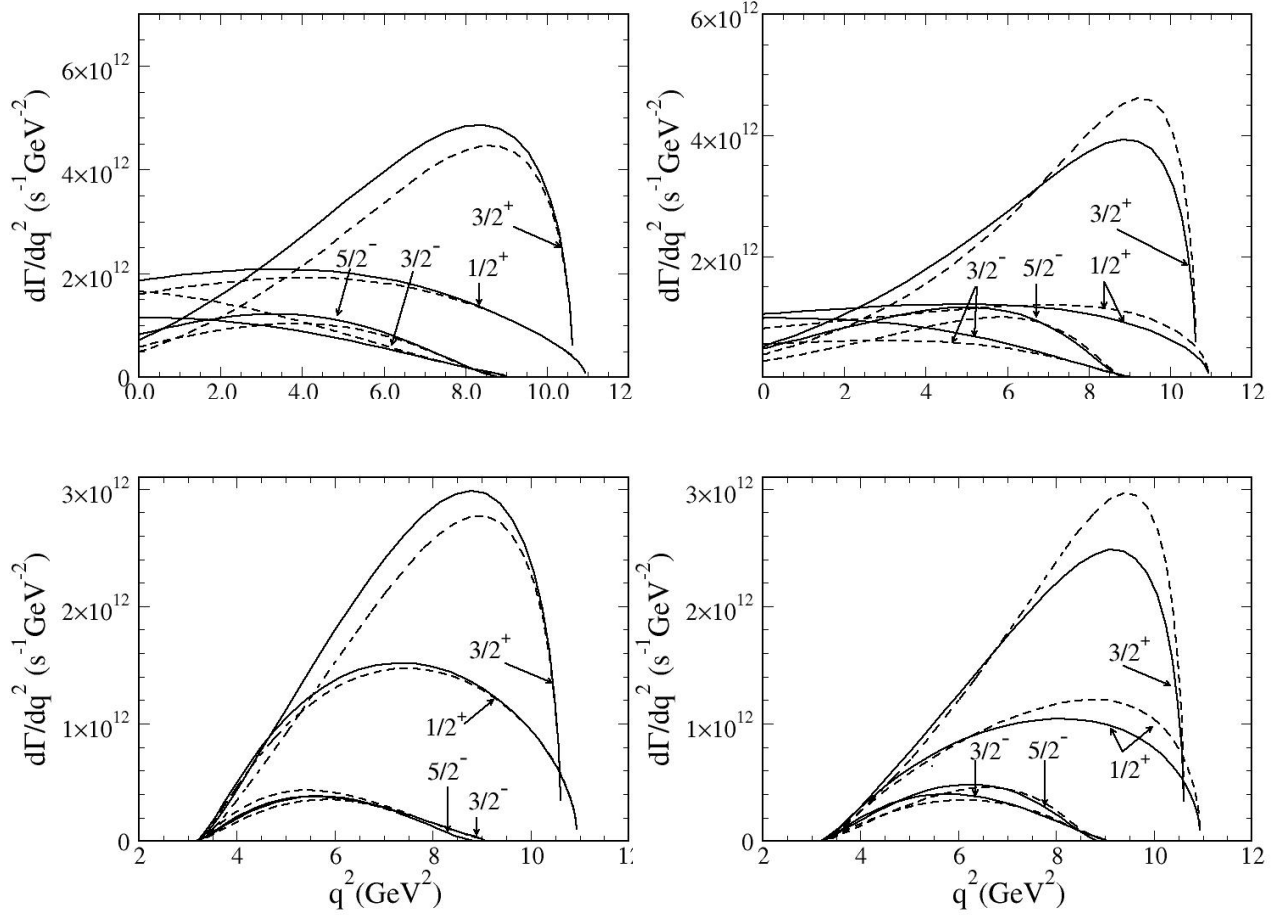


Figure 5.10: The differential decay rates for different $\Omega_b \rightarrow \Omega_c^{(*)}$ transitions, in the various models that we use. The curves on the left arise from the two versions of the harmonic oscillator model, while those on the right are from the Sturmian models. The upper panels are for $\Omega_b \rightarrow \Omega_c^{(*)} l \bar{\nu}_l$, where l is e^- or μ^- . The lower panels are for $\Omega_b \rightarrow \Omega_c^{(*)} \tau \bar{\nu}_\tau$. The curves are for final states with $J^P = 3/2^+, 1/2^+, 3/2^-$ and $5/2^-$.

In Table 5.17 we have shown only the rates to those spin states of $\Omega_c^{(*)}$ which have a significant branching fraction. However, we have calculated the rates of Ω_b decaying to the majority of states listed in Eq. 3.6, and we have found that the rates for states not shown in the table are small (of the order of 1%).

Table 5.17: Integrated decay rates for $\Omega_b \rightarrow \Omega_c^{(*)}$ in units of $10^{10}s^{-1}$, for different Ω_c states in the four models we consider. The top part of the table represents the decay rates with lepton (electron and muon case) mass zero, and the bottom part corresponds to the rates with non-vanishing mass for the τ lepton.

	$\Omega_b \rightarrow \Omega_c^{(*)} \ell^- \bar{\nu}_\ell$			
Spin	$\Gamma(\text{HONR})$	$\Gamma(\text{HOSR})$	$\Gamma(\text{STNR})$	$\Gamma(\text{STSR})$
$3/2^+$	2.16	2.51	1.91	1.86
$1/2^+$	1.30	1.40	0.84	0.87
$3/2^-$	0.63	0.75	0.32	0.46
$1/2^-$	0.30	0.38	0.16	0.22
$5/2^-$	0.50	0.59	0.44	0.56
$3/2_1^-$	0.33	0.35	0.23	0.24
$1/2_1^-$	0.38	0.43	0.21	0.28
total	5.59	6.41	4.11	4.49
$\Gamma_{\Omega_c}/\Gamma_{\text{total}}$	0.62	0.61	0.67	0.61
	$\Omega_b \rightarrow \Omega_c^{(*)} \tau^- \bar{\nu}_\tau$			
Spin	$\Gamma(\text{HONR})$	$\Gamma(\text{HOSR})$	$\Gamma(\text{STNR})$	$\Gamma(\text{STSR})$
$3/2^+$	0.95	1.06	0.91	0.83
$1/2^+$	0.62	0.64	0.48	0.44
$3/2^-$	0.12	0.13	0.10	0.11
$1/2^-$	0.06	0.07	0.05	0.05
$5/2^-$	0.09	0.10	0.12	0.13
$3/2_1^-$	0.06	0.06	0.07	0.06
$1/2_1^-$	0.06	0.06	0.05	0.05
total	1.96	2.12	1.78	1.67

5.3.2 $\Omega_c \rightarrow \Xi^{(*)}$ Decay

The $\Omega_c \rightarrow \Xi^{(*)}$ decay is a heavy to light decay process, where the charm quark of Ω_c is decaying to a light (down) quark. Such a process would best be described in the framework of HQET as a heavy to light transition. Nonetheless, it is interesting to compare the quark model predictions for these decay processes with the heavy to heavy predictions of HQET.

Table 5.18 shows the values of the form factors at the non-recoil point for the two elastic decay processes of $\Omega_c \rightarrow \Xi$. The difference between the harmonic oscillator and Sturmian model values arise because of the significant mixing in the $J^P = 3/2^+$ and $J^P = 1/2^+$ state Sturmian wave functions for both Ω_c and Ξ , whereas the harmonic oscillator models

predict mostly single component wave functions for these states. We may also compare our model-predicted form factor values, shown in Table 5.18, with the HQET predictions. As we discussed in the previous section for final state $J^P = 1/2^+$, we expect F_1 and G_1 to be $-1/3$ at the non-recoil point in the heavy quark limit. The large deviation of F_1 from the value of $-1/3$ can be traced to the presence of a $1/m_q$ term in the form factor, and with q being a u quark in the case of Ξ , this next to leading order term makes a large contribution, comparable to the leading order term. Similar effects, coming from the next to leading order terms, occur in F_3 and G_2 . In the same way we compare the spin $3/2^+$ model form factor values with HQET predictions at the non-recoil point. A comparison between the form factor values presented in Table 5.18 and HQET predictions shows that the numbers are compatible when there is no $1/m_q$ term present in the form factors, such as G_3 and G_4 . Otherwise, we notice significant deviation in our model-predicted form factor values from the HQET predictions.

Table 5.18: The form factors for $\Omega_c \rightarrow \Xi^{(*)}$ transitions, calculated at the non-recoil point, in the four models used here.

spin	model	F_1	F_2	F_3	F_4	G_1	G_2	G_3	G_4
$1/2^+$	HONR	-0.82	0.51	1.25	-	-0.31	0.38	-0.13	-
$1/2^+$	HOSR	-0.88	0.45	1.38	-	-0.32	0.42	-0.12	-
$1/2^+$	STNR	-0.98	0.41	1.59	-	-0.34	0.51	-0.12	-
$1/2^+$	STSR	-0.97	0.23	1.66	-	-0.31	0.57	-0.09	-
$3/2^+$	HONR	1.14	0.0	-1.14	2.28	0.0	-0.42	0.72	-0.96
$3/2^+$	HOSR	1.37	0.0	-1.37	2.75	0.0	-0.61	0.76	-1.08
$3/2^+$	STNR	1.82	0.0	-1.82	3.64	0.0	-0.87	0.85	-1.32
$3/2^+$	STSR	1.70	0.0	-1.70	3.40	0.0	-0.94	0.71	-1.08

The form factors for the $\Omega_c \rightarrow \Xi(1/2^+)$ are shown in Figure 5.11 as a function of q^2 . The left panel shows the form factors obtained in the HONR and HOSR and the right panel shows the results from the STNR and STSR models. The pattern of the form factors (Sturmian form factors having larger slopes than those of the harmonic oscillator) in the different models is similar to what we have seen previously in other decays we have considered.

The differential decay rates, $d\Gamma/dq^2$, for Ω_c to the dominant final states of $\Xi^{(*)}$ are plotted as a function of q^2 and shown in Figure 5.12. The right panel shows the differential decay

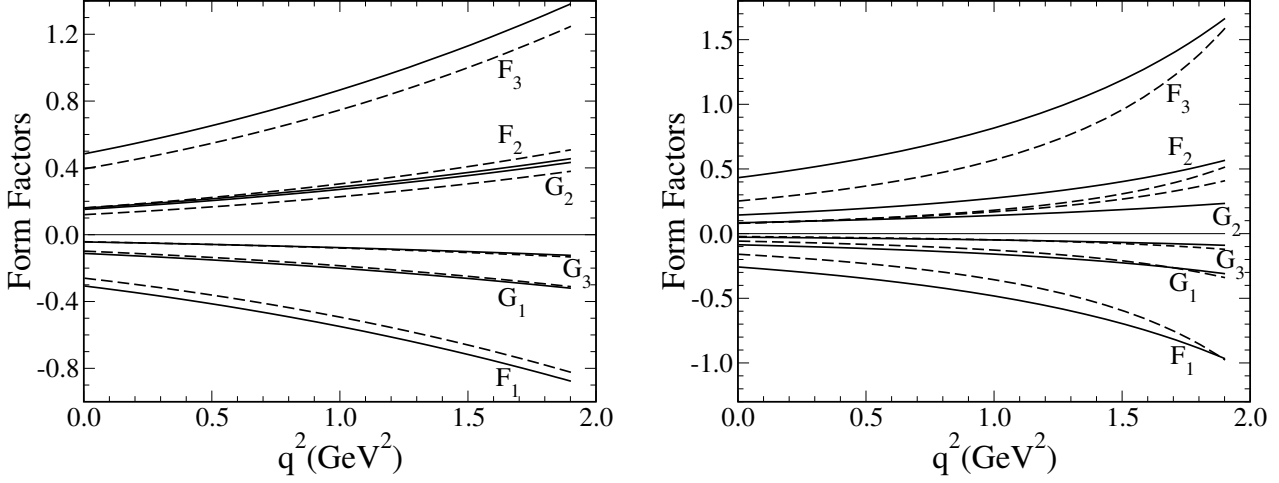


Figure 5.11: Form factors for $\Omega_c \rightarrow \Xi(1/2^+)$ obtained using harmonic oscillator wave functions (left panel, HOSR and HONR models) and Sturmian wave functions (right panel, STSR and STSR models). In each panel, the solid curves arise from the semirelativistic version of the model, while the dashed curves arise from the non-relativistic version.

rates obtained in the HONR and HOSR models and the left panel shows the results from the STNR and STSR models. In both harmonic oscillator and Sturmian models we see significant differences between the non-relativistic and semi-relativistic predictions. Although the different size parameters obtained in various models play a role in these differences, we should also note here that this particular decay rate is very sensitive to the values of m_σ ($\sigma = s$ in this decay). Our fitted values for the strange quark mass in different models, shown in Table 5.1, show significant variation. We have seen similar differences between NR and SR model differential decay rates for the $\Lambda_c \rightarrow n$ decay mode, as shown in Figure 5.8.

The integrated decay rates of Ω_c to various states of Ξ are shown in Table 5.19 in the four different models we use in this project. The last two rows give the total decay rate and the branching fraction to the ‘elastic decay’ modes. Even though a small fraction of Ω_c decays to the orbitally excited $\Xi^{(*)}$, we note that the two elastic decay modes dominate the decay. We also note that the rates obtained in Sturmian models are smaller than those obtained in harmonic oscillator models, with the exceptions of the final state $3/2^+$ and $5/2^-$ rates. In addition, we see that the predictions for the integrated rates are quite different in

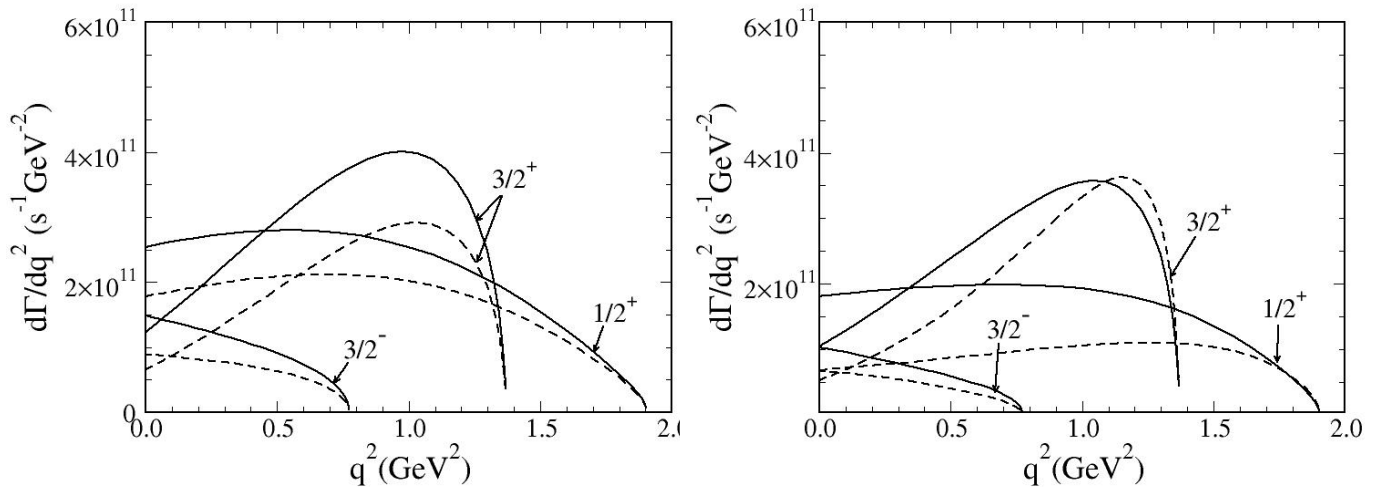


Figure 5.12: The differential decay rates for different $\Omega_c \rightarrow \Xi^{(*)}$ transitions, in the various models that we use. The curve on the left arise from the harmonic oscillator model, while those on the right are from the Sturmian model. The curves are for final states with $J^P = 3/2^+$, $1/2^+$, and $3/2^-$.

the NR and SR models. Nevertheless, the predicted elastic fraction shows very little model dependence.

5.3.3 $\Omega_c \rightarrow \Omega^{(*)}$ Decay

Table 5.20 shows the integrated rates for Ω_c decaying to Ω in the two harmonic oscillator models we use. We note that the decay to the ground state ($J^P = 3/2^+$) almost saturates the decay, providing 94% of the total decay rate. The lack of phase space suppresses the decays to the excited Ω . We do not present results for Sturmian models.

Table 5.19: Integrated decay rates for $\Omega_c \rightarrow \Xi^{(*)}$ in units of $10^{10} s^{-1}$, for different Ξ states in the four models we consider.

Spin	$\Gamma(\text{HONR})$	$\Gamma(\text{HOSR})$	$\Gamma(\text{STNR})$	$\Gamma(\text{STSR})$
$3/2^+$	0.52	0.76	0.55	0.65
$1/2^+$	0.60	0.78	0.32	0.58
$3/2^-$	0.10	0.15	0.07	0.10
$1/2^-$	0.05	0.07	0.02	0.03
$1/2_1^-$	0.07	0.10	0.04	0.06
$3/2_1^-$	0.01	0.02	0.01	0.02
$5/2^-$	0.01	0.02	0.03	0.03
total	1.36	1.90	1.04	1.47
$\Gamma_{\Xi}/\Gamma_{\text{total}}$	0.82	0.81	0.84	0.84

Table 5.20: Integrated decay rates for $\Omega_c \rightarrow \Omega^{(*)}$ in units of $10^{11} s^{-1}$, for different Ω states in the four models we consider. The last row shows the ‘elastic fraction’ obtained in our model, where the decays shown in the table are assumed to saturate the semileptonic decays.

Spin	$\Gamma(\text{HONR})$	$\Gamma(\text{HOSR})$
$3/2^+$	2.57	3.60
$3/2^-$	0.08	0.10
$1/2^-$	0.06	0.08
$1/2^+$	0.03	0.03
total	2.74	3.81
$\Gamma_{\Omega}/\Gamma_{\text{total}}$	0.94	0.94

5.4 Conclusions and Outlook

A constituent quark model calculation of semileptonic decays of heavy baryons, which has several novel features, is described here. Analytic results for the form factors for the decays to ground states and excited states with different quantum numbers are evaluated, and compared to HQET predictions. For both $\Lambda_b \rightarrow \Lambda_c$ and $\Omega_b \rightarrow \Omega_c$ transitions, the relations among the form factors, predicted by HQET, are satisfied by the form factors obtained in the model, independent of the basis used to describe the baryon wave functions. For $\Lambda_b \rightarrow \Lambda_c$ decays, the elastic form factors, as well as the form factors for decays to the $(1/2^-, 3/2^-)$ doublet satisfy the HQET relationships up to the order we have examined, namely $1/m_b$ and $1/m_c$. For states of higher spin, we have compared our model form factors to the HQET predictions at leading order, and the expected relations hold at that order. A similar observation for $\Omega_b \rightarrow \Omega_c$ transitions shows that the HQET relationships among the form factors in the $(1/2^+, 3/2^+)$, $(1/2^-, 3/2^-)$, $(3/2^-, 5/2^-)$, and $(3/2^+, 5/2^+)$ doublets are respected in our predicted form factors at leading order.

These form factors depend on the size parameters of the initial and final baryon wave functions, and so a fit is made to the spectrum of the states treated here. Two model Hamiltonians are used, with either a nonrelativistic or semi-relativistic kinetic energy term, and with Coulomb and spin-spin contact interactions. The wave functions are expanded in either a harmonic oscillator or Sturmian basis, up to second-order polynomials, and our numerical results for form factors and rates are calculated using the resulting mixed wave functions. Four sets of predictions are made for form factors and rates, with wave functions, size parameters and mixing coefficients arising from fits using both the non-relativistic and semi-relativistic Hamiltonians, and using the two different bases. The variation among these predictions can be used to assess the model dependence in the results we obtain.

Interestingly, the form factors for decays to ground state daughter baryons evaluated using the Sturmian basis for the wave functions have slopes at the non-recoil point that are significantly larger than those evaluated using the harmonic oscillator basis. As a result, the corresponding integrated decay rates for $\Lambda_c \rightarrow \Lambda$ elastic decays, calculated using the Sturmian wave functions, are smaller than those obtained using the harmonic oscillator basis wave functions. The Sturmian rates are both consistent within errors with the experimentally reported $\Lambda_c \rightarrow \Lambda$ rate of $1.05 \pm 0.35 \times 10^{11} \text{ s}^{-1}$, while those calculated using the harmonic

oscillator basis are significantly larger. As pointed out by Keister and Polyzou [69], although calculations using the Sturmian basis are not as simple as those using the harmonic oscillator basis, the resulting form factors have shapes which are expansions in inverse powers of $1 + k^2/\Lambda^2$, with k the decay three-momentum (in a non-relativistic decay calculation like ours), and Λ a constant which is calculated in terms of quark masses and wave function size parameters. This is closer to the form expected from experimental studies of hadron decay form factors, and so the use of Sturmian basis functions produces realistic results for decay calculations even with the inevitable truncations of the basis required for tractability. Larger scale numerical calculations using the Sturmian basis require fewer basis states than those using the harmonic oscillator basis to yield accurate energies and decay form factors for excited states.

Although the use of a semi-relativistic Hamiltonian does not necessarily lead to a better fit to the spectrum, in calculations using both bases it results in an integrated decay rate for the $\Lambda_c \rightarrow \Lambda$ elastic channel that is closer to the central value that has been experimentally reported. However, the rate obtained in the nonrelativistic version of the Sturmian model is also consistent (within 1σ) with the experimentally reported value.

Decay form factors and rates to all available excited state daughter baryons are evaluated using these four models. Significant branching fractions are found for Λ_c inelastic semileptonic decays in all four calculations, with the total to all excited states ranging from 11 to 19%. This has important consequences for the absolute normalization of the branching fractions to the many observed final states in Λ_c^+ decay, most of which are measured relative to the decay mode $\Lambda_c^+ \rightarrow pK^-\pi^+$. The extraction of the absolute branching fraction of this mode, from measurements of the cross section for $\Lambda_c^+ X$ production in e^+e^- annihilation, requires knowledge of the fraction f of semi-leptonic decays $\Lambda_c^+ \rightarrow X_s \ell^+ \nu_\ell$ to the elastic channel. Our predictions for the inelastic branching fraction contradicts the available CLEO analyses, in which it is assumed that the elastic decay of the Λ_c saturates its semileptonic decays. A larger fraction, from 23 \rightarrow 38%, of $\Lambda_b \rightarrow \Lambda_c$ semileptonic decays are found to be inelastic. Elastic decays of the Λ_b involving tau leptons in the final state are suppressed by roughly a factor of two because of the reduction in the final-state phase space, and those to excited baryon states are suppressed more strongly.

HQET predicts that the form factors ξ_1 and ξ_2 , defined earlier, should be the same for the decays $\Lambda_b \rightarrow N^0$ and $\Lambda_c \rightarrow N^+$, up to $1/m_b$ or $1/m_c$ corrections. Within our approaches,

we find that the two form factors are very similar, but not identical, with the differences arising from differences in the size parameters for the Λ_b and Λ_c . In the case of the decay of the Λ_b to nucleons, we find that the ‘elastic’ fraction is quite small, of the order of 35% when the leptons produced in the decay are light. A number of excited nucleons contribute to the total rate, with the radially excited Roper having the next largest branching fraction. This may be used as a test of the structure of this resonance, if ample Λ_b ’s can be produced.

A few features which have been observed in the decays of Λ_b and Λ_c are also present in our quark model calculation of Ω_b and Ω_c decays. The slopes of the form factors for Ω_b and Ω_c decays obtained in the Sturmian model are larger than those obtained in the HO models. As a consequence, the integrated rates for various decay modes of Ω_b and Ω_c obtained in the Sturmian models are smaller than rates obtained in the HO models.

Experimental measurements of the semileptonic decay rates of Ω_Q are essentially non-existent, which implies that a comparison of our model predictions with experiment is not possible. Nevertheless, it is instructive to examine our predictions for the various integrated rates for Ω_b and Ω_c decays in light of HQET predictions for these decays. There are a number of pairs of degenerate states, such as states with $J^P = (1/2^+, 3/2^+)$, $J^P = (1/2^-, 3/2^-)$, $J^P = (3/2_1^-, 5/2^-)$, for which HQET predicts the relationships between the form factors as well as the ratio of rates of the degenerate pairs. According to this prediction, the rate for the $\Omega_b \rightarrow \Omega_c(3/2^+)$ decay is expected to be twice as large as the rate for $\Omega_b \rightarrow \Omega_c(1/2^+)$ decay, and the rate for the $J^P = 3/2^-$ final state decay is also expected to be twice as large as the rate for the $J^P = 1/2^-$ final state decay. In the same way the ratio of the rates for the final states of the $(3/2_1^-, 5/2^-)$ doublets is expected to be 2:3. These relationships among the rates of the degenerate pairs are well respected in all our quark model calculations for the semileptonic decays of Ω_b .

It is also interesting to note that our predictions for the elastic branching fraction of $\Omega_b \rightarrow \Omega_c^{(*)}$ decay are almost independent of the four models we use and we obtain a fraction $(63\% \pm 2)$ similar to the fraction we obtained for the $\Lambda_b \rightarrow \Lambda_c^{(*)}$ decays. The elastic fraction for $\Omega_c \rightarrow \Xi^{(*)}$ decays is significantly higher $(82\% \pm 2)$. For semileptonic decay of $\Omega_c \rightarrow \Omega^{(*)}$, 94% of all decays are elastic. Interestingly, the elastic fraction is essentially model independent for all Ω_Q decays.

The work presented in this dissertation can be extended in a number of directions. We can apply our model to the description of the semileptonic decays of the light baryons, although

these are already successfully described by Cabibbo theory. Essentially all experimentally accessible observables for these decays have been measured, and it will be interesting to see if our model, constructed with no special reference to chiral symmetry or current algebra, can describe the results of these measurements.

We have not examined the predictions of our model for the many polarization observables which can, in principle, be measured in semileptonic decays. One example is the asymmetry parameter α_{Λ_c} in the decays of the Λ_c , which has already been extracted by the CLEO collaboration. The predictions of our model for this and similar quantities are therefore of some interest. In addition, the rare decays of heavy baryons, such as $\Lambda_b \rightarrow \Lambda$ can easily be treated in the framework that we have developed. Such processes, along with their meson analogs, are used in searches for physics beyond the standard model. However, the interpretation of the measured rates depend strongly on estimates of the form factors involved (in much the same way that extraction of CKM matrix elements depends on the form factors that describe semileptonic decays). Finally, if factorization, in some form, is valid, the semileptonic form factors calculated in the dissertation may also be useful in the description of nonleptonic weak decays.

It may also be possible to systematically improve the quark model used in the present calculation. An obvious first step is the implementation of full symmetrization of the spatial wave functions in the Sturmian basis, which would allow calculation of results for decays to final state nucleons in this basis.

We also plan to modify and expand all our baryon spectrum codes to make predictions for baryons containing quarks with three different masses. One advantage of this modification is that it will allow us to examine the semileptonic decays of Ξ_Q . This study will be interesting as some of the Ξ_Q states have an antisymmetric (Λ_Q -like) light diquark, while some have a symmetric (Ω_Q -like) light diquark [70].

APPENDIX A

Wave Functions and Semileptonic Operators

A.1 Λ_Q Baryon

As mentioned in the text, our wave functions are expanded in two different bases. For the states of different spins and parities considered here, the expansions are given in this Appendix. For Λ_Q states with $J^P = 1/2^+$, the expansion reads

$$\begin{aligned}
 \Psi_{\Lambda_Q, 1/2^+ M} &= \phi_{\Lambda_Q} \left(\left[\eta_1^{\Lambda_Q} \psi_{000000}(\mathbf{p}_\rho, \mathbf{p}_\lambda) + \eta_2^{\Lambda_Q} \psi_{001000}(\mathbf{p}_\rho, \mathbf{p}_\lambda) + \eta_3^{\Lambda_Q} \psi_{000010}(\mathbf{p}_\rho, \mathbf{p}_\lambda) \right] \chi_{1/2}^\rho(M) \right. \\
 &+ \eta_4^{\Lambda_Q} \psi_{000101}(\mathbf{p}_\rho, \mathbf{p}_\lambda) \chi_{1/2}^\lambda(M) + \eta_5^{\Lambda_Q} \left[\psi_{1M_L 0101}(\mathbf{p}_\rho, \mathbf{p}_\lambda) \chi_{3/2}^S(M - M_L) \right]_{1/2, M} \\
 &+ \eta_6^{\Lambda_Q} \left[\psi_{1M_L 0101}(\mathbf{p}_\rho, \mathbf{p}_\lambda) \chi_{1/2}^\lambda(M - M_L) \right]_{1/2, M} \\
 &+ \left. \eta_7^{\Lambda_Q} \left[\psi_{2M_L 0101}(\mathbf{p}_\rho, \mathbf{p}_\lambda) \chi_{3/2}^S(M - M_L) \right]_{1/2, M} \right), \tag{A.1}
 \end{aligned}$$

where $[\psi_{LM_L n_\rho \ell_\rho n_\lambda \ell_\lambda}(\mathbf{p}_\rho, \mathbf{p}_\lambda) \chi_S(M - M_L)]_{JM}$ is a shorthand notation that denotes the Clebsch-Gordan sum $\sum_{M_L} \langle JM | LM_L, SM - M_L \rangle \psi_{LM_L n_\rho \ell_\rho n_\lambda \ell_\lambda}(\mathbf{p}_\rho, \mathbf{p}_\lambda) \chi_S(M - M_L)$.

For Λ_Q states with $J^P = 1/2^-$ and $3/2^-$, the expansion is

$$\begin{aligned}
 \Psi_{\Lambda_Q, J^- M} &= \phi_{\Lambda_Q} \left(\eta_1^{\Lambda_Q} \left[\psi_{1M_L 0100}(\mathbf{p}_\rho, \mathbf{p}_\lambda) \chi_{3/2}^S(M - M_L) \right]_{JM} \right. \\
 &+ \eta_2^{\Lambda_Q} \left[\psi_{1M_L 0100}(\mathbf{p}_\rho, \mathbf{p}_\lambda) \chi_{1/2}^\lambda(M - M_L) \right]_{JM} \\
 &+ \left. \eta_3^{\Lambda_Q} \left[\psi_{1M_L 0001}(\mathbf{p}_\rho, \mathbf{p}_\lambda) \chi_{1/2}^\rho(M - M_L) \right]_{JM} \right), \tag{A.2}
 \end{aligned}$$

where J can take the values $1/2$ or $3/2$.

For Λ_Q states with $J^P = 3/2^+$, the expansion is

$$\begin{aligned}
\Psi_{\Lambda_Q, 3/2^+M} &= \phi_{\Lambda_Q} \left(\eta_1^{\Lambda_Q} \psi_{000101}(\mathbf{p}_\rho, \mathbf{p}_\lambda) \chi_{3/2}^S(M) + \eta_2^{\Lambda_Q} [\psi_{1M_L0101}(\mathbf{p}_\rho, \mathbf{p}_\lambda) \chi_{3/2}^S(M - M_L)]_{3/2,M} \right. \\
&+ \eta_3^{\Lambda_Q} [\psi_{1M_L0101}(\mathbf{p}_\rho, \mathbf{p}_\lambda) \chi_{1/2}^\lambda(M - M_L)]_{3/2,M} \\
&+ \eta_4^{\Lambda_Q} [\psi_{2M_L0200}(\mathbf{p}_\rho, \mathbf{p}_\lambda) \chi_{1/2}^\rho(M - M_L)]_{3/2,M} \\
&+ \eta_5^{\Lambda_Q} [\psi_{2M_L0101}(\mathbf{p}_\rho, \mathbf{p}_\lambda) \chi_{3/2}^S(M - M_L)]_{3/2,M} \\
&+ \eta_6^{\Lambda_Q} [\psi_{2M_L0101}(\mathbf{p}_\rho, \mathbf{p}_\lambda) \chi_{1/2}^\lambda(M - M_L)]_{3/2,M} \\
&\left. + \eta_7^{\Lambda_Q} [\psi_{2M_L0002}(\mathbf{p}_\rho, \mathbf{p}_\lambda) \chi_{1/2}^\rho(M - M_L)]_{3/2,M} \right) \quad (\text{A.3})
\end{aligned}$$

For $J^P = 5/2^+$, the expansion is

$$\begin{aligned}
\Psi_{\Lambda_Q, 5/2^+M} &= \phi_{\Lambda_Q} \left(\eta_1^{\Lambda_Q} \psi_{1M_L0101}(\mathbf{p}_\rho, \mathbf{p}_\lambda) \chi_{3/2}^S(M) + \eta_2^{\Lambda_Q} [\psi_{2M_L0101}(\mathbf{p}_\rho, \mathbf{p}_\lambda) \chi_{3/2}^S(M - M_L)]_{5/2,M} \right. \\
&+ \eta_3^{\Lambda_Q} [\psi_{2M_L0101}(\mathbf{p}_\rho, \mathbf{p}_\lambda) \chi_{1/2}^\lambda(M - M_L)]_{5/2,M} \\
&+ \eta_4^{\Lambda_Q} [\psi_{2M_L0200}(\mathbf{p}_\rho, \mathbf{p}_\lambda) \chi_{1/2}^\rho(M - M_L)]_{5/2,M} \\
&\left. + \eta_5^{\Lambda_Q} [\psi_{2M_L0002}(\mathbf{p}_\rho, \mathbf{p}_\lambda) \chi_{1/2}^\rho(M - M_L)]_{5/2,M} \right) \quad (\text{A.4})
\end{aligned}$$

No other states are expected to have significant overlap with the decaying ground-state Λ_Q in the spectator approximation that we use.

The wave function components for nucleons are different from those shown above, due to the different (12) symmetry in the wave functions, and are shown below. For $J^P = 1/2^+$, nucleon wave functions are expanded as

$$\begin{aligned}
\Psi_{N, 1/2^+M} &= \phi_N \left([\eta_1^N \psi_{000000}(\mathbf{p}_\rho, \mathbf{p}_\lambda) + \eta_2^N \psi_{001000}(\mathbf{p}_\rho, \mathbf{p}_\lambda) + \eta_3^N \psi_{000010}(\mathbf{p}_\rho, \mathbf{p}_\lambda)] \chi_{1/2}^\lambda(M) \right. \\
&+ \eta_4^N \psi_{000101}(\mathbf{p}_\rho, \mathbf{p}_\lambda) \chi_{1/2}^\rho(M) + \eta_5^N [\psi_{1M_L0101}(\mathbf{p}_\rho, \mathbf{p}_\lambda) \chi_{1/2}^\rho(M - M_L)]_{1/2,M} \\
&+ \eta_6^N [\psi_{2M_L0200}(\mathbf{p}_\rho, \mathbf{p}_\lambda) \chi_{3/2}^S(M - M_L)]_{1/2,M} \\
&\left. + \eta_7^N [\psi_{2M_L0002}(\mathbf{p}_\rho, \mathbf{p}_\lambda) \chi_{3/2}^S(M - M_L)]_{1/2,M} \right), \quad (\text{A.5})
\end{aligned}$$

For $J^P = 1/2^-$ and $3/2^-$, the expansion is

$$\begin{aligned}\Psi_{N,J-M} &= \phi_N \left(\eta_1^N \left[\psi_{1M_L 0100}(\mathbf{p}_\rho, \mathbf{p}_\lambda) \chi_{1/2}^\rho(M - M_L) \right]_{JM} \right. \\ &\quad + \eta_2^N \left[\psi_{1M_L 0001}(\mathbf{p}_\rho, \mathbf{p}_\lambda) \chi_{3/2}^S(M - M_L) \right]_{JM} \\ &\quad \left. + \eta_3^N \left[\psi_{1M_L 0001}(\mathbf{p}_\rho, \mathbf{p}_\lambda) \chi_{1/2}^\lambda(M - M_L) \right]_{JM} \right),\end{aligned}\quad (\text{A.6})$$

where J can take the values $1/2$ or $3/2$.

A.2 Ω_Q Baryon

The wave function components for states that we consider are shown here. These components are valid for both the Ω_Q and Ξ states that are treated in this manuscript. For $J^P = 1/2^+$, wave functions are expanded as

$$\begin{aligned}\Psi_{1/2^+M}^{\Omega_Q} &= \phi_{\Omega_Q} \left(\left[\eta_1^{\Omega_Q} \psi_{000000}(\mathbf{p}_\rho, \mathbf{p}_\lambda) + \eta_2^{\Omega_Q} \psi_{001000}(\mathbf{p}_\rho, \mathbf{p}_\lambda) + \eta_3^{\Omega_Q} \psi_{000010}(\mathbf{p}_\rho, \mathbf{p}_\lambda) \right] \chi_{1/2}^\lambda(M) \right. \\ &\quad + \eta_4^{\Omega_Q} \psi_{000101}(\mathbf{p}_\rho, \mathbf{p}_\lambda) \chi_{1/2}^\rho(M) + \eta_5^{\Omega_Q} \left[\psi_{1M_L 0101}(\mathbf{p}_\rho, \mathbf{p}_\lambda) \chi_{1/2}^\rho(M - M_L) \right]_M^{1/2} \\ &\quad + \eta_6^{\Omega_Q} \left[\psi_{2M_L 0200}(\mathbf{p}_\rho, \mathbf{p}_\lambda) \chi_{3/2}^S(M - M_L) \right]_M^{1/2} \\ &\quad \left. + \eta_7^{\Omega_Q} \left[\psi_{2M_L 0002}(\mathbf{p}_\rho, \mathbf{p}_\lambda) \chi_{3/2}^S(M - M_L) \right]_M^{1/2} \right),\end{aligned}\quad (\text{A.7})$$

For Ω_Q states with $J^P = 3/2^+$, the expansion is

$$\begin{aligned}\Psi_{3/2^+M}^{\Omega_Q} &= \phi_{\Omega_Q} \left(\left[\eta_1^{\Omega_Q} \psi_{000000}(\mathbf{p}_\rho, \mathbf{p}_\lambda) + \eta_2^{\Omega_Q} \psi_{001000}(\mathbf{p}_\rho, \mathbf{p}_\lambda) + \eta_3^{\Omega_Q} \psi_{000010}(\mathbf{p}_\rho, \mathbf{p}_\lambda) \right] \chi_{3/2}^S(M) \right. \\ &\quad + \eta_4^{\Omega_Q} \left[\psi_{1M_L 0101}(\mathbf{p}_\rho, \mathbf{p}_\lambda) \chi_{1/2}^\rho(M - M_L) \right]_M^{3/2} \\ &\quad + \eta_5^{\Omega_Q} \left[\psi_{2M_L 0200}(\mathbf{p}_\rho, \mathbf{p}_\lambda) \chi_{3/2}^S(M - M_L) \right]_M^{3/2} \\ &\quad + \eta_6^{\Omega_Q} \left[\psi_{2M_L 0200}(\mathbf{p}_\rho, \mathbf{p}_\lambda) \chi_{1/2}^\lambda(M - M_L) \right]_M^{3/2} \\ &\quad + \eta_7^{\Omega_Q} \left[\psi_{2M_L 0101}(\mathbf{p}_\rho, \mathbf{p}_\lambda) \chi_{1/2}^\rho(M - M_L) \right]_M^{3/2} \\ &\quad + \eta_8^{\Omega_Q} \left[\psi_{2M_L 0002}(\mathbf{p}_\rho, \mathbf{p}_\lambda) \chi_{3/2}^S(M - M_L) \right]_M^{3/2} \\ &\quad \left. + \eta_9^{\Omega_Q} \left[\psi_{2M_L 0002}(\mathbf{p}_\rho, \mathbf{p}_\lambda) \chi_{1/2}^\lambda(M - M_L) \right]_M^{3/2} \right),\end{aligned}\quad (\text{A.8})$$

where $\left[\psi_{LM_L n_\rho \ell_\rho n_\lambda \ell_\lambda}(\mathbf{p}_\rho, \mathbf{p}_\lambda) \chi_S(M - M_L) \right]_M^J$ is a shorthand notation that denotes the Clebsch-Gordan sum $\sum_{M_L} \langle JM | LM_L, SM - M_L \rangle \psi_{LM_L n_\rho \ell_\rho n_\lambda \ell_\lambda}(\mathbf{p}_\rho, \mathbf{p}_\lambda) \chi_S(M - M_L)$.

For $J^P = 1/2^-$ and $3/2^-$, the expansion is

$$\begin{aligned}\Psi_{J^-M}^{\Omega_Q} &= \phi_{\Omega_Q} \left(\eta_1^{\Omega_Q} \left[\psi_{1M_L0100}(\mathbf{p}_\rho, \mathbf{p}_\lambda) \chi_{1/2}^\rho(M - M_L) \right]_M^J \right. \\ &\quad + \eta_2^{\Omega_Q} \left[\psi_{1M_L0001}(\mathbf{p}_\rho, \mathbf{p}_\lambda) \chi_{3/2}^S(M - M_L) \right]_M^J \\ &\quad \left. + \eta_3^{\Omega_Q} \left[\psi_{1M_L0001}(\mathbf{p}_\rho, \mathbf{p}_\lambda) \chi_{1/2}^\lambda(M - M_L) \right]_M^J \right),\end{aligned}\tag{A.9}$$

where J can take the values $1/2$ or $3/2$.

For $J^P = 5/2^+$, the expansion is

$$\begin{aligned}\Psi_{5/2^+M}^{\Omega_Q} &= \phi_{\Omega_Q} \left(\eta_1^{\Omega_Q} \psi_{2M_L0101}(\mathbf{p}_\rho, \mathbf{p}_\lambda) \chi_{1/2}^\rho(M - M_L) + \eta_2^{\Omega_Q} \left[\psi_{2M_L0200}(\mathbf{p}_\rho, \mathbf{p}_\lambda) \chi_{3/2}^S(M - M_L) \right]_M^{5/2} \right. \\ &\quad + \eta_3^{\Omega_Q} \left[\psi_{2M_L0200}(\mathbf{p}_\rho, \mathbf{p}_\lambda) \chi_{1/2}^\lambda(M - M_L) \right]_M^{5/2} + \eta_4^{\Omega_Q} \left[\psi_{2M_L0002}(\mathbf{p}_\rho, \mathbf{p}_\lambda) \chi_{3/2}^S(M - M_L) \right]_M^{5/2} \\ &\quad \left. + \eta_5^{\Omega_Q} \left[\psi_{2M_L0002}(\mathbf{p}_\rho, \mathbf{p}_\lambda) \chi_{1/2}^\lambda(M - M_L) \right]_M^{5/2} \right)\end{aligned}\tag{A.10}$$

For $J^P = 5/2^-$, the wave function is

$$\Psi_{J^-M}^{\Omega_Q} = \phi_{\Omega_Q} \left[\psi_{1M_L0001}(\mathbf{p}_\rho, \mathbf{p}_\lambda) \chi_{3/2}^S(M - M_L) \right]_M^{5/2},\tag{A.11}$$

No other states are expected to have significant overlap with the decaying ground-state Ω_Q in the spectator approximation that we use.

A.3 Semileptonic Operators

Table A.1: Quark matrix elements of $\langle q(p_Q, s_Q) | \mathcal{O}_i | Q(p_q, s_q) \rangle$, where \mathcal{O} are combination of γ -matrices with $i = 0, +, -, 3$ and $\mathcal{O}_+ = \mathcal{O}_1 + i\mathcal{O}_2$, $\mathcal{O}_- = \mathcal{O}_1 - i\mathcal{O}_2$. The superscripts of \mathcal{O} , such as ‘+’ implies the spin projection of the initial and final quarks.

\mathcal{O}	\mathcal{O}^{++}	\mathcal{O}^{--}	\mathcal{O}^{+-}	\mathcal{O}^{-+}
V_0	$1 + \frac{\mathbf{p}_Q \cdot \mathbf{p}_q + i(\mathbf{p}_{q1}\mathbf{p}_{Q2} - \mathbf{p}_{q2}\mathbf{p}_{Q1})}{4m_q m_Q}$	$1 + \frac{\mathbf{p}_Q \cdot \mathbf{p}_q + i(\mathbf{p}_{q1}\mathbf{p}_{Q2} - \mathbf{p}_{q2}\mathbf{p}_{Q1})}{4m_q m_Q}$	$\frac{\mathbf{p}_{q3}\mathbf{p}_{Q-} - \mathbf{p}_{q-}\mathbf{p}_{Q3}}{4m_q m_Q}$	$\frac{\mathbf{p}_q + \mathbf{p}_{Q3} - \mathbf{p}_{q3}\mathbf{p}_{Q+}}{4m_q m_Q}$
V_+	$\frac{\mathbf{p}_{Q+}}{m_q}$	$\frac{\mathbf{p}_{q+}}{m_q}$	$\frac{\mathbf{p}_{q3}}{m_q} - \frac{\mathbf{p}_{Q3}}{m_Q}$	0
V_-	$\frac{\mathbf{p}_{q-}}{m_q}$	$\frac{\mathbf{p}_{Q-}}{m_Q}$	0	$-\frac{\mathbf{p}_{q3}}{m_q} + \frac{\mathbf{p}_{Q3}}{m_Q}$
V_3	$\frac{\mathbf{p}_{q3}}{2m_q} + \frac{\mathbf{p}_{Q3}}{2m_Q}$	$\frac{\mathbf{p}_{q3}}{2m_q} + \frac{\mathbf{p}_{Q3}}{2m_Q}$	$-\frac{\mathbf{p}_{q-}}{2m_q} + \frac{2\mathbf{p}_{Q-}}{m_Q}$	$\frac{\mathbf{p}_{q+}}{2m_q} - \frac{2\mathbf{p}_{Q+}}{m_Q}$
A_0	$\frac{\mathbf{p}_{q3}}{2m_q} + \frac{\mathbf{p}_{Q3}}{2m_Q}$	$-\frac{\mathbf{p}_{q3}}{2m_q} - \frac{\mathbf{p}_{Q3}}{2m_Q}$	$\frac{\mathbf{p}_{q-}}{2m_q} + \frac{2\mathbf{p}_{Q-}}{m_Q}$	$\frac{\mathbf{p}_{q+}}{2m_q} + \frac{2\mathbf{p}_{Q+}}{m_Q}$
A_+	$\frac{\mathbf{p}_{q3}\mathbf{p}_{Q+}}{2m_q m_Q}$	$-\frac{\mathbf{p}_{q+}\mathbf{p}_{Q3}}{2m_q m_Q}$	$2 + \frac{\mathbf{p}_q - \mathbf{p}_{Q+} - 2\mathbf{p}_Q \cdot \mathbf{p}_q + \mathbf{p}_q + \mathbf{p}_{Q-}}{4m_q m_Q}$	$\frac{\mathbf{p}_q + \mathbf{p}_{Q+}}{2m_q m_Q}$
A_-	$\frac{\mathbf{p}_q - \mathbf{p}_{Q3}}{2m_q m_Q}$	$-\frac{\mathbf{p}_{q3}\mathbf{p}_{Q-}}{2m_q m_Q}$	$\frac{\mathbf{p}_q - \mathbf{p}_{Q-}}{2m_q m_Q}$	$2 + \frac{\mathbf{p}_q - \mathbf{p}_{Q+} - 2\mathbf{p}_Q \cdot \mathbf{p}_q + \mathbf{p}_q + \mathbf{p}_{Q-}}{4m_q m_Q}$
A_3	$1 + \frac{2\mathbf{p}_{q3}\mathbf{p}_{Q3} - \mathbf{p}_Q \cdot \mathbf{p}_q + i(\mathbf{p}_q \times \mathbf{p}_Q)_3}{4m_q m_Q}$	$-1 + \frac{-2\mathbf{p}_{q3}\mathbf{p}_{Q3} + \mathbf{p}_Q \cdot \mathbf{p}_q + i(\mathbf{p}_q \times \mathbf{p}_Q)_3}{4m_q m_Q}$	$\frac{\mathbf{p}_q - \mathbf{p}_{Q3} + \mathbf{p}_{q3}\mathbf{p}_{Q-}}{4m_q m_Q}$	$\frac{\mathbf{p}_q + \mathbf{p}_{Q3} + \mathbf{p}_{q3}\mathbf{p}_{Q+}}{4m_q m_Q}$

Table A.2: Quark matrix elements of $\langle q(p_Q, s_Q) | \mathcal{O}_i | Q(p_q, s_q) \rangle$ in terms of spherical harmonics. The notations are same as in Table A.1. The momenta involved in the spherical harmonics are defined in Section 3.4.

\mathcal{O}	\mathcal{O}^{++}	\mathcal{O}^{--}
V_0	$\sqrt{4\pi} \left[\left(1 + \frac{p_\lambda^2}{6m_b m_c} \right) \mathcal{Y}_{00} - \frac{\sqrt{2}p}{12m_b m_c} \mathcal{Y}_{10} \right]$	$\sqrt{4\pi} \left[\left(1 + \frac{p_\lambda^2}{6m_b m_c} \right) \mathcal{Y}_{00} - \frac{\sqrt{2}p}{12m_b m_c} \mathcal{Y}_{10} \right]$
V_+	$\frac{4\sqrt{\pi}}{3m_b} \mathcal{Y}_{11}$	$\frac{4\sqrt{\pi}}{3m_c} \mathcal{Y}_{11}$
V_-	$-\frac{4\sqrt{\pi}}{3m_c} \mathcal{Y}_{1-1}$	$-\frac{4\sqrt{\pi}}{3m_b} \mathcal{Y}_{1-1}$
V_3	$\frac{\sqrt{4\pi}p}{2m_c} \mathcal{Y}_{00} - \frac{\sqrt{8\pi}}{6} \left(\frac{1}{m_b} + \frac{1}{m_c} \right) \mathcal{Y}_{10}$	$\frac{\sqrt{4\pi}p}{2m_c} \mathcal{Y}_{00} - \frac{\sqrt{8\pi}}{6} \left(\frac{1}{m_b} + \frac{1}{m_c} \right) \mathcal{Y}_{10}$
A_0	$\frac{\sqrt{4\pi}p}{2m_c} \mathcal{Y}_{00} - \frac{\sqrt{8\pi}}{6} \left(\frac{1}{m_b} + \frac{1}{m_c} \right) \mathcal{Y}_{10}$	$-\frac{\sqrt{4\pi}p}{2m_c} \mathcal{Y}_{00} + \frac{\sqrt{8\pi}}{6} \left(\frac{1}{m_b} + \frac{1}{m_c} \right) \mathcal{Y}_{10}$
A_+	$\frac{2\sqrt{\pi}}{3m_b m_c} (p\mathcal{Y}_{11} - \sqrt{\frac{2}{15}}\mathcal{Y}_{21})$	$\frac{2}{3m_b m_c} \sqrt{\frac{2\pi}{15}} \mathcal{Y}_{21}$
A_-	$\frac{2}{3m_b m_c} \sqrt{\frac{2\pi}{15}} \mathcal{Y}_{2-1}$	$\frac{2\sqrt{\pi}}{3m_b m_c} (p\mathcal{Y}_{1-1} - \sqrt{\frac{2}{15}}\mathcal{Y}_{2-1})$
A_3	$\sqrt{4\pi} \mathcal{Y}_{00} + \frac{1}{4m_b m_c} \left[-\sqrt{\frac{8\pi}{9}} p \mathcal{Y}_{10} + \frac{16}{9} \sqrt{\frac{\pi}{5}} \mathcal{Y}_{20} - \frac{2\sqrt{4\pi}}{9} p_\lambda^2 \mathcal{Y}_{00} \right]$	$-\sqrt{4\pi} \mathcal{Y}_{00} - \frac{1}{4m_b m_c} \left[-\sqrt{\frac{8\pi}{9}} p \mathcal{Y}_{10} + \frac{16}{9} \sqrt{\frac{\pi}{5}} \mathcal{Y}_{20} - \frac{2\sqrt{4\pi}}{9} p_\lambda^2 \mathcal{Y}_{00} \right]$
\mathcal{O}	\mathcal{O}^{+-}	\mathcal{O}^{-+}
V_0	$-\frac{\sqrt{\pi}p}{3m_b m_c} \mathcal{Y}_{1-1}$	$-\frac{\sqrt{\pi}p}{3m_b m_c} \mathcal{Y}_{11}$
V_+	$\frac{\sqrt{4\pi}p}{m_c} \mathcal{Y}_{00} + \frac{\sqrt{8\pi}}{3} \left(\frac{1}{m_b} - \frac{1}{m_c} \right) \mathcal{Y}_{10}$	0
V_-	0	$-\frac{\sqrt{4\pi}p}{m_c} \mathcal{Y}_{00} - \frac{\sqrt{8\pi}}{3} \left(\frac{1}{m_b} - \frac{1}{m_c} \right) \mathcal{Y}_{10}$
V_3	$\frac{2\sqrt{\pi}}{3} \left(\frac{1}{m_c} - \frac{1}{m_b} \right) \mathcal{Y}_{1-1}$	$\frac{2\sqrt{\pi}}{3} \left(\frac{1}{m_c} - \frac{1}{m_b} \right) \mathcal{Y}_{11}$
A_0	$-\frac{2\sqrt{\pi}}{3} \left(\frac{1}{m_c} + \frac{1}{m_b} \right) \mathcal{Y}_{1-1}$	$\frac{2\sqrt{\pi}}{3} \left(\frac{1}{m_c} + \frac{1}{m_b} \right) \mathcal{Y}_{11}$
A_+	$2\sqrt{4\pi} \mathcal{Y}_{00} + \frac{1}{4m_b m_c} \left[2\sqrt{\frac{8\pi}{9}} p \mathcal{Y}_{10} - \frac{16}{9} \sqrt{\frac{\pi}{5}} \mathcal{Y}_{20} - \frac{4\sqrt{4\pi}}{9} p_\lambda^2 \mathcal{Y}_{00} \right]$	$\frac{4}{3m_b m_c} \sqrt{\frac{2\pi}{15}} \mathcal{Y}_{2-2}$
A_-	$\frac{4}{3m_b m_c} \sqrt{\frac{2\pi}{15}} \mathcal{Y}_{2-2}$	$2\sqrt{4\pi} \mathcal{Y}_{00} + \frac{1}{4m_b m_c} \left[2\sqrt{\frac{8\pi}{9}} p \mathcal{Y}_{10} - \frac{16}{9} \sqrt{\frac{\pi}{5}} \mathcal{Y}_{20} - \frac{4\sqrt{4\pi}}{9} p_\lambda^2 \mathcal{Y}_{00} \right]$
A_3	$\frac{\sqrt{\pi}}{3m_b m_c} \left(2\sqrt{\frac{2}{15}} \mathcal{Y}_{2-1} - p\mathcal{Y}_{1-1} \right)$	$\frac{\sqrt{\pi}}{3m_b m_c} (p\mathcal{Y}_{11} - 2\sqrt{\frac{2}{15}} \mathcal{Y}_{21})$

APPENDIX B

Integrals in the SturmianBasis

Wave functions expanded in the Sturmian basis have been used by other authors in exploring aspects of heavy meson phenomenology [83]. However, to the best of our knowledge, there have been no prior applications to baryon phenomenology. We therefore believe that it is useful to outline some of the steps needed in using this basis for calculations of the kind that we present.

B.0.1 Integrals for Hamiltonian Matrix Elements

We begin by reminding the reader that, in coordinate space, say, the spatial wave function components are written as

$$\psi_{LMn_\rho\ell_\rho n_\lambda\ell_\lambda}(\boldsymbol{\rho}, \boldsymbol{\lambda}) = \sum_m \langle LM | \ell_\rho m, \ell_\lambda M - m \rangle \psi_{n_\rho\ell_\rho m}(\boldsymbol{\rho}) \psi_{n_\lambda\ell_\lambda M - m}(\boldsymbol{\lambda}),$$

with $\boldsymbol{\rho}$ and $\boldsymbol{\lambda}$ as defined in the main text.

In the Sturmian basis, evaluation of the matrix elements of the non-relativistic kinetic energy operator, as well as those of the parts of the potential that depend only on $r_{12} \equiv |\mathbf{r}_1 - \mathbf{r}_2|$, are relatively straightforward, in the latter case because $\rho = r_{12}/\sqrt{2}$. However, the evaluation of terms that depend on r_{13} or r_{23} is not as straightforward. To illustrate the way in which such calculations are carried out, we consider the linear potential, and examine the term

$$V_{13}^{\text{lin}} = b |\mathbf{r}_1 - \mathbf{r}_3| = br_{13}. \quad (\text{B.1})$$

We begin by writing

$$r_{13} = \frac{1}{\sqrt{2}} \left| \boldsymbol{\rho} + \sqrt{3}\boldsymbol{\lambda} \right| \equiv |\boldsymbol{\rho}' + \boldsymbol{\lambda}'| = \frac{1}{\sqrt{2}} (\rho^2 + 2\sqrt{3}\boldsymbol{\rho} \cdot \boldsymbol{\lambda} + 3\lambda^2)^{1/2}. \quad (\text{B.2})$$

In the above, $\boldsymbol{\rho}' \equiv \boldsymbol{\rho}/\sqrt{2}$ and $\boldsymbol{\lambda}' \equiv \sqrt{3/2}\boldsymbol{\lambda}$. The latter form is expanded in spherical harmonics, yielding

$$r_{13} = 4\pi \sum_l \frac{1}{(2l+1)} \frac{\rho'^l}{\lambda'^{l+1}} \left(\frac{\rho'^2}{(2l+3)} - \frac{\lambda'^2}{(2l-1)} \right) \left(Y_l(\hat{\rho}) \cdot Y_l(\hat{\lambda}) \right) \quad (\text{B.3})$$

for $\rho' < \lambda'$, and a similar expression with $\rho' \leftrightarrow \lambda'$ otherwise. In this expansion,

$$\left(Y_l(\hat{\rho}) \cdot Y_l(\hat{\lambda}) \right) \equiv \sum_m (-1)^m Y_l^m(\hat{\rho}) Y_l^{-m}(\hat{\lambda}) \quad (\text{B.4})$$

Calculation of $\langle r_{13} \rangle$ then requires the evaluation of the matrix element $\langle L'n'_\rho l'_\rho n'_\lambda l'_\lambda | \mathcal{Y}_l(\hat{\rho}) \cdot \mathcal{Y}_l(\hat{\lambda}) | Ln_\rho l_\rho n_\lambda l_\lambda \rangle$, which symbolically denotes integrations over the angles defining $\boldsymbol{\rho}$ and $\boldsymbol{\lambda}$. This is done with the use of 6-J symbols, leaving integrals over the magnitudes of ρ and λ which can be done either numerically or analytically. For the potentials we use, all terms can be handled analytically. Terms in the potential that depend on r_{23} are handled in a similar manner.

B.0.2 Integrals for Current Matrix Elements

In order to evaluate the form factors in the Sturmian basis, integrals of the form

$$\mathcal{I}_{n_1, n_2}^{\ell_1, \ell_2, \ell_3} = \int d^3p \frac{\mathcal{Y}_{\ell_1}(\mathbf{p}) \mathcal{Y}_{\ell_2}(\mathbf{p} + a\mathbf{k}) \mathcal{Y}_{\ell_3}(\mathbf{p})}{(p^2 + \alpha^2)^{n_1} [(p + a\mathbf{k})^2 + \alpha'^2]^{n_2}} \quad (\text{B.5})$$

must be calculated. In the above, p represents an internal momentum conjugate to one of the Jacobi coordinates (for these integrals, p_λ), while \mathbf{k} is the momentum of the daughter baryon in the frame in which the parent is at rest. The constant $a = -2\sqrt{3/2} m_\sigma / m_{\Lambda_q}$, with m_{Λ_q} being the mass of the daughter baryon in the decay. The quantities $\mathcal{Y}_\ell(\mathbf{p})$ are the vector harmonics, with $\ell_{1,2}$ being the orbital angular momentum in the initial or final state, respectively, while $\mathcal{Y}_{\ell_3}(\mathbf{p})$ arises from the Pauli reduction of the vector or axial current. For simplicity we choose $\ell_1 = \ell_3 = 0$, but this will still be sufficient to illustrate the method.

With the use of Feynman parametrization, this integral is first rewritten as

$$\begin{aligned}
\mathcal{I}_{n_1, n_2}^{0, \ell, 0} &= \frac{1}{\sqrt{4\pi}} \frac{\Gamma(n_1 + n_2)}{\Gamma(n_1)\Gamma(n_2)} \int_0^1 dx \int d^3p \frac{x^{n_1-1}(1-x)^{n_2-1} \mathcal{Y}_0(\mathbf{p}) \mathcal{Y}_\ell(\mathbf{p} + a\mathbf{k})}{\{x(p^2 + \alpha^2) + (1-x)[(\mathbf{p} + a\mathbf{k})^2 + \beta^2]\}^{n_1+n_2}} \\
&= \frac{1}{\sqrt{4\pi}} \frac{\Gamma(n_1 + n_2)}{\Gamma(n_1)\Gamma(n_2)} \int_0^1 dx \int d^3p \\
&\quad \times \frac{x^{n_1-1}(1-x)^{n_2-1} \mathcal{Y}_0(\mathbf{p}) \mathcal{Y}_\ell(\mathbf{p} + a\mathbf{k})}{[p^2 + 2a(1-x)\mathbf{p} \cdot \mathbf{k} + a^2k^2(1-x) + \beta^2(1-x) + \alpha^2x]^{n_1+n_2}} \\
&= \frac{1}{\sqrt{4\pi}} \frac{\Gamma(n_1 + n_2)}{\Gamma(n_1)\Gamma(n_2)} \int_0^1 dx \int d^3p \\
&\quad \times \frac{x^{n_1-1}(1-x)^{n_2-1} \mathcal{Y}_0(\mathbf{p}) \mathcal{Y}_\ell(\mathbf{p} + a\mathbf{k})}{\{[\mathbf{p} + a(1-x)\mathbf{k}]^2 + a^2k^2x(1-x) + \alpha^2x + \beta^2(1-x)\}^{n_1+n_2}}, \tag{B.6}
\end{aligned}$$

where the factor of $1/\sqrt{4\pi}$ arises from one of the vector harmonics with $\ell = 0$.

Defining

$$\mathbf{u} = \mathbf{p} + a(1-x)\mathbf{k} \tag{B.7}$$

and substituting into the integral gives

$$\mathcal{I}_{n_1, n_2}^{0, \ell, 0} = \frac{1}{\sqrt{4\pi}} \frac{\Gamma(n_1 + n_2)}{\Gamma(n_1)\Gamma(n_2)} \int_0^1 dx \int d^3u \frac{x^{n_1-1}(1-x)^{n_2-1} \mathcal{Y}_0(\mathbf{u}) \mathcal{Y}_\ell(\mathbf{u} + ax\mathbf{k})}{[u^2 + a^2k^2x(1-x) + \alpha^2x + \beta^2(1-x)]^{n_1+n_2}}. \tag{B.8}$$

The angular integration can be performed after expanding the $\mathcal{Y}_\ell(\mathbf{u} + ax\mathbf{k})$ to give

$$\mathcal{I}_{n_1, n_2}^\ell = a^\ell \mathcal{Y}_\ell(\mathbf{k}) \frac{\Gamma(n_1 + n_2)}{\Gamma(n_1)\Gamma(n_2)} \int_0^1 dx \int du u^2 \frac{x^{n_1-1+\ell}(1-x)^{n_2-1}}{[u^2 + a^2k^2x(1-x) + \alpha^2x + \beta^2(1-x)]^{n_1+n_2}}.$$

Using

$$\int_0^\infty du \frac{u^{2m}}{(u^2 + \mathcal{A})^n} = \frac{1}{2\mathcal{A}^{n-m-1/2}} \frac{\Gamma(m+1/2)\Gamma(n-m-1/2)}{\Gamma(n)} \tag{B.9}$$

in the above equation gives

$$\begin{aligned}
\mathcal{I}_{n_1, n_2}^\ell &= a^\ell \mathcal{Y}_\ell(\mathbf{k}) \frac{\Gamma(n_1 + n_2)}{\Gamma(n_1)\Gamma(n_2)} \frac{\Gamma(3/2)\Gamma(n_1 + n_2 - 3/2)}{\Gamma(n_1 + n_2)} \\
&\quad \times \int_0^1 dx \frac{x^{n_1-1+\ell}(1-x)^{n_2-1}}{2[a^2k^2x(1-x) + \alpha^2x + \beta^2(1-x)]^{n_1+n_2-3/2}} \\
&= a^\ell \mathcal{Y}_\ell(\mathbf{k}) \frac{\Gamma(3/2)\Gamma(n_1 + n_2 - 3/2)}{\Gamma(n_1)\Gamma(n_2)} \int_0^1 dx \frac{x^{n_1-1+\ell}(1-x)^{n_2-1}}{2[a^2k^2x(1-x) + \alpha^2x + \beta^2(1-x)]^{n_1+n_2-3/2}}.
\end{aligned}$$

This integral can now be written as a sum of terms \mathcal{J}_n^m , with

$$\mathcal{J}_n^m \equiv \int_0^1 dx \frac{x^m}{(c_0 + c_1x + c_2x^2)^{n+1/2}}, \tag{B.10}$$

where

$$c_0 = \beta^2, \quad c_1 = a^2 k^2 + \alpha^2 - \beta^2, \quad c_2 = -a^2 k^2.$$

Each of these terms can be then be integrated analytically to give the required matrix element.

This procedure works as long as $2n > m$. When $2n \leq m$, the last integration leads to logarithms. Such terms are expanded around $k = 0$ before the form factors are extracted.

APPENDIX C

Quark Model Form Factors

C.1 Form factors for Λ_Q decay

The analytic expressions that we obtain for the form factors are shown in the following subsections. The results shown are valid for single-component wave functions. We separate the results obtained using the harmonic oscillator basis from those obtained using the Sturmian basis.

C.1.1 $1/2^+, |100000\rangle$

Harmonic Oscillator Form Factors

$$\begin{aligned}
 F_1 &= I_H \left[1 + \frac{m_\sigma}{\alpha_{\lambda\lambda'}^2} \left(\frac{\alpha_{\lambda'}^2}{m_q} + \frac{\alpha_\lambda^2}{m_Q} \right) \right], \\
 F_2 &= -I_H \left[\frac{m_\sigma}{m_q} \frac{\alpha_{\lambda'}^2}{\alpha_{\lambda\lambda'}^2} - \frac{\alpha_\lambda^2 \alpha_{\lambda'}^2}{4\alpha_{\lambda\lambda'}^2 m_q m_Q} \right], \\
 F_3 &= -I_H \frac{m_\sigma}{m_Q} \frac{\alpha_\lambda^2}{\alpha_{\lambda\lambda'}^2}, \\
 G_1 &= I_H \left[1 - \frac{\alpha_\lambda^2 \alpha_{\lambda'}^2}{12\alpha_{\lambda\lambda'}^2 m_q m_Q} \right], \\
 G_2 &= -I_H \left[\frac{m_\sigma}{m_q} \frac{\alpha_{\lambda'}^2}{\alpha_{\lambda\lambda'}^2} + \frac{\alpha_\lambda^2 \alpha_{\lambda'}^2}{12m_q m_Q \alpha_{\lambda\lambda'}^2} \left(1 + \frac{12m_\sigma^2}{\alpha_{\lambda\lambda'}^2} \right) \right], \\
 G_3 &= I_H \left[\frac{m_\sigma}{m_Q} \frac{\alpha_\lambda^2}{\alpha_{\lambda\lambda'}^2} + \frac{m_\sigma^2 \alpha_\lambda^2 \alpha_{\lambda'}^2}{m_q m_Q \alpha_{\lambda\lambda'}^4} \right]
 \end{aligned}$$

where

$$I_H = \left(\frac{\alpha_\lambda \alpha_{\lambda'}}{\alpha_{\lambda\lambda'}^2} \right)^{3/2} \exp \left(-\frac{3m_\sigma^2}{2m_{\Lambda_q}^2} \frac{p^2}{\alpha_{\lambda\lambda'}^2} \right),$$

$\alpha_{\lambda\lambda'}^2 = \frac{1}{2}(\alpha_\lambda^2 + \alpha_{\lambda'}^2)$, and m_σ is the mass of the light quark.

Sturmian Form Factors

$$\begin{aligned}
 F_1 &= I_S \left[1 + \frac{m_\sigma}{\beta_{\lambda\lambda'}} \left(\frac{\beta_{\lambda'}}{m_q} + \frac{\beta_\lambda}{m_Q} \right) \right], \\
 F_2 &= -I_S \left[\frac{m_\sigma}{m_q} \frac{\beta_{\lambda'}}{\beta_{\lambda\lambda'}} - \frac{\beta_\lambda \beta_{\lambda'}}{6m_q m_Q} \right], \\
 F_3 &= -I_S \frac{m_\sigma}{m_Q} \frac{\beta_\lambda}{\beta_{\lambda\lambda'}}, \\
 G_1 &= I_S \left[1 - \frac{\beta_\lambda \beta_{\lambda'}}{18m_q m_Q} \right], \\
 G_2 &= -I_S \left[\frac{m_\sigma \beta_{\lambda'}}{m_q \beta_{\lambda\lambda'}} + \frac{4m_\sigma^2 \beta_\lambda \beta_{\lambda'}}{5m_q m_Q \beta_{\lambda\lambda'}^2} + \frac{\beta_\lambda \beta_{\lambda'}}{18m_q m_Q} \right], \\
 G_3 &= I_S \left[\frac{m_\sigma \beta_\lambda}{m_Q \beta_{\lambda\lambda'}} + \frac{4m_\sigma^2 \beta_\lambda \beta_{\lambda'}}{5m_q m_Q \beta_{\lambda\lambda'}^2} \right],
 \end{aligned}$$

where

$$I_S = \frac{\left(\frac{\beta_\lambda \beta_{\lambda'}}{\beta_{\lambda\lambda'}} \right)^{3/2}}{\left[1 + \frac{3}{2} \frac{m_\sigma^2}{m_{\Lambda_q}^2} \frac{p^2}{\beta_{\lambda\lambda'}} \right]^2},$$

and $\beta_{\lambda\lambda'} = \frac{1}{2}(\beta_\lambda + \beta_{\lambda'})$.

C.1.2 $1/2_1^+, |100010\rangle$

Harmonic Oscillator Form Factors

$$\begin{aligned}
F_1 &= I_H \frac{1}{2\alpha_{\lambda\lambda'}^2} \left[(\alpha_\lambda^2 - \alpha_{\lambda'}^2) - \frac{m_\sigma}{3\alpha_{\lambda\lambda'}^2} \left(\frac{\alpha_{\lambda'}^2}{m_q} (7\alpha_\lambda^2 - 3\alpha_{\lambda'}^2) + \frac{\alpha_\lambda^2}{m_Q} (7\alpha_{\lambda'}^2 - 3\alpha_\lambda^2) \right) \right], \\
F_2 &= -I_H \frac{\alpha_{\lambda'}^2}{6m_q\alpha_{\lambda\lambda'}^4} (7\alpha_\lambda^2 - 3\alpha_{\lambda'}^2) \left[m_\sigma - \frac{\alpha_\lambda^2}{4m_Q} \right], \\
F_3 &= I_H \frac{\alpha_\lambda^2 m_\sigma}{6m_Q\alpha_{\lambda\lambda'}^4} (7\alpha_{\lambda'}^2 - 3\alpha_\lambda^2), \\
G_1 &= I_H \left[\frac{(\alpha_\lambda^2 - \alpha_{\lambda'}^2)}{2\alpha_{\lambda\lambda'}^2} - \frac{\alpha_\lambda^2 \alpha_{\lambda'}^2}{72\alpha_{\lambda\lambda'}^4 m_q m_Q} (7\alpha_\lambda^2 - 3\alpha_{\lambda'}^2) \right], \\
G_2 &= -I_H \frac{\alpha_{\lambda'}^2}{6m_q\alpha_{\lambda\lambda'}^4} \left[(7\alpha_\lambda^2 - 3\alpha_{\lambda'}^2) \left(m_\sigma + \frac{\alpha_\lambda^2}{6m_Q} \right) + \frac{7m_\sigma^2 \alpha_\lambda^2}{m_Q \alpha_{\lambda\lambda'}^2} (\alpha_\lambda^2 - \alpha_{\lambda'}^2) \right], \\
G_3 &= -I_H \frac{\alpha_\lambda^2 m_\sigma}{6m_Q\alpha_{\lambda\lambda'}^4} \left[(7\alpha_{\lambda'}^2 - 3\alpha_\lambda^2) - \frac{7m_\sigma \alpha_{\lambda'}^2}{m_q \alpha_{\lambda\lambda'}^2} (\alpha_\lambda^2 - \alpha_{\lambda'}^2) \right],
\end{aligned}$$

where

$$I_H = \sqrt{\frac{3}{2}} \left(\frac{\alpha_\lambda \alpha_{\lambda'}}{\alpha_{\lambda\lambda'}^2} \right)^{3/2} \exp \left(-\frac{3m_\sigma^2}{2m_{\Lambda_q}^2} \frac{p^2}{\alpha_{\lambda\lambda'}^2} \right).$$

Sturmian Form Factors

$$\begin{aligned}
F_1 &= I_S \frac{1}{2\beta_{\lambda'}\beta_\lambda} \left[(\beta_\lambda^2 - \beta_{\lambda'}^2) - \frac{2m_\sigma}{3} \left(\frac{\beta_\lambda}{m_Q} (5\beta_{\lambda'} - 3\beta_\lambda) - \frac{\beta_{\lambda'}}{m_q} (5\beta_\lambda - 3\beta_{\lambda'}) \right) \right], \\
F_2 &= -I_S \frac{(5\beta_\lambda - 3\beta_{\lambda'})}{3m_q} \left[\frac{m_\sigma}{\beta_\lambda} - \frac{\beta_{\lambda\lambda'}}{3m_Q} \right], \\
F_3 &= I_S \frac{m_\sigma}{6m_Q\beta_{\lambda'}} (5\beta_{\lambda'} - 3\beta_\lambda), \\
G_1 &= I_S \left[\frac{(\beta_\lambda^2 - \beta_{\lambda'}^2)}{2\beta_{\lambda'}\beta_\lambda} - \frac{\beta_{\lambda\lambda'}}{54m_q m_Q} (5\beta_\lambda - 3\beta_{\lambda'}) \right], \\
G_2 &= -I_S \frac{m_\sigma}{3m_q\beta_\lambda} \left[(5\beta_\lambda - 3\beta_{\lambda'}) + \frac{4m_\sigma\beta_\lambda}{m_Q\beta_{\lambda\lambda'}} (\beta_\lambda - \beta_{\lambda'}) + \frac{\beta_{\lambda\lambda'}}{18m_Q} (5\beta_\lambda - \beta_{\lambda'}) \right], \\
G_3 &= -I_S \frac{m_\sigma}{3m_Q\beta_{\lambda'}} \left[(5\beta_{\lambda'} - 3\beta_\lambda) - \frac{4m_\sigma\beta_{\lambda'}}{m_Q\beta_{\lambda\lambda'}} (\beta_\lambda - \beta_{\lambda'}) \right],
\end{aligned}$$

where

$$I_S = \frac{\sqrt{3}}{2} \frac{\left(\frac{\beta_\lambda \beta_{\lambda'}}{\beta_{\lambda\lambda'}} \right)^{5/2}}{\left[1 + \frac{3}{2} \frac{m_\sigma^2}{m_{\Lambda_q}^2} \frac{p^2}{\beta_{\lambda\lambda'}^2} \right]^3}.$$

C.1.3 $1/2^-, |110001\rangle$

Harmonic Oscillator Form Factors

$$\begin{aligned}
F_1 &= I_H \frac{\alpha_\lambda}{6} \left[\frac{3}{m_q} - \frac{1}{m_Q} \right], \\
F_2 &= -I_H \left[\frac{2m_\sigma}{\alpha_\lambda} - \frac{\alpha_\lambda}{2m_q} + \frac{2m_\sigma^2 \alpha_\lambda}{m_Q \alpha_{\lambda\lambda'}^2} - \frac{m_\sigma \alpha_\lambda}{6m_q m_Q \alpha_{\lambda\lambda'}^2} (3\alpha_\lambda^2 - 2\alpha_{\lambda'}^2) \right], \\
F_3 &= I_H \frac{2m_\sigma^2 \alpha_\lambda}{m_Q \alpha_{\lambda\lambda'}^2}, \\
G_1 &= I_H \left[\frac{2m_\sigma}{\alpha_\lambda} - \frac{\alpha_\lambda}{6m_Q} + \frac{m_\sigma \alpha_\lambda}{6m_q m_Q \alpha_{\lambda\lambda'}^2} (3\alpha_\lambda^2 - 2\alpha_{\lambda'}^2) \right], \\
G_2 &= I_H \left[-\frac{2m_\sigma}{\alpha_\lambda} + \frac{\alpha_\lambda}{2m_q} + \frac{\alpha_\lambda}{3m_Q} \right], \\
G_3 &= I_H \frac{\alpha_\lambda}{3m_Q} \left[1 - \frac{m_\sigma}{2m_q \alpha_{\lambda\lambda'}^2} (3\alpha_\lambda^2 - 2\alpha_{\lambda'}^2) \right],
\end{aligned}$$

where

$$I_H = \left(\frac{\alpha_\lambda \alpha_{\lambda'}}{\alpha_{\lambda\lambda'}^2} \right)^{5/2} \exp \left(-\frac{3m_\sigma^2 p^2}{2m_{\Lambda_q}^2 \alpha_{\lambda\lambda'}^2} \right),$$

Sturmian Form Factors

$$\begin{aligned}
F_1 &= I_S \frac{\beta_{\lambda\lambda'}}{12} \left[\frac{3}{m_q} - \frac{1}{m_Q} \right], \\
F_2 &= -I_S \left[\frac{2m_\sigma}{\beta_\lambda} - \frac{\beta_{\lambda\lambda'}}{4m_q} + \frac{2m_\sigma^2}{\beta_{\lambda\lambda'} m_Q} - \frac{m_\sigma}{12m_q m_Q} (5\beta_\lambda - 3\beta_{\lambda'}) \right], \\
F_3 &= I_S \frac{2m_\sigma^2}{m_Q \beta_{\lambda\lambda'}}, \\
G_1 &= I_S \left[\frac{2m_\sigma}{\beta_\lambda} - \frac{\beta_{\lambda\lambda'}}{12m_Q} + \frac{m_\sigma}{36m_q m_Q} (11\beta_\lambda - 5\beta_{\lambda'}) \right], \\
G_2 &= -I_S \left[\frac{2m_\sigma}{\beta_\lambda} - \frac{\beta_{\lambda\lambda'}}{4m_q} - \frac{\beta_{\lambda\lambda'}}{6m_Q} + \frac{m_\sigma}{18m_q m_Q} (\beta_\lambda - \beta_{\lambda'}) \right], \\
G_3 &= I_S \frac{\beta_{\lambda\lambda'}}{6m_Q} \left[1 + \frac{m_\sigma}{2m_q \beta_{\lambda\lambda'}} (\beta_{\lambda'} - 3\beta_\lambda) \right],
\end{aligned}$$

where

$$I_S = \sqrt{2} \frac{\left(\frac{\beta_\lambda \beta_{\lambda'}}{\beta_{\lambda\lambda'}} \right)^{5/2}}{\left[1 + \frac{3}{2} \frac{m_\sigma^2 p^2}{m_{\Lambda_q}^2 \beta_{\lambda\lambda'}^2} \right]^3}.$$

C.1.4 $3/2^-, |110001\rangle$

Harmonic Oscillator Form Factors

$$\begin{aligned}
 F_1 &= I_H \frac{3m_\sigma}{\alpha_\lambda} \left[1 + \frac{m_\sigma}{\alpha_{\lambda\lambda'}^2} \left(\frac{\alpha_{\lambda'}^2}{m_q} + \frac{\alpha_\lambda^2}{m_Q} \right) \right], \\
 F_2 &= -I_H \left[\frac{3m_\sigma^2}{m_q} \frac{\alpha_{\lambda'}^2}{\alpha_{\lambda\lambda'}^2 \alpha_\lambda} - \frac{5\alpha_\lambda \alpha_{\lambda'}^2 m_\sigma}{4\alpha_{\lambda\lambda'}^2 m_q m_Q} \right], \\
 F_3 &= -I_H \left[\frac{3m_\sigma^2}{m_Q} \frac{\alpha_\lambda}{\alpha_{\lambda\lambda'}^2} + \frac{\alpha_\lambda}{2m_Q} \right], \\
 F_4 &= I_H \frac{\alpha_\lambda}{m_Q}, \\
 G_1 &= I_H \left[\frac{3m_\sigma}{\alpha_\lambda} - \frac{\alpha_\lambda}{2m_Q} \left(1 + \frac{3m_\sigma \alpha_{\lambda'}^2}{2m_q \alpha_{\lambda\lambda'}^2} \right) \right], \\
 G_2 &= -I_H \left[\frac{3m_\sigma^2}{m_q} \frac{\alpha_{\lambda'}^2}{\alpha_{\lambda\lambda'}^2 \alpha_\lambda} + \frac{m_\sigma \alpha_\lambda \alpha_{\lambda'}^2}{4m_q m_Q \alpha_{\lambda\lambda'}^4} (\alpha_{\lambda\lambda'}^2 + 12m_\sigma^2) \right], \\
 G_3 &= I_H \frac{\alpha_\lambda}{m_Q \alpha_{\lambda\lambda'}^2} \left[\frac{\alpha_{\lambda\lambda'}^2}{2} + 3m_\sigma^2 + \frac{\alpha_{\lambda'}^2 m_\sigma}{m_q \alpha_{\lambda\lambda'}^2} (\alpha_{\lambda\lambda'}^2 + 6m_\sigma^2) \right], \\
 G_4 &= -I_H \left[\frac{\alpha_\lambda}{m_Q} + \frac{m_\sigma}{m_q m_Q} \frac{\alpha_{\lambda'}^2 \alpha_\lambda}{\alpha_{\lambda\lambda'}^2} \right],
 \end{aligned}$$

where

$$I_H = -\frac{1}{\sqrt{3}} \left(\frac{\alpha_\lambda \alpha_{\lambda'}}{\alpha_{\lambda\lambda'}^2} \right)^{5/2} \exp \left(-\frac{3m_\sigma^2}{2m_{\Lambda_q}^2} \frac{p^2}{\alpha_{\lambda\lambda'}^2} \right),$$

Sturmian Form Factors

$$\begin{aligned}
F_1 &= I_S \frac{3m_\sigma}{\beta_\lambda} \left[1 + \frac{m_\sigma}{\beta_{\lambda\lambda'}} \left(\frac{\beta_{\lambda'}}{m_q} + \frac{\beta_\lambda}{m_Q} \right) \right], \\
F_2 &= -I_S \left[\frac{3m_\sigma^2}{m_q} \frac{\beta_{\lambda'}}{\beta_{\lambda\lambda'}\beta_\lambda} - \frac{m_\sigma}{4m_q m_Q} (\beta_\lambda - 3\beta_{\lambda'}) \right], \\
F_3 &= -I_S \left[\frac{3m_\sigma^2}{m_Q \beta_{\lambda\lambda'}} + \frac{\beta_{\lambda\lambda'}}{4m_Q} \right], \\
F_4 &= I_S \frac{\beta_{\lambda\lambda'}}{2m_Q}, \\
G_1 &= I_S \left[\frac{3m_\sigma}{\beta_\lambda} - \frac{\beta_{\lambda\lambda'}}{4m_Q} + \frac{m_\sigma}{60m_q m_Q} (5\beta_\lambda - 23\beta_{\lambda'}) \right], \\
G_2 &= -I_S \left[\frac{3m_\sigma^2}{m_q} \frac{\beta_{\lambda'}}{\beta_\lambda \beta_{\lambda\lambda'}} - \frac{m_\sigma}{60m_q m_Q} (5\beta_\lambda - 11\beta_{\lambda'}) + \frac{18m_\sigma^3 \beta_{\lambda'}}{7\beta_{\lambda\lambda'}^2 m_q m_Q} \right], \\
G_3 &= I_S \frac{1}{m_Q} \left[\frac{3m_\sigma^2}{\beta_{\lambda\lambda'}} + \frac{\beta_{\lambda\lambda'}}{4} + \frac{m_\sigma \beta_{\lambda'}}{5m_q} + \frac{18m_\sigma^3 \beta_{\lambda'}}{7\beta_{\lambda\lambda'}^2 m_q} \right], \\
G_4 &= -I_S \frac{1}{m_Q} \left[\frac{\beta_{\lambda\lambda'}}{2} + \frac{2m_\sigma \beta_{\lambda'}}{5m_q} \right],
\end{aligned}$$

where

$$I_S = -\frac{\sqrt{2}}{3} \frac{\left(\frac{\beta_\lambda \beta_{\lambda'}}{\beta_{\lambda\lambda'}} \right)^{5/2}}{\left[1 + \frac{3}{2} \frac{m_\sigma^2}{m_{\lambda q}^2} \frac{p^2}{\beta_{\lambda\lambda'}^2} \right]^3}.$$

C.1.5 $3/2^+, |120002\rangle$

Harmonic Oscillator Form Factors

$$\begin{aligned}
F_1 &= -I_H \frac{m_\sigma}{2} \left[\frac{5}{m_q} - \frac{3}{m_Q} \right], \\
F_2 &= I_H \frac{m_\sigma}{\alpha_\lambda} \left[\frac{6m_\sigma}{\alpha_\lambda} - \frac{5\alpha_\lambda}{2m_q} + \frac{6m_\sigma^2 \alpha_\lambda}{\alpha_{\lambda\lambda'}^2 m_Q} - \frac{m_\sigma \alpha_\lambda}{2\alpha_{\lambda\lambda'}^2 m_q m_Q} (\alpha_\lambda^2 - 2\alpha_{\lambda'}^2) \right], \\
F_3 &= -I_H \frac{m_\sigma}{m_Q} \left[1 + \frac{6m_\sigma^2}{\alpha_{\lambda\lambda'}^2} \right], \\
F_4 &= I_H \frac{2m_\sigma}{m_Q}, \\
G_1 &= -I_H \left[\frac{6m_\sigma^2}{\alpha_\lambda^2} - \frac{m_\sigma}{2m_Q} + \frac{m_\sigma^2}{6\alpha_{\lambda\lambda'}^2 m_q m_Q} (11\alpha_\lambda^2 - 6\alpha_{\lambda'}^2) \right], \\
G_2 &= I_H \left[\frac{6m_\sigma^2}{\alpha_\lambda^2} - \frac{5m_\sigma}{2m_q} - \frac{2m_\sigma}{m_Q} + \frac{5\alpha_\lambda^2}{12m_q m_Q} - \frac{2m_\sigma^2 \alpha_\lambda^2}{3\alpha_{\lambda\lambda'}^2 m_q m_Q} \right], \\
G_3 &= -I_H \left[\frac{m_\sigma}{2m_Q} - \frac{5\alpha_\lambda^2}{24m_q m_Q} - \frac{m_\sigma^2}{4m_q m_Q \alpha_{\lambda\lambda'}^2} (5\alpha_\lambda^2 - 2\alpha_{\lambda'}^2) \right], \\
G_4 &= -I_H \frac{5\alpha_\lambda^2}{6m_q m_Q},
\end{aligned}$$

where

$$I_H = \frac{1}{\sqrt{5}} \left(\frac{\alpha_\lambda \alpha_{\lambda'}}{\alpha_{\lambda\lambda'}^2} \right)^{7/2} \exp \left(-\frac{3m_\sigma^2}{2m_{\Lambda_q}^2} \frac{p^2}{\alpha_{\lambda\lambda'}^2} \right),$$

Sturmian Form Factors

$$\begin{aligned}
F_1 &= I_S \frac{m_\sigma \beta_{\lambda\lambda'}}{2\beta_\lambda} \left[\frac{1}{m_Q} - \frac{5}{3m_q} \right], \\
F_2 &= I_S \frac{m_\sigma}{\beta_\lambda} \left[\frac{6m_\sigma}{\beta_\lambda} - \frac{5\beta_{\lambda\lambda'}}{6m_q} + \frac{6m_\sigma^2}{\beta_{\lambda\lambda'} m_Q} - \frac{m_\sigma}{6m_q m_Q} (5\beta_\lambda - \beta_{\lambda'}) \right], \\
F_3 &= -I_S \frac{m_\sigma}{3\beta_\lambda m_Q} \left[\beta_{\lambda\lambda'} + \frac{18m_\sigma^2}{\beta_{\lambda\lambda'}} \right], \\
F_4 &= I_S \frac{2m_\sigma \beta_{\lambda\lambda'}}{3m_Q \beta_\lambda}, \\
G_1 &= -I_S \frac{m_\sigma}{\beta_\lambda} \left[\frac{6m_\sigma}{\beta_\lambda} - \frac{\beta_{\lambda\lambda'}}{6m_Q} + \frac{m_\sigma}{6m_q m_Q} (5\beta_\lambda - \beta_{\lambda'}) \right], \\
G_2 &= I_S \frac{\beta_{\lambda\lambda'}}{\beta_\lambda} \left[\frac{6m_\sigma^2}{\beta_\lambda \beta_{\lambda\lambda'}} - \frac{5m_\sigma}{6m_q} - \frac{2m_\sigma}{3m_Q} + \frac{\beta_{\lambda\lambda'}}{72m_q m_Q} (5\beta_\lambda + \beta_{\lambda'}) \right], \\
G_3 &= -I_S \frac{\beta_{\lambda\lambda'}}{3\beta_\lambda m_Q} \left[m_\sigma - \frac{m_\sigma^2}{2m_q \beta_{\lambda\lambda'}} (5\beta_\lambda - \beta_{\lambda'}) + \frac{\beta_{\lambda\lambda'}}{24m_q} (5\beta_\lambda + \beta_{\lambda'}) \right], \\
G_4 &= -I_S \frac{\beta_{\lambda\lambda'}^2}{36m_q m_Q \beta_\lambda} (\beta_{\lambda'} + 5\beta_\lambda),
\end{aligned}$$

where

$$I_S = \frac{\sqrt{6}}{5} \frac{\left(\frac{\beta_\lambda \beta_{\lambda'}}{\beta_{\lambda\lambda'}} \right)^{7/2}}{\left[1 + \frac{3}{2} \frac{m_\sigma^2}{m_{\Lambda q}^2} \frac{p^2}{\beta_{\lambda\lambda'}^2} \right]^4}.$$

C.1.6 $5/2^+, |120002\rangle$

Harmonic Oscillator Form Factors

$$\begin{aligned}
F_1 &= I_H \frac{3m_\sigma^2}{\alpha_\lambda^2} \left[1 + \frac{m_\sigma}{\alpha_{\lambda\lambda'}^2} \left(\frac{\alpha_{\lambda'}^2}{m_q} + \frac{\alpha_\lambda^2}{m_Q} \right) \right], \\
F_2 &= -I_H \frac{m_\sigma^2}{m_q \alpha_{\lambda\lambda'}^2} \left[\frac{3m_\sigma \alpha_{\lambda'}^2}{\alpha_\lambda^2} - \frac{1}{4m_Q} (8\alpha_\lambda^2 + 7\alpha_{\lambda'}^2) \right], \\
F_3 &= -I_H \frac{m_\sigma}{m_Q} \left[1 + \frac{3m_\sigma^2}{\alpha_{\lambda\lambda'}^2} \right], \\
F_4 &= I_H \frac{2m_\sigma}{m_Q}, \\
G_1 &= I_H \left[\frac{3m_\sigma^2}{\alpha_\lambda^2} - \frac{m_\sigma}{m_Q} - \frac{m_\sigma^2}{12m_q m_Q \alpha_{\lambda\lambda'}^2} (8\alpha_\lambda^2 + 15\alpha_{\lambda'}^2) \right], \\
G_2 &= -I_H \frac{m_\sigma^2}{m_q \alpha_{\lambda\lambda'}^2} \left[\frac{3m_\sigma \alpha_{\lambda'}^2}{\alpha_\lambda^2} + \frac{1}{12m_Q} (8\alpha_\lambda^2 + 3\alpha_{\lambda'}^2) + \frac{3m_\sigma^2 \alpha_{\lambda'}^2}{m_Q \alpha_{\lambda\lambda'}^2} \right], \\
G_3 &= I_H \frac{m_\sigma}{m_Q} \left[1 + \frac{3m_\sigma^2}{\alpha_{\lambda\lambda'}^2} + \frac{m_\sigma \alpha_{\lambda'}^2}{m_q \alpha_{\lambda\lambda'}^2} \left(1 + \frac{6m_\sigma^2}{\alpha_{\lambda\lambda'}^2} \right) \right], \\
G_4 &= -I_H \frac{2m_\sigma}{m_Q} \left[1 + \frac{m_\sigma}{m_q} \frac{\alpha_{\lambda'}^2}{\alpha_{\lambda\lambda'}^2} \right],
\end{aligned}$$

where

$$I_H = \frac{1}{\sqrt{2}} \left(\frac{\alpha_\lambda \alpha_{\lambda'}}{\alpha_{\lambda\lambda'}^2} \right)^{7/2} \exp \left(-\frac{3m_\sigma^2}{2m_{\Lambda_q}^2} \frac{p^2}{\alpha_{\lambda\lambda'}^2} \right),$$

Sturmian Form Factors

$$\begin{aligned}
F_1 &= I_S \frac{3m_\sigma^2}{\beta_\lambda^2} \left[1 + \frac{m_\sigma}{\beta_{\lambda\lambda'}} \left(\frac{\beta_{\lambda'}}{m_q} + \frac{\beta_\lambda}{m_Q} \right) \right], \\
F_2 &= -I_S \frac{m_\sigma^2 \beta_{\lambda'}}{m_q \beta_\lambda^2} \left[\frac{3m_\sigma}{\beta_{\lambda\lambda'}} - \frac{\beta_\lambda}{2m_Q} \right], \\
F_3 &= -I_S \frac{m_\sigma}{3m_Q \beta_\lambda} \left[\beta_{\lambda\lambda'} + \frac{9m_\sigma^2}{\beta_{\lambda\lambda'}} \right], \\
F_4 &= I_S \frac{2m_\sigma}{3m_Q} \frac{\beta_{\lambda\lambda'}}{\beta_\lambda}, \\
G_1 &= I_S \left[\frac{3m_\sigma^2}{\beta_\lambda^2} - \frac{m_\sigma}{m_Q \beta_\lambda} \left(\frac{\beta_{\lambda\lambda'}}{3} + \frac{5m_\sigma \beta_{\lambda'}}{14m_q} \right) \right], \\
G_2 &= -I_S \frac{m_\sigma^2 \beta_{\lambda'}}{m_q \beta_{\lambda\lambda'} \beta_\lambda} \left[\frac{3m_\sigma}{\beta_\lambda} + \frac{\beta_{\lambda\lambda'}}{14m_Q} + \frac{8m_\sigma^2}{3m_Q \beta_{\lambda\lambda'}} \right], \\
G_3 &= I_S \frac{m_\sigma}{m_Q \beta_\lambda} \left[\frac{\beta_{\lambda\lambda'}}{3} + \frac{3m_\sigma^2}{\beta_{\lambda\lambda'}} + \frac{m_\sigma \beta_{\lambda'}}{m_q} \left(\frac{2}{7} + \frac{8m_\sigma^2}{3\beta_{\lambda\lambda'}^2} \right) \right], \\
G_4 &= -I_S \frac{2m_\sigma}{m_Q} \left[\frac{\beta_{\lambda\lambda'}}{3\beta_\lambda} + \frac{2m_\sigma}{7m_q} \frac{\beta_{\lambda'}}{\beta_\lambda} \right],
\end{aligned}$$

where

$$I_S = -\sqrt{3} \frac{\left(\frac{\beta_\lambda \beta_{\lambda'}}{\beta_{\lambda\lambda'}} \right)^{7/2}}{\left[1 + \frac{3}{2} \frac{m_\sigma^2}{m_q^2} \frac{p^2}{\beta_{\lambda\lambda'}^2} \right]^4}.$$

C.2 Form factors for Ω_Q decay

In this section, we present the analytic expressions we obtained for the form factors, assuming single component wave functions. For most of the J^P we treat, there are usually more than one example of the state: the exception is $5/2^-$, for which there is a single state up to $N = 2$. We therefore distinguish among the different states with the same J^P by presenting their quark model quantum numbers, in the notation $|I_S, L, n_\rho, \ell_\rho, n_\lambda, \ell_\lambda \rangle$. Here I_S takes values between 1 and 3, with 1 denoting total quark spin 1/2, with spin wave function of type χ_ρ , 2 denoting total quark spin 1/2, with spin wave function of type χ_λ , and 3 denoting total quark spin 3/2.

C.2.1 $1/2^+, |200000\rangle$

Harmonic Oscillator Form Factors

$$\begin{aligned}
 F_1 &= -I_H \left[1 + \frac{m_\sigma}{\alpha_{\lambda\lambda'}^2} \left(\frac{\alpha_{\lambda'}^2}{m_q} + \frac{\alpha_\lambda^2}{m_Q} \right) \right], \\
 F_2 &= 2I_H \left[1 - \frac{m_\sigma}{\alpha_{\lambda\lambda'}^2} \left(\frac{\alpha_{\lambda'}^2}{2m_q} - \frac{\alpha_\lambda^2}{m_Q} \right) \right], \\
 F_3 &= 2I_H \left[1 + \frac{m_\sigma}{\alpha_{\lambda\lambda'}^2} \left(\frac{\alpha_{\lambda'}^2}{m_q} - \frac{\alpha_\lambda^2}{2m_Q} \right) \right], \\
 G_1 &= -I_H, \\
 G_2 &= I_H \frac{m_\sigma}{m_q} \frac{\alpha_{\lambda'}^2}{\alpha_{\lambda\lambda'}^2}, \\
 G_3 &= -I_H \frac{m_\sigma}{m_Q} \frac{\alpha_\lambda^2}{\alpha_{\lambda\lambda'}^2}
 \end{aligned}$$

where

$$I_H = 1/3 \left(\frac{\alpha_\lambda \alpha_{\lambda'}}{\alpha_{\lambda\lambda'}^2} \right)^{3/2} \exp \left(\frac{-3m_\sigma^2 p^2}{2m_{\Omega_q}^2 \alpha_{\lambda\lambda'}^2} \right),$$

Sturmian Form Factors

$$\begin{aligned}
 F_1 &= -I_S \left[1 + \frac{m_\sigma}{\beta_{\lambda\lambda'}} \left(\frac{\beta_{\lambda'}}{m_q} + \frac{\beta_\lambda}{m_Q} \right) \right], \\
 F_2 &= 2I_S \left[1 - \frac{m_\sigma}{\beta_{\lambda\lambda'}} \left(\frac{\beta_{\lambda'}}{2m_q} - \frac{\beta_\lambda}{m_Q} \right) \right], \\
 F_3 &= 2I_S \left[1 + \frac{m_\sigma}{\beta_{\lambda\lambda'}} \left(\frac{\beta_{\lambda'}}{m_q} - \frac{\beta_\lambda}{2m_Q} \right) \right], \\
 G_1 &= -I_S, \\
 G_2 &= I_S \frac{m_\sigma \beta_{\lambda'}}{m_q \beta_{\lambda\lambda'}}, \\
 G_3 &= -I_S \frac{m_\sigma \beta_\lambda}{m_Q \beta_{\lambda\lambda'}}
 \end{aligned}$$

where

$$I_S = \frac{\left(\frac{\beta_\lambda \beta_{\lambda'}}{\beta_{\lambda\lambda'}^2} \right)^{3/2}}{3 \left[1 + \frac{3}{2} \frac{m_\sigma^2}{m_{\Omega_q}^2} \frac{p^2}{\beta_{\lambda\lambda'}^2} \right]^2},$$

and $\beta_{\lambda\lambda'} = \frac{1}{2}(\beta_\lambda + \beta_{\lambda'})$.

C.2.2 $1/2_1^+, |200010 \rangle$

Harmonic Oscillator Form Factors

$$\begin{aligned}
F_1 &= -I_H \frac{1}{2\alpha_{\lambda\lambda'}^2} \left[(\alpha_\lambda^2 - \alpha_{\lambda'}^2) + \frac{m_\sigma}{3\alpha_{\lambda\lambda'}^2} \left(\frac{\alpha_{\lambda'}^2(7\alpha_\lambda^2 - 3\alpha_{\lambda'}^2)}{m_q} + \frac{\alpha_\lambda^2(3\alpha_\lambda^2 - 7\alpha_{\lambda'}^2)}{m_Q} \right) \right], \\
F_2 &= I_H \frac{1}{\alpha_{\lambda\lambda'}^2} \left[(\alpha_\lambda^2 - \alpha_{\lambda'}^2) + \frac{m_\sigma}{3\alpha_{\lambda\lambda'}^2} \left(\frac{\alpha_{\lambda'}^2(7\alpha_\lambda^2 - 3\alpha_{\lambda'}^2)}{2m_q} - \frac{\alpha_\lambda^2(3\alpha_\lambda^2 - 7\alpha_{\lambda'}^2)}{m_Q} \right) \right] \\
F_3 &= I_H \frac{1}{\alpha_{\lambda\lambda'}^2} \left[(\alpha_\lambda^2 - \alpha_{\lambda'}^2) + \frac{m_\sigma}{3\alpha_{\lambda\lambda'}^2} \left(\frac{\alpha_{\lambda'}^2(7\alpha_\lambda^2 - 3\alpha_{\lambda'}^2)}{m_q} - \frac{\alpha_\lambda^2(3\alpha_\lambda^2 - 7\alpha_{\lambda'}^2)}{2m_Q} \right) \right], \\
G_1 &= -I_H \frac{1}{\alpha_{\lambda\lambda'}^2} (\alpha_\lambda^2 - \alpha_{\lambda'}^2), \\
G_2 &= I_H \frac{m_\sigma}{6m_q} \frac{\alpha_{\lambda'}^2}{\alpha_{\lambda\lambda'}^4} (7\alpha_\lambda^2 - 3\alpha_{\lambda'}^2), \\
G_3 &= -I_H \frac{m_\sigma}{6m_Q} \frac{\alpha_\lambda^2}{\alpha_{\lambda\lambda'}^4} (3\alpha_\lambda^2 - 7\alpha_{\lambda'}^2),
\end{aligned}$$

where

$$I_H = \sqrt{\frac{1}{6}} \left(\frac{\alpha_\lambda \alpha_{\lambda'}}{\alpha_{\lambda\lambda'}^2} \right)^{3/2} \exp \left(\frac{-3m_\sigma^2 p^2}{2m_{\Lambda_b}^2 \alpha_{\lambda\lambda'}^2} \right),$$

Sturmian Form Factors

$$\begin{aligned}
F_1 &= -I_S \frac{1}{2\beta_\lambda \beta_{\lambda'}} \left[(\beta_\lambda^2 - \beta_{\lambda'}^2) + \frac{2m_\sigma}{3} \left(\frac{\beta_{\lambda'}(5\beta_\lambda - 3\beta_{\lambda'})}{m_q} + \frac{\beta_\lambda(3\beta_\lambda - 5\beta_{\lambda'})}{m_Q} \right) \right], \\
F_2 &= I_S \frac{1}{\beta_\lambda \beta_{\lambda'}} \left[(\beta_\lambda^2 - \beta_{\lambda'}^2) - \frac{m_\sigma}{3} \left(\frac{\beta_{\lambda'}(5\beta_\lambda - 3\beta_{\lambda'})}{m_q} - \frac{2\beta_\lambda(3\beta_\lambda - 5\beta_{\lambda'})}{m_Q} \right) \right] \\
F_3 &= I_S \frac{1}{\beta_\lambda \beta_{\lambda'}} \left[(\beta_\lambda^2 - \beta_{\lambda'}^2) + \frac{m_\sigma}{3} \left(\frac{2\beta_{\lambda'}(5\beta_\lambda - 3\beta_{\lambda'})}{m_q} - \frac{\beta_\lambda(3\beta_\lambda - 5\beta_{\lambda'})}{m_Q} \right) \right], \\
G_1 &= -I_S \frac{(\beta_\lambda^2 - \beta_{\lambda'}^2)}{2\beta_\lambda \beta_{\lambda'}}, \\
G_2 &= I_S \frac{m_\sigma}{3m_q} \frac{(5\beta_\lambda - 3\beta_{\lambda'})}{\beta_\lambda}, \\
G_3 &= -I_S \frac{m_\sigma}{3m_Q} \frac{(3\beta_\lambda - 5\beta_{\lambda'})}{\beta_{\lambda'}},
\end{aligned}$$

where

$$I_S = \frac{\left(\frac{\beta_\lambda \beta_{\lambda'}}{\beta_{\lambda\lambda'}^2} \right)^{5/2}}{2\sqrt{3} \left[1 + \frac{3}{2} \frac{m_\sigma^2 p^2}{m_{\Lambda_b}^2 \beta_{\lambda\lambda'}^2} \right]^2},$$

C.2.3 $1/2_2^+, |320002\rangle$

Harmonic Oscillator Form Factors

$$\begin{aligned}
 F_1 &= -m_\sigma I_H \left(\frac{1}{m_q} - \frac{1}{m_Q} \right), \\
 F_2 &= I_H \frac{m_\sigma}{2} \left(\frac{1}{m_q} - \frac{1}{m_Q} \right), \\
 F_3 &= I_H \frac{m_\sigma}{2} \left(\frac{1}{m_q} - \frac{1}{m_Q} \right), \\
 G_1 &= 0, \\
 G_2 &= I_H \frac{m_\sigma}{\alpha_\lambda} \left[\frac{18m_\sigma}{5\alpha_\lambda} - \frac{\alpha_\lambda}{2} \left(\frac{4}{m_q} + \frac{3}{m_Q} \right) \right], \\
 G_3 &= -I_H \frac{m_\sigma}{\alpha_\lambda} \left(\frac{18m_\sigma}{5\alpha_\lambda} + \frac{\alpha_\lambda}{2m_Q} \right),
 \end{aligned}$$

where

$$I_H = -\frac{1}{3} \sqrt{\frac{10}{3}} \left(\frac{\alpha_\lambda \alpha_{\lambda'}}{\alpha_{\lambda\lambda'}^2} \right)^{7/2} \exp \left(-\frac{3m_\sigma^2 p^2}{2m_{\Omega_q}^2 \alpha_{\lambda\lambda'}^2} \right),$$

Sturmian Form Factors

$$\begin{aligned}
 F_1 &= -I_S \frac{m_\sigma \beta_{\lambda'}}{\beta_{\lambda\lambda'}} \left(\frac{1}{m_q} - \frac{1}{m_Q} \right), \\
 F_2 &= I_S \frac{m_\sigma \beta_{\lambda'}}{2\beta_{\lambda\lambda'}} \left(\frac{1}{m_q} - \frac{1}{m_Q} \right), \\
 F_3 &= I_S \frac{m_\sigma \beta_{\lambda'}}{2\beta_{\lambda\lambda'}} \left(\frac{1}{m_q} - \frac{1}{m_Q} \right), \\
 G_1 &= 0, \\
 G_2 &= -I_S \frac{m_\sigma \beta_\lambda}{\beta_{\lambda\lambda'}^2} \left[\frac{108m_\sigma \beta_{\lambda'}}{5\beta_\lambda} - \beta_{\lambda'} \left(\frac{4}{m_q} + \frac{3}{m_Q} \right) \right], \\
 G_3 &= -I_S \frac{m_\sigma \beta_{\lambda'}}{\beta_{\lambda\lambda'}^2} \left(\frac{108m_\sigma}{5\beta_\lambda} + \frac{\beta_{\lambda\lambda'}}{m_Q} \right),
 \end{aligned}$$

where

$$I_S = -\frac{2}{9} \sqrt{5} \frac{\left(\frac{\beta_\lambda \beta_{\lambda'}}{\beta_{\lambda\lambda'}^2} \right)^{5/2}}{\left[1 + \frac{3}{2} \frac{m_\sigma^2 p^2}{m_{\Omega_q}^2 \beta_{\lambda\lambda'}^2} \right]^4}.$$

C.2.4 $1/2^-, |210001\rangle$

Harmonic Oscillator Form Factors

$$\begin{aligned}
F_1 &= -I_H \frac{\alpha_\lambda}{6} \left(\frac{1}{m_q} + \frac{5}{m_Q} \right), \\
F_2 &= I_H \left\{ \frac{2m_\sigma}{\alpha_\lambda} \left[1 - \frac{m_\sigma}{\alpha_{\lambda\lambda'}^2} \left(\frac{2\alpha_{\lambda'}^2}{m_q} - \frac{\alpha_\lambda^2}{m_Q} \right) \right] - \frac{\alpha_\lambda}{6m_q} \right\}, \\
F_3 &= I_H \frac{2m_\sigma}{\alpha_\lambda} \left[2 + \frac{m_\sigma}{\alpha_{\lambda\lambda'}^2} \left(\frac{2\alpha_{\lambda'}^2}{m_q} - \frac{\alpha_\lambda^2}{m_Q} \right) \right], \\
G_1 &= I_H \left(\frac{2m_\sigma}{\alpha_\lambda} - \frac{5\alpha_\lambda}{6m_Q} \right), \\
G_2 &= I_H \left[-\frac{2m_\sigma}{\alpha_\lambda} + \alpha_\lambda \left(\frac{1}{2m_q} + \frac{2}{3m_Q} \right) \right], \\
G_3 &= I_H \frac{2\alpha_\lambda}{3m_Q},
\end{aligned}$$

where

$$I_H = -\frac{1}{3} \left(\frac{\alpha_\lambda \alpha_{\lambda'}}{\alpha_{\lambda\lambda'}^2} \right)^{5/2} \exp \left(-\frac{3m_\sigma^2}{2m_{\Omega_q}^2} \frac{p^2}{\alpha_{\lambda\lambda'}^2} \right),$$

Sturmian Form Factors

$$\begin{aligned}
F_1 &= -I_S \frac{\beta_{\lambda\lambda'}}{12} \left(\frac{1}{m_q} + \frac{5}{m_Q} \right), \\
F_2 &= I_S \left\{ \frac{2m_\sigma}{\beta_\lambda} \left[1 + \frac{m_\sigma}{\beta_{\lambda\lambda'}} \left(\frac{2\beta_{\lambda'}}{m_q} - \frac{\beta_\lambda}{m_Q} \right) \right] - \frac{\beta_{\lambda\lambda'}}{12m_q} \right\}, \\
F_3 &= I_S \frac{2m_\sigma}{\beta_\lambda} \left[2 + \frac{m_\sigma}{\beta_{\lambda\lambda'}} \left(\frac{2\beta_{\lambda'}}{m_q} - \frac{\beta_\lambda}{m_Q} \right) \right], \\
G_1 &= I_S \left(\frac{2m_\sigma}{\beta_\lambda} - \frac{5\beta_{\lambda\lambda'}}{12m_Q} \right), \\
G_2 &= I_S \left[-\frac{2m_\sigma}{\beta_\lambda} + \beta_{\lambda\lambda'} \left(\frac{1}{4m_q} + \frac{1}{3m_Q} \right) \right], \\
G_3 &= I_S \frac{\beta_{\lambda\lambda'}}{3m_Q},
\end{aligned}$$

where

$$I_S = -\frac{\sqrt{2}}{3} \frac{\left(\frac{\beta_\lambda \beta_{\lambda'}}{\beta_{\lambda\lambda'}^2} \right)^{5/2}}{\left[1 + \frac{3}{2} \frac{m_\sigma^2}{m_{\Omega_q}^2} \frac{p^2}{\beta_{\lambda\lambda'}^2} \right]^3}.$$

C.2.5 $3/2^-, |210001\rangle$

Harmonic Oscillator Form Factors

$$\begin{aligned}
 F_1 &= -I_H \frac{m_\sigma}{\alpha_\lambda} \left[1 + \frac{m_\sigma}{\alpha_{\lambda\lambda'}} \left(\frac{\alpha_{\lambda'}^2}{m_q} + \frac{\alpha_\lambda^2}{m_Q} \right) \right], \\
 F_2 &= I_H \left\{ \frac{m_\sigma}{\alpha_\lambda} \left[2 - \frac{m_\sigma}{\alpha_{\lambda\lambda'}} \left(\frac{\alpha_{\lambda'}^2}{m_q} - \frac{2\alpha_\lambda^2}{m_Q} \right) \right] - \frac{\alpha_\lambda}{3m_q} \right\}, \\
 F_3 &= I_H \left\{ \frac{m_\sigma}{\alpha_\lambda} \left[2 + \frac{m_\sigma}{\alpha_{\lambda\lambda'}} \left(\frac{2\alpha_{\lambda'}^2}{m_q} - \frac{\alpha_\lambda^2}{m_Q} \right) \right] - \frac{\alpha_\lambda}{6} \left(\frac{2}{m_q} + \frac{1}{m_Q} \right) \right\}, \\
 F_4 &= I_H \frac{\alpha_\lambda}{3} \left(\frac{2}{m_q} + \frac{1}{m_Q} \right), \\
 G_1 &= -I_H \left(\frac{m_\sigma}{\alpha_\lambda} + \frac{\alpha_\lambda}{6m_Q} \right), \\
 G_2 &= I_H \frac{m_\sigma^2}{m_q} \frac{\alpha_{\lambda'}^2}{\alpha_{\lambda\lambda'} \alpha_\lambda}, \\
 G_3 &= I_H \frac{\alpha_\lambda}{m_Q \alpha_{\lambda\lambda'}^2} \left(\frac{\alpha_{\lambda\lambda'}^2}{6} - m_\sigma^2 \right), \\
 G_4 &= -I_H \frac{\alpha_\lambda}{3m_Q},
 \end{aligned}$$

where

$$I_H = -\frac{1}{\sqrt{3}} \left(\frac{\alpha_\lambda \alpha_{\lambda'}}{\alpha_{\lambda\lambda'}^2} \right)^{5/2} \exp \left(-\frac{3m_\sigma^2}{2m_{\Omega_q}^2} \frac{p^2}{\alpha_{\lambda\lambda'}^2} \right),$$

Sturmian Form Factors

$$\begin{aligned}
F_1 &= -I_S \frac{m_\sigma}{\beta_\lambda} \left[1 + \frac{m_\sigma}{\beta_{\lambda\lambda'}} \left(\frac{\beta_{\lambda'}}{m_q} + \frac{\beta_\lambda}{m_Q} \right) \right], \\
F_2 &= I_S \left\{ \frac{m_\sigma}{\beta_\lambda} \left[2 - \frac{m_\sigma}{\beta_{\lambda\lambda'}} \left(\frac{\beta_{\lambda'}}{m_q} - \frac{2\beta_\lambda}{m_Q} \right) \right] - \frac{\beta_{\lambda\lambda'}}{6m_q} \right\}, \\
F_3 &= I_S \left\{ \frac{m_\sigma}{\beta_\lambda} \left[2 + \frac{m_\sigma}{\beta_{\lambda\lambda'}} \left(\frac{2\beta_{\lambda'}}{m_q} - \frac{\beta_\lambda}{m_Q} \right) \right] - \frac{\beta_{\lambda\lambda'}}{6} \left(\frac{2}{m_q} + \frac{1}{m_Q} \right) \right\}, \\
F_4 &= I_S \frac{\beta_{\lambda\lambda'}}{6} \left(\frac{2}{m_q} + \frac{1}{6m_Q} \right), \\
G_1 &= -I_S \left(\frac{m_\sigma}{\beta_\lambda} + \frac{\beta_{\lambda\lambda'}}{12m_Q} \right), \\
G_2 &= I_S \frac{m_\sigma^2}{m_q} \frac{\beta_{\lambda'}}{\beta_\lambda \beta_{\lambda\lambda'}}, \\
G_3 &= -I_S \frac{1}{m_Q} \left(\frac{m_\sigma^2}{\beta_{\lambda\lambda'}} - \frac{\beta_{\lambda\lambda'}}{12} \right), \\
G_4 &= -I_S \frac{\beta_{\lambda\lambda'}}{6m_Q},
\end{aligned}$$

where

$$I_S = -\sqrt{\frac{2}{3}} \frac{\left(\frac{\beta_\lambda \beta_{\lambda'}}{\beta_{\lambda\lambda'}^2} \right)^{5/2}}{\left[1 + \frac{3}{2} \frac{m_\sigma^2}{m_{\Omega q}^2} \frac{p^2}{\beta_{\lambda\lambda'}^2} \right]^3}.$$

C.2.6 $1/2_1^-, |310001\rangle$

Harmonic Oscillator Form Factors

$$\begin{aligned}
 F_1 &= -I_H \frac{\alpha_\lambda}{3} \left(\frac{1}{m_q} - \frac{1}{m_Q} \right), \\
 F_2 &= I_H \left\{ \frac{m_\sigma}{\alpha_\lambda} \left[1 + \frac{m_\sigma}{\alpha_{\lambda\lambda'}}^2 \left(\frac{\alpha_{\lambda'}^2}{m_q} + \frac{\alpha_\lambda^2}{m_Q} \right) \right] - \frac{\alpha_\lambda}{3m_Q} \right\}, \\
 F_3 &= -I_H \frac{m_\sigma}{\alpha_\lambda} \left[1 + \frac{m_\sigma}{\alpha_{\lambda\lambda'}^2} \left(\frac{\alpha_{\lambda'}^2}{m_q} + \frac{\alpha_\lambda^2}{m_Q} \right) \right], \\
 G_1 &= -I_H \left(\frac{2m_\sigma}{\alpha_\lambda} - \frac{\alpha_\lambda}{3m_Q} \right), \\
 G_2 &= -I_H \left[\frac{m_\sigma}{\alpha_\lambda} - \frac{\alpha_\lambda}{3} \left(\frac{3}{m_q} - \frac{1}{m_Q} \right) \right], \\
 G_3 &= I_H \left(\frac{3m_\sigma}{\alpha_\lambda} + \frac{\alpha_\lambda}{3m_Q} \right),
 \end{aligned}$$

where

$$I_H = -\frac{\sqrt{2}}{3} \left(\frac{\alpha_\lambda \alpha_{\lambda'}}{\alpha_{\lambda\lambda'}^2} \right)^{5/2} \exp \left(-\frac{3m_\sigma^2}{2m_{\Omega_q}^2} \frac{p^2}{\alpha_{\lambda\lambda'}^2} \right),$$

Sturmian Form Factors

$$\begin{aligned}
 F_1 &= -I_S \frac{\beta_{\lambda\lambda'}}{6} \left(\frac{1}{m_q} - \frac{1}{m_Q} \right), \\
 F_2 &= I_S \left\{ \frac{m_\sigma}{\beta_\lambda} \left[1 + \frac{m_\sigma}{\beta_{\lambda\lambda'}} \left(\frac{\beta_{\lambda'}}{m_q} + \frac{\beta_\lambda}{m_Q} \right) \right] - \frac{\beta_{\lambda\lambda'}}{6m_q} \right\}, \\
 F_3 &= -I_S \frac{m_\sigma}{\beta_\lambda} \left[1 + \frac{m_\sigma}{\beta_{\lambda\lambda'}} \left(\frac{\beta_{\lambda'}}{m_q} + \frac{\beta_\lambda}{m_Q} \right) \right], \\
 G_1 &= -I_H \left(\frac{2m_\sigma}{\beta_\lambda} - \frac{\beta_{\lambda\lambda'}}{6m_Q} \right), \\
 G_2 &= -I_S \left[\frac{m_\sigma}{\beta_\lambda} - \frac{\beta_{\lambda\lambda'}}{6} \left(\frac{3}{m_q} + \frac{1}{m_Q} \right) \right], \\
 G_3 &= I_S \left(\frac{3m_\sigma}{\beta_\lambda} + \frac{\beta_{\lambda\lambda'}}{6m_Q} \right),
 \end{aligned}$$

where

$$I_S = -\frac{1}{3} \frac{\left(\frac{\beta_\lambda \beta_{\lambda'}}{\beta_{\lambda\lambda'}^2} \right)^{5/2}}{\left[1 + \frac{3}{2} \frac{m_\sigma^2}{m_{\Omega_q}^2} \frac{p^2}{\beta_{\lambda\lambda'}^2} \right]^3}.$$

C.2.7 $3/2_1^-, |310001\rangle$

Harmonic Oscillator Form Factors

$$\begin{aligned}
 F_1 &= I_H \frac{2m_\sigma}{\alpha_\lambda} \left[1 + \frac{m_\sigma}{\alpha_{\lambda\lambda'}^2} \left(\frac{\alpha_{\lambda'}^2}{m_q} + \frac{\alpha_\lambda^2}{m_Q} \right) \right], \\
 F_2 &= I_H \left\{ \frac{2m_\sigma}{\alpha_\lambda} \left[1 + \frac{m_\sigma}{\alpha_{\lambda\lambda'}^2} \left(\frac{\alpha_{\lambda'}^2}{m_q} + \frac{\alpha_\lambda^2}{m_Q} \right) \right] - \frac{\alpha_\lambda}{6} \left(\frac{3}{m_q} + \frac{2}{m_Q} \right) \right\}, \\
 F_3 &= -I_H \left\{ \frac{4m_\sigma}{\alpha_\lambda} \left[1 + \frac{m_\sigma}{\alpha_{\lambda\lambda'}^2} \left(\frac{\alpha_{\lambda'}^2}{m_q} + \frac{\alpha_\lambda^2}{m_Q} \right) \right] + \frac{\alpha_\lambda}{2} \left(\frac{1}{m_q} - \frac{1}{m_Q} \right) \right\}, \\
 F_4 &= I_H \alpha_\lambda \left(\frac{1}{m_q} - \frac{1}{m_Q} \right), \\
 G_1 &= -I_H \left(\frac{4m_\sigma}{\alpha_\lambda} - \frac{\alpha_\lambda}{6m_Q} \right), \\
 G_2 &= -I_H \left(\frac{2\alpha_\lambda}{3m_Q} + \frac{2m_\sigma^2 \alpha_{\lambda'}^2}{m_q \alpha_{\lambda\lambda'}^2 \alpha_\lambda} \right), \\
 G_3 &= I_H \left(\frac{6m_\sigma}{\alpha_\lambda} - \frac{5\alpha_\lambda}{6m_Q} \right), \\
 G_4 &= -I_H \left(\frac{12m_\sigma}{\alpha_\lambda} - \frac{5\alpha_\lambda}{3m_Q} \right),
 \end{aligned}$$

where

$$I_H = -\frac{1}{\sqrt{15}} \left(\frac{\alpha_\lambda \alpha_{\lambda'}}{\alpha_{\lambda\lambda'}^2} \right)^{5/2} \exp \left(-\frac{3m_\sigma^2}{2m_{\Omega_q}^2} \frac{p^2}{\alpha_{\lambda\lambda'}^2} \right),$$

Sturmian Form Factors

$$\begin{aligned}
F_1 &= I_S \frac{2m_\sigma}{\beta_\lambda} \left[1 + \frac{m_\sigma}{\beta_{\lambda\lambda'}} \left(\frac{\beta_{\lambda'}}{m_q} + \frac{\beta_\lambda}{m_Q} \right) \right], \\
F_2 &= I_H \left\{ \frac{2m_\sigma}{\beta_\lambda} \left[1 + \frac{m_\sigma}{\beta_{\lambda\lambda'}} \left(\frac{\beta_{\lambda'}}{m_q} + \frac{\beta_\lambda}{m_Q} \right) \right] - \frac{\beta_{\lambda\lambda'}}{12} \left(\frac{3}{m_q} + \frac{2}{m_Q} \right) \right\}, \\
F_3 &= -I_H \left\{ \frac{4m_\sigma}{\beta_\lambda} \left[1 + \frac{m_\sigma}{\beta_{\lambda\lambda'}} \left(\frac{\beta_{\lambda'}}{m_q} + \frac{\beta_\lambda}{m_Q} \right) \right] + \frac{\beta_{\lambda\lambda'}}{4} \left(\frac{1}{m_q} - \frac{1}{m_Q} \right) \right\}, \\
F_4 &= I_S \beta_{\lambda\lambda'} \left(\frac{1}{m_q} - \frac{1}{m_Q} \right), \\
G_1 &= -I_H \left(\frac{4m_\sigma}{\beta_\lambda} - \frac{\beta_\lambda}{12m_Q} \right), \\
G_2 &= -I_S \left(\frac{\beta_{\lambda\lambda'}}{3m_Q} + \frac{2m_\sigma^2 \beta_{\lambda'}}{m_q \beta_{\lambda\lambda'} \beta_\lambda} \right), \\
G_3 &= I_S \left(\frac{6m_\sigma}{\beta_\lambda} - \frac{5\beta_{\lambda\lambda'}}{12m_Q} - \frac{2m_\sigma^2}{m_Q \beta_{\lambda\lambda'}} \right), \\
G_4 &= -I_S \left(\frac{12m_\sigma}{\beta_\lambda} - \frac{5\beta_\lambda}{6m_Q} \right),
\end{aligned}$$

where

$$I_S = -\sqrt{\frac{2}{15}} \frac{\left(\frac{\beta_\lambda \beta_{\lambda'}}{\beta_{\lambda\lambda'}^2} \right)^{5/2}}{\left[1 + \frac{3}{2} \frac{m_\sigma^2}{m_{\Omega q}^2} \frac{p^2}{\beta_{\lambda\lambda'}} \right]^3}.$$

C.2.8 $3/2^+, |300000\rangle$

Harmonic Oscillator Form Factors

$$\begin{aligned}
 F_1 &= I_H \left[1 + \frac{m_\sigma}{\alpha_{\lambda\lambda'}^2} \left(\frac{\alpha_{\lambda'}^2}{m_q} + \frac{\alpha_\lambda^2}{m_Q} \right) \right], \\
 F_2 &= 0, \\
 F_3 &= -I_H \left[1 + \frac{m_\sigma}{\alpha_{\lambda\lambda'}^2} \left(\frac{\alpha_{\lambda'}^2}{m_q} + \frac{\alpha_\lambda^2}{m_Q} \right) \right], \\
 F_4 &= 2I_H \left[1 + \frac{m_\sigma}{\alpha_{\lambda\lambda'}^2} \left(\frac{\alpha_{\lambda'}^2}{m_q} + \frac{\alpha_\lambda^2}{m_Q} \right) \right], \\
 G_1 &= 0, \\
 G_2 &= -I_H \frac{m_\sigma}{m_q} \frac{\alpha_{\lambda'}^2}{\alpha_{\lambda\lambda'}^2}, \\
 G_3 &= I_H \left(1 + \frac{m_\sigma}{m_Q} \frac{\alpha_\lambda^2}{\alpha_{\lambda\lambda'}^2} \right), \\
 G_4 &= -2I_H,
 \end{aligned}$$

where

$$I_H = \sqrt{1/3} \left(\frac{\alpha_\lambda \alpha_{\lambda'}}{\alpha_{\lambda\lambda'}^2} \right)^{3/2} \exp \left(\frac{-3m_\sigma^2 p^2}{2m_{\Lambda_b}^2 \alpha_{\lambda\lambda'}^2} \right),$$

Sturmian Form Factors

$$\begin{aligned}
 F_1 &= I_S \left[1 + \frac{m_\sigma}{\beta_{\lambda\lambda'}} \left(\frac{\beta_{\lambda'}}{m_q} + \frac{\beta_\lambda}{m_Q} \right) \right], \\
 F_2 &= 0, \\
 F_3 &= -I_S \left[1 + \frac{m_\sigma}{\beta_{\lambda\lambda'}} \left(\frac{\beta_{\lambda'}}{m_q} + \frac{\beta_\lambda}{m_Q} \right) \right], \\
 F_4 &= 2I_S \left[1 + \frac{m_\sigma}{\beta_{\lambda\lambda'}} \left(\frac{\beta_{\lambda'}}{m_q} + \frac{\beta_\lambda}{m_Q} \right) \right], \\
 G_1 &= 0, \\
 G_2 &= -I_S \frac{m_\sigma}{m_q} \frac{\beta_{\lambda'}}{\beta_{\lambda\lambda'}}, \\
 G_3 &= I_S \left(1 + \frac{m_\sigma}{m_Q} \frac{\beta_\lambda}{\beta_{\lambda\lambda'}} \right), \\
 G_4 &= -2I_S
 \end{aligned}$$

where

$$I_S = \sqrt{\frac{1}{3}} \frac{\left(\frac{\beta_\lambda \beta_{\lambda'}}{\beta_{\lambda\lambda'}^2}\right)^{3/2}}{\left[1 + \frac{3}{2} \frac{m_\sigma^2}{m_{\Omega_q}^2} \frac{p^2}{\beta_{\lambda\lambda'}^2}\right]^2},$$

C.2.9 $3/2^+, |300010\rangle$

Harmonic Oscillator Form Factors

$$\begin{aligned} F_1 &= I_H \left[\frac{3(\alpha_\lambda^2 - \alpha_{\lambda'}^2)}{\alpha_\lambda \alpha_{\lambda'}} + \frac{\alpha_{\lambda'}(7\alpha_\lambda^2 - 3\alpha_{\lambda'}^2)}{m_q \alpha_{\lambda'} \alpha_{\lambda\lambda'}^2} + \frac{\alpha_\lambda(3\alpha_\lambda^2 - 7\alpha_{\lambda'}^2)}{m_Q \alpha_{\lambda'} \alpha_{\lambda\lambda'}^2} \right], \\ F_2 &= 0, \\ F_3 &= -I_H \left[\frac{3(\alpha_\lambda^2 - \alpha_{\lambda'}^2)}{\alpha_\lambda \alpha_\lambda} + \frac{\alpha_{\lambda'}(7\alpha_\lambda^2 - 3\alpha_{\lambda'}^2)}{m_q \alpha_\lambda \alpha_{\lambda\lambda'}^2} + \frac{\alpha_\lambda(3\alpha_\lambda^2 - 7\alpha_{\lambda'}^2)}{m_Q \alpha_{\lambda'} \alpha_{\lambda\lambda'}^2} \right], \\ F_4 &= 2I_H \left[\frac{3(\alpha_\lambda^2 - \alpha_{\lambda'}^2)}{\alpha_\lambda \alpha_\lambda} + \frac{\alpha_{\lambda'}(7\alpha_\lambda^2 - 3\alpha_{\lambda'}^2)}{m_q \alpha_\lambda \alpha_{\lambda\lambda'}^2} + \frac{\alpha_\lambda(3\alpha_\lambda^2 - 7\alpha_{\lambda'}^2)}{m_Q \alpha_{\lambda'} \alpha_{\lambda\lambda'}^2} \right], \\ G_1 &= 0, \\ G_2 &= -I_H \frac{m_\sigma}{m_q} \frac{\alpha_{\lambda'}(7\alpha_\lambda^2 - 3\alpha_{\lambda'}^2)}{\alpha_\lambda \alpha_{\lambda\lambda'}^2}, \\ G_3 &= I_H \left[\frac{3(\alpha_\lambda^2 - \alpha_{\lambda'}^2)}{\alpha_\lambda \alpha_{\lambda'}} + \frac{m_\sigma}{m_Q} \frac{\alpha_\lambda(3\alpha_\lambda^2 - 7\alpha_{\lambda'}^2)}{\alpha_{\lambda'} \alpha_{\lambda\lambda'}^2} \right], \\ G_4 &= -I_H, \frac{6(\alpha_\lambda^2 - \alpha_{\lambda'}^2)}{\alpha_\lambda \alpha_\lambda} \end{aligned}$$

where

$$I_H = \frac{1}{6} \sqrt{1/2} \left(\frac{\alpha_\lambda^{5/2} \alpha_{\lambda'}^{5/2}}{\alpha_{\lambda\lambda'}^5} \right) \exp\left(\frac{-3m_\sigma^2}{2m_{\Lambda_b}^2} \frac{p^2}{\alpha_{\lambda\lambda'}^2}\right),$$

Sturmian Form Factors

$$\begin{aligned}
F_1 &= I_S \left[\frac{3(\beta_\lambda^2 - \beta_{\lambda'}^2)}{2\beta_\lambda\beta_{\lambda'}} + \frac{(5\beta_\lambda - 3\beta_{\lambda'})}{m_q\beta_{\lambda'}} + \frac{(3\beta_\lambda - 5\beta_{\lambda'})}{m_Q\beta_{\lambda'}} \right], \\
F_2 &= 0, \\
F_3 &= -I_S \left[\frac{3(\beta_\lambda^2 - \beta_{\lambda'}^2)}{2\beta_\lambda\beta_{\lambda'}} + \frac{(5\beta_\lambda - 3\beta_{\lambda'})}{m_q\beta_{\lambda'}} + \frac{(3\beta_\lambda - 5\beta_{\lambda'})}{m_Q\beta_{\lambda'}} \right], \\
F_4 &= 2I_S \left[\frac{3(\beta_\lambda^2 - \beta_{\lambda'}^2)}{2\beta_\lambda\beta_{\lambda'}} + \frac{(5\beta_\lambda - 3\beta_{\lambda'})}{m_q\beta_{\lambda'}} + \frac{(3\beta_\lambda - 5\beta_{\lambda'})}{m_Q\beta_{\lambda'}} \right], \\
G_1 &= 0, \\
G_2 &= -I_S \frac{m_\sigma}{m_q} \frac{(5\beta_\lambda - 3\beta_{\lambda'})}{\beta_\lambda}, \\
G_3 &= I_S \left[\frac{3(\beta_\lambda^2 - \beta_{\lambda'}^2)}{2\beta_\lambda\beta_{\lambda'}} + \frac{m_\sigma}{m_Q} \frac{(3\beta_\lambda - 5\beta_{\lambda'})}{\beta_{\lambda'}} \right], \\
G_4 &= -I_S \frac{3(\beta_\lambda^2 - \beta_{\lambda'}^2)}{\beta_\lambda\beta_{\lambda'}},
\end{aligned}$$

where

$$I_S = \frac{1}{6} \frac{\left(\frac{\beta_\lambda\beta_{\lambda'}}{\beta_{\lambda\lambda'}} \right)^{5/2}}{\left[1 + \frac{3}{2} \frac{m_\sigma^2}{m_{\Omega_q}^2} \frac{p^2}{\beta_{\lambda\lambda'}} \right]^3},$$

C.2.10 $3/2_2^+, |220002\rangle$

Harmonic Oscillator Form Factors

$$\begin{aligned}
F_1 &= I_H \frac{m_\sigma}{2} \left(\frac{1}{m_q} - \frac{7}{m_Q} \right), \\
F_2 &= I_H \left\{ \frac{6m_\sigma^2}{\alpha_\lambda^2} \left[1 - \frac{m_\sigma}{\alpha_{\lambda\lambda'}} \left(\frac{2\alpha_{\lambda'}^2}{m_q} - \frac{\alpha_\lambda^2}{m_Q} \right) \right] - \frac{3m_\sigma}{2m_q} \right\}, \\
F_3 &= I_H \left\{ \frac{6m_\sigma^2}{\alpha_\lambda^2} \left[2 + \frac{m_\sigma}{\alpha_{\lambda\lambda'}} \left(\frac{2\alpha_{\lambda'}^2}{m_q} - \frac{\alpha_\lambda^2}{m_Q} \right) \right] - m_\sigma \left(\frac{2}{m_q} + \frac{1}{m_Q} \right) \right\}, \\
F_4 &= 2I_H m_\sigma \left(\frac{2}{m_q} + \frac{1}{m_Q} \right), \\
G_1 &= I_H \frac{3m_\sigma}{\alpha_\lambda} \left(\frac{2m_\sigma}{\alpha_\lambda} - \frac{3}{2m_Q} \right), \\
G_2 &= -I_H \left[\frac{6m_\sigma^2}{\alpha_\lambda^2} - m_\sigma \left(\frac{5}{2m_q} - \frac{3}{m_Q} \right) \right], \\
G_3 &= I_H \frac{4m_\sigma}{m_Q}, \\
G_4 &= 0,
\end{aligned}$$

where

$$I_H = \frac{1}{3\sqrt{5}} \left(\frac{\alpha_\lambda \alpha_{\lambda'}}{\alpha_{\lambda\lambda'}^2} \right)^{7/2} \exp \left(-\frac{3m_\sigma^2}{2m_{\Omega_q}^2} \frac{p^2}{\alpha_{\lambda\lambda'}^2} \right),$$

Sturmian Form Factors

$$\begin{aligned} F_1 &= I_S \frac{m_\sigma}{2} \left(\frac{1}{m_q} - \frac{7}{m_Q} \right), \\ F_2 &= I_S \frac{m_\sigma}{\beta_\lambda} \left\{ \frac{18m_\sigma}{\beta_{\lambda\lambda'}} \left[1 - \frac{m_\sigma}{\beta_{\lambda\lambda'}} \left(\frac{2\beta_{\lambda'}}{m_q} - \frac{\beta_\lambda}{m_Q} \right) \right] - \frac{3\beta_\lambda}{2m_q} \right\}, \\ F_3 &= I_S \frac{m_\sigma}{\beta_\lambda} \left\{ \frac{18m_\sigma}{\beta_{\lambda\lambda'}} \left[2 + \frac{m_\sigma}{\beta_{\lambda\lambda'}} \left(\frac{2\beta_{\lambda'}}{m_q} - \frac{\beta_\lambda}{m_Q} \right) \right] - \beta_\lambda \left(\frac{2}{m_q} + \frac{1}{m_Q} \right) \right\}, \\ F_4 &= 2I_S m_\sigma \left(\frac{2}{m_q} + \frac{1}{m_Q} \right), \\ G_1 &= -9I_S \frac{m_\sigma}{\beta_\lambda} \left(\frac{2m_\sigma}{\beta_{\lambda\lambda'}} - \frac{\beta_\lambda}{2m_Q} \right), \\ G_2 &= -I_S \frac{m_\sigma}{\beta_\lambda} \left[\frac{18m_\sigma}{\beta_{\lambda\lambda'}} - \beta_\lambda \left(\frac{5}{2m_q} + \frac{3}{m_Q} \right) \right], \\ G_3 &= I_S \frac{4m_\sigma}{m_Q}, \\ G_4 &= 0, \end{aligned}$$

where

$$I_S = \sqrt{\frac{2}{15}} \frac{\left(\frac{\beta_\lambda \beta_{\lambda'}}{\beta_{\lambda\lambda'}^2} \right)^{7/2}}{3\beta_\lambda \left[1 + \frac{3}{2} \frac{m_\sigma^2}{m_{\Omega_q}^2} \frac{p^2}{\beta_{\lambda\lambda'}^2} \right]^4}.$$

C.2.11 $3/2_3^+, |320002\rangle$

Harmonic Oscillator Form Factors

$$\begin{aligned}
F_1 &= I_H m_\sigma \left(\frac{1}{m_q} - \frac{1}{m_Q} \right), \\
F_2 &= I_H \frac{3m_\sigma}{\alpha_\lambda} \left\{ \frac{2m_\sigma}{\alpha_\lambda} \left[1 + \frac{m_\sigma}{\alpha_{\lambda\lambda'}^2} \left(\frac{\alpha_{\lambda'}^2}{m_q} + \frac{\alpha_\lambda^2}{m_Q} \right) \right] + \frac{\alpha_\lambda}{m_q} \right\}, \\
F_3 &= -I_H \frac{2m_\sigma}{\alpha_\lambda} \left\{ \frac{3m_\sigma}{\alpha_\lambda} \left[1 + \frac{m_\sigma}{\alpha_{\lambda\lambda'}^2} \left(\frac{\alpha_{\lambda'}^2}{m_q} + \frac{\alpha_\lambda^2}{m_Q} \right) \right] + 2\alpha_\lambda \left(\frac{1}{m_q} - \frac{1}{m_Q} \right) \right\}, \\
F_4 &= 8I_H m_\sigma \left(\frac{1}{m_q} - \frac{1}{m_Q} \right), \\
G_1 &= -I_H \frac{3m_\sigma}{\alpha_\lambda} \left(\frac{4m_\sigma^2}{\alpha_\lambda} - \frac{\alpha_\lambda}{m_Q} \right), \\
G_2 &= -I_H \frac{m_\sigma}{\alpha_\lambda} \left[\frac{6m_\sigma}{\alpha_\lambda} - \alpha_\lambda \left(\frac{5}{m_q} + \frac{3}{m_Q} \right) \right], \\
G_3 &= I_H \frac{m_\sigma}{\alpha_\lambda} \left(\frac{18m_\sigma}{\alpha_\lambda} - \frac{\alpha_\lambda}{m_Q} \right), \\
G_4 &= 0,
\end{aligned}$$

where

$$I_H = \frac{1}{3\sqrt{5}} \left(\frac{\alpha_\lambda \alpha_{\lambda'}}{\alpha_{\lambda\lambda'}^2} \right)^{7/2} \exp \left(-\frac{3m_\sigma^2 p^2}{2m_{\Omega_q}^2 \alpha_{\lambda\lambda'}^2} \right),$$

Sturmian Form Factors

$$\begin{aligned}
F_1 &= I_S m_\sigma \left(\frac{1}{m_q} - \frac{1}{m_Q} \right), \\
F_2 &= I_S \frac{m_\sigma}{\beta_\lambda} \left\{ \frac{6m_\sigma}{\beta_{\lambda\lambda'}} \left[1 + \frac{m_\sigma}{\beta_{\lambda\lambda'}} \left(\frac{\beta_{\lambda'}}{m_q} + \frac{\beta_\lambda}{m_Q} \right) \right] - \frac{\beta_\lambda}{m_q} \right\}, \\
F_3 &= -I_S \frac{2m_\sigma}{\beta_\lambda} \left\{ \frac{9m_\sigma}{\beta_{\lambda\lambda'}} \left[1 + \frac{m_\sigma}{\beta_{\lambda\lambda'}} \left(\frac{\beta_{\lambda'}}{m_q} + \frac{\beta_\lambda}{m_Q} \right) \right] + 2\beta_\lambda \left(\frac{1}{m_q} - \frac{1}{m_Q} \right) \right\}, \\
F_4 &= 8I_S m_\sigma \left(\frac{1}{m_q} - \frac{1}{m_Q} \right), \\
G_1 &= -I_S \frac{3m_\sigma}{\beta_\lambda} \left(\frac{6m_\sigma}{\beta_{\lambda\lambda'}} - \frac{\beta_\lambda}{m_Q} \right), \\
G_2 &= -I_S \frac{m_\sigma}{\beta_\lambda} \left[\frac{18m_\sigma}{\beta_{\lambda\lambda'}} - \beta_\lambda \left(\frac{5}{m_q} - \frac{3}{m_Q} \right) \right], \\
G_3 &= I_S \frac{m_\sigma}{\beta_\lambda} \left(\frac{54m_\sigma}{\beta_{\lambda\lambda'}} - \frac{\beta_\lambda}{m_Q} \right), \\
G_4 &= 0,
\end{aligned}$$

where

$$I_S = \sqrt{\frac{2}{15}} \frac{\left(\frac{\beta_\lambda \beta_{\lambda'}}{\beta_{\lambda\lambda'}^2}\right)^{7/2}}{3\beta_\lambda \left[1 + \frac{3}{2} \frac{m_\sigma^2}{m_{\Omega_q}^2} \frac{p^2}{\beta_{\lambda\lambda'}^2}\right]^4}.$$

C.2.12 $5/2^-, |310001\rangle$

Harmonic Oscillator Form Factors

$$\begin{aligned} F_1 &= I_H \frac{m_\sigma}{\alpha_\lambda} \left[1 + \frac{m_\sigma}{\alpha_{\lambda\lambda'}^2} \left(\frac{\alpha_{\lambda'}^2}{m_q} + \frac{\alpha_\lambda^2}{m_Q}\right)\right], \\ F_2 &= 0, \\ F_3 &= -I_H \frac{m_\sigma}{\alpha_\lambda} \left[1 + \frac{m_\sigma}{\alpha_{\lambda\lambda'}^2} \left(\frac{\alpha_{\lambda'}^2}{m_q} + \frac{\alpha_{\lambda'}^2}{m_Q}\right)\right], \\ F_4 &= I_H \frac{2m_\sigma}{\alpha_\lambda} \left[1 + \frac{m_\sigma}{\alpha_{\lambda\lambda'}^2} \left(\frac{\alpha_{\lambda'}^2}{m_q} + \frac{\alpha_\lambda^2}{m_Q}\right)\right], \\ G_1 &= 0, \\ G_2 &= -I_H \frac{m_\sigma^2 \alpha_{\lambda'}^2}{m_q \alpha_\lambda \alpha_{\lambda\lambda'}^2}, \\ G_3 &= I_H \frac{m_\sigma}{\alpha_\lambda} \left(1 + \frac{m_\sigma \alpha_\lambda^2}{m_Q \alpha_{\lambda\lambda'}^2}\right), \\ G_4 &= -I_H \frac{2m_\sigma}{\alpha_\lambda}, \end{aligned}$$

where

$$I_H = - \left(\frac{\alpha_\lambda \alpha_{\lambda'}}{\alpha_{\lambda\lambda'}^2}\right)^{5/2} \exp\left(-\frac{3m_\sigma^2}{2m_{\Omega_q}^2} \frac{p^2}{\alpha_{\lambda\lambda'}^2}\right),$$

Sturmian Form Factors

$$\begin{aligned}
 F_1 &= I_S \frac{m_\sigma}{\beta_\lambda} \left[1 + \frac{m_\sigma}{\beta_{\lambda\lambda'}} \left(\frac{\beta_{\lambda'}}{m_q} + \frac{\beta_\lambda}{m_Q} \right) \right], \\
 F_2 &= 0, \\
 F_3 &= -I_S \frac{m_\sigma}{\beta_\lambda} \left[1 + \frac{m_\sigma}{\beta_{\lambda\lambda'}} \left(\frac{\beta_{\lambda'}}{m_q} + \frac{\beta_\lambda}{m_Q} \right) \right], \\
 F_4 &= I_S \frac{2m_\sigma}{\beta_\lambda} \left[1 + \frac{m_\sigma}{\beta_{\lambda\lambda'}} \left(\frac{\beta_{\lambda'}}{m_q} + \frac{\beta_\lambda}{m_Q} \right) \right], \\
 G_1 &= 0, \\
 G_2 &= -I_S \frac{m_\sigma^2 \beta_{\lambda'}}{m_q \beta_\lambda \beta_{\lambda\lambda'}}, \\
 G_3 &= I_S \frac{m_\sigma}{\beta_\lambda} \left(1 + \frac{m_\sigma \beta_\lambda}{m_Q \beta_{\lambda\lambda'}} \right), \\
 G_4 &= -I_S \frac{2m_\sigma}{\beta_\lambda},
 \end{aligned}$$

where

$$I_S = -\sqrt{2} \frac{\left(\frac{\beta_\lambda \beta_{\lambda'}}{\beta_{\lambda\lambda'}^2} \right)^{5/2}}{\left[1 + \frac{3}{2} \frac{m_\sigma^2}{m_{\Omega_q}^2} \frac{p^2}{\beta_{\lambda\lambda'}^2} \right]^3}.$$

C.2.13 $5/2^+, |220002\rangle$

Harmonic Oscillator Form Factors

$$\begin{aligned}
 F_1 &= -I_H \frac{3m_\sigma^2}{\alpha_\lambda^2} \left[1 + \frac{m_\sigma}{\alpha_{\lambda\lambda'}^2} \left(\frac{\alpha_{\lambda'}^2}{m_q} + \frac{\alpha_\lambda^2}{m_Q} \right) \right], \\
 F_2 &= I_H \frac{m_\sigma}{\alpha_\lambda} \left\{ \frac{3m_\sigma}{\alpha_\lambda} \left[2 - \frac{m_\sigma}{\alpha_{\lambda\lambda'}^2} \left(\frac{\alpha_{\lambda'}^2}{m_q} - \frac{2\alpha_\lambda^2}{m_Q} \right) \right] - \frac{2\alpha_\lambda}{m_q} \right\}, \\
 F_3 &= I_H \frac{m_\sigma}{\alpha_\lambda} \left\{ \frac{3m_\sigma}{\alpha_\lambda} \left[2 + \frac{m_\sigma}{\alpha_{\lambda\lambda'}^2} \left(\frac{2\alpha_{\lambda'}^2}{m_q} - \frac{\alpha_\lambda^2}{m_Q} \right) \right] - \alpha_\lambda \left(\frac{2}{m_q} + \frac{1}{m_Q} \right) \right\}, \\
 F_4 &= 2I_H m_\sigma \left(\frac{2}{m_q} + \frac{1}{m_Q} \right), \\
 G_1 &= -I_H \frac{m_\sigma}{\alpha_\lambda} \left(\frac{3m_\sigma}{\alpha_\lambda} + \frac{\alpha_\lambda}{m_Q} \right), \\
 G_2 &= I_H \frac{m_\sigma^3}{2m_q} \frac{\alpha_{\lambda'}^2}{\alpha_{\lambda\lambda'}^2 \alpha_\lambda^2}, \\
 G_3 &= I_H \frac{m_\sigma}{m_Q} \left(1 - \frac{3m_\sigma^2}{\alpha_{\lambda\lambda'}^2} \right), \\
 G_4 &= -I_H \frac{2m_\sigma}{m_Q},
 \end{aligned}$$

where

$$I_H = \frac{1}{3\sqrt{2}} \left(\frac{\alpha_\lambda \alpha_{\lambda'}}{\alpha_{\lambda\lambda'}^2} \right)^{7/2} \exp \left(-\frac{3m_\sigma^2}{2m_{\Omega_q}^2} \frac{p^2}{\alpha_{\lambda\lambda'}^2} \right),$$

Sturmian Form Factors

$$\begin{aligned}
F_1 &= -I_S \frac{9m_\sigma^2}{\beta_\lambda \beta_{\lambda\lambda'}} \left[1 + \frac{m_\sigma}{\beta_{\lambda\lambda'}} \left(\frac{\beta_{\lambda'}}{m_q} + \frac{\beta_\lambda}{m_Q} \right) \right], \\
F_2 &= I_S \frac{m_\sigma}{\beta_\lambda} \left\{ \frac{9m_\sigma}{\beta_{\lambda\lambda'}} \left[2 - \frac{m_\sigma}{\beta_{\lambda\lambda'}} \left(\frac{\beta_{\lambda'}}{m_q} - \frac{2\beta_\lambda}{m_Q} \right) \right] - \frac{2\beta_\lambda}{m_q} \right\}, \\
F_3 &= I_S \frac{m_\sigma}{\beta_\lambda} \left\{ \frac{9m_\sigma}{\beta_{\lambda\lambda'}} \left[2 + \frac{m_\sigma}{\beta_{\lambda\lambda'}} \left(\frac{2\beta_{\lambda'}}{m_q} - \frac{\beta_\lambda}{m_Q} \right) \right] - \beta_\lambda \left(\frac{2}{m_q} + \frac{1}{m_Q} \right) \right\}, \\
F_4 &= 2I_S m_\sigma \left(\frac{2}{m_q} + \frac{1}{m_Q} \right), \\
G_1 &= -I_S \frac{m_\sigma}{\beta_\lambda} \left(\frac{9m_\sigma}{\beta_{\lambda\lambda'}} + \frac{\beta_\lambda}{m_Q} \right), \\
G_2 &= I_S \frac{9m_\sigma^3 \beta_{\lambda'}}{m_q \beta_\lambda \beta_{\lambda\lambda'}^2}, \\
G_3 &= I_S \frac{m_\sigma}{m_Q} \left(1 - \frac{9m_\sigma^2}{\beta_{\lambda\lambda'}^2} \right), \\
G_4 &= -I_S \frac{2m_\sigma}{m_Q},
\end{aligned}$$

where

$$I_S = \sqrt{\frac{1}{3}} \frac{\left(\frac{\beta_\lambda \beta_{\lambda'}}{\beta_{\lambda\lambda'}^2} \right)^{5/2} \frac{\beta_{\lambda'}}{\beta_{\lambda\lambda'}}}{3 \left[1 + \frac{3}{2} \frac{m_\sigma^2}{m_{\Omega_q}^2} \frac{p^2}{\beta_{\lambda\lambda'}^2} \right]^4}.$$

C.2.14 $5/2_1^+, |320002\rangle$

Harmonic Oscillator Form Factors

$$\begin{aligned}
F_1 &= -I_H \frac{3m_\sigma^2}{\alpha_\lambda^2} \left[1 + \frac{m_\sigma}{\alpha_{\lambda\lambda'}} \left(\frac{\alpha_{\lambda'}^2}{m_q} + \frac{\alpha_\lambda^2}{m_Q} \right) \right], \\
F_2 &= I_H \frac{m_\sigma}{\alpha_\lambda} \left\{ \frac{3m_\sigma}{\alpha_\lambda} \left[1 + \frac{m_\sigma}{\alpha_{\lambda\lambda'}} \left(\frac{\alpha_{\lambda'}^2}{m_q} + \frac{\alpha_{\lambda'}^2}{m_Q} \right) \right] - \frac{\alpha_\lambda}{4} \left(\frac{1}{m_q} + \frac{6}{m_Q} \right) \right\}, \\
F_3 &= -I_H \frac{m_\sigma}{\alpha_\lambda} \left\{ \frac{6m_\sigma}{\alpha_\lambda} \left[1 + \frac{m_\sigma}{\alpha_{\lambda\lambda'}} \left(\frac{\alpha_{\lambda'}^2}{m_q} + \frac{\alpha_{\lambda'}^2}{m_Q} \right) \right] + \frac{\alpha_\lambda}{4} \left(\frac{1}{m_q} - \frac{1}{m_Q} \right) \right\}, \\
F_4 &= I_H \frac{m_\sigma}{2} \left(\frac{1}{m_q} - \frac{1}{m_Q} \right), \\
G_1 &= -I_H \frac{m_\sigma}{\alpha_\lambda} \left(\frac{6m_\sigma}{\alpha_\lambda} - \frac{7\alpha_\lambda}{4m_Q} \right), \\
G_2 &= -I_H \frac{3m_\sigma^3 \alpha_{\lambda'}^2}{m_q \alpha_{\lambda\lambda'}^2 \alpha_\lambda^2}, \\
G_3 &= I_H \frac{m_\sigma}{\alpha_\lambda} \left[\frac{9m_\sigma}{\alpha_\lambda} + \frac{\alpha_\lambda}{m_Q} \left(\frac{3m_\sigma^2}{\alpha_{\lambda\lambda'}^2} - \frac{7}{4} \right) \right], \\
G_4 &= -I_H \frac{m_\sigma}{\alpha_\lambda} \left(\frac{18m_\sigma}{\alpha_\lambda} - \frac{7\alpha_\lambda}{2m_Q} \right),
\end{aligned}$$

where

$$I_H = \frac{2}{3\sqrt{7}} \left(\frac{\alpha_\lambda \alpha_{\lambda'}}{\alpha_{\lambda\lambda'}^2} \right)^{7/2} \exp \left(-\frac{3m_\sigma^2}{2m_{\Omega_q}^2} \frac{p^2}{\alpha_{\lambda\lambda'}^2} \right),$$

Sturmian Form Factors

$$\begin{aligned}
F_1 &= -I_S \frac{6m_\sigma^2}{\beta_\lambda \beta_{\lambda\lambda'}} \left[1 + \frac{m_\sigma}{\beta_{\lambda\lambda'}} \left(\frac{\beta_{\lambda'}}{m_q} + \frac{\beta_\lambda}{m_Q} \right) \right], \\
F_2 &= I_S \frac{m_\sigma}{\beta_\lambda} \left\{ \frac{6m_\sigma}{\beta_{\lambda\lambda'}} \left[1 + \frac{m_\sigma}{\beta_{\lambda\lambda'}} \left(\frac{\beta_{\lambda'}}{m_q} + \frac{\beta_\lambda}{m_Q} \right) \right] - \frac{\beta_\lambda}{6} \left(\frac{1}{m_q} + \frac{6}{m_Q} \right) \right\}, \\
F_3 &= -I_S \frac{m_\sigma}{\beta_\lambda} \left\{ \frac{12m_\sigma}{\beta_{\lambda\lambda'}} \left[1 + \frac{m_\sigma}{\beta_{\lambda\lambda'}} \left(\frac{\beta_{\lambda'}}{m_q} + \frac{\beta_\lambda}{m_Q} \right) \right] + \frac{\beta_\lambda}{6} \left(\frac{1}{m_q} - \frac{1}{m_Q} \right) \right\}, \\
F_4 &= I_S \frac{m_\sigma}{3} \left(\frac{1}{m_q} - \frac{1}{m_Q} \right), \\
G_1 &= -I_S \frac{m_\sigma}{\beta_\lambda} \left(12 - \frac{7\beta_\lambda}{6m_Q} \right), \\
G_2 &= -I_S \frac{6m_\sigma^3 \beta_{\lambda'}}{m_q \beta_{\lambda\lambda'} \beta_{\lambda\lambda'}^2}, \\
G_3 &= I_S \frac{m_\sigma}{\beta_\lambda} \left[\frac{18m_\sigma}{\beta_{\lambda\lambda'}} + \frac{\beta_\lambda}{m_Q} \left(\frac{6m_\sigma^2}{\beta_{\lambda\lambda'}^2} - \frac{7}{4} \right) \right], \\
G_4 &= -I_S \frac{m_\sigma}{\beta_\lambda} \left(\frac{36m_\sigma}{\beta_{\lambda\lambda'}} - \frac{7\beta_\lambda}{3m_Q} \right),
\end{aligned}$$

where

$$I_S = \sqrt{\frac{2}{21}} \frac{\beta_{\lambda'} \left(\frac{\beta_\lambda \beta_{\lambda'}}{\beta_{\lambda\lambda'}^2} \right)^{5/2}}{\beta_{\lambda\lambda'} \left[1 + \frac{3}{2} \frac{m_\sigma^2}{m_{\Omega_q}^2} \frac{p^2}{\beta_{\lambda\lambda'}^2} \right]^4}.$$

C.3 HQET Quark Model Form Factors

C.3.1 $1/2^-, j = 0$

Harmonic Oscillator Form Factors

$$\begin{aligned}
 F_1 &= I_H \frac{\alpha_\lambda}{6} \left(\frac{1}{m_q} - \frac{3}{m_Q} \right), \\
 F_2 &= \frac{1}{6m_q \alpha_\lambda} I_H \left(\alpha_\lambda^2 - \frac{12\alpha_{\lambda'}^2 m_\sigma^2}{\alpha_{\lambda\lambda'}^2} \right), \\
 F_3 &= \frac{2m_\sigma}{\alpha_\lambda} I_H \left(1 + \frac{m_\sigma \alpha_{\lambda'}^2}{m_q \alpha_{\lambda\lambda'}^2} \right), \\
 G_1 &= I_H \left(\frac{2m_\sigma}{\alpha_\lambda} - \frac{\alpha_\lambda}{2m_Q} \right), \\
 G_2 &= -\frac{\alpha_\lambda}{2m_q} I_H, \\
 G_3 &= -\frac{2m_\sigma}{\alpha_\lambda} I_H,
 \end{aligned}$$

where

$$I_H = \frac{1}{\sqrt{3}} \left(\frac{\alpha_\lambda \alpha_{\lambda'}}{\alpha_{\lambda\lambda'}^2} \right)^{5/2} \exp \left(-\frac{3m_\sigma^2}{2m_{\Omega_q}^2} \frac{p^2}{\alpha_{\lambda\lambda'}^2} \right),$$

Sturmian Form Factors

$$\begin{aligned}
 F_1 &= I_S \frac{\beta_{\lambda\lambda'}}{24} \left(\frac{1}{m_q} - \frac{3}{m_Q} \right), \\
 F_2 &= \frac{1}{m_q} I_S \left(\frac{\beta_{\lambda\lambda'}}{24} - \frac{\beta_{\lambda'} m_\sigma^2}{\beta_\lambda \beta_{\lambda\lambda'}} \right), \\
 F_3 &= \frac{m_\sigma}{\beta_\lambda} I_S \left(1 + \frac{m_\sigma \beta_{\lambda'}}{m_q \beta_{\lambda\lambda'}} \right), \\
 G_1 &= I_S \left(\frac{m_\sigma}{\beta_\lambda} - \frac{\beta_{\lambda\lambda'}}{8m_Q} \right), \\
 G_2 &= -\frac{\beta_{\lambda\lambda'}}{8m_q} I_S, \\
 G_3 &= -\frac{m_\sigma}{\beta_\lambda} I_S,
 \end{aligned}$$

where

$$I_S = 2\sqrt{\frac{2}{3}} \frac{\left(\frac{\beta_\lambda \beta_{\lambda'}}{\beta_{\lambda\lambda'}} \right)^{5/2}}{\left[1 + \frac{3}{2} \frac{m_\sigma^2}{m_{\Omega_q}^2} \frac{p^2}{\beta_{\lambda\lambda'}^2} \right]^3}.$$

C.3.2 $1/2^-$, $j = 1$

Harmonic Oscillator Form Factors

$$\begin{aligned}
F_1 &= \frac{\alpha_\lambda}{6} I_H \left(\frac{1}{m_q} + \frac{1}{m_Q} \right), \\
F_2 &= I_H \left\{ -\frac{m_\sigma}{\alpha_\lambda} \left[1 - \frac{m_\sigma}{\alpha_{\lambda\lambda'}}^2 \left(\frac{\alpha_{\lambda'}^2}{m_q} - \frac{\alpha_\lambda^2}{m_Q} \right) \right] + \frac{\alpha_\lambda}{6m_q} \right\}, \\
F_3 &= -\frac{m_\sigma}{\alpha_\lambda} I_H \left[1 + \frac{m_\sigma}{\alpha_{\lambda\lambda'}^2} \left(\frac{\alpha_{\lambda'}^2}{m_q} - \frac{\alpha_\lambda^2}{m_Q} \right) \right], \\
G_1 &= \frac{\alpha_\lambda}{6m_Q} I_H, \\
G_2 &= I_H \left[\frac{m_\sigma}{\alpha_\lambda} - \frac{\alpha_\lambda}{6} \left(\frac{3}{m_q} + \frac{2}{m_Q} \right) \right], \\
G_3 &= -I_H \left(\frac{m_\sigma^2}{\alpha_\lambda} + \frac{\alpha_\lambda}{3m_Q} \right),
\end{aligned}$$

where

$$I_H = \sqrt{\frac{2}{3}} \left(\frac{\alpha_\lambda \alpha_{\lambda'}}{\alpha_{\lambda\lambda'}^2} \right)^{5/2} \exp \left(-\frac{3m_\sigma^2 p^2}{2m_{\Omega_q}^2 \alpha_{\lambda\lambda'}^2} \right),$$

Sturmian Form Factors

$$\begin{aligned}
F_1 &= I_S \frac{\beta_{\lambda\lambda'}}{6} \left(\frac{1}{m_q} + \frac{1}{m_Q} \right), \\
F_2 &= I_S \left\{ -\frac{2m_\sigma}{\beta_\lambda} \left[1 - \frac{m_\sigma}{\beta_{\lambda\lambda'}} \left(\frac{\beta_{\lambda'}}{m_q} - \frac{\beta_\lambda}{m_Q} \right) \right] + \frac{\beta_{\lambda\lambda'}}{6m_q} \right\}, \\
F_3 &= -\frac{2m_\sigma}{\beta_\lambda} I_S \left[1 + \frac{m_\sigma}{\beta_{\lambda\lambda'}} \left(\frac{\beta_{\lambda'}}{m_q} - \frac{\beta_\lambda}{m_Q} \right) \right], \\
G_1 &= \frac{\beta_{\lambda\lambda'}}{6m_Q} I_S, \\
G_2 &= I_S \left[\frac{2m_\sigma}{\beta_\lambda} - \frac{\beta_{\lambda\lambda'}}{6} \left(\frac{3}{m_q} + \frac{2}{m_Q} \right) \right], \\
G_3 &= -I_S \left(\frac{2m_\sigma}{\beta_\lambda} + \frac{\beta_{\lambda\lambda'}}{3m_Q} \right),
\end{aligned}$$

where

$$I_S = \frac{1}{\sqrt{3}} \frac{\left(\frac{\beta_\lambda \beta_{\lambda'}}{\beta_{\lambda\lambda'}^2} \right)^{5/2}}{\left[1 + \frac{3}{2} \frac{m_\sigma^2 p^2}{m_{\Omega_q}^2 \beta_{\lambda\lambda'}^2} \right]^4}.$$

C.3.3 $3/2^+$, $j = 1$

Harmonic Oscillator Form Factors

$$\begin{aligned}
F_1 &= I_H \frac{m_\sigma}{6} \left(\frac{1}{m_q} + \frac{5}{m_Q} \right), \\
F_2 &= -I_H \frac{m_\sigma}{2m_q} \left(1 - \frac{12m_\sigma^2 \alpha_{\lambda'}^2}{\alpha_\lambda^2 \alpha_{\lambda\lambda'}} \right), \\
F_3 &= -\frac{m_\sigma}{\alpha_\lambda} I_H \left[\frac{6m_\sigma}{\alpha_\lambda} \left(1 + \frac{m_\sigma \alpha_{\lambda'}^2}{m_q \alpha_{\lambda\lambda'}} \right) + \frac{\alpha_\lambda}{3} \left(\frac{2}{m_q} - \frac{5}{m_Q} \right) \right], \\
F_4 &= \frac{2m_\sigma}{3} I_H \left(\frac{2}{m_q} - \frac{5}{m_Q} \right), \\
G_1 &= -\frac{m_\sigma}{\alpha_\lambda} I_H \left(\frac{6m_\sigma}{\alpha_\lambda} - \frac{5\alpha_\lambda}{2m_Q} \right), \\
G_2 &= I_H \frac{5m_\sigma}{6m_q}, \\
G_3 &= \frac{m_\sigma}{\alpha_\lambda} I_H \left(\frac{6m_\sigma}{\alpha_\lambda} - \frac{5\alpha_\lambda}{3m_Q} \right), \\
G_4 &= 0,
\end{aligned}$$

where

$$I_H = \sqrt{\frac{1}{10}} \left(\frac{\alpha_\lambda \alpha_{\lambda'}}{\alpha_{\lambda\lambda'}^2} \right)^{5/2} \exp \left(-\frac{3m_\sigma^2}{2m_{\Omega_q}^2} \frac{p^2}{\alpha_{\lambda\lambda'}^2} \right),$$

Sturmian Form Factors

$$\begin{aligned}
F_1 &= I_S \frac{\beta_{\lambda\lambda'} m_\sigma}{108\beta_\lambda} \left(\frac{1}{m_q} + \frac{5}{m_Q} \right), \\
F_2 &= -I_S \frac{m_\sigma \beta_{\lambda\lambda'}}{36m_q \beta_\lambda} \left(1 - \frac{36m_\sigma^2 \beta_{\lambda'}}{\beta_\lambda \beta_{\lambda\lambda'}} \right), \\
F_3 &= I_S \left[-\frac{m_\sigma^2}{\beta_\lambda^2} \left(1 + \frac{m_\sigma \beta_{\lambda'}}{m_q \beta_{\lambda\lambda'}} \right) + \frac{\beta_{\lambda\lambda'}}{54\beta_\lambda} \left(\frac{5}{m_Q} - \frac{2}{m_q} \right) \right], \\
F_4 &= \frac{\beta_{\lambda\lambda'} m_\sigma}{27\beta_\lambda} I_H \left(\frac{2}{m_q} - \frac{5}{m_Q} \right), \\
G_1 &= -\frac{m_\sigma}{\beta_\lambda} I_S \left(\frac{m_\sigma}{\beta_\lambda} - \frac{5\beta_{\lambda\lambda'}}{36m_Q} \right), \\
G_2 &= \frac{5m_\sigma \beta_{\lambda\lambda'}}{108m_Q \beta_\lambda} I_S, \\
G_3 &= \frac{m_\sigma}{\beta_\lambda} I_S \left(\frac{m_\sigma}{\beta_\lambda} - \frac{5\beta_{\lambda\lambda'}}{54m_Q} \right), \\
G_4 &= 0,
\end{aligned}$$

where

$$I_S = 6\sqrt{\frac{3}{5}} \frac{\left(\frac{\beta_\lambda \beta_{\lambda'}}{\beta_{\lambda\lambda'}^2}\right)^{7/2}}{\left[1 + \frac{3}{2} \frac{m_\sigma^2}{m_{\Omega_q}^2} \frac{p^2}{\beta_{\lambda\lambda'}^2}\right]^4}. \quad (\text{C.1})$$

C.3.4 $3/2^+$, $j = 2$

Harmonic Oscillator Form Factors

$$\begin{aligned} F_1 &= \frac{m_\sigma}{4} I_H \left(\frac{1}{m_q} - \frac{3}{m_Q} \right), \\ F_2 &= I_H \left\{ \frac{2m_\sigma^2}{\alpha_\lambda^2} \left[1 + \frac{m_\sigma}{2\alpha_{\lambda\lambda'}^2} \left(\frac{2\alpha_\lambda^2}{m_Q} - \frac{\alpha_{\lambda'}^2}{m_q} \right) \right] - \frac{3m_\sigma}{4m_Q} \right\}, \\ F_3 &= I_H \left\{ \frac{m_\sigma^2}{\alpha_\lambda^2} \left[1 + \frac{m_\sigma}{\alpha_{\lambda\lambda'}^2} \left(\frac{\alpha_{\lambda'}^2}{m_q} - \frac{2\alpha_\lambda^2}{m_Q} \right) \right] + m_\sigma \left(\frac{1}{2m_Q} - \frac{1}{m_q} \right) \right\}, \\ F_4 &= m_\sigma I_H \left(\frac{2}{m_q} - \frac{1}{m_Q} \right), \\ G_1 &= -m_\sigma I_H \left(\frac{m_\sigma}{\alpha_\lambda^2} + \frac{1}{4m_Q} \right), \\ G_2 &= \frac{m_\sigma}{\alpha_\lambda} I_H \left[-\frac{2m_\sigma}{\alpha_\lambda} + \frac{\alpha_\lambda}{4} \left(\frac{5}{m_q} + \frac{4}{m_Q} \right) \right], \\ G_3 &= \frac{m_\sigma}{\alpha_\lambda} I_H \left(\frac{3m_\sigma}{\alpha_\lambda} + \frac{\alpha_\lambda}{2m_Q} \right), \\ G_4 &= 0, \end{aligned}$$

where

$$I_H = \sqrt{\frac{2}{5}} \left(\frac{\alpha_\lambda \alpha_{\lambda'}}{\alpha_{\lambda\lambda'}^2} \right)^{5/2} \exp \left(-\frac{3m_\sigma^2}{2m_{\Omega_q}^2} \frac{p^2}{\alpha_{\lambda\lambda'}^2} \right),$$

Sturmian Form Factors

$$\begin{aligned}
F_1 &= \frac{m_\sigma \beta_{\lambda\lambda'}}{24\beta_\lambda} I_S \left(\frac{1}{m_q} - \frac{3}{m_Q} \right), \\
F_2 &= \frac{m_\sigma}{\beta_\lambda} I_S \left\{ \frac{m_\sigma}{\beta_\lambda} \left[1 + \frac{m_\sigma}{2\beta_{\lambda\lambda'}} \left(\frac{2\beta_\lambda}{m_Q} - \frac{\beta_{\lambda'}}{m_q} \right) \right] - \frac{\beta_{\lambda\lambda'}}{8m_q} \right\}, \\
F_3 &= \frac{m_\sigma}{\beta_\lambda} I_S \left\{ \frac{m_\sigma}{2\beta_\lambda} \left[1 + \frac{m_\sigma}{\beta_{\lambda\lambda'}} \left(\frac{\beta_{\lambda'}}{m_q} - \frac{2\beta_\lambda}{m_Q} \right) \right] + \frac{\beta_{\lambda\lambda'}}{12} \left(\frac{1}{m_Q} - \frac{2}{m_q} \right) \right\}, \\
F_4 &= \frac{m_\sigma \beta_{\lambda\lambda'}}{6\beta_\lambda} I_S \left(\frac{2}{m_q} - \frac{1}{m_Q} \right), \\
G_1 &= -\frac{m_\sigma}{2\beta_\lambda} I_S \left(\frac{m_\sigma}{\beta_\lambda} + \frac{\beta_{\lambda\lambda'}}{12m_Q} \right), \\
G_2 &= \frac{m_\sigma}{\beta_\lambda} I_S \left[-\frac{m_\sigma}{\beta_\lambda} + \frac{\beta_{\lambda\lambda'}}{24} \left(\frac{5}{m_q} + \frac{4}{m_Q} \right) \right], \\
G_3 &= \frac{m_\sigma}{2\beta_\lambda} I_S \left(\frac{3m_\sigma}{\beta_\lambda} + \frac{\beta_{\lambda\lambda'}}{6m_Q} \right), \\
G_4 &= 0,
\end{aligned}$$

where

$$I_S = 4\sqrt{\frac{3}{5}} \frac{\left(\frac{\beta_\lambda \beta_{\lambda'}}{\beta_{\lambda\lambda'}^2} \right)^{7/2}}{\left[1 + \frac{3}{2} \frac{m_\sigma^2}{m_{\Omega_q}^2} \frac{p^2}{\beta_{\lambda\lambda'}^2} \right]^4}.$$

C.3.5 $3/2^-$, $j = 1$

Harmonic Oscillator Form Factors

$$\begin{aligned}
F_1 &= -I_H \frac{m_\sigma}{\alpha_\lambda} \left[1 + \frac{m_\sigma}{\alpha_{\lambda\lambda'}^2} \left(\frac{\alpha_{\lambda'}^2}{m_q} + \frac{\alpha_\lambda^2}{m_Q} \right) \right], \\
F_2 &= I_H \left[-\frac{m_\sigma^2 \alpha_{\lambda'}^2}{m_q \alpha_\lambda \alpha_{\lambda\lambda'}^2} + \frac{\alpha_\lambda}{18} \left(\frac{1}{m_q} + \frac{2}{m_Q} \right) \right], \\
F_3 &= I_H \left\{ \frac{2m_\sigma}{\alpha_\lambda} \left[1 + \frac{m_\sigma}{2\alpha_{\lambda\lambda'}^2} \left(\frac{\alpha_\lambda^2}{m_Q} + \frac{2\alpha_{\lambda'}^2}{m_q} \right) \right] + \frac{\alpha_\lambda}{18} \left(\frac{1}{m_q} - \frac{4}{m_Q} \right) \right\}, \\
F_4 &= \frac{\alpha_\lambda}{9} I_H \left(\frac{4}{m_Q} - \frac{1}{m_q} \right), \\
G_1 &= I_H \left(\frac{m_\sigma}{\alpha_\lambda} - \frac{\alpha_\lambda}{9m_Q} \right), \\
G_2 &= 2I_H \left(\frac{\alpha_\lambda}{9m_Q} + \frac{m_\sigma^2 \alpha_{\lambda'}^2}{2m_q \alpha_\lambda \alpha_{\lambda\lambda'}^2} \right), \\
G_3 &= I_H \left[-\frac{2m_\sigma}{\alpha_\lambda} \left(1 + \frac{m_\sigma \alpha_\lambda^2}{2m_Q \alpha_{\lambda\lambda'}^2} \right) + \frac{\alpha_\lambda}{3m_Q} \right], \\
G_4 &= 2I_H \left(\frac{2m_\sigma}{\alpha_\lambda} - \frac{\alpha_\lambda}{3m_Q} \right),
\end{aligned}$$

where

$$I_H = -\frac{1}{\sqrt{3}} \left(\frac{\alpha_\lambda \alpha_{\lambda'}}{\alpha_{\lambda\lambda'}^2} \right)^{5/2} \exp \left(-\frac{3m_\sigma^2}{2m_{\Omega_q}^2} \frac{p^2}{\alpha_{\lambda\lambda'}^2} \right). \quad (\text{C.2})$$

Sturmian Form Factors

$$\begin{aligned}
F_1 &= -I_S \frac{m_\sigma}{\beta_\lambda} \left[1 + \frac{m_\sigma}{\beta_{\lambda\lambda'}} \left(\frac{\beta_{\lambda'}}{m_q} + \frac{\beta_\lambda}{m_Q} \right) \right], \\
F_2 &= I_S \left[-\frac{m_\sigma^2 \beta_{\lambda'}}{m_q \beta_\lambda \beta_{\lambda\lambda'}} + \frac{\beta_{\lambda\lambda'}}{36} \left(\frac{1}{m_q} + \frac{2}{m_Q} \right) \right], \\
F_3 &= I_S \left\{ \frac{2m_\sigma}{\beta_\lambda} \left[1 + \frac{m_\sigma}{2\beta_{\lambda\lambda'}} \left(\frac{2\beta_{\lambda'}}{m_q} + \frac{\beta_\lambda}{m_Q} \right) \right] - \frac{\beta_{\lambda\lambda'}}{36} \left(\frac{1}{m_q} + \frac{4}{m_Q} \right) \right\}, \\
F_4 &= I_S \frac{\beta_{\lambda\lambda'}}{18} \left(\frac{4}{m_Q} - \frac{1}{m_q} \right), \\
G_1 &= I_S \left(\frac{m_\sigma}{\beta_\lambda} - \frac{\beta_{\lambda\lambda'}}{18m_Q} \right), \\
G_2 &= I_S \left(\frac{m_\sigma^2 \beta_{\lambda'}}{m_q \beta_\lambda \beta_{\lambda\lambda'}} + \frac{\beta_{\lambda\lambda'}}{9m_Q} \right), \\
G_3 &= I_S \left[\frac{-2m_\sigma}{\beta_\lambda} + \frac{1}{m_Q} \left(\frac{\beta_{\lambda\lambda'}}{6} - \frac{m_\sigma^2}{\beta_{\lambda\lambda'}} \right) \right], \\
G_4 &= I_S \left(\frac{4m_\sigma}{\beta_\lambda} - \frac{\beta_{\lambda\lambda'}}{3m_Q} \right),
\end{aligned}$$

where

$$I_S = \frac{\left(\frac{\beta_\lambda \beta_{\lambda'}}{\beta_{\lambda\lambda'}^2} \right)^{5/2}}{\left[1 + \frac{3}{2} \frac{m_\sigma^2}{m_{\Omega_q}^2} \frac{p^2}{\beta_{\lambda\lambda'}^2} \right]^3}. \tag{C.3}$$

C.3.6 $3/2^-$, $j = 2$

Harmonic Oscillator Form Factors

$$\begin{aligned}
F_1 &= I_H \frac{m_\sigma}{\alpha_\lambda} \left[1 + \frac{m_\sigma}{\alpha_{\lambda\lambda'}} \left(\frac{\alpha_{\lambda'}^2}{m_q} + \frac{\alpha_\lambda^2}{m_Q} \right) \right], \\
F_2 &= I_H \left\{ \frac{2m_\sigma}{\alpha_\lambda} \left[-2 + \frac{m_\sigma}{2\alpha_{\lambda\lambda'}} \left(\frac{\alpha_{\lambda'}^2}{m_q} - \frac{4\alpha_\lambda^2}{m_Q} \right) \right] + \frac{\alpha_\lambda}{18} \left(\frac{13}{m_q} + \frac{2}{m_Q} \right) \right\}, \\
F_3 &= I_H \left\{ \frac{2m_\sigma}{\alpha_\lambda} \left[-1 + \frac{m_\sigma}{2\alpha_{\lambda\lambda'}} \left(\frac{3\alpha_\lambda^2}{m_Q} - \frac{2\alpha_{\lambda'}^2}{m_q} \right) \right] + \frac{\alpha_\lambda}{18} \left(\frac{13}{m_q} + \frac{2}{m_Q} \right) \right\}, \\
F_4 &= -\frac{\alpha_\lambda}{9} I_H \left(\frac{13}{m_q} + \frac{2}{m_Q} \right), \\
G_1 &= I_H \left(\frac{3m_\sigma}{\alpha_\lambda} + \frac{2\alpha_\lambda}{9m_Q} \right), \\
G_2 &= I_H \left(\frac{2\alpha_\lambda}{9m_Q} - \frac{m_\sigma^2 \alpha_{\lambda'}^2}{m_q \alpha_{\lambda\lambda'}^2 \alpha_\lambda} \right), \\
G_3 &= \frac{2m_\sigma}{\alpha_\lambda} I_H \left(-1 + \frac{m_\sigma \alpha_\lambda^2}{2m_Q \alpha_{\lambda\lambda'}^2} \right), \\
G_4 &= \frac{4m_\sigma}{\alpha_\lambda} I_H,
\end{aligned}$$

where

$$I_H = -\frac{1}{\sqrt{10}} \left(\frac{\alpha_\lambda \alpha_{\lambda'}}{\alpha_{\lambda\lambda'}^2} \right)^{5/2} \exp \left(-\frac{3m_\sigma^2}{2m_{\Omega_q}^2} \frac{p^2}{\alpha_{\lambda\lambda'}^2} \right),$$

Sturmian Form Factors

$$\begin{aligned}
F_1 &= I_S \frac{m_\sigma}{\beta_\lambda} \left[1 + \frac{m_\sigma}{\beta_{\lambda\lambda'}} \left(\frac{\beta_{\lambda'}}{m_q} + \frac{\beta_\lambda}{m_Q} \right) \right], \\
F_2 &= I_S \left\{ \frac{2m_\sigma}{\beta_\lambda} \left[-2 + \frac{m_\sigma}{2\beta_{\lambda\lambda'}} \left(\frac{\beta_{\lambda'}}{m_q} - \frac{4\beta_\lambda}{m_Q} \right) \right] + \frac{\beta_{\lambda\lambda'}}{36} \left(\frac{13}{m_q} + \frac{2}{m_Q} \right) \right\}, \\
F_3 &= I_S \left\{ \frac{2m_\sigma}{\beta_\lambda} \left[-1 + \frac{m_\sigma}{2\beta_{\lambda\lambda'}} \left(\frac{3\beta_\lambda}{m_Q} - \frac{2\beta_{\lambda'}}{m_q} \right) \right] + \frac{\beta_{\lambda\lambda'}}{36} \left(\frac{13}{m_q} + \frac{2}{m_Q} \right) \right\}, \\
F_4 &= -I_S \frac{\beta_{\lambda\lambda'}}{18} \left(\frac{13}{m_q} + \frac{2}{m_Q} \right), \\
G_1 &= I_S \left(\frac{3m_\sigma}{\beta_\lambda} + \frac{\beta_{\lambda\lambda'}}{9m_Q} \right), \\
G_2 &= I_S \left(\frac{\beta_{\lambda\lambda'}}{9m_Q} - \frac{m_\sigma^2 \beta_{\lambda'}}{m_q \beta_\lambda \beta_{\lambda\lambda'}} \right), \\
G_3 &= -\frac{2m_\sigma}{\beta_\lambda} \left(1 - \frac{m_\sigma \beta_\lambda}{2m_Q \beta_{\lambda\lambda'}} \right), \\
G_4 &= \frac{4m_\sigma}{\beta_\lambda} I_S,
\end{aligned}$$

where

$$I_S = \sqrt{\frac{1}{5}} \frac{\left(\frac{\beta_\lambda \beta_{\lambda'}}{\beta_{\lambda\lambda'}^2} \right)^{5/2}}{\left[1 + \frac{3}{2} \frac{m_\sigma^2}{m_{\tilde{\nu}_q}^2} \frac{p^2}{\beta_{\lambda\lambda'}^2} \right]^3}.$$

C.3.7 $5/2^+$, $j = 2$

Harmonic Oscillator Form Factors

$$\begin{aligned}
 F_1 &= \frac{m_\sigma^2}{\alpha_\lambda^2} I_H \left[1 + \frac{m_\sigma}{\alpha_{\lambda\lambda'}^2} \left(\frac{\alpha_{\lambda'}^2}{m_q} + \frac{\alpha_\lambda^2}{m_Q} \right) \right], \\
 F_2 &= m_\sigma I_H \left[\frac{1}{6} \left(\frac{1}{m_q} - \frac{2}{m_Q} \right) + \frac{m_\sigma^2 \alpha_{\lambda'}^2}{m_q \alpha_\lambda^2 \alpha_{\lambda\lambda'}^2} \right], \\
 F_3 &= I_H \left\{ -\frac{2m_\sigma^2}{\alpha_\lambda^2} I_H \left[1 + \frac{m_\sigma}{2\alpha_{\lambda\lambda'}^2} \left(\frac{2\alpha_{\lambda'}^2}{m_q} + \frac{\alpha_\lambda^2}{m_Q} \right) \right] + \frac{m_\sigma}{6} \left(\frac{1}{m_q} + \frac{1}{m_Q} \right) \right\}, \\
 F_4 &= -\frac{m_\sigma}{3} I_H \left(\frac{1}{m_q} + \frac{1}{m_Q} \right), \\
 G_1 &= \frac{m_\sigma}{\alpha_\lambda} I_H \left(-\frac{m_\sigma}{\alpha_\lambda} + \frac{\alpha_\lambda}{2m_Q} \right), \\
 G_2 &= -\frac{m_\sigma^3 \alpha_{\lambda'}^2}{m_q \alpha_\lambda^2 \alpha_{\lambda\lambda'}^2} I_H, \\
 G_3 &= \frac{m_\sigma}{\alpha_\lambda} I_H \left[\frac{2m_\sigma}{\alpha_\lambda} \left(1 + \frac{m_\sigma \alpha_\lambda^2}{2m_Q \alpha_{\lambda\lambda'}^2} \right) - \frac{\alpha_\lambda}{2m_Q} \right], \\
 G_4 &= m_\sigma I_H \left(-\frac{4m_\sigma}{\alpha_\lambda^2} + \frac{1}{m_Q} \right),
 \end{aligned}$$

where

$$I_H = \left(\frac{\alpha_\lambda \alpha_{\lambda'}}{\alpha_{\lambda\lambda'}^2} \right)^{7/2} \exp \left(-\frac{3m_\sigma^2}{2m_{\Omega_q}^2} \frac{p^2}{\alpha_{\lambda\lambda'}^2} \right),$$

Sturmian Form Factors

$$\begin{aligned}
F_1 &= \frac{m_\sigma^2}{\beta_\lambda^2} I_S \left[1 + \frac{m_\sigma}{\beta_{\lambda\lambda'}} \left(\frac{\beta_{\lambda'}}{m_q} + \frac{\beta_\lambda}{m_Q} \right) \right], \\
F_2 &= \frac{m_\sigma}{\beta_\lambda} I_S \left[\frac{\beta_{\lambda\lambda'} m_\sigma}{18\beta_\lambda} \left(\frac{1}{m_q} - \frac{2}{m_Q} \right) + \frac{m_\sigma^2 \beta_{\lambda'}}{m_q \beta_\lambda \beta_{\lambda\lambda'}} \right], \\
F_3 &= \frac{m_\sigma}{\beta_\lambda} I_S \left\{ -\frac{2m_\sigma}{\beta_\lambda} I_S \left[1 + \frac{m_\sigma}{2\beta_{\lambda\lambda'}} \left(\frac{2\beta_{\lambda'}}{m_q} + \frac{\beta_\lambda}{m_Q} \right) \right] + \frac{\beta_{\lambda\lambda'}}{18} \left(\frac{1}{m_q} + \frac{1}{m_Q} \right) \right\}, \\
F_4 &= -\frac{m_\sigma \beta_{\lambda\lambda'}}{9\beta_\lambda} I_S \left(\frac{1}{m_q} + \frac{1}{m_Q} \right), \\
G_1 &= -\frac{m_\sigma}{\beta_\lambda} I_S \left(\frac{m_\sigma}{\beta_\lambda} - \frac{\beta_{\lambda\lambda'}}{6m_Q} \right), \\
G_2 &= -\frac{m_\sigma^3 \beta_{\lambda'}}{m_q \beta_\lambda^2 \beta_{\lambda\lambda'}} I_S, \\
G_3 &= \frac{m_\sigma}{\beta_\lambda} I_S \left[\frac{2m_\sigma}{\beta_\lambda} \left(1 + \frac{m_\sigma \beta_\lambda}{2m_Q \beta_{\lambda'}} \right) - \frac{\beta_{\lambda\lambda'}}{6m_Q} \right], \\
G_4 &= \frac{m_\sigma}{\beta_\lambda} I_S \left(-\frac{4m_\sigma}{\beta_\lambda} + \frac{\beta_{\lambda\lambda'}}{3m_Q} \right),
\end{aligned}$$

where

$$I_S = \sqrt{6} \frac{\left(\frac{\beta_\lambda \beta_{\lambda'}}{\beta_{\lambda\lambda'}^2} \right)^{7/2}}{\left[1 + \frac{3}{2} \frac{m_\sigma^2}{m_{\Omega_q}^2} \frac{p^2}{\beta_{\lambda\lambda'}^2} \right]^4}.$$

C.3.8 $5/2^+$, $j = 3$

Harmonic Oscillator Form Factors

$$\begin{aligned}
F_1 &= -\frac{m_\sigma^2}{\alpha_\lambda^2} I_H \left[1 + \frac{m_\sigma}{\alpha_{\lambda\lambda'}^2} \left(\frac{\alpha_{\lambda'}^2}{m_q} + \frac{\alpha_\lambda^2}{m_Q} \right) \right], \\
F_2 &= I_H \left\{ \frac{2m_\sigma^2}{\alpha_\lambda^2} \left[3 + \frac{m_\sigma}{2\alpha_{\lambda\lambda'}^2} \left(\frac{6\alpha_\lambda^2}{m_Q} - \frac{\alpha_{\lambda'}^2}{m_q} \right) \right] - \frac{m_\sigma}{3} \left(\frac{5}{m_q} + \frac{2}{m_Q} \right) \right\}, \\
F_3 &= I_H \left\{ \frac{2m_\sigma}{\alpha_\lambda} \left[1 + \frac{m_\sigma}{2\alpha_{\lambda\lambda'}^2} \left(\frac{2\alpha_{\lambda'}^2}{m_q} - \frac{5\alpha_\lambda^2}{m_Q} \right) \right] - \frac{m_\sigma}{3} \left(\frac{5}{m_q} + \frac{2}{m_Q} \right) \right\}, \\
F_4 &= \frac{2m_\sigma}{3} I_H \left(\frac{2}{2m_Q} + \frac{5}{m_q} \right), \\
G_1 &= -\frac{5m_\sigma^2}{\alpha_\lambda^2} I_H, \\
G_2 &= \frac{m_\sigma^3 \alpha_{\lambda'}^2}{m_q \alpha_\lambda^2 \alpha_{\lambda\lambda'}^2} I_H, \\
G_3 &= \frac{2m_\sigma^2}{\alpha_\lambda^2} I_H \left(2 - \frac{m_\sigma \alpha_\lambda^2}{2m_Q \alpha_{\lambda\lambda'}^2} \right), \\
G_4 &= -\frac{8m_\sigma^2}{\alpha_\lambda^2} I_H,
\end{aligned}$$

where

$$I_H = \frac{1}{\sqrt{14}} \left(\frac{\alpha_\lambda \alpha_{\lambda'}}{\alpha_{\lambda\lambda'}^2} \right)^{7/2} \exp \left(-\frac{3m_\sigma^2}{2m_{\Omega_q}^2} \frac{p^2}{\alpha_{\lambda\lambda'}^2} \right),$$

Sturmian Form Factors

$$\begin{aligned}
F_1 &= -\frac{m_\sigma^2}{\beta_\lambda^2} I_S \left[1 + \frac{m_\sigma}{\beta_{\lambda\lambda'}} \left(\frac{\beta_{\lambda'}}{m_q} + \frac{\beta_\lambda}{m_Q} \right) \right], \\
F_2 &= \frac{m_\sigma}{\beta_\lambda} I_S \left\{ \frac{2m_\sigma}{\beta_\lambda} I_S \left[3 + \frac{m_\sigma}{2\beta_{\lambda\lambda'}} \left(\frac{6\beta_\lambda}{m_Q} - \frac{\beta_{\lambda'}}{m_q} \right) \right] - \frac{\beta_{\lambda\lambda'}}{9} \left(\frac{5}{m_q} + \frac{2}{m_Q} \right) \right\}, \\
F_3 &= \frac{m_\sigma}{\beta_\lambda} I_S \left\{ \frac{2m_\sigma}{\beta_\lambda} I_S \left[1 + \frac{m_\sigma}{2\beta_{\lambda\lambda'}} \left(\frac{2\beta_{\lambda'}}{m_q} - \frac{5\beta_\lambda}{m_Q} \right) \right] - \frac{\beta_{\lambda\lambda'}}{9} \left(\frac{5}{m_q} + \frac{2}{m_Q} \right) \right\}, \\
F_4 &= \frac{2m_\sigma\beta_{\lambda\lambda'}}{9\beta_\lambda} I_S \left(\frac{5}{m_q} + \frac{2}{m_Q} \right), \\
G_1 &= -\frac{5m_\sigma^2}{\beta_\lambda^2} I_S, \\
G_2 &= \frac{m_\sigma^3\beta_{\lambda'}}{m_q\beta_\lambda^2\beta_{\lambda\lambda'}} I_S, \\
G_3 &= \frac{m_\sigma^2}{\beta_\lambda} I_S \left(\frac{4}{\beta_\lambda} - \frac{m_\sigma}{m_Q\beta_{\lambda\lambda'}} \right), \\
G_4 &= -\frac{8m_\sigma^2}{\beta_\lambda^2} I_S,
\end{aligned}$$

where

$$I_S = \sqrt{\frac{3}{7}} \frac{\left(\frac{\beta_\lambda\beta_{\lambda'}}{\beta_{\lambda\lambda'}^2} \right)^{7/2}}{\left[1 + \frac{3}{2} \frac{m_\sigma^2}{m_{\Omega_q}^2} \frac{p^2}{\beta_{\lambda\lambda'}^2} \right]^4}.$$

APPENDIX D

Hadronic Tensor

The hadronic tensor for these semileptonic decays takes the form

$$\begin{aligned}
 H_{\mu\nu} &= -\alpha G_{\mu\nu} + \beta_{++}(p+p')_{\mu}(p+p')_{\nu} + \beta_{+-}(p+p')_{\mu}(p-p')_{\nu} \\
 &+ \beta_{-+}(p-p')_{\mu}(p+p')_{\nu} + \beta_{--}(p-p')_{\mu}(p-p')_{\nu} \\
 &+ i\gamma\epsilon_{\mu\nu\rho\sigma}(p+p')^{\rho}(p-p')^{\sigma}.
 \end{aligned}$$

The forms of the terms α , $\beta_{\pm\pm}$ and γ for the different final states we consider are given in the subsections below.

D.0.9 $1/2^+$

$$\alpha(1/2^+) = 2 \{ [(m_{B_Q} - m_{B_q})^2 - q^2] F_1^2 + [(m_{B_Q} + m_{B_q})^2 - q^2] G_1^2 \}, \quad (\text{D.1})$$

$$\beta_{++}(1/2^+) = \sum_{i,j=1}^3 (A_{ij} F_i F_j + A'_{ij} G_i G_j), \quad (\text{D.2})$$

with

$$\begin{aligned}
A_{11} &= A'_{11} = 2, \\
A_{22} &= \frac{1}{2m_{B_Q}^2} [(m_{B_Q} + m_{B_q})^2 - q^2], \\
A_{33} &= \frac{1}{2m_{B_q}^2} [(m_{B_Q} + m_{B_q})^2 - q^2], \\
A_{12} &= \frac{1}{m_{B_Q}} (m_{B_Q} + m_{B_q}), \\
A_{23} &= \frac{1}{m_{B_Q} m_{B_q}} [(m_{B_Q} + m_{B_q})^2 - q^2], \\
A_{31} &= \frac{2}{m_{B_q}} (m_{B_Q} + m_{B_q}), \\
A'_{22} &= \frac{1}{2m_{B_Q}^2} [(m_{B_Q} - m_{B_q})^2 - q^2], \\
A'_{33} &= \frac{1}{2m_{B_q}^2} [(m_{B_Q} - m_{B_q})^2 - q^2], \\
A'_{12} &= \frac{1}{m_{B_Q}} (m_{B_Q} - m_{B_q}), \\
A'_{23} &= \frac{1}{m_{B_Q} m_{B_q}} [(m_{B_Q} - m_{B_q})^2 - q^2], \\
A'_{31} &= \frac{2}{m_{B_q}} (m_{B_Q} - m_{B_q}),
\end{aligned}$$

$$\gamma(1/2^+) = 4F_1 G_1. \quad (\text{D.3})$$

D.0.10 $1/2^-$

$$\alpha(1/2^-) = 2\{[(m_{B_Q} + m_{B_q})^2 - q^2]F_1^2 + [(m_{B_Q} - m_{B_q})^2 - q^2]G_1^2\}, \quad (\text{D.4})$$

$$\beta_{++}(1/2^-) = \sum_{i,j=1}^3 (A_{ij}F_iF_j + A'_{ij}G_iG_j), \quad (\text{D.5})$$

with

$$\begin{aligned} A_{11} &= A'_{11} = 2, \\ A_{22} &= \frac{1}{2m_{B_Q}^2} [(m_{B_Q} - m_{B_q})^2 - q^2], \\ A_{33} &= \frac{1}{2m_{B_q}^2} [(m_{B_Q} - m_{B_q})^2 - q^2], \\ A_{12} &= \frac{1}{m_{B_Q}} (m_{B_Q} - m_{B_q}), \\ A_{23} &= \frac{1}{m_{B_Q}m_{B_q}} [(m_{B_Q}m_{B_q})^2 - q^2], \\ A_{31} &= \frac{2}{m_{B_q}} (m_{B_Q} - m_{B_q}), \\ A'_{22} &= \frac{1}{2m_{B_Q}^2} [(m_{B_Q} + m_{B_q})^2 - q^2], \\ A'_{33} &= \frac{1}{2m_{B_q}^2} [(m_{B_Q} + m_{B_q})^2 - q^2], \\ A'_{12} &= \frac{1}{m_{B_Q}} (m_{B_Q} + m_{B_q}), \\ A'_{23} &= \frac{1}{m_{B_Q}m_{B_q}} [(m_{B_Q} + m_{B_q})^2 - q^2], \\ A'_{31} &= \frac{2}{m_{B_q}} (m_{B_Q} + m_{B_q}), \end{aligned}$$

$$\gamma(1/2^-) = 4F_1G_1. \quad (\text{D.6})$$

D.0.11 $3/2^-$

$$\alpha(3/2^-) = \sum_{i,j=1}^4 \frac{1}{Y'} (B_{ij} F_i F_j + B'_{ij} G_i G_j), \quad (\text{D.7})$$

where $Y' = 3m_{B_Q}^2 m_{B_q}^2$, and the non-vanishing coefficients are

$$\begin{aligned} B_{11} &= X[(m_{B_Q} + m_{B_q})^2 - q^2], \\ B_{44} &= 4m_{B_Q}^2 m_{B_q}^2 [(m_{B_Q} + m_{B_q})^2 - q^2], \\ B_{14} &= B'_{14} = m_{B_Q} m_{B_q} [m_{B_Q}^4 - 2(m_{B_q}^2 + q^2)m_{B_Q}^2 + (m_{B_q}^2 - q^2)^2], \\ B'_{11} &= X[(m_{B_Q} - m_{B_q})^2 - q^2], \\ B'_{44} &= 4m_{B_Q}^2 m_{B_q}^2 [(m_{B_Q} - m_{B_q})^2 - q^2], \end{aligned}$$

$$\beta_{++}(3/2^-) = \sum_{i,j=1}^4 \frac{1}{Y} (A_{ij} F_i F_j + A'_{ij} G_i G_j), \quad (\text{D.8})$$

where $Y = 12m_{B_Q}^4 m_{B_q}^4$, $X = (m_{B_Q}^2 + m_{B_q}^2 - q^2)^2 - 4m_{B_Q}^2 m_{B_q}^2$, and the A_{ij} are

$$\begin{aligned} A_{11} &= A'_{11} = 4Xm_{B_Q}^2 m_{B_q}^2, \\ A_{22} &= Xm_{B_q}^2 [(m_{B_Q} + m_{B_q})^2 - q^2], \\ A_{33} &= Xm_{B_Q}^2 [(m_{B_Q} + m_{B_q})^2 - q^2], \\ A_{44} &= 4m_{B_Q}^4 m_{B_q}^2 [(m_{B_Q} + m_{B_q})^2 - q^2], \\ A_{12} &= 4Xm_{B_Q} m_{B_q}^2 (m_{B_Q} + m_{B_q}), \\ A_{23} &= 2Xm_{B_Q} m_{B_q} [(m_{B_Q} + m_{B_q})^2 - q^2], \\ A_{31} &= 4Xm_{B_Q}^2 m_{B_q} (m_{B_Q} + m_{B_q}), \\ A_{14} &= -8m_{B_Q}^3 m_{B_q}^2 [m_{B_Q} q^2 - (m_{B_Q} - m_{B_q})(m_{B_Q} + m_{B_q})^2], \\ A_{24} &= 4m_{B_Q}^2 m_{B_q}^2 [(m_{B_Q} + m_{B_q})^2 - q^2] [m_{B_Q}^2 - m_{B_q}^2 - q^2], \\ A_{34} &= 4m_{B_Q}^3 m_{B_q} [(m_{B_Q} + m_{B_q})^2 - q^2] [m_{B_Q}^2 - m_{B_q}^2 - q^2], \end{aligned}$$

$$\begin{aligned}
A'_{22} &= X m_{B_q}^2 [(m_{B_Q} - m_{B_q})^2 - q^2], \\
A'_{33} &= X m_{B_Q}^2 [(m_{B_Q} - m_{B_q})^2 - q^2], \\
A'_{44} &= 4 m_{B_Q}^4 m_{B_q}^2 [(m_{B_Q} - m_{B_q})^2 - q^2], \\
A'_{12} &= 4 X m_{B_Q} m_{B_q}^2 (m_{B_q} - m_{B_Q}), \\
A'_{23} &= 2 X m_{B_Q} m_{B_q} [(m_{B_Q} - m_{B_q})^2 - q^2], \\
A'_{31} &= 4 X m_{B_Q}^2 m_{B_q} (m_{B_q} - m_{B_Q}), \\
A'_{14} &= 8 m_{B_Q}^3 m_{B_q}^2 [m_{B_Q} q^2 - (m_{B_Q} + m_{B_q})(m_{B_Q} - m_{B_q})^2], \\
A'_{24} &= 4 m_{B_Q}^2 m_{B_q}^2 [(m_{B_Q} - m_{B_q})^2 - q^2] [m_{B_Q}^2 - m_{B_q}^2 - q^2], \\
A'_{34} &= 4 m_{B_Q}^3 m_{B_q} [(m_{B_Q} - m_{B_q})^2 - q^2] [m_{B_Q}^2 - m_{B_q}^2 - q^2],
\end{aligned}$$

$$\begin{aligned}
\gamma(3/2^-) &= \frac{2}{3 m_{B_Q}^2 m_{B_q}^2} \{ [(m_{B_Q} - m_{B_q})^2 - q^2] (F_1 G_4 m_{B_Q} m_{B_q} + F_1 G_1 [(m_{B_Q} + m_{B_q})^2 - q^2]) \\
&+ F_4 G_4 m_{B_Q}^2 m_{B_q}^2 + F_4 G_1 m_{B_Q} m_{B_q} [(m_{B_Q} + m_{B_q})^2 - q^2] \}. \tag{D.9}
\end{aligned}$$

D.0.12 $3/2^+$

$$\alpha(3/2^+) = \sum_{i,j=1}^4 \frac{1}{Y'} (B_{ij} F_i F_j + B'_{ij} G_i G_j), \tag{D.10}$$

where the non-vanishing coefficients are

$$\begin{aligned}
B_{11} &= X [(m_{B_Q} - m_{B_q})^2 - q^2], \\
B_{44} &= 4 m_{B_Q}^2 m_{B_q}^2 [(m_{B_Q} - m_{B_q})^2 - q^2], \\
B_{14} &= B'_{14} = m_{B_Q} m_{B_q} [m_{B_Q}^4 - 2(m_{B_q}^2 + q^2) m_{B_Q}^2 + (m_{B_q}^2 - q^2)^2], \\
B'_{11} &= X [(m_{B_Q} + m_{B_q})^2 - q^2], \\
B'_{44} &= 4 m_{B_Q}^2 m_{B_q}^2 [(m_{B_Q} + m_{B_q})^2 - q^2],
\end{aligned}$$

$$\beta_{++}(3/2^+) = \sum_{i,j=1}^4 \frac{1}{Y} (A_{ij} F_i F_j + A'_{ij} G_i G_j), \quad (\text{D.11})$$

where $Y = 12m_{B_Q}^4 m_{B_q}^4$, $X = (m_{B_Q}^2 + m_{B_q}^2 - q^2)^2 - 4m_{B_Q}^2 m_{B_q}^2$, and

$$\begin{aligned} A_{11} &= A'_{11} = 4X m_{B_Q}^2 m_{B_q}^2, \\ A_{22} &= X m_{B_q}^2 [(m_{B_Q} - m_{B_q})^2 - q^2], \\ A_{33} &= X m_{B_Q}^2 [(m_{B_Q} - m_{B_q})^2 - q^2], \\ A_{44} &= 4m_{B_Q}^4 m_{B_q}^2 [(m_{B_Q} - m_{B_q})^2 - q^2], \\ A_{12} &= 4X m_{B_Q} m_{B_q}^2 (m_{B_q} - m_{B_Q}), \\ A_{23} &= 2X m_{B_Q} m_{B_q} [(m_{B_Q} - m_{B_q})^2 - q^2], \\ A_{31} &= 4X m_{B_Q}^2 m_{B_q} (m_{B_q} - m_{B_Q}), \\ A_{14} &= 8m_{B_Q}^3 m_{B_q}^2 [m_{B_Q} q^2 - (m_{B_Q} + m_{B_q})(m_{B_Q} - m_{B_q})^2], \\ A_{24} &= 4m_{B_Q}^2 m_{B_q}^2 [(m_{B_Q} - m_{B_q})^2 - q^2] [m_{B_Q}^2 - m_{B_q}^2 - q^2], \\ A_{34} &= 4m_{B_Q}^3 m_{B_q} [(m_{B_Q} - m_{B_q})^2 - q^2] [m_{B_Q}^2 - m_{B_q}^2 - q^2], \\ A'_{22} &= X m_{B_q}^2 [(m_{B_Q} + m_{B_q})^2 - q^2], \\ A'_{33} &= X m_{B_Q}^2 [(m_{B_Q} + m_{B_q})^2 - q^2], \\ A'_{44} &= 4m_{B_Q}^4 m_{B_q}^2 [(m_{B_Q} + m_{B_q})^2 - q^2], \\ A'_{12} &= 4X m_{B_Q} m_{B_q}^2 (m_{B_q} + m_{B_Q}), \\ A'_{23} &= 2X m_{B_Q} m_{B_q} [(m_{B_Q} + m_{B_q})^2 - q^2], \\ A'_{31} &= 4X m_{B_Q}^2 m_{B_q} (m_{B_q} + m_{B_Q}), \\ A'_{14} &= -8m_{B_Q}^3 m_{B_q}^2 [m_{B_Q} q^2 - (m_{B_Q} - m_{B_q})(m_{B_Q} + m_{B_q})^2], \\ A'_{24} &= 4m_{B_Q}^2 m_{B_q}^2 [(m_{B_Q} + m_{B_q})^2 - q^2] [m_{B_Q}^2 - m_{B_q}^2 - q^2], \\ A'_{34} &= 4m_{B_Q}^3 m_{B_q} [(m_{B_Q} + m_{B_q})^2 - q^2] [m_{B_Q}^2 - m_{B_q}^2 - q^2], \end{aligned}$$

$$\begin{aligned} \gamma(3/2^+) &= \frac{2}{3m_{B_Q}^2 m_{B_q}^2} \{ [(m_{B_Q} + m_{B_q})^2 - q^2] (F_1 G_4 m_{B_Q} m_{B_q} + F_1 G_1 [(m_{B_Q} - m_{B_q})^2 - q^2]) \\ &+ F_4 G_4 m_{B_Q}^2 m_{B_q}^2 + F_4 G_1 m_{B_Q} m_{B_q} [(m_{B_Q} - m_{B_q})^2 - q^2] \}. \quad (\text{D.12}) \end{aligned}$$

D.0.13 $5/2^+$

$$\alpha(5/2^+) = \sum_{i,j=1}^4 \frac{1}{Y_2} X(B_{ij}F_iF_j + B'_{ij}G_iG_j), \quad (\text{D.13})$$

where the non-vanishing coefficients are

$$\begin{aligned} B_{11} &= X[(m_{B_Q} - m_{B_q})^2 - q^2], \\ B_{44} &= 3m_{B_Q}^2 m_{B_q}^2 [(m_{B_Q} + m_{B_q})^2 - q^2], \\ B_{14} &= B'_{14} = 2Xm_{B_Q}m_{B_q}, \\ B'_{11} &= X[(m_{B_Q} + m_{B_q})^2 - q^2], \\ B'_{44} &= 3m_{B_Q}^2 m_{B_q}^2 [(m_{B_Q} - m_{B_q})^2 - q^2], \end{aligned}$$

$$\beta_{++}(5/2^+) = \sum_{i,j=1}^4 \frac{1}{Y_1} (A_{ij}F_iF_j + A'_{ij}G_iG_j), \quad (\text{D.14})$$

where $Y_1 = 80m_{B_Q}^6 m_{B_q}^6$, and

$$\begin{aligned} A_{11} &= A'_{11} = 4X^2m_{B_Q}^2 m_{B_q}^2, \\ A_{22} &= X^2m_{B_q}^2 [(m_{B_Q} + m_{B_q})^2 - q^2], \\ A_{33} &= X^2m_{B_Q}^2 [(m_{B_Q} + m_{B_q})^2 - q^2], \\ A_{44} &= 4m_{B_Q}^4 m_{B_q}^2 [(m_{B_Q} + m_{B_q})^2 - q^2][q^4 - (2m_{B_Q}^2 + m_{B_q}^2)q^2 + (m_{B_Q}^2 - m_{B_q}^2)^2], \\ A_{12} &= 4X^2m_{B_Q}m_{B_q}^2 (m_{B_Q} + m_{B_q}), \\ A_{23} &= 2X^2m_{B_Q}m_{B_q} [(m_{B_Q} + m_{B_q})^2 - q^2], \\ A_{31} &= 4X^2m_{B_Q}^2 m_{B_q} (m_{B_Q} + m_{B_q}), \\ A_{14} &= -8Xm_{B_Q}^3 m_{B_q}^2 [m_{B_Q}q^2 - (m_{B_Q} - m_{B_q})(m_{B_Q} + m_{B_q})^2], \\ A_{24} &= 4Xm_{B_Q}^2 m_{B_q}^2 [(m_{B_Q} + m_{B_q})^2 - q^2][m_{B_Q}^2 - m_{B_q}^2 - q^2], \\ A_{34} &= 4Xm_{B_Q}^3 m_{B_q} [(m_{B_Q} + m_{B_q})^2 - q^2][m_{B_Q}^2 - m_{B_q}^2 - q^2], \end{aligned}$$

$$\begin{aligned}
A'_{22} &= X^2 m_{B_q}^2 [(m_{B_Q} - m_{B_q})^2 - q^2], \\
A'_{33} &= X^2 m_{B_Q}^2 [(m_{B_Q} - m_{B_q})^2 - q^2], \\
A'_{44} &= 4m_{B_Q}^4 m_{B_q}^2 [(m_{B_Q} - m_{B_q})^2 - q^2] [q^4 - (2m_{B_Q}^2 + m_{B_q}^2)q^2 + (m_{B_Q}^2 - m_{B_q}^2)^2], \\
A'_{12} &= 4X^2 m_{B_Q} m_{B_q}^2 (m_{B_q} - m_{B_Q}), \\
A'_{23} &= 2X^2 m_{B_Q} m_{B_q} [(m_{B_Q} - m_{B_q})^2 - q^2], \\
A'_{31} &= 4X^2 m_{B_Q}^2 m_{B_q} (m_{B_q} - m_{B_Q}), \\
A'_{14} &= 8X m_{B_Q}^3 m_{B_q}^2 [m_{B_Q} q^2 - (m_{B_Q} + m_{B_q})(m_{B_Q} - m_{B_q})^2], \\
A'_{24} &= 4X m_{B_Q}^2 m_{B_q}^2 [(m_{B_Q} - m_{B_q})^2 - q^2] [m_{B_Q}^2 - m_{B_q}^2 - q^2], \\
A'_{34} &= 4X m_{B_Q}^3 m_{B_q} [(m_{B_Q} - m_{B_q})^2 - q^2] [m_{B_Q}^2 - m_{B_q}^2 - q^2],
\end{aligned}$$

$$\begin{aligned}
\gamma(5/2^+) &= \frac{m_{B_Q}^4 - 2m_{B_Q}^2(m_{B_q}^2 + q^2) + (m_{B_q}^2 + q^2)^2}{10m_{B_Q}^4 m_{B_q}^4} \left\{ F_4 G_4 m_{B_Q}^2 m_{B_q}^2 \right. \\
&+ F_4 G_1 m_{B_Q} m_{B_q} [(m_{B_Q} - m_{B_q})^2 - q^2] \\
&+ [(m_{B_Q} + m_{B_q})^2 - q^2] \left(F_1 G_4 m_{B_Q} m_{B_q} + F_1 G_1 [(m_{B_Q} - m_{B_q})^2 - q^2] \right) \left. \right\}.
\end{aligned}$$

APPENDIX E

Constructing Higher Spin Representations and Quark Matrix Elements

It is necessary to construct explicit representations for the spin-3/2 and spin- 5/2 baryons that we treat. In the case of the former, the vector-spinor field $u^\alpha(p', s')$ must satisfy

$$p'_\alpha u^\alpha(p', s') = 0, \quad \gamma_\alpha u^\alpha(p', s') = 0, \quad \not{p}' u^\alpha(p', s') = m_{\Lambda_q^{(3/2)}} u^\alpha(p', s'). \quad (\text{E.1})$$

A suitable representation can be constructed by using the usual Dirac spin-1/2 spinors, together with the ‘polarization’ vectors $\epsilon_\mu(p', s_z)$. These vectors satisfy

$$p'_\mu \epsilon^\mu(p', s_z) = 0, \quad \epsilon_\mu^*(p', s_z) \epsilon^\mu(p', s'_z) = -\delta_{s_z, s'_z}. \quad (\text{E.2})$$

Our representation of the spin-3/2 Rarita-Schwinger vector-spinor $u_\mu(p', M)$ is given by the Clebsch-Gordan sum

$$u_\mu(p', M) = \sum_m \epsilon_\mu(p', m) u(p', M - m) \langle 3/2 M | 1m, 1/2, M - m \rangle. \quad (\text{E.3})$$

This satisfies all of the conditions required.

A representation of the spin-5/2 spinor $u^{\alpha\beta}(p', s)$ can be constructed in a similar way, but there are two additional constraints that must be satisfied. The first is that the spinor must be symmetric in its Lorentz indices, and the second is that it must be traceless when the two indices are contracted, i.e.

$$u^\alpha_\alpha(p', s) = 0. \quad (\text{E.4})$$

Such a representation can be built in one of two ways. We can use the previously constructed spin-3/2 spinor, and the vector ϵ , to write

$$u_{\mu\nu}(p', M) = \sum_m \epsilon_\mu(p', m) u_\nu(p', M - m) \langle 5/2 M | 1m, 3/2, M - m \rangle. \quad (\text{E.5})$$

Alternatively, we can first construct a spin-2 tensor $A_{\mu\nu}$ from two of the ϵ vectors as

$$A_{\mu\nu}(p', M) = \sum_m \epsilon_\mu(p', m) \epsilon_\nu(p', M - m) \langle 2M | 1m, 1, M - m \rangle \quad (\text{E.6})$$

The symmetry properties of the Clebsch-Gordan coefficients guarantee that this tensor is symmetric in its indices. The spin-5/2 spinor is then

$$u_{\mu\nu}(p', M) = \sum_m A_{\mu\nu}(p', m) u(p', M - m) \langle 5/2M | 2m, 1/2, M - m \rangle. \quad (\text{E.7})$$

These two representations are equivalent, but the manifest symmetry of the second representation allows us to see the symmetry in $u_{\mu\nu}$ in an obvious way.

The conditions

$$p'_\alpha u^{\alpha\beta}(p', s') = p'_\beta u^{\alpha\beta}(p', s') = 0 \quad (\text{E.8})$$

are clearly satisfied, since each vector ϵ satisfies $p' \cdot \epsilon = 0$ (and the second equality also follows from the symmetry in the indices). It is easy to check that the auxiliary conditions

$$\gamma_\alpha u^{\alpha\beta}(p', s') = \gamma_\beta u^{\alpha\beta}(p', s') = 0 \quad (\text{E.9})$$

are satisfied, as are

$$p' u^{\alpha\beta}(p', s') = m_{\Lambda_q^{(5/2)}} u^{\alpha\beta}(p', s'). \quad (\text{E.10})$$

The traceless condition

$$g_{\alpha\beta} u^{\alpha\beta}(p', s') = 0, \quad (\text{E.11})$$

is less obvious, but follows from the tracelessness of $A_{\mu\nu}$. This, in turn, follows from the symmetry properties of the Clebsch-Gordan sum in $A_{\mu\nu}$, and the properties of the ϵ vectors.

REFERENCES

- [1] J. I. Friedman and H. W. Kendall, *Ann. Rev. Nucl. Part. Sci.* **22** 203(1972), M. Breidenbach *et al.*, *Phys. Rev. Lett.* **23**, 935 (1969), G. Miller *et al.*, *Phys. Rev. D* **5**, 528 (1972).
- [2] S. L. Glashow, *Nucl. Phys.* **22**, 579 (1961), A. Salam, *Elementary Particle Theory*,(1968), S. Weinberg , *Phys. Rev. Lett.* **19**, 1264 (1967).
- [3] P. W. Higgs, *Phys. Lett.* **12**, 132 (1964).
- [4] M. Kobayashi and T. Maskawa, *Prog. Theor. Phys.* **49**, 652 (1973).
- [5] S. Eidelman *et al.*, *Phys. Lett.* **B592**, 1 (2004).
- [6] H. Abramowicz *et al.*, *Z. Phys. C* **15**, 19 (1982).
- [7] S. A. Rabinowitz *et al.*, *Phys. Rev. Lett.* **70**, 134 (1993), A. O bazarko *et al.*, *Z. Phys. C* **65**, 189 (1995).
- [8] P. Abreu *et al.* [DELPHI Collaboration], *Phys. Lett. B* **439**, 209 (1998), R. Barate *et al.* [ALEPH Collaboration], *Phys. Lett. B* **465**, 349 (1999).
- [9] N. Isgur and M. B. Wise, *Phys. Lett.* **B232**, 113 (1989); *Phys. Lett.* **B237**,527 (1990).
- [10] M. E. Luke, *Phys. Lett. B* **252**, 447 (1990).
- [11] S. Eidelman *et al.*, *Phys. Lett.* **B592**, 786 (2004).
- [12] S. Eidelman *et al.*, *Phys. Lett.* **B592**, 793 (2004).
- [13] T. Affolder *et al.*, *Phys. Rev. Lett.* **86**, 3233 (2001).
- [14] M. Gell-Mann, *Phys. Rev.* **125**, 1067 (1962), Y. Ne'eman, *Nucl. Phys.* **26**, 222 (1961).
- [15] CERN Preprints 8182/Th.401, 8419/Th.412(1964) unpublished.
- [16] M. Gell-Mann, *Phys. Lett.* **8**, 214 (1964).
- [17] O. W. Greenberg *Phys. Rev. Lett.* **13**, 1598 (1964).
- [18] M. Y. Han and Y. Nambu, *Phys. Rev.* **139** (1965) B1006.

- [19] S. L. Adler and W. A. Bardeen, Phys. Rev. **182**, 1517(1969) , S. L. Adler, Phys. Rev. **177**, 2426 (1969),
R. Jackiw and K. Johnson, Phys. Rev. **182** (1969) 1459.
- [20] D. J. Gross and F. Wilczek, Phys. Rev. D **8**, 3633 (1973), Phys. Rev. D **9**, 980 (1974).
- [21] H. D. Politzer, Phys. Rev. Lett. **30**, 1346 (1973), Phys. Rev. D **9**, 2174 (1974).
- [22] R. H. Dalitz in High Energy Physics, (Les Houches, 1965) eds. C. DeWitt and M. Jacob (Gordon and Breach, New York, 1966).
O. W. Greenberg, Phys. Rev. Lett. **13**, 598 (1964), D. R. Divgi and O. W. Greenberg, Phys. Rev. **175**, 2024 (1968).
- [23] A. De Rujula, H. Georgi and S. L. Glashow, Phys. Rev. Lett. **35**, 628 (1975).
- [24] N. Isgur and G. Karl, Phys. Rev. D **18**, 4187 (1978).
- [25] N. Isgur and G. Karl, Phys. Lett. **72B**, 109 (1977); **74B** 353(1978); Phys. Rev. **D19**, 2653 (1979).
- [26] See previous references, A. B. Henriques, B. H. Kellett and R. G. Moorhouse, Phys. Lett. B **64**, 85 (1976),
H. J. Schnitzer, Phys. Lett. B **65**, 239 (1976), Phys. Lett. B **69**, 477 (1977), Phys. Rev. D **18**, 3482 (1978).
- [27] N. Isgur and G. Karl, Phys. Rev. D **19**, 2653 (1979).
- [28] See the following article and many other works referred in this paper. S. Capstick and W. Roberts Prog. Part. Nucl. Phys. **45**, S241 (2000)
- [29] S. Capstick and N. Isgur, Phys. Rev. D **34** (86) 2809.
- [30] W. Pauli, <http://www.slac.stanford.edu/spires/find/hep/www?irn=1959247SPIRES>
- [31] F. Reines, C. L. Cowan, F. B. Harrison, A. D. McGuire and H. W. Kruse, Phys. Rev. **117**, 159 (1960)
- [32] S. Eidelman *et al.*, Phys. Lett. **B592**, 980 (2004).
- [33] M. Ademollo and R. Gatto, Phys. Rev. Lett. **13**, 264 (1964).
- [34] M. Wirbel, B. Stech and M. Bauer, Z. Phys. C **29**, 637(1985).
- [35] M. Bauer and M. Wirbel, Z. Phys. C **42**, 671 (1989).
- [36] N. Isgur, D. Scora, B. Grinstein and M. Wise, Phys. Rev. D **39**, 799 (1989).
- [37] N. Isgur and D. Scora, Phys. Rev. D **52**, 2783 (1989).

- [38] M. A. Shifman and M. B. Voloshin, Sov. J. Nucl. Phys. **47**, 511 (1988) [Yad. Fiz. **47**, 801 (1988)].
- [39] M. A. Ivanov and P. Santorelli, hep-ph/9910434.
- [40] W. Roberts, Nucl. Phys. B **389**, 549 (1993).
- [41] A. K. Leibovich and I. W. Stewart, Phys. Rev. D **57**, 5620 (1998).
- [42] J. G. Körner and M. Krämer, Phys. Lett. B **275**, 495 (1992).
- [43] B. Singleton, Phys. Rev. D **43**, 293 (1991).
- [44] C. Albertus, E. Hernandez and J. Nieves, arXiv:hep-ph/0408065.
- [45] K. C. Bowler *et al.* [UKQCD Collaboration], Phys. Rev. D **57**, 6948 (1998).
- [46] S. A. Gottlieb and S. Tamhankar, Nucl. Phys. Proc. Suppl. **119**, 644 (2003)
- [47] R. Pérez-Marcial, R. Huerta, A. Garca, and M. Avila-Aoki, Phys. Rev. **D40**, 2944 (1989); *ibid.* 2955 (1989).
- [48] F. Cardarelli and S. Simula, *Prepared for 3rd International Conference in Quark Confinement and Hadron Spectrum (Confinement III), Newport News, Virginia, 7-12 Jun 1998*;
F. Cardarelli and S. Simula, Phys. Lett. B **421**, 295 (1998);
L. A. Kondratyuk and D. V. Chekin, Phys. Atom. Nucl. **61**, 302 (1998) [Yad. Fiz. **61**, 355 (1998)].
- [49] M. Q. Huang, J. P. Lee, C. Liu and H. S. Song, Phys. Lett. B **502**, 133 (2001);
R. S. Marques de Carvalho and M. Nielsen, *Prepared for 7th Hadron Physics 2000, Caraguatatuba, Sao Paulo, Brazil, 10-15 Apr 2000*;
H. G. Dosch, E. Ferreira, M. Nielsen and R. Rosenfeld, Phys. Lett. B **431**, 173 (1998);
Y. B. Dai, C. S. Huang, M. Q. Huang and C. Liu, Phys. Lett. B **387**, 379 (1996).
- [50] X. H. Guo and T. Muta, Phys. Rev. D **54**, 4629 (1996).
- [51] M. Sadzikowski and K. Zalewski, Z. Phys. C **59**, 677 (1993).
- [52] M. A. Ivanov and V. E. Lyubovitskij, arXiv:hep-ph/9502202;
R. K. Das, A. R. Panda, R. K. Sahoo and M. R. Swain, Pramana **58**, 551 (2002);
D. Chakraverty, T. De, B. Dutta-Roy and K. S. Gupta, Mod. Phys. Lett. A **12**, 195 (1997);
B. Konig, J. G. Korner, M. Kramer and P. Kroll, Phys. Rev. D **56**, 4282 (1997).
- [53] C. K. Chow, Phys. Rev. D **54**, 873 (1996);
C. Liu, Phys. Rev. D **57**, 1991 (1998);
C. K. Chow, Phys. Rev. D **51**, 1224 (1995);
E. Jenkins, A. V. Manohar and M. B. Wise, Nucl. Phys. B **396**, 38 (1993).

- [54] P. Guo, H. W. KB, X. Q. Li and C. D. Lu, arXiv:hep-ph/0501058.
- [55] M. Q. Huang and D. W. Wang, Phys. Rev. D **69**, 094003 (2004).
- [56] A. Datta, arXiv:hep-ph/9504429.
- [57] D. J. Scora, PhD. thesis UMI-315-82807-2.
- [58] M. Sutherland, Z. Phys. C **63**, 111 (1994), Q. P. Xu, Phys. Rev. D **48**, 5429 (1993), C. G. Boyd and D. E. Brahm, Phys. Lett. B **254**, 468 (1991).
- [59] H. Albrecht *et al.* [ARGUS Collaboration], Phys. Lett **B269** 234 (1991).
- [60] G. D. Crawford *et al.* [CLEO Collaboration], Phys. Rev. Lett. **75**, 624 (1995).
- [61] J. Abdallah *et al.* [DELPHI Collaboration], Phys. Lett. B **585**, 63 (2004).
- [62] S. Capstick and W. Roberts, Phys. Rev. D **47**, 1994 (1993); Phys. Rev. D **49**, 4570 (1994); Prog. Part. Nucl. Phys. **45**, S241 (2000); Phys. Rev. D **58**, 074011 (1998).
- [63] S. Capstick and B. D. Keister, Phys. Rev. D **51**, 3598 (1995).
- [64] S. Capstick, Phys. Rev. D **46**, 1965 (1992), S. Capstick, Phys. Rev. D **46**, 2864 (1992).
- [65] N. Isgur and M. Wise, Phys. Lett. **B232** (1989) 113; Phys.Lett. **B237** (1990) 527; B. Grinstein, Nucl. Phys. **B339** (1990) 253; H. Georgi, Phys. Lett. **B240** (1990) 447; A. Falk, H. Georgi, B. Grinstein and M. Wise, Nucl. Phys. **B343** (1990) 1; A. Falk and B. Grinstein, Phys. Lett. **B247** (1990) 406; T. Mannel, W. Roberts and Z. Ryzak, Nucl. Phys. **B368** (1992) 204.
- [66] For a pedagogical description see N. Isgur and M. B. Wise, Phys. Lett. B **237**, 527 (1990) H. Georgi, <http://www.slac.stanford.edu/spires/find/hep/www?r=hutp-91-a039SPIRES> entry B. Grinstein, <http://www.slac.stanford.edu/spires/find/hep/www?r=sscl-preprint-17SPIRES> entry T. Mannel, arXiv:hep-ph/9611411.
- [67] A. Falk, SLAC preprint 5689, 1991.
- [68] N. Isgur and M. B. Wise, Phys. Rev. **D43** (1991) 819; N. Isgur, M. B. Wise and M. Youssefmir, Phys. Lett. **B254** (1991) 215.
- [69] B. D. Keister and W. N. Polyzou, J. Comput. Phys. **134**, 231 (1997).
- [70] Article on Charmed Baryons by C.G. Wohl, Phys. Lett. **B592**, 977 (2004)
- [71] S. Capstick, pp. 311, in Hadron Spectroscopy and the Confinement Problem, Ed. D.V. Bugg (Queen Mary and Westfield College, London, England), Plenum Press (New York, 1996).
- [72] A. Falk and M. Neubert, Phy. Rev. **D47**, 2982 (1993).

- [73] B. K. Jennings, Phys. Lett. B **176**, 229 (1986); A. Ramos, E. Oset, C. Bennhold, D. Jido, J. A. Oller and U. G. Meissner, arXiv:nucl-th/0312013.
- [74] See, for example, S. Choe, Eur. Phys. J. A **3**, 65 (1998), and references therein.
- [75] H. Albrecht *et al.* [ARGUS Collaboration], Phys. Rept. **276**, 223 (1996).
- [76] P. Avery *et al.* [CLEO Collaboration], Phys. Rev. **D43**, 3599 (1991).
- [77] D. Scora and N. Isgur, Phys. Rev. **D52**, 2783 (1995).
- [78] M. - Q. Huang, H. - Y. Jin, J. G. Körner and C. Liu, arXiv hep-ph/0502004.
- [79] A. Le Yaouanc, L. Oliver and J. C. Raynal, Phys. Rev. D **69**, 094022 (2004).
- [80] R. L. Jaffe and F. Wilczek, Phys. Rev. Lett. **91**, 232003 (2003).
- [81] O. Krehl, C. Hanhart, S. Krewald and J. Speth, Phys. Rev. C **62**, 025207 (2000)
- [82] L. S. Kisslinger and Z. P. Li, Phys. Rev. D **51**, 5986 (1995).
- [83] M. G. Olsson, S. Veseli and K. Williams, Phys. Rev. **D51**, 5079 (1995).

BIOGRAPHICAL SKETCH

Muslema Pervin

Education

- Florida State University, Tallahassee, Florida, USA, 2000-Present
Ph. D. in Physics, Expected in Summer 2005
Major Professor: Dr. Simon Capstick
Thesis title: “Quark Model of Baryon Semileptonic Decays”.
- University of Dhaka, Dhaka, Bangladesh, 1992-1993 (Academic Year)
M. Sc. in Physics, 1997
Thesis supervisor: Professor L. M. Nath
Thesis title: “CP violation in neutral kaon decays and the standard model”.
- University of Dhaka, Dhaka, Bangladesh, 1989-1992 (Academic Year)
B. Sc. with Honors in Physics, 1994

Research Experience

- Research Assistant:
Department of Physics, Florida State University, Tallahassee, Florida
2002-Present
- Research Fellow:
University Grants Commission, Dhaka, Bangladesh
1998-1999

Teaching Experience

- Teaching Assistant:
Department of Physics, Florida State University, Tallahassee, Florida
2000-2001
- Teaching Assistant:
Department of Physics, Southern Illinois University, Carbondale, Illinois
1999-2000

Publications

- K. Kabir, T. K. Dutta, M. Pervin, L. M. Nath, *The Role of $\Delta(1232)$ in Two-pion Exchange Three-nucleon Potential*, Int. J. Mod. Phys. E9, 157(2000).
- M. Pervin, N. Ahsan, K. Kabir, L. M. Nath, *Standard model and CP violations in neutral K- and B-meson systems*, J. Phys. G24, 1693(1998).
- M. Pervin, W. Roberts and S. Capstick, *Semileptonic Decays of Heavy Lambda Baryons in a Quark Model*, nucl-th/0503030, accepted for publication in Phys. Rev. C.
- M. Pervin, W. Roberts and S. Capstick, *Semileptonic Decays of Heavy Omega Baryons in a Constituent Quark Model*, in preparation.